Diplomarbeit

Environmental External Costs from Power Generation by Renewable Energies

Martin Braun

Environmental External Costs from Power Generation by Renewable Energies

Diplomarbeit

angefertigt von
cand. BWL techn. Martin Braun
Karl-Klingler Str. 12
71336 Waiblingen
Matr. Nr.: 1931482

Betreuer:	Prof. Dr.-Ing. habil. R. Friedrich, Dipl.-Ing. P. Preiss, IER
	Prof. Dr. H. Majer, IVR

Studienrichtung:	Technisch orientierte Betriebswirtschaftslehre
Wahlpflichtfächer:	Energiewirtschaft; Planung;
	Marketing, insbes. Investitionsgütermarketing
Technisches	
Schwerpunktfach:	Elektrotechnik

Beginn der Arbeit:	16. April 2004
Ende der Arbeit:	16. Juli 2004

Institut für Energiewirtschaft und Rationelle Energieanwendung, Stuttgart
Prof. Dr.-Ing. A. Voß
Abteilung Technikfolgenabschätzung und Umwelt (TFU)
Prof. Dr.-Ing. habil. R. Friedrich

Index of Contents

List of Figures

List of Tables

List of Abbreviations

$(NH_4)_2SO_4$	Ammonium sulphate
a-Si	Amorphous silicon
AC	Alternating current
AFC	Alkaline fuel cell
APME	Association of Plastics Manufacturers in Europe
B	Boron
BF	Bio-fuelled
BM	Biomass
BMU	Bundesministerium für Umwelt, Naturschutz und Reaktorsicherheit
BMWA	Bundesministerium für Wirtschaft und Arbeit
BoP	Balance of plant
BOS	Balance of System
BUWAL	Bundesamt für Umwelt, Wald und Landwirtschaft (Switzerland)
C	Carbon
c-Si	Crystalline silicon
C-CFB	Coal-fired pressurized circulating fluidised bed power plant analysed in /BMWA 2004/
C-IGCC	Coal-fired Integrated Gasification Combined Cycle power plants analysed in /BMWA 2004/
C-ST	Coal-fired steam turbine power plants analysed in /BMWA 2004/
c&c	Contraction and convergence
CC	Direct co-combustion
CCl_4	Carbon tetrachloride
CdTe	Cadmium telluride
CFB	Circulating fluidised bed
CFBC	Circulating fluidised bed combustion
CFBC+additive	Circulating fluidised bed combustion with addition of limestone
CFBC+FGD	Circulating fluidised bed combustion with flue gas desulphurization
CFBG	Circulating fluidised bed gasification
CFBG+CC	Circulating fluidised bed gasification combined with co-combustion
CFB+FGC	CFB boiler with steam power technology, crude bio fuel and flue gas condensation
CFC	Chlorofluorocarbon
CH_4	Methane
CHP	Combined heat and power
CIGS	One of the alloys of $Cu(In,Ga)(S,Se)_2$
CIS	Cooper Indium Diselenide

CO	Carbon monoxide
CO_2	Carbon dioxide
$CO_{2,equ}$	Equivalent carbon dioxide (cf. chapter 4.7)
Cu	Copper
DC	Direct current
DENOX	NO_x reduction
DLR	Deutsches Zentrum für Luft- und Raumfahrt
DWD	Deutscher Wetterdienst
EAA	European Aluminum Association
ECLIPSE	Environmental and Ecological Life Cycle Inventories for present and future Power Systems in Europe
EcoSenseLE	EcoSense Look-up Edition
ECU	Environmental Change Unit
E.E.I.G.	European Economic Interest Grouping
EG-Si	Electronic-grade silicon
EI99	Eco-Indicator 99
EU	European Union
EU-15	European Union (Austria, Belgium, Denmark, Finland, France, Germany, Greece, Ireland, Italy, Luxembourg, Netherlands, Poland, Portugal, Spain, Sweden and United Kingdom)
EU-25	European Union (Austria, Belgium, Cyprus, Czech Republic, Denmark, Estonia, Finland, France, Germany, Greece, Hungary, Ireland, Italy, Latvia, Lithonia, Luxembourg, Malta, Netherlands, Portugal, Slovakia, Slovenia, Spain, Sweden and United Kingdom)
EVA	Ethyl-vinyl-acetate
EWEA	European Wind Energy Association
ExternE	External Costs of Energy
ExternE-Coal	Coal-fired power plant analysed in /European Commission 1999c/
ExternE-Gas	Natural gas-fired power plant analysed in /European Commission 1999c/
ExternE-Lignite	Lignite-fired power plant analysed in /European Commission 1999c/
ExternE-Oil	Oil fired power plant analysed in /European Commission 1999c/
FC	Fuel Cell
FG	Fire grate
FG+FGC	Fire grate with steam cycle, crude bio fuel and flue gas condensation
FG+dry	Fire grate with steam cycle and integrated steam dryer for bio fuel drying
FGD	Flue gas desulphurization
FfE	Forschungsstelle für Energiewirtschaft e.V.
FfE-Coal	Coal-fired power plant analysed in /FfE 1999/
FfE-Lignite	Lignite-fired power plant analysed in /FfE 1999/

FfE-Gas	Natural gas-fired power plant analysed in /FfE 1999/
FfE-Nuclear	Nuclear power plant analysed in /FfE 1999/
FUND	Climate Framework for Uncertainty, Negotiation and Distribution
Ga	Gallium
Gas+dry	Pressurized gasification, combined cycle and integrated steam dryer for biofuel drying
Gas-Engines	Circulating fluidised bed gasification at atmospheric pressure with two downstream gas engines analysed in /Briem 2003/
GNP	Gross national product
GT	Geothermal
GWP	Global Warming Potential
GWP-100a	Global Warming Potential with a time horizon of 100 years
H_2O	Water
H_2SO_4	Sulphuric acid
H_3PO_4	Phosphoric acid
HCFC-22	Chlorodifluoromethane
HCl	Hydrochloride acid
HDR	Hot Dry Rock
HFC	Hydro fluorocarbon
HNO_3	Nitric acid
IEA	International Energy Agency
IEA PVPS	IEA Photovoltaics Power Systems Programme
IGCC	Integrated Gasification Combined Cycle
IISI	International Iron and Steel Institute
In	Indium
IPCC	Intergovernmental Panel on Climate Change
ISET	Institut für Solare Energieversorgungstechnik
ISO	International Organization for Standardization
L-IGCC	Lignite-fired Integrated Gasification Combined Cycle power plants analysed in /BMWA 2004/
L-ST	Lignite-fired steam turbine power plant with integrated coal dryer analysed in /BMWA 2004/
LCA	Life cycle assessment
LCI	Life cycle inventory
LUKO	Air-cooled condenser
MAC	Marginal abatement costs
MEC	Marginal external costs
MEC_{opt}	Optimal marginal external costs
mc-Si	Multi-crystalline silicon

MCFC	Molten carbonate fuel cell
MG-Si	Metallurgical-grade silicon
MIC	Marginal internal costs
MIC_{opt}	Optimal marginal internal costs
MNPB	Marginal net private benefits
$MNPB_{opt}$	Optimal marginal net private benefits
NMVOC	Non methane volatile organic compounds
NewExt	New Elements for the Assessment of External Costs from Energy Technologies
N_2	Nitrogen
N_2O	Nitrous oxide
N_2O_5	Nitric pentoxide
NG-GS	Natural gas-fired gas and steam power plant analysed in /BMWA 2004/
NH_3	Ammonia
NH_4NO_3	Ammonium nitrate
NO	Nitrogen monoxide
NO_2	Nitrogen dioxide
NO_3	Nitrogen trioxide
NO_x	Nitrogen oxides
NPV	Net present value
NTM	Network for Transportation and Environment
O	Oxygen atom
O_2	Oxygen molecule
O_3	Ozone
OECD	Organisation for Economic Co-operation and Development
OF	Open Framework for Climate Change Impact Assessment
OH	Hydroxyl
ORC	Organic Rankine Cycle
P	Phosphor
PAFC	Phosphoric acid fuel cell
PEFC	Polymer electrolyte fuel cell
PEM	Proton exchange membrane
PFBC	Pressurized fluidised bed combustion
PFC	Per fluorocarbons
PM	Particulates matter
PM10	Particulates matter with a diameter of less than 10 μm
PM2.5	Particulates matter with a diameter of less than 2.5 μm
poly-Si	Non-prime direct poly-crystalline silicon
PV	Photovoltaic

PVC	Polyvinyl chloride
REISI	Renewable Energy Information System on Internet
River-3.1	River power plant with 3.1 MW
River-0.3	River power plant with 0.3 MW
S	Sulphur
Se	Selenium
Si	Silicon
sc-Si	Single crystalline silicon
SF_6	Sulphur hexafluoride
SG-Si	Solar-grade silicon
$SiCl_4$	Silicon tetrachloride
$SiHCl_3$	Trichlorosilane
SiO_2	Silicon dioxide
SNCR	Selective Non-Catalytic Reaction
SO_2	Sulphur dioxide
SOFC	Solid oxide fuel cell
SRES	Special Report on Emission Scenarios
ST	Solar thermal
TiO_2	Titanium dioxide
UBP97	Umweltbelastungspunkte 97
UCTE	Union for the Co-ordination of Transmission of Electricity
UN	United Nations
UNDP	United Nations Development Programme
VLYL	Value of a life year lost
VOC	Volatile organic compounds
VSL	Value of a statistical life
WBGU	Wissenschaftlicher Beirat der Bundesregierung globale Umwelt-veränderungen
Wp	Watt peak
WRE	Name of scenarios which are proposed by Wigley, Richels and Edmonds in /IPCC 2001a/
WT	Wind turbine
WTA	Willingness to accept
WTP	Willingness to pay
YCl_3	Yttrium chloride
$ZrCl_4$	Zirconium tetrachloride

Nomenclature

A	Area
a	Year (annum)
AGWP	Absolute global warming potential
all_{el}	Allocation factor for electricity
all_{th}	Allocation factor for heat
a_x	Radiative efficiency
C	Cost per unit
CC	Capacity credit
d	Day
dis	Distance
E	Electrical energy
ex_{el}	Exergy content of an electricity unit
ex_{th}	Exergy content of a heat unit
E_c	Energy production of a single conventional energy system
E_m	Energy production of a mixed (conventional + renewable) energy system
E_r	Energy production of a single renewable energy system
Ex_{el}	Exergy of electrical energy
Ex_{th}	Exergy of heat
f_c	Full load hours of the conventional energy system
f_r	Full load hours of the renewable energy system
g	Growth rate of real consumption per capita
g_{earth}	Acceleration of gravity
GWP	Global warming potential
$h\upsilon$	Energy of a photon (h is Planck's constant and υ is the frequency)
h	Hour
h_1	Height of the head water
h_2	Height of the run-off water
I	Annual solar radiation on optimal tilt angle
L	Learning factor
m	Mass
MEC_{opt}	Optimal marginal external costs
MIC_{opt}	Optimal marginal internal costs
p	Price
p_1	Pressure of the head water
p_2	Pressure of the run-off water
P_{wind}	Power of the wind
P	Produced quantity

$P_{c,m}$ Capacity of a conventional energy system in a mixed energy system

$P_{c,s}$ Capacity of a single conventional energy system

$P_{c,tot}$ Capacity of a conventional energy system needed to produce E_m

P_r Capacity of a renewable energy system

Q Heat

$r_{fix,c,s}$ Ratio of the specific fixed costs over the specific total costs of a single conventional energy system

R Penetration (proportion of the electricity generation of the renewable energy system to the total electricity generation)

s_b Specific backup costs per kWh for the electricity generation of the renewable energy system in a mixed energy system

$s_{c,s}$ Specific costs of a single conventional energy system for the electricity generation E_c

$s_{var,c,s}$ Specific variable costs per energy unit of a single conventional energy system

$s_{fix,c,s}$ Specific fixed costs per energy unit of a single conventional energy system

S Reaction entropy

S_b Backup costs

$S_{c,s}$ Costs of a single conventional energy system for the electricity generation E_c

$S_{c,m}$ Cost of a conventional energy system in a mixed energy system with the costs S_m

S_{fix} Fixed costs

$S_{fix,c,s}$ Fixed costs of a single conventional energy system

$S_{fix,c,m}$ Fixed costs of a conventional energy system in a mixed energy system

S_m Costs of a mixed energy system (conventional + renewable) for the electricity generation E_m

S_r Costs of a renewable energy system for the electricity generation E_r

S_{var} Variable costs

SDR Social discount rate

STP Social rate of time preference

T Temperature

T_0 Ambient temperature

T_{in} Temperature fed into a local heat network

T_m Thermodynamic mean temperature

TH Time horizon

T_{out} Temperature returning from a local heat network

v Velocity

v_1 Velocity of the head water

v_2	Velocity of the run-off water
V	Volume
W	Energy of fuel
ΔG_T	Free reaction enthalpy
ΔH	Enthalpy change
ΔT	Temperature change compared to the 1901-1995 average
ε	Elasticity of marginal utility with respect to consumption
ζ	Utilization degree
$\zeta_{c,s}$	Utilization degree of a single conventional energy system
$\zeta_{c,m}$	Utilization degree of a conventional energy system in a mixed energy system
η	Energetic conversion rate
$\eta_{BOS,el}$	BOS efficiency
η_{Carnot}	Carnot efficiency
η_{el}	Efficiency of generating electricity
η_{inv}	BOS inverter efficiency
η_{loss}	BOS losses efficiency
η_{max}	Maximum theoretical efficiency
η_{mod}	Module efficiency
η_{PV}	Total PV efficiency
η_{th}	Efficiency of generating heat
η_{tot}	BOS total efficiency
λ_{max}	Maximum wave length
ρ	Density
Index 1	Head water
Index 2	Run-off water
Index c	Conventional energy system
Index el	Electric
Index fix	Fixed part (of the costs)
Index m	Mixed energy system
Index r	Renewable energy system
Index R	Related to a specific penetration
Index th	Thermal
Index var	Variable part (of the costs)

Abstract

In the following decades there will be a fundamental structural change in the European power supply system. This structural change is forced by several factors, e.g. the European Union Greenhouse Gas Emission Trading Scheme, the strategic goal for the European Union of a more sustainable development, energy policy targets to double the share of renewable energies, the phase out or moratoria of the nuclear industry in some European Union member states, and the need of more than 200 GW of new power plant capacities in EU-15. The structural change has to be embedded into an economic, social and ecological framework. Within this framework, there is a variety of possible options to create a future power supply which fulfils the multiple criteria. Generally, different technologies can be chosen which all have their own advantages and disadvantages. It is a challenging decision-making process because fossil-fired power plants tend to be economically advantageous and ecologically disadvantageous whereas renewable energy systems tend to be ecologically advantageous and economically disadvantageous.

This study gives a comparison of the estimated external costs (environmental aspects) and internal costs (economic aspects) of different power generation technologies in the year 2010 in order to support the decision-making process of future power plant investments in the framework of a sustainable development. A life cycle analysis gives considerable life cycle data for photovoltaic systems, wind turbines, fuel cells, bio-fuelled combined heat and power plants, biomass, water, solar thermal, geothermal, coal-fired, lignite-fired and natural gas-fired power plants as well as nuclear power plants. This database is used for the estimation of external costs which is based on updated factors of damage and avoidance costs for selected emissions. The damage factors are calculated with the software tool EcoSense following the impact pathway approach. Global warming and discounting are considered to be the hot spots in the external costs discussion. An avoidance costs approach is applied which is assumed to fulfil sustainability criteria.

The comparison of the external costs of the technologies analysed shows that external costs of power generation technologies using renewable energies and nuclear power plants are in the range of 0.03-3.79 €-Cent/kWh$_{el}$ whereas the external costs of power generation technologies using organic fossil fuels are in the range of 3.37-27.98 €-Cent/kWh$_{el}$. However, the comparison of the internal costs shows that fossil-fuelled power plants have the lowest internal costs compared to the other technologies analysed. This trade-off between external and internal costs requires a comparison of the social costs which are the sum of internal and external costs. The comparison of the social costs shows five social cost clusters for the analysed technologies for the year 2010. Nuclear power plants have social costs of less than 10 €-Cent/kWh$_{el}$. Wind turbines and river power plants have slightly higher social costs of 10-15 €-Cent/kWh$_{el}$. Biomass power plants, bio-fuelled combined heat and power plants, solar thermal power plants, geothermal power plants and natural gas-fired power plants have social

costs in the range of 15-20 €-Cent/kWh$_{el}$. Photovoltaic systems in Spain, fuel cells, coal-fired power plants and lignite-fired power plants have social costs in the range of 20-35 €-Cent/kWh$_{el}$. The highest social costs are caused by Photovoltaic systems in Germany with more than 35 €-Cent/kWh$_{el}$.

1   Introduction

In the following decades, there will be a fundamental structural change in the European power supply system. This structural change is forced by several factors. Ratifying the Kyoto protocol in 1997 the *European Union* (EU) committed to reducing greenhouse gas emissions by 8 % from the 1990 level by 2008-2012. In order to reach this target, the *European Union Greenhouse Gas Emission Trading Scheme* will start in January 2005 based on the Directive 2003/87/EC. Another important influencing factor for the structural change is the strategic goal for the EU of a more sustainable development[1] in order to achieve an enduring development which includes equity between people, regions and generations with the holistic view of the economic, ecological and social system. Motivated by the goals of sustainable development and reduction of greenhouse gas emissions, the EU set a clear energy policy target to double the share of renewable energies from 6 % of the gross inland energy production in 1997 to 12 % in 2010 (COM(97)99). Another energy policy target is to maintain the security of supply (COM(2002)231) which may be at risk, e.g. due to a high import dependency on limited resources with very volatile prices on world markets and the phase out or moratoria of the nuclear industry in some EU member states. Additionally, many present European power plants are over aged and have to be replaced in the following decades. For the period 2010-2020 it is estimated that there is a need of more than 200 GW of new power plant capacities in EU-15 /BMWA 2003/.

The structural change has to be embedded into an economic, social and ecological framework. Within this framework there is a variety of possible options to create a future power supply which fulfils the multiple criteria. Generally, different technologies can be chosen which all have their own advantages and disadvantages. Possible technologies are nuclear power plants, coal-fired power plants, gas-fired power plants as well as renewable power plants which use regenerative energies, e.g. solar radiation, wind or biomass. It is a challenging decision-making process because fossil-fired power plants tend to be economically advantageous and ecologically disadvantageous whereas renewable energy systems tend to be ecologically advantageous and economically disadvantageous. The difficulty is that economic and ecological criteria can not be compared directly as the former are normally available in monetary terms (*internal costs*) whereas the latter are usually not. Thus, an attempt is made to estimate ecological aspects in monetary terms (*external costs*) in order to enable a comparison of the different technologies with economic and ecological criteria. A further advance would be the inclusion of social criteria which is not performed in this study.

In the study at hand, the term *external costs* is explained from the point of view of environmental economics in chapter 2. Chapter 3 describes the methodology for the estimation of external costs whereby it concentrates on emissions whose economic impacts have been in-

---

[1]   Sustainable development in this study follows the concept of /Majer 2003b/.

vestigated in detail in previous studies. One of the main contributors to external costs is global warming which is caused by the emission of greenhouse gases. Its economic consequences are described in detail in chapter 4. After explaining the theory of external costs in the first four chapters, an analysis of the external and internal costs of different power generation technologies is performed with a European scope. Firstly, a life cycle inventory of different power generating systems is given in chapter 5. This chapter is based on studies which have been published in 2004 and is thus up to date. Secondly, in chapter 6 the environmental external costs are estimated with this life cycle inventory. Thirdly, chapter 7 summarizes the internal costs for the inclusion of the economic criteria in a further comparison of the analysed technologies. Fourthly, in chapter 8, an analysis is made of how the uncertainty of fluctuating power generation technologies, which are, for instance, dependent on solar radiation or wind velocity, can be taken into account for the estimations. Finally, a comparison of the sum of external and internal costs, the so-called *social costs*, is performed in chapter 9. This comparison claims to comprise economic as well as ecological aspects which should be considered in the decision-making process for future power plant investments. However, it is not claimed to be an exact calculation because of a variety of uncertainties which are inherent in the estimation of external as well as internal costs. Additionally, only a part of the environmental aspects and no social aspects are taken into account. Due to this incompleteness the results of this study represent an intermediate step which can be used to make decisions on future power plant investments in the framework of a sustainable development.

2   External costs in environmental economics[2]

Originally, environmental economics is derived from the neo-classical paradigm in micro-economics. The main assumption of this paradigm is perfect competition on all markets. This means, on the one hand, that all economic subjects act in the rational way of a homo oeconomicus, who maximizes his utility with universal knowledge to his own interest without accounting for the interests of other people. On the other hand, perfect competition means that all economic subjects do not have a significant market share to influence the market in any noticeable way. With neo-classical assumptions there is a pareto-optimal market equilibrium on all markets so that supply and demand are equal and no economic subject is able to improve its own situation without deteriorating the situation of another one.

Usually, these pareto-optimal results are not achieved in real market conditions which are characterized by market imperfections, e.g. transaction costs, significant market powers, incomplete information, public goods and externalities. In order to regain pareto-optimal results there is a need for public interventions, e.g. rules of competition. For an appropriate intervention market imperfections should be analysed. In the context of this study, public goods and externalities are surveyed.

Public goods, e.g. clean air, differ from private goods, e.g. a car, in two ways. On the one hand, consumers of private goods are excluded from consuming the good if they do not pay the claimed price. In contrast, consumers of public goods can not be excluded because they do not need to pay for the use of the good. On the other hand, there exists no rivalry in consumption of public goods compared to private goods because the good can be used by all consumers at the same time, generally, without interference. With this definition of public goods, there will be no market for them since they can be used by everyone without the need to pay for them. In many cases public goods are used in a careless way because no compensation has to be paid for damages because nothing has to be paid for their use.

Externalities exist in the form of external costs and external benefits. External costs occur when an economic subject causes a loss of welfare to another one and does not compensate the change of welfare. In contrast, external benefits occur when an economic subject causes an increase of welfare to another one and is not compensated for this change of welfare. On perfect markets, the utility of a good would be compensated by the utility of the money paid for this good. A compensation for this change of welfare due to external costs of benefits would eliminate the market imperfection caused by externalities. This procedure is called *internalisation of externalities* because external costs and benefits are considered in market prices. In a situation where all externalities are internalised, the compensation corresponds to the same utility as the change of welfare so that there is no externality anymore.

---

[2]   Further literature: /Pearce; Turner 1994/, /Friedrich 2003a/, /Majer 2003a/, /Clarkson; Deyes 2002/ and /Endres 2000/

The market mechanism of this internalisation can be illustrated with a cost-benefit-diagram which is shown in **Figure 2-1**. In this diagram, the abscissa displays the amount of a predefined emission, e.g. particulates, which corresponds approximately to a certain economic activity. Marginal costs and benefits are displayed by the ordinate. The following description is based on the assumption that the only market imperfections are the considered public goods and externalities.

The clean air as a public good can be used and polluted unlimited, e.g. with particulates from coal-fired power plants. These particulates affect the health of people due to inhalation. It is assumed that with increasing amount of emissions the damage to the injured party increases more than proportionally. In the case of particulates, little concentration in the inhaled air will not be recognized as there is no noticeable interference of the health. With increasing concentration levels, the damage becomes more obvious, initially, with cases of cough and, eventually, with cases of asthma. Therefore, the function of *marginal external cost* (MEC) has a positive slope in **Figure 2-1**. However, there are also benefits as the power produced increases the welfare of the consumers, which represent the injuring party. The function of *marginal net private benefits* (MNPB) has a negative slope as an additional unit of power at a lower supply level has a higher additional benefit compared to higher supply levels. At a certain level, there is no additional demand for power because the willingness to pay is less than the production costs. This function may also be interpreted in terms of opportunity costs as a function of *marginal abatement costs* (MAC) because the abatement of emissions corresponds approximately to the reduction of economic activity so that the welfare (area below the MNPB curve) decreases. The injuring party produces with the highest economic activity possible in order to gain the maximum of benefit (area below the MNPB curve) causing external costs (area below the MEC curve) to the injured party.

The goal of society is to maximise the sum of benefits minus the sum of costs. In the situation described above, the MEC of the last units of economic activity are higher than the MNPB. Therefore, a reduction of the economic activity leads to a higher reduction of external costs than the reduction of net private benefits. Using social criteria, the economic activity has to be reduced until the MAC is as high as the MEC. A further reduction would lead to more loss of benefits than a reduction of external costs. This equilibrium (MAC = MEC) is pareto-optimal because any deviation would lead to a worse situation for society. Thus, the optimal level of economic activity, emission and pollution is defined. The need for a perfect market can be derived from this description.

This pareto-optimum can be achieved by the internalisation of the external costs which means the allocation of the external costs to the polluter. Assuming the MEC curve as well as the MAC curve is known, the pareto-optimal equilibrium, which should be achieved, can be derived. The MEC_{opt} in this equilibrium should be added to the *marginal internal costs* (MIC_{opt}) needed to produce the considered unit of power. In perfect market conditions the *price* (p) of a unit of power would be equal to this sum:

$$p = MEC_{opt} + MIC_{opt} \qquad\qquad (2\text{-}1)$$

Thus, one possibility for the internalisation of the external costs would be a tax equal to MEC_{opt} which is raised on every unit of power, a so-called Pigouvian tax. Another possibility is the use of tradable permits with an amount of permits according to the optimal level of emission with internalisation.[3]

It should be noted that the determination of this optimum does only work with a static point of view. Since the MEC and MAC functions vary over time on real markets and a variety of uncertainties is inherent in the functions (cf. next chapter) the estimation of the optimal level of pollution as well as the optimal Pigouvian tax is difficult.
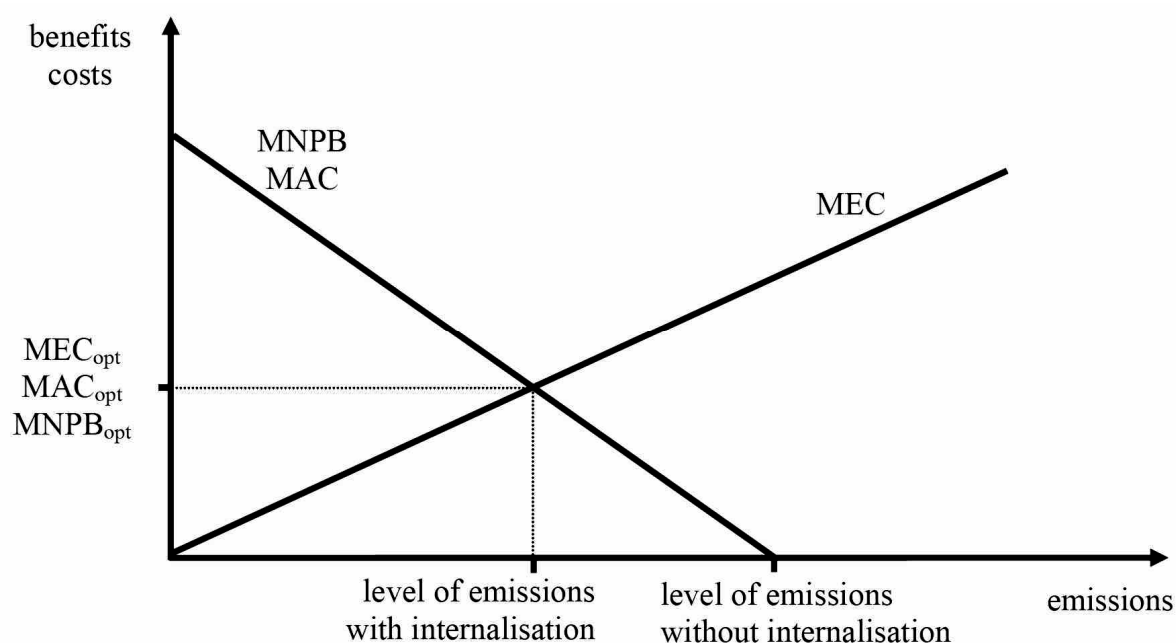
Figure 2-1:   Cost-benefit-diagram

---

[3]   Detailed descriptions of internalisation strategies (Pigovian tax, marketable pollution permits, property rights) are available in /Endres 2000/ and /Bartmann 1996/.

3 Methodology for the estimation of external costs[4]

In this study, only selected types of emissions are considered for external costs. This restriction has to be adopted as there is a large variety of impacts which are very difficult to survey. Additionally, uncertainties, which are specified in this chapter, are very large and reliable data on the emissions is hardly available. Therefore, only well studied emissions with good data quality are taken into account.

The estimation of external costs with a cost-benefit analysis requires the estimation of the MEC- and MAC-function, initially. These functions should be comparable in the same diagram with the same dimensions in order to determine the optimum. The only reasonable dimension which enables to compare costs and benefits is a monetary one. Therefore, the *impact pathway approach* is used in order to estimate the benefits and costs of emissions. With this assessment method, a general path from emissions to the costs and benefits is followed to estimate them as transparently, consistently and comprehensively as possible. The pathway consists of the following steps.

At a certain location the considered emissions are released. From this location the meteorological conditions determine the dispersion of the emissions. During the transport process, chemical conversion processes may appear depending on the considered type of emission. The emissions cause a certain level of concentration or deposition on the considered impact area. There, receptors will show a certain response in form of a physical impact. This will lead to a change in utility and thus to a change in welfare. Finally, the welfare change is expressed in monetary terms in order to determine costs or benefits.

Sometimes it is not possible to estimate the change in utility. In these cases a second path is used which is based on sustainability standards defined for concentrations or physical impacts. These sustainability standards specify thresholds, e.g. critical loads or critical levels, which should not be exceeded. Therefore, cost-effective reduction strategies have to be performed to reach these standards. Instead of a change in welfare the costs for the reduction are taken into account. Both possible impact pathways are described in chapter 4 with the example of global warming.

With this structured calculation procedure the application of a software tool seems reasonable. Within the project series *External Costs of Energy* (ExternE) the EcoSense model was developed. Features of this software tool are, for example, a database containing information about receptor distribution (population, production of crops and inventory of materials) as well as meteorological data (wind speed, wind direction and precipitation). This tool is described in more detail in /European Commission 1999a/.

In the study at hand, the external costs of different power generation technologies are estimated. For this purpose, a *life cycle assessment* (LCA) is necessary to determine the differ-

---

[4] /Friedrich 2003a/ and /European Commission 1999a/

ent locations and amounts of emissions during the whole life cycle of a plant from the cradle, e.g. fuel extraction, to the grave, e.g. waste disposal. Therefore, all the upstream processes, e.g. material supply for the construction, and downstream processes, e.g. network for energy supply to the households, have to be taken into account. With these site specific emission data from the LCA an impact pathway has to be calculated for the emissions from every relevant location to all the affected receptors. Obviously, this is too complex because of changing processes and emission sites as well as the lack of detailed information (see chapter 3.1).

An all-embracing LCA is only achievable for one specific power plant, at a specific site and with unchanging upstream and downstream processes. For this study, it is not feasible to calculate in a high level of detail because in the high dynamic market of renewable energies, the process chain is changing permanently and small decentral power plants are widespread.

Therefore, in this study the external costs are considered as average values for the EU-15. This simplified estimate of external costs is based on the multi-source version of EcoSense. With this software, the external costs per kg of a pollutant are calculated by marginal variation of the CORINAIR database for emission. The calculation is performed with a 10 % increment of the emissions from all sources and the associated increase of damages. The division of the determined damage costs by the additional mass of emissions results in damage factors. These damage factors indicate the marginal external costs corresponding to damages which are caused by one mass unit of the considered type of emission. The values are taken from /European Commission 2004/[5]. Within /European Commission 2004/, a new and extended methodology to estimate external costs is developed.

Table 3-1 lists the damage factors for an average emission change in EU-15 of 1 kg and shows the range with a lower and an upper estimate which determines the damage factor of EU-15-countries with the lowest and EU-15-countries with the highest damage factor. The range is estimated with *EcoSenseLE* (EcoSense Look-up Edition)*,* a web-based tool for the estimation of external costs. This tool can be used for quick, approximate estimates of damage costs. Specific *sulphur dioxide* (SO_2) and *nitrogen oxides* (NO_x) damage costs are thus assumed to be in the range of ca. 25-200 % relative to the mean value. The estimation of damage costs of specific *particulates matter with diameter of less than 10 μm* (PM10) results in a range of 70-130 % relative to the mean value. For *non methane volatile organic compounds* (NMVOC) emissions, no range is estimated because it only contributes less than 1 % to the total external costs (cf. chapter 6).

Further uncertainties emerging in the estimation of external costs are described in chapter 3.1. The considered impact pathways covering the emissions with the main impact on external costs are characterised in chapter 3.2. Finally, chapter 3.3 gives an overview of different monetary evaluation methods.

---

[5]   The damage costs in $€_{2000}$ are inflation adjusted to $€_{2003}$.

Table 3-1: Damage factors ($€_{2003}$/kg) of emissions in EU-15 /European Commission 2004/

Emissions	Lower estimate	Damage factor	Upper estimate
SO_2	0.937	3.750	7.499
NO_x	0.804	3.214	6.429
PM10	20.141	28.774	37.406
NMVOC	1.196	1.196	1.196

3.1 Uncertainties[6]

Besides uncertainties inherent in any set of data, specific uncertainties exist in the determination of the MEC function as well as the MAC function. In the following, important uncertainties are summarised and then described in more detail:

- uncertainty in emission levels
- uncertainty in meteorological conditions, concentration and deposition
- uncertainty in response of the receptors
- uncertainty in valuing the costs and benefits of the physical impacts

3.1.1 Uncertainty in emission levels

It is very difficult to determine the current level of emissions. In order to achieve exact figures every emission source should be under permanent measurement. This is economically not feasible. Therefore, estimations of the emissions about similar sources are based on a representative source. Often, the combusted fuels are used as a proxy. The composition of the fuels is assumed to be similar. Therefore, the same combustion processes generate more or less the same emissions. This results in quite good estimations in the case of *carbon dioxide* (CO_2) because CO_2 emissions are related to the carbon content of the fuel. In case of other emissions, e.g. SO_2, it is not appropriate to relate the emission of SO_2 to the sulphur content because different combustion processes use specific flue gas treatment technologies. Therefore, the estimation has to rely on data from the power plant operator.

Natural sources of emissions, e.g. methane, are quite difficult to estimate in contrast to emissions from man-made processes because the sources are widespread and not well investigated. Thus, a distinction between natural and anthropogenic emissions is mostly difficult because natural sources and emissions are not well known.

---

[6] Further discussions on uncertainties are available in /Clarkson; Deyes 2002/, /European Commission 1999a/ and /Friedrich; Bickel 2001/.

Some calculations need data on future emissions, e.g. in the case of avoidance costs. Avoidance costs can be determined by estimating the difference between a business as usual emission scenario and a scenario with fewer emissions. The costs to achieve these reductions are avoidance costs. For such calculations even future emission levels should be estimated with corresponding uncertainties inherent in every scenario about future developments.

3.1.2   Uncertainty in meteorological conditions, concentration and deposition

Emissions do not only have impacts on the emissions site. Following the impact pathway they are dispersed in the atmosphere and transported to distant receptors. Therefore, meteorological conditions should be estimated because they determine the direction, distance and velocity of the dispersion. This estimation of the meteorological conditions is gained from records of the past and often averaged over certain timescales. However, weather forecasts are generally uncertain because of the complex behaviour of the regional and local wheather. Also uncertainties remain about the modelling of various conversion processes, which occur during the dispersion. All these complex processes determine the concentrations and depositions at the receptors site.

3.1.3   Uncertainty in response of the receptors

Following the impact pathway, the next step concerns the response of the receptors to the concentrations and depositions resulting in physical impacts.

A very critical factor is the considered time horizon. For example, in the case of CO_2 emissions, higher CO_2 concentrations are responsible for global warming (cf. chapter 4) with the following cause-and-effect chain over time (cf. **Figure 4-11**). Higher atmospheric CO_2 concentrations cause a greenhouse effect which leads to increasing temperatures over centuries. These higher temperatures are responsible for increasing sea levels over millennia due to thermal expansion and melting of ice sheets. Because of these long time periods it is highly speculative to estimate the response of the receptors in the coming centuries.

Another factor concerning the uncertainties in response of the receptors is the receptor's individual sensitivity. Every human being, every type of material and every organism can respond in an individual way. For instance, some people are sensitive to only small concentrations of tropospheric ozone while others do not notice it until much higher concentrations occur. Furthermore, organisms tend to adapt to changing environments so that new conditions seem to be disadvantageous at first hand while they get more and more common over time and thus loose their negative impact.

A difficult research process is the determination of various complex effects which normally take place in the natural environment. It is not possible to conduct all the measurements outside the laboratory as the molecules and their reactions are not observable without precise

laboratory instruments. Therefore, many models and investigations are performed under ceteris paribus conditions. Uncertainties arise with the transfer of the results from the laboratory to the natural environment because the natural environment is influenced by a multitude of other factors.

In the case of human beings, there is a lack of detailed information with respect to their behaviour and preferences. This makes it very difficult to determine the severity of the impacts.

3.1.4   Uncertainty in valuing the costs and benefits of the physical impacts

It is not possible to value all costs and benefits with market prices because, mostly, market prices are not available. Therefore, an attempt is made to estimate the *willingness to pay* (WTP) for a benefit and the *willingness to accept* (WTA) compensation for a detriment with a variety of evaluation methods. These evaluation methods are described in more detail in chapter 3.3. Market prices are sometimes very volatile at a specific market and vary between different markets. This variability makes a correct valuation impossible. Also the evaluation methods generate data with a high variance which is mostly averaged. Moreover, it is not possible to perform the evaluation with every affected person. This directly concerns the interpersonal, interregional and intergenerational equity as fundamental criteria for sustainability.

The interpersonal equity has to be considered if only parts of a society are affected while other parts are not. In this case, the evaluation should be performed with a fair distribution, which is difficult to achieve.

In the case of interregional equity, differences between people in the developed as well as people in less developed countries should be taken into account, for instance. This is necessary because people in less developed countries are frequently more affected than those in the developed countries, e.g. in the case of global warming. They often live in areas which are more affected and do not have the necessary economic background to compensate arising costs. This situation is especially critical because air as a public good circulates over the whole globe so that emissions in developed countries do also affect the less developed ones without the obligation of compensation. In an evaluation it is necessary to take this market failure into account. At present, most evaluations are performed in developed countries. Generally, less developed countries are either not included or only considered with weighting factors.

The interregional equity can be taken into account because previously mostly neglected people actually are at hand. In contrast, in the case of intergenerational equity, future generations can not be questioned personally. Thus, they can not be included into evaluations. Intergenerational equity is a problem which is difficult to solve. It is necessary to correct this market failure which arises from the use of public goods and the situation that affected people,

e.g. affected by the sea level rise in the coming centuries (cf. chapter 4), can not state their WTA a compensation for the environmental impacts caused by the present generation. Therefore, it is necessary that the present generation accounts for future generations. From a sustainability's point of view, the present generation is responsible for the future impacts which it causes. So, the present generation has to determine how to compensate the impacts they will cause. It is impossible to determine the correct value of compensation because the impacts arise in the coming centuries and millennia. In the meantime, there are developments which are hardly possible to determine in any way. It is possible that some problems will be solved whereas other problems, which are not known today, arise. Therefore, present models generally use a time horizon of one hundred years and thus neglect long-term impacts because future development would be highly speculative and therefore highly uncertain.

Another hot spot in the estimation of future impact costs is the use of discount rates. The high sensitivity of the results to different discount rates is exemplarily shown in chapter 4.4. In this chapter **Table 3-2** shows the different *net present values* (NPVs) in the year 2000 which arise by discounting with different discount rates. The table illustrates that future costs are reduced to a marginal value by using higher discount rates. A discount rate of 5 % reduces the costs of 1,000,000 € in 2100 to a NPV of 7,604 € in 2000. The same calculation using a 3 % discount rate results in a NPV of 52,033 €. It can be stated that higher discount rates reduce future costs very much so that they are less relevant compared to present costs. Thus, using a positive discount rate, even extremely high costs arising in the coming centuries are negligible.

Table 3-2:   Net present value (NPV) depending on the discount rate

Discount rate	5 %	3 %	1 %	0.1 %	0 %	-0.1 %	-1 %
Damage 2100	1,000,000	1,000,000	1,000,000	1,000,000	1,000,000	1,000,000	1,000,000
NPV in 2000	7,604	52,033	369,711	904,883	1,000,000	1,105,226	2,731,999

The *social discount rate* SDR, which is used in the case of external costs, is determined by the sum of the *social rate of time preference* STP with the product of the *growth rate of real consumption per capita* g and the *elasticity of marginal utility with respect to consumption* ε. The elasticity describes the relative change of the marginal utility with respect to the relative change of consumption level:

$$SDR = STP + \varepsilon \cdot g \qquad\qquad (3\text{-}1)$$

The first component (STP) is assumed to be zero because in case of a positive value present generation would benefits whereas in case of a negative value future generations would benefit. Sustainability criteria do not allow a benefit of any generation by means of a detriment of

another generation.[7] The growth rate of real consumption per capita is often derived from its recent development. However, it should be noted that this approach includes some problems. **Figure 3-1** shows the changes of the German *gross national product* (GNP) per capita over the last three decades following a negative sloped trend, which is illustrated as a dotted line. This is a trend which can be observed in most developed countries. Besides this behaviour it is not certain that the relatively constant growth over recent years will continue. It may also be possible that recessions with negative growth may occur, e.g. due to oil crises, terror acts, or financial crisis as the Asian one in 1997.
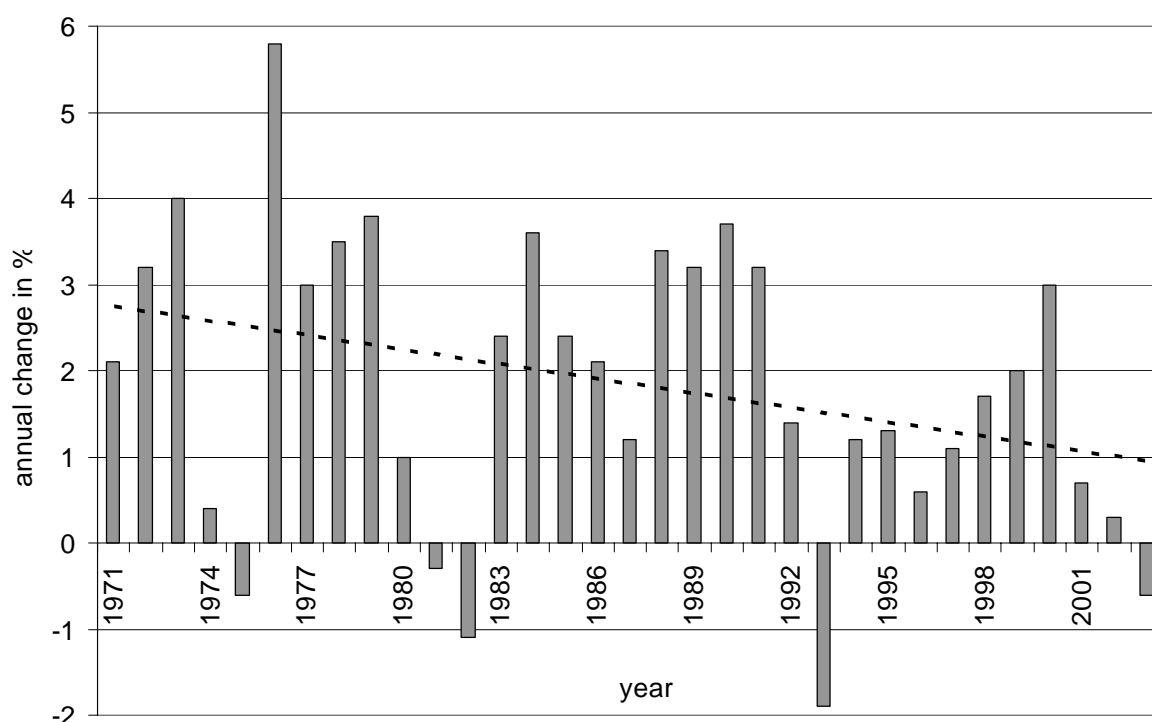
Figure 3-1:   Annual changes of the gross national product per capita in Germany with prices from 1995 over the years 1971-2003 /Statistisches Bundesamt Deutschland 2004/

Therefore, a positive growth rate g is mostly based on the assumption that the economic growth of the recent years continues. It seems necessary to conduct sensitivity analyses in order to compare the results of different discount rates, which can be positive, zero and negative. However, it is not easy to implement negative discount because future costs may have even higher net present values (cf. **Table 3-2**), which increase with longer time horizons. Nevertheless, it seems not fulfilling sustainability criteria to use only positive discount rates assuming that future generations do have a higher GNP per capita.

The elasticity ε is the third uncertain component determining the discount rate. It is varying between societies and generations and is derived by a utility estimation which again is based on controversially discussed assumptions. Mostly ε is assumed to be one.

---

[7] A more detailed discussion is given in /Azar; Sterner 1996/.

Summarizing the above mentioned hot spots of valuing, it can be concluded that the uncertainties are extremely high because evaluation has to be performed accounting for all affected persons. However, in the case of future generations, it is not possible to account for their needs because they do not exist at present and can therefore not influence negotiations and decisions. Due to the uncertainties concerning future developments the discount rate seems to be one of the most influencing parameters. A sensitivity analysis to different discount rates leads to a large range of results. However, which discount rate to choose is still a contentious issue.

Altogether it seems necessary to quantify the uncertainties which are described above in order to include them in the calculation or at least mention them in the results.

3.2 Considered Impact Pathways[8]

Actually, for the estimation of external costs it is necessary to assess every emitted substance with reference to their impact on the possible receptors. Moreover, there are other categories such as resource depletion or land use which cause externalities. However, for the investigated technologies only few substances cause the major part of the total external costs and therefore theses substances are studied in more detail. This study will take into account the pollutants in **Table 3-3** which can be characterized by the four different receptors:

- climate,
- human health,
- crops and
- building materials.

The effects are given in **Table 3-3** in form of an overview. The main part of the external costs arises due to impacts on the climate Therefore, it is analysed in an extra chapter 4. About 90 % of the remaining external costs can be attributed to human health impacts of the non-greenhouse emissions. Impacts on crops and building materials do only contribute a minor part to the external costs. It should be noted that impacts on the climate include impacts to human health, crops and building materials.

3.2.1 Emissions

CO_2 and SO_2 emissions are determined by the carbon and sulphur content of the fuel. In contrast, NO_x is created by the oxidation of nitrogen during the combustion of fuels. The nitrogen may originate from the fuel or from the combustion air. *Nitrogen monoxide* (NO) is the first combustion product. Later in the atmosphere it reacts with the aerial oxygen to *nitrogen dioxide* (NO_2). NO and NO_2 are included in the collective name *nitrogen oxides* (NO_x).

---

[8]   /Friedrich 2003a/, /Friedrich; Bickel 2001/ and /European Commission 1999a/

Volatile organic compounds (VOC) are a collective name of a variety of hydrocarbons, halogenated hydrocarbon and organic compounds with oxygen which are in the fuels or created during the combustion. VOC also contains *methane* (CH_4) which is an important greenhouse gas. Therefore, CH_4 is separated from VOC. The remaining substances are named as *non methane volatile organic compounds* (NMVOC).

Particulates consist of elementary carbon or condensated hydrocarbons due to the lack of oxygen during the combustion or a carbon-hydrogen-ratio which is too large.

Table 3-3:   Considered Emissions

Emission	Receptor	Effects
CO_2	Climate	World-wide effects on mortality, morbidity, coastal impacts, agriculture, energy demand and economic impacts due to temperature change, sea level rise etc. (see chapter 4)
CH_4		
NO_x (tropospheric O_3 and nitrates as secondary particulates)	Human health	Chronic and acute mortality (reduction of life expectancy) as well as morbidity (respiratory hospital admissions, cerebrovascular hospital admissions, restricted activity days, bronchodilator usage, cough, lower respiratory symptoms, asthma attacks, congestive heart failure, chronic bronchitis and cases of chronic cough)
	Crops	Yield change, acidification compensated by liming and fertilisation
	Materials	Ageing of galvanised steel, limestone, natural stone, mortar, sand-stone, paint, rendering and zinc for utilitarian buildings
SO_2 (sulphates as secondary particulates)	Human health	See above Human health
	Crops	Yield change and acidification compensated by liming
	Materials	Ageing of galvanised steel, limestone, mortar, sand-stone, paint, rendering and zinc for utilitarian buildings
Particulates	Human health	See above Human health
NMVOC (tropospheric O_3)	Human health	Asthma attacks
	Crops	Yield change

3.2.2   Emission reactions

The mean residence time in atmosphere:

The considered gases exist in a dynamic balance in the atmosphere. In this balance the gases which are produced by emissions and chemical reactions are chemically degraded and deposited. Their mean residence time in the atmosphere can be calculated by their mass over their generation rate. This estimation results in values given in **Table 3-4**.

Table 3-4:   Mean residence time in atmosphere of the considered emissions

Emissions	Mean residence time in atmosphere
CO_2	100 a
CH_4	7 a
SO_2	1-40 d
NO_x	1-2 d

Generation of ozone from NO_2 with hydrocarbons:

The photolysis (by photons with the energy hυ) of NO_2 to NO and O and the following recombination of the O with free *oxygen* (O_2) generates *ozone* (O_3) in the troposphere. NO together with O_3 reacts immediately afterwards to NO_2 and O_2. These reaction processes result in a balance between NO, NO_2 and O_3:

$$NO_2 + hυ \rightarrow NO + O$$
$$O + O_2 \rightarrow O_3$$
$$NO + O_3 \rightarrow NO_2 + O_2$$
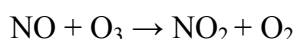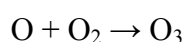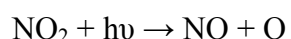
The concentration of O_3 depends on the insulation conditions and the concentration ratio of NO and NO_2. An additional reaction of NMVOC increases the concentration of O_3 by transforming the NO to NO_2 without degrading O_3 as in the other process. With an increasing concentration of NO_2 a higher concentration of O_3 through photolysis arises.

Acid deposition:

SO_2 passes through multiple reactions, e.g. with O_2, H_2O, OH and O_3, in gas and liquid phase to *sulphuric acid* (H_2SO_4).

During the day, NO_2 reacts with a *hydroxyl* (OH) to *nitric acid* (HNO_3) and reduces thus the NO_2-concentration and with it the ozone concentration. At night the concentration of OH

declines and thus the described reaction declines. Additionally, during the day, NO_3 immediately splits up into NO_2 and O by photolysis.

$$NO_2 + OH \rightarrow HNO_3$$
$$NO_3 + h\upsilon \rightarrow NO_2 + O$$
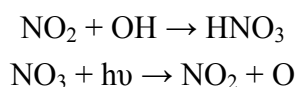
Instead of this reaction, by night NO_2 reacts with O_3 to *nitrogen trioxide* (NO_3) which reacts with NO_2 to *nitric pentoxide* (N_2O_5) and then with H_2O to HNO_3. This reaction degrades NO_2 and thus O_3. During the day the NO_3 immediately splits up into NO_2 and O by photolysis and hinders the described reaction.

$$NO_2 + O_3 \rightarrow NO_3 + O_2$$
$$NO_3 + NO_2 \rightarrow N_2O_5$$
$$N_2O_5 + H_2O \rightarrow 2HNO_3$$
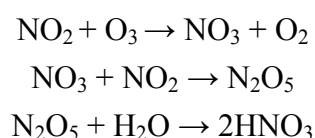
Nitric acid and sulphuric acid are the main parts of the acid rain (wet deposition) and acid deposition in general (wet and dry deposition).

Particulates deposition:

Ammonia (NH_3) reacts with HNO_3 to *ammonium nitrate* (NH_4NO_3) and with H_2SO_4 to *ammonium sulphate* ((NH_4)$_2SO_4$). H_2SO_4, NH_4NO_3 and (NH_4)$_2SO_4$ are solids and hence added to atmospheric aerosol. Within the aerosols primary and secondary particulates can be differentiated. Primary particulates are particulates which are emitted directly into the atmosphere. Secondary particulates are particulates which are created by accumulation of primary particulates and gaseous molecules as ammonium nitrate or ammonium sulphate.

$$NH_3 + HNO_3 \rightarrow NH_4NO_3$$
$$NH_3 + H_2SO_4 \rightarrow (NH_4)_2SO_4$$
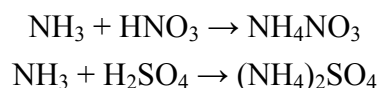
3.2.3 Exposure-response functions

There is a large variety of exposure–response functions which determine the relation between the exposure of a certain receptor with an emitted substance and the response of the receptor. The exposure–response functions can be linear or not linear. Linear means that each additional exposure unit results in the same number of response units. Not linear means that each additional exposure unit results not in the same number of response units. Special functions are functions with thresholds. The response is zero until a threshold of the exposure is reached and the response thereafter increases with the exposure. Another type is the function

with fertilizer effect which occurs in the impact category crops and describes that higher exposures result in higher crop yields. Examples are given in the following.

The impacts of SO_2 to crop yield are estimated with an exposure-response function which leads to an increase in crop yield until a certain level and a decrease thereafter. In contrast, the effects from O_3 to crop yield are estimated with a linear exposure-response function between an ozone level above a threshold and the yield loss. The effects from acid inputs to crop yield are estimated with a linear exposure-response function between acid deposition and additional lime requirements. Particularly, the fertilisation effect of nitrogen deposition is estimated with a linear exposure-response function between nitrogen deposition and reduction of fertiliser requirement.

3.2.4   Impacts[9]

Impact on human health:

SO_2 as well as NO_2 are highly soluble irritant gases affecting the mucous membranes of the respiratory tracts.

Particulates deposit in the respiratory tracts in dependence on their physical and chemical characteristics and the diameter of the respiratory tracts. Those particulates with a diameter of more than 10 μm do seldom reach the lung. In contrast, p*articulates matter with a diameter of less than 2.5 μm* (PM2.5) do deposit even in the alveoli. Generally, p*articulates matter with a diameter of less than 10 μm* (PM10) are particulates which can be inhaled.

Ozone has a high chemical reactivity and is only slightly water soluble. Therefore, it reaches easily the alveoli where it oxidises elements of the cell membrane damaging cells of the respiratory tracts.

Impact on materials:

All materials exposed to the atmosphere are damaged due to natural weathering, e.g. caused by precipitation and temperature changes. In addition, anthropogenic air pollution is oxidising and acid-forming and thus leading to corrosion. Another impact is the soiling of materials due to depositing particulates leading to aesthetical nuisance as well as cleaning costs and damages.

SO_2 and HNO_3 as acid-forming gases are deposited on the materials in two different ways. One way is the dry deposition. The gaseous SO_2 and NO_2 are solubilised in the water on the surfaces. The other way of deposition is the wet acid deposition. Here the SO_2 and NO_2 are already solubilised in the precipitation forming an acid precipitation.

---

[9]   /Friedrich 2003b/

Ozone and NO_2 as oxidising gases may have direct and indirect impacts on materials. Direct effects concerning organic materials are alterations in the structure of the molecules leading to a change in physical characteristics (e.g. embrittlement). The indirect effect is the oxidisation in liquid films on the surface leading to a more stable chemical compounds increasing the time of possible damages.

The damage of metals is mainly caused by SO_2. Corrosion is an electrochemical process and the electrolyte is the liquid on the surface of the metal. There are local elements of anodes and cathodes which lead to oxidisation together with the electrolyte. The damage to calcareous natural stone is caused by an increase of the water solubility of the lime-compounds by SO_2 and acid rain resulting in increased natural weathering.

Impacts on crops:

There are two impact pathways. On the one hand the direct impact pathway with the absorption of air pollutants and on the other hand the indirect pathway through the soil.

In the case of direct impacts, biochemical and physiological processes of phytotoxic pollutants such as SO_2, NO_2 and O_3 may lead to damages as the functions of the cells are interfered (e.g. by reduction of photosynthesis).

The main indirect impacts are acidification and eutrophication. H_2SO_4, HNO_3 and $(NH_4)_2SO_4$ formed by SO_2, NO_x and NH_3 lead to a long term accumulation of acids in the soil. This leads to damages to all soils apart from agriculture where regular liming balances the pH-value. In other soils the acidification causes a change in the chemical ambience repressing the nutrient uptake of plants and changing the consistence of organisms in the soils. Eutrophication is the harmful increase of nitrogen concentration. It is a nutrient for plants and therefore regarded as a fertilizer. However, nitrogen has also negative effects due to repression of other nutrients causing imbalances and lacks. Another negative impact is the repression of organisms which need an environment with low nitrogen concentration.

All the described impacts are extremely influenced, e.g. by location, time, type and age of humans, corn and material and interaction with other pollutants.

3.3   Monetary evaluation methods[10]

The last step of the impact pathway is the monetarisation of the impacts on welfare. For this evaluation different methods can be characterised:
- Market prices
- Indirect evaluation methods

---

[10]   /Friedrich 2003a/ and /Endres; Holm-Müller 1998/

- Direct evaluation methods

Market prices can only be used for goods which are traded on markets. For all non-market goods the indirect and direct evaluation methods should be used. Following the economic welfare-theory the concepts *willingness to pay* (WTP) for a reduction of the risk of the damage (from the perspective of the entitlement for a worse environment) and *willingness to accept* (WTA) the risk of the damage for an appropriate compensation (from the perspective of the entitlement for a better environment) are used in the latter two methods to reveal the preferences of individuals towards public goods compared to private goods.

Market prices:

An example for the evaluation with market prices is the loss of agricultural crops which can be rated with the market price of the considered type of corn.

Indirect evaluation methods:

Hedonic pricing and the travel cost approach can be differentiated as indirect evaluation methods:

One example for hedonic pricing is the extra pay for difficult working conditions, e.g. due to heat, cold, dirt or possible accidents. Another example is the lower price of houses or rents due to more air or noise pollution compared to the average conditions.

With the travel cost approach the time and money expended for enjoying a public good, e.g. a recreation area, is used to estimate the inherent benefit value of this public good.

Direct evaluation methods:

In the case of direct evaluation methods, households are directly asked for their WTP or WTA. Survey based techniques of contingent valuation are used for this evaluation method. In contrast to the prior methods, there has to be no market. Hence, even intangible benefits of public goods which can not be traded on markets can be evaluated. The disadvantages of this method are several types of bias, e.g. interviewer bias, and the difficulty of including all affected people..

An extensive description of these evaluation methods provides /Endres; Holm-Müller 1998/.

4 Global warming

/Luterbacher et al. 2004/ describes the European temperature variability, trends and extremes since 1500. In **Figure 4-1**, /Luterbacher et al. 2004/ illustrate the European annual mean temperature from 1500 to 2003. With ΔT^{11} = -0.32 °C the 19th century was the coldest century in the last 500 years. In contrast the 20th century was the warmest with a strong warming trend of +0.08 +/- 0.03 °C per decade. The last 30 years have been the warmest since 1500 with ΔT = +0.43 °C. And even more dramatically, the nine warmest European years have occurred since 1989. 1989 was the warmest year with ΔT = +1.3 °C and the decade 1994-2003 was the warmest decade with ΔT = +0.84 °C.
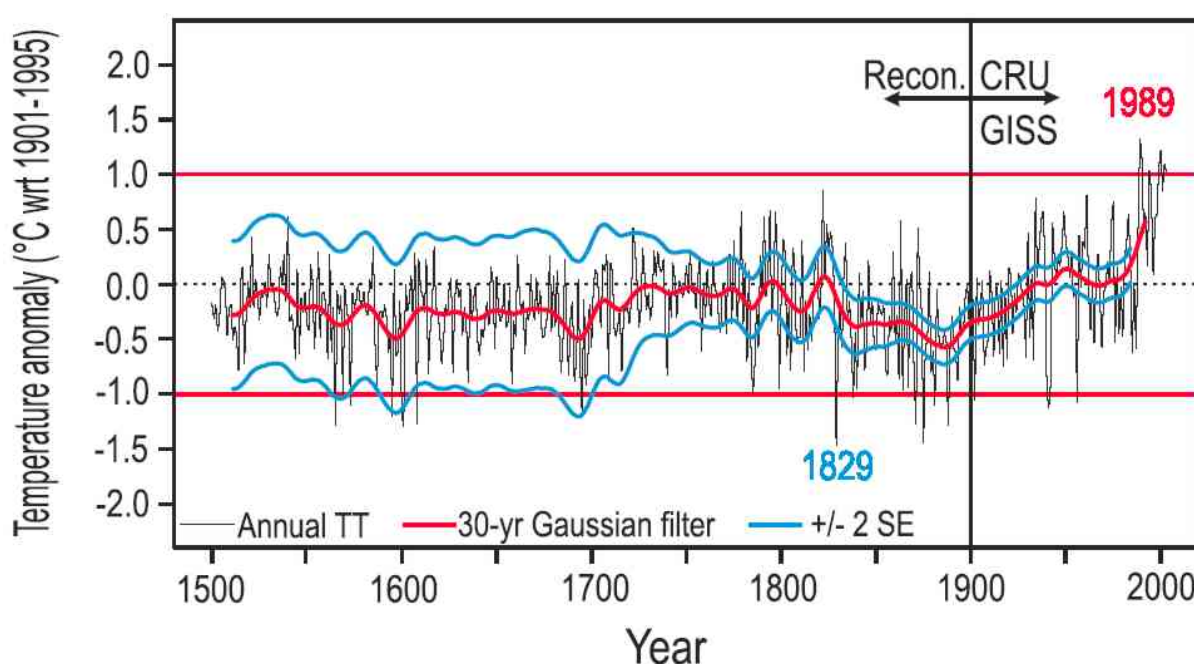
Figure 4-1: European annual mean temperature 1500-2003 /Luterbacher et al. 2004/

SE = Standard Error
wrt = as compared to
TT = temperature
yr = year
Recon. = reconstructed
GISS = Goddard Institute for Space Studies
CRU = Climatic Research Unit

Similar results were found by the *Intergovernmental Panel und Climate Change* (IPCC). The essential results are described in the following chapters.

---

[11] ΔT is the temperature change from the 1901-1995 average.

4.1   Global warming in the past

The atmospheric concentrations of the three main greenhouse gases *carbon dioxide* (CO_2), *methane* (CH_4) and *nitrous oxide* (N_2O) over the last millennium are displayed in **Figure 4-2**. It shows that the atmospheric concentration of the greenhouse gases had been relatively constant in the time period 1000-1750 and has been rising exponentially since 1750.
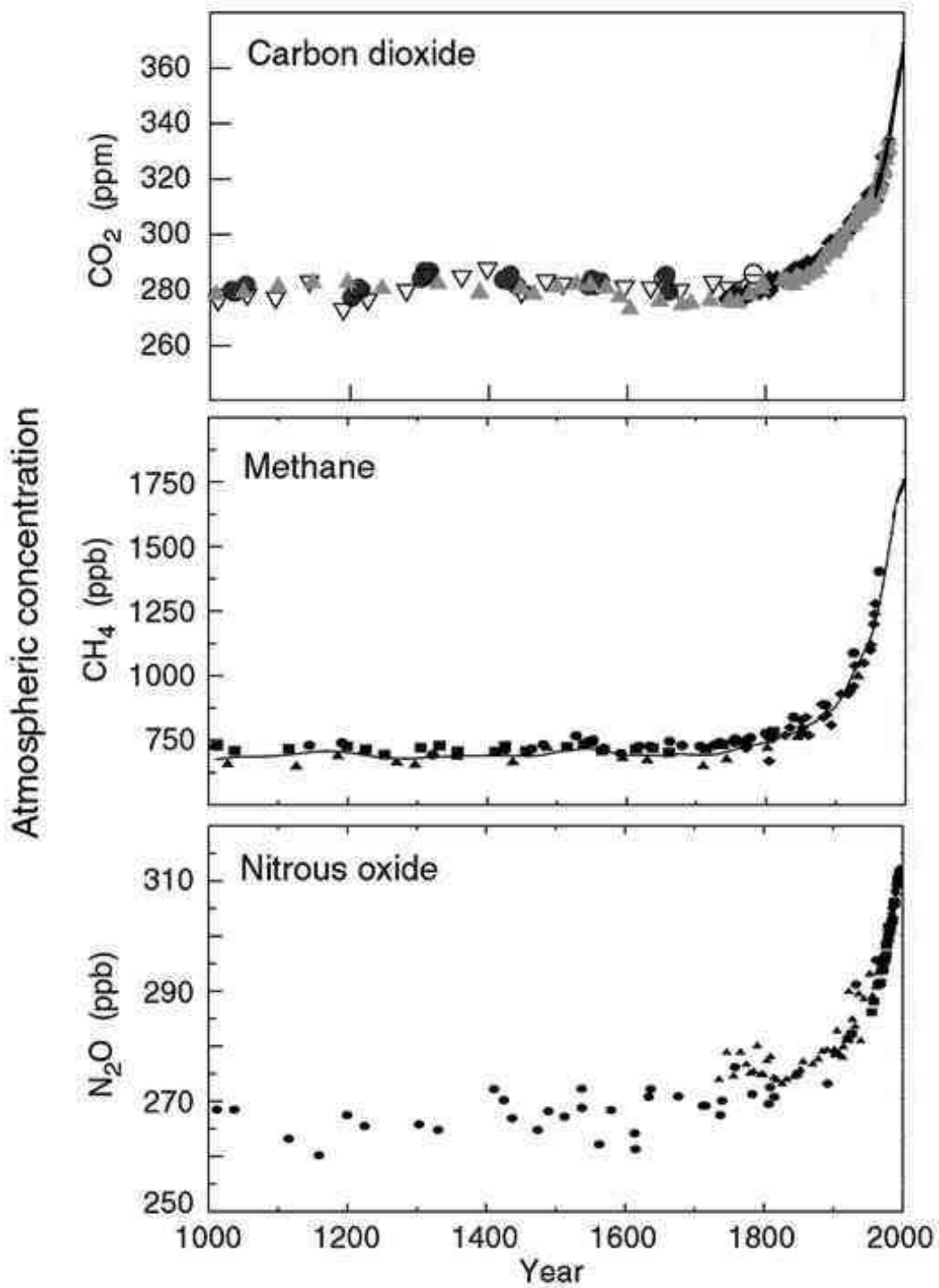
Figure 4-2:   Changes in atmospheric composition /IPCC 2001d/

The present atmospheric CO_2 concentration of approximately 370 ppm has not been exceeded during the past 420,000 years with a maximum of approximately 300 ppm as shown in **Figure 4-3**. This has been measured by means of air trapped in ice cores from Antarctica. **Figure 4-3** also shows that there is a correlation between the atmospheric concentration of greenhouse gases and the temperature as well as the glacial periods. Correlating to the high greenhouse gas concentration at present, the temperature is one of the highest in the last 420,000 years.
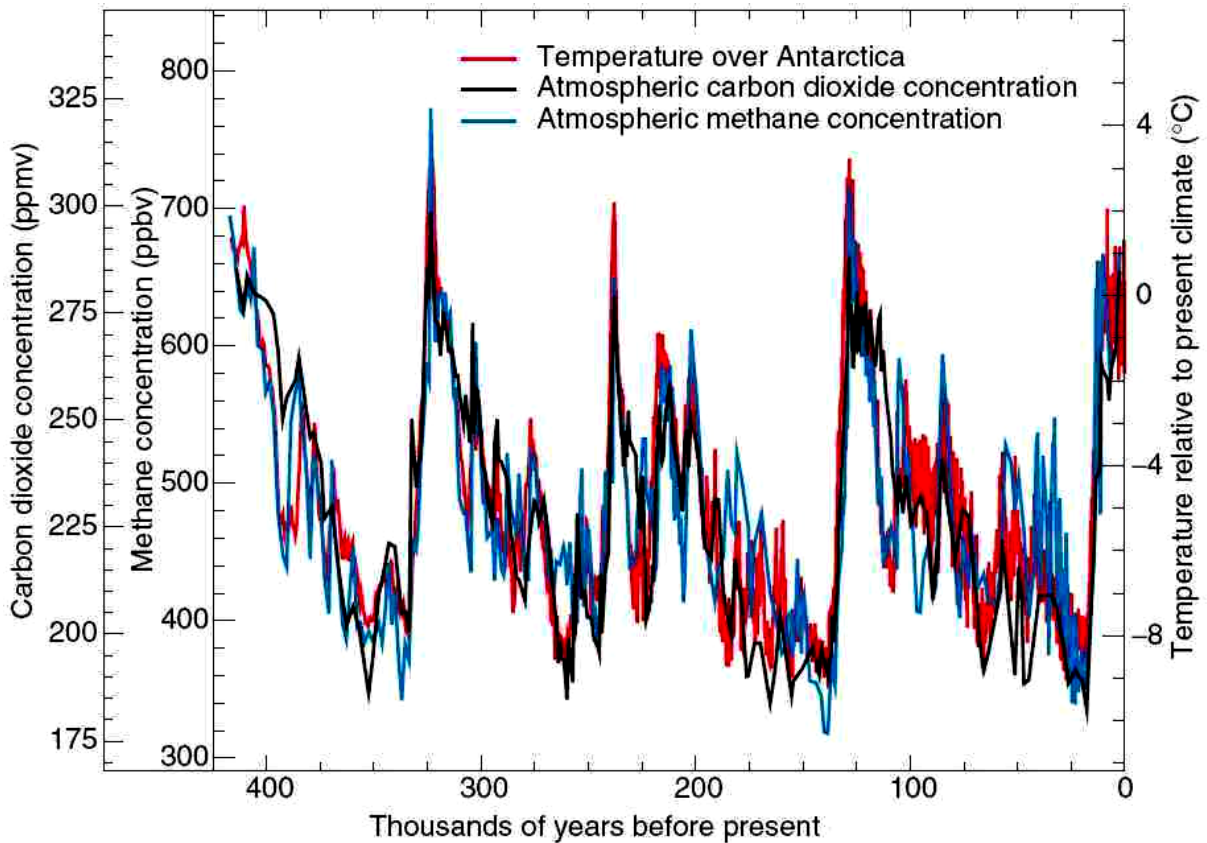
Figure 4-3: CO_2 concentration, CH_4 concentration and temperature relative to the pre-industrial level over the last 420,000 years /IPCC 2001a/

Figure 4-4 shows the Northern hemisphere temperature of the last 1,000 years. From 1000 to 1900 there is a declining linear temperature trend which ends in the years around 1900 and changes into a steep rise in the last century so that the temperature between the 19th century and 1998 has been risen by approximately 1 °C. This increase over the last 140 years is illustrated in **Figure 4-5**.
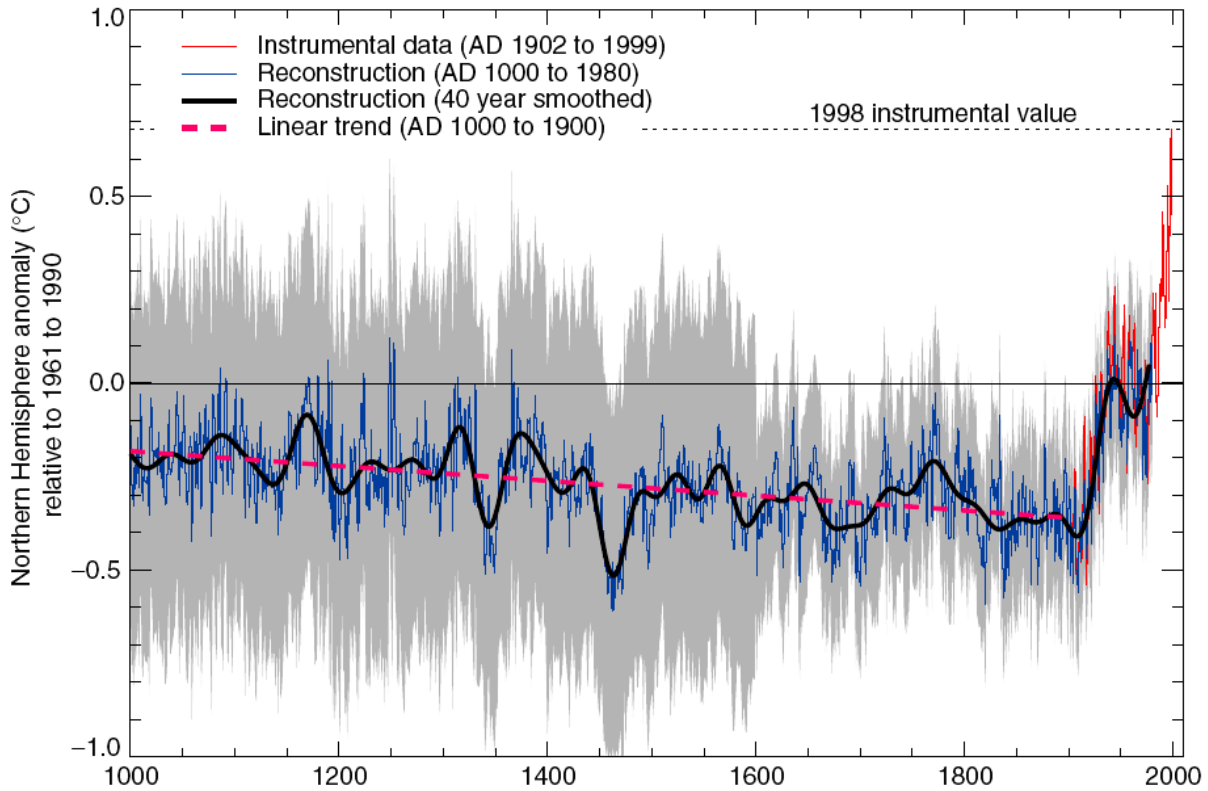
Figure 4-4:   Northern hemisphere temperature anomaly relative to 1961-1990 over the last millen-
nium /IPCC 2001a/
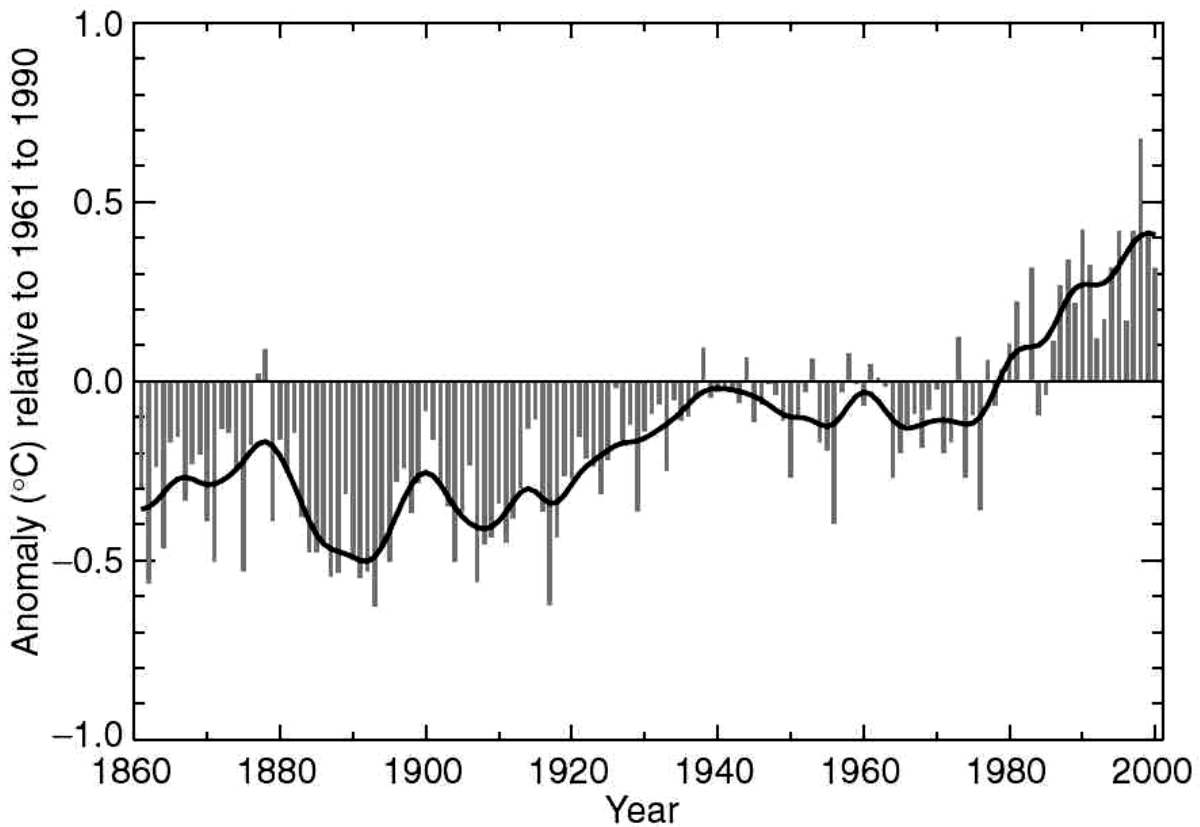
Figure 4-5:   Global temperature anomaly relative to 1961-1990 over the last 140 years /IPCC
2001a/

Besides atmospheric concentration levels and temperature changes, several other changes in the earth's atmosphere, climate and biochemical system occurred in the 20th century. Some of the very likely changes are listed in **Table 4-1**.

Table 4-1: Overview of some 20th century changes in the earth's atmosphere, climate and bio-physical system with a high confidence (adapted from /IPCC 2001d/)

Indicator	Observed Changes
Concentration indicators	
Atmospheric concentration of CO_2	280 ppm (1000-1750) to 368 ppm in year 2000 (31±4 % increase).
Atmospheric concentration of CH_4	700 ppb (1000-1750) to 1,750 ppb in year 2000 (151±25 % increase).
Atmospheric concentration of N_2O	270 ppb (1000-1750) to 316 ppb in year 2000 (17±5 % increase).
Tropospheric concentration of O_3	Increased by 35±15 % from the years 1750 to 2000 and varies with region.
Stratospheric concentration of O_3	Decreased over the years 1970 to 2000, varies with altitude and latitude.
Atmospheric concentrations of HFCs, PFCs and SF_6	Increased globally over the last 50 years.
Weather indicators	
Global mean surface temperature	Increased by 0.6±0.2°C over the 20th century.
Cold / frost days	Decreased for nearly all land areas during the 20th century.
Continental precipitation	Increased by 5-10 % over the 20th century in the Northern Hemisphere, although decreased in some regions (e.g., north and west Africa).
Numbers of global extreme weather events	Increased by ca. 50 % over the last 50 years.
Biological and physical indicators	
Global mean sea level	Increased at an average annual rate of 1-2 mm during the 20th century.
Non-polar glaciers	Widespread retreat during the 20th century.
Snow cover	Decreased in area by 10 % since global observations became available from satellites in the 1960s.
Permafrost	Thawed, warmed and degraded in parts.
El Niño events	Became more frequent, persistent and intense during the last 20 to 30 years compared to the previous 100 years.
Growing season	Lengthened by about 1 to 4 days per decade during the last 40 years in the Northern Hemisphere.
Plant and animal ranges	Shifted pole wards and up in elevation for plants, insects, birds and fish.
Coral reef bleaching	Increased frequency, especially during El Niño events.
Economic indicators	
Weather-related economic losses	Global inflation-adjusted losses rose an order of magnitude over the last 40 years. Part of the observed upward trend is linked to socio-economic factors and part is linked to climatic factors.

4.2   The global energy balance

The global energy balance is displayed in **Figure 4-6**. Averaged over the year, each square metre of the earth's spherical surface outside the atmosphere receives 342 W solar radiation. 31 % of the solar radiation is reflected back into space, 20 % is absorbed by atmosphere and the remaining 49 % is absorbed by the earth's surface and is thus warming the earth. The heat is returned to the atmosphere in form of sensible heat (thermals), water vapour (evapotranspiration) condensing in higher atmosphere and infrared radiation. The solar radiation has its *maximum wave length* λ_{max} approximately at 0.5 µm (due to the sun's body temperature of ca. 5800 K) whereas the earth's radiation has its maximum wave length at ca. 10 µm in the infrared spectrum (due to the earth's temperature of ca. 300 K). This can be derived from Wien's displacement law resulting in a relation of the temperature T in Kelvin:

$$\lambda_{max} = \frac{2.8978 \cdot 10^3 \, \mu m \cdot K}{T} \tag{4-1}$$

This difference between the sun's and the earth's radiation is essential because the atmosphere contains trace gases, so called greenhouse gases, which absorb and emit infrared radiation with the exception of a transparent part of the spectrum (atmospheric window). Thus, a part of the emissions of the atmosphere is radiated back to the earth's surface. In contrast, the sun's radiation is not absorbed that much. Thus, heat is trapped between the earth's surface and the atmosphere. This is the natural greenhouse effect. In the case of a stable climate the incoming radiation of 235 W/m² has to be emitted as well. This corresponds to a temperature of -19 °C. However, the earth's surface has an average temperature of 14 °C due to the natural greenhouse effect. The contribution to this greenhouse effect of the different greenhouse gases is approximately 20.6 °C for water vapour, 7.2 °C for 350 ppm CO_2, 2.4 °C for 30 ppb tropospheric O_3, 1.4 °C for 300 ppb N_2O, 0.8 °C for 1.7 ppm CH_4 and 0.6 °C for other greenhouse gases /Voß 2003/.

An imbalance between the solar radiation and the infrared radiation is called radiative forcing. The surface is warmed in the case of positive radiative forcing and cooled in the case of negative radiative forcing. This imbalance occurs naturally because the components of the climate system have non-linear interactions and different times of response. The radiative forcing is fluctuating with high amplitudes as can be seen in **Figure 4-3**. **Figure 4-3** illustrates the alternation of glacial and interglacial periods. Besides this natural fluctuation of the radiative forcing there is a anthropogenic perturbation of the atmospheric composition. This anthropogenic perturbation originates mainly from combustion processes of organic fossil resources which cause a positive radiative forcing because of the increase of greenhouse gases in the atmosphere (see **Table 4-2**).
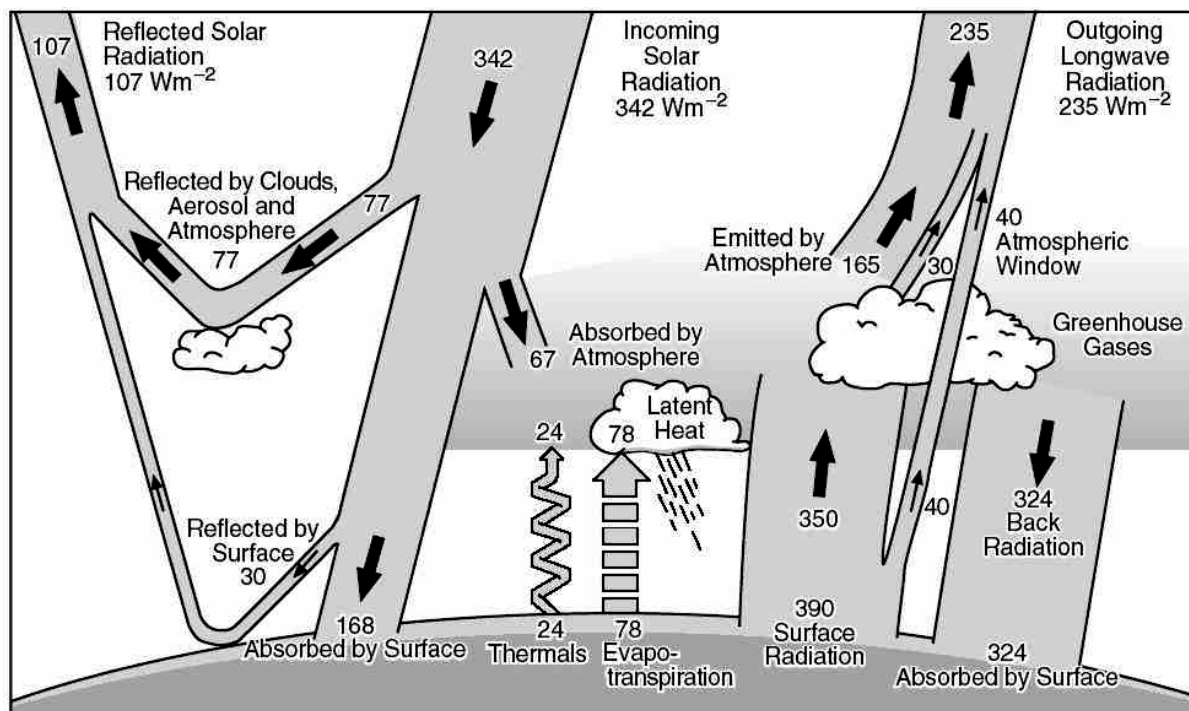
Figure 4-6:   The global energy balance /IPCC 2001a/

Table 4-2:   Pre-industrial (1750) and present (1998) atmospheric concentration of the main greenhouse gases and the radiative forcing due to the change in abundance (adapted from /IPCC 2001a/)

Gas	Atmospheric concentration in 1750	Atmospheric concentration in 1998	Radiative forcing (W/m²)
CO_2	278 ppm	365 ppm	1.46
CH_4	700 ppb	1745 ppb	0.48
N_2O	270 ppb	314 ppb	0.15
CFC-11	0 ppt	268 ppt	0.07
CFC-12	0 ppt	533 ppt	0.17
CFC-113	0 ppt	84 ppt	0.03
CCl_4	0 ppt	102 ppt	0.01
HCFC-22	0 ppt	132 ppt	0.03

In the next chapter possible scenarios for the global warming in the next century are described.

4.3   Global warming in the future

The IPCC developed six scenario groups which span a wide range of possible futures. They are described in **Table 4-3**. Besides these scenarios a further scenario is used for comparison, the IS92 scenario which was developed in previous IPCC reports. **Figure 4-7** displays the simulation of the future global warming in different scenarios. The assumed cause-and-effect chain is described in the following.

With CO_2 emissions the concentration in the atmosphere increases. The projected concentrations of CO_2 in the year 2100 range from 540 to 970 ppm, compared to about 280 ppm in the pre-industrial era and about 368 ppm in the year 2000. This increase of concentrations causes a positive radiative forcing. Thus; the global averaged surface temperature is forced to increase by 1.4-5.8 °C over the period from 1990 to 2100. It is very likely that the projected rate of warming has not taken place at least in the last 10,000 years. This statement is based on paleoclimate data. The development of the temperature after the year 1000 is illustrated in **Figure 4-8**. In this figure, temperature data for the time period of the years 1000-1860 are based on proxy data, for the years 1860-2000 they are based on instrumental observations and for the future until 2100 it is based on the scenario projections. Because of the higher temperatures the global mean sea level is projected to rise by 0.09-0.88 m between the years 1990 to 2100, primarily, due to thermal expansion and loss of mass from glaciers and ice caps. Due to the long time scales in which the deep ocean with its large heat capacity adjusts to climate changes the rise will continue for hundreds of years. Ice sheets will continue to react to climate change for thousands of years (cf **Figure 4-11**).

The scenario analysis in /IPCC 2001a/ shows several further results. It is projected that the global averaged annual precipitation will increase during the 21st century and that very likely[12] nearly all land areas will warm more rapidly than the global average. Larger year-to-year variations in precipitation are very likely over most areas where an increase in mean precipitation is projected. Glaciers and ice caps are projected to continue their widespread retreat during the 21st century.

---

[12]   The definition of *very likely* in the context of the IPCC reports means that the chance for the correctness of the predication is 90-99%.

Table 4-3:   Special Report on Emission Scenarios (SRES) in /IPCC 2001d/

Scenario	Description
A1	Storyline: Future world of very rapid economic growth, global population which peaks in mid-century and declines thereafter and rapid introduction of new and more efficient technologies. Major underlying themes: Convergence among regions, capacity-building and increased cultural and social interactions, with a substantial reduction in regional differences in per capita income Alternative directions of technological change in energy system are distinguished by three different scenario groups (A1FI, A1T, A1B)
A1FI	Fossil intensive
A1T	Non-fossil energy sources
A1B	Balance across all source
A2	Storyline: Very heterogeneous world, fertility patterns across regions converge very slowly which results in continuously increasing population, per capita economic growth and technological change more fragmented and slower than in the other scenarios Major underlying themes: Self-reliance and preservation of local identities
B1	Storyline: Convergent world, global population which peaks in mid-century and declines thereafter, very rapid change in economic structures towards a service and information economy with reductions in material intensity and the introduction of clean and resource-efficient technologies Major underlying themes: Global solutions to economic, social and environmental sustainability, including improved equity, but without additional climate initiatives.
B2	Storyline: World in which the emphasis is on local solutions to economic, social and environmental sustainability, increasing global population at a lower rate than A2, intermediate levels of economic development and less rapid and more diverse technological change than in the B1 and A1 scenarios Major underlying themes: Environmental protection, social equity, local and regional levels

CO$_2$ emissions (Gt C)

CO$_2$ concentration (ppm)

Radiative forcing (Wm^{-2})

Temperature change (°C)

Sea-level rise (m)

Model ensemble
all SRES envelope

All SRES envelope
including land-ice
uncertainty

All IS92

- A1B
- A1T
- A1FI
- A2
- B1
- B2
- IS92a
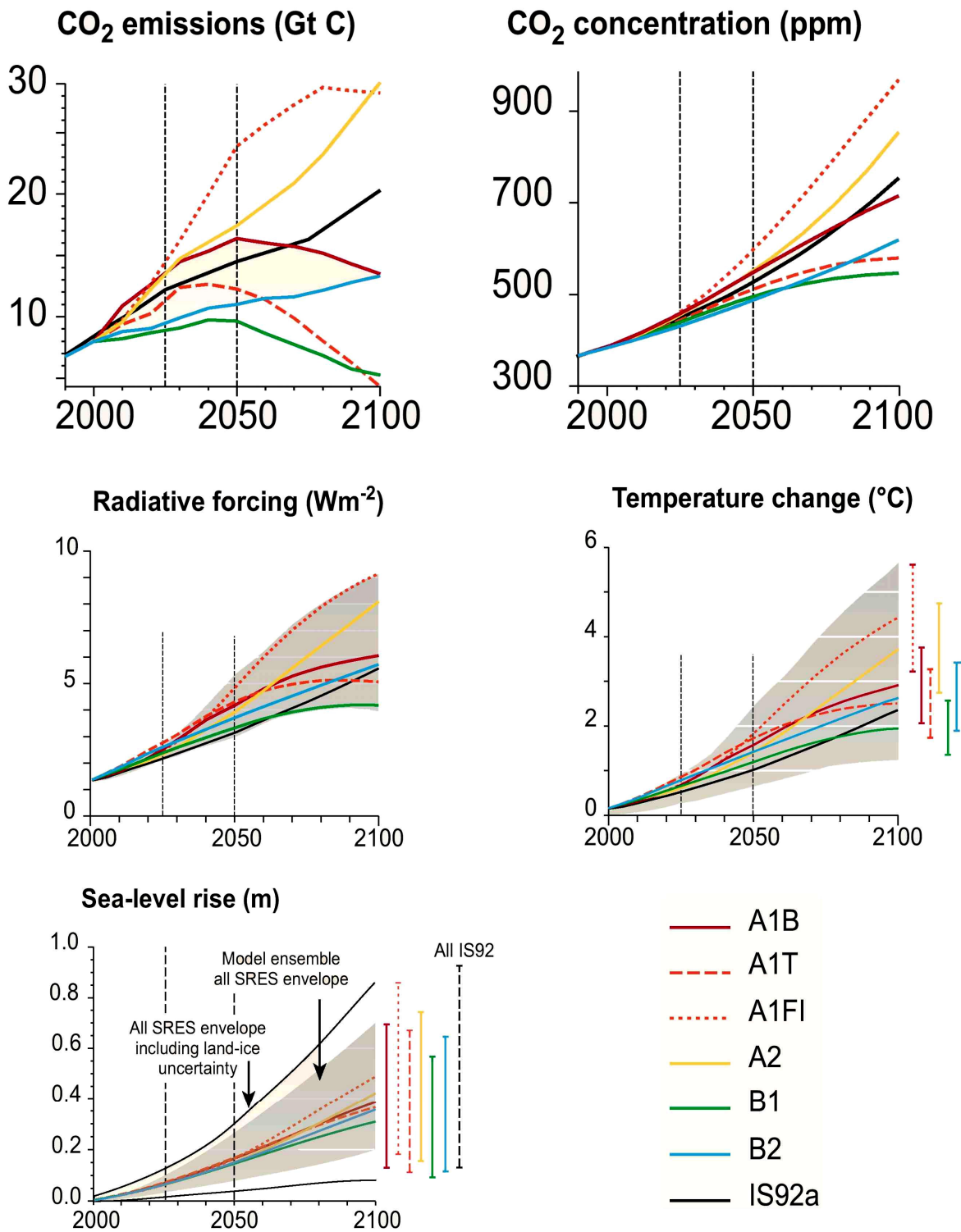
Figure 4-7:   IPCC scenarios[13] /IPCC 2001d/

The bars on the right hand side show the range within the respective scenario and the
shaded area the range of all scenarios together.

---

[13]   SRES = Special Report on Emission Scenarios
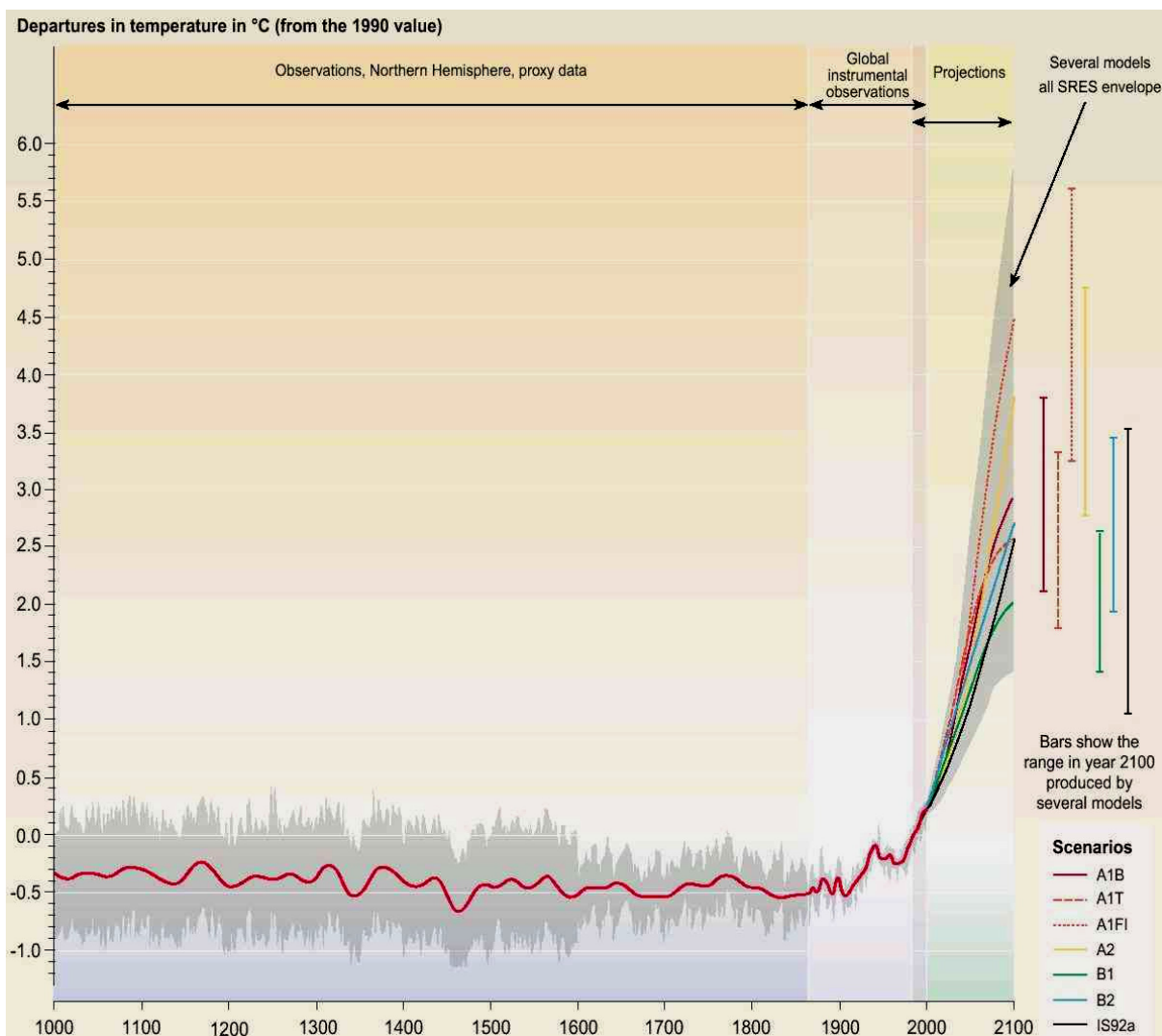
Figure 4-8:   Earth's surface temperature in the years 1000 to 2100 /IPCC 2100d/

The bars on the right hand side show the range within the respective scenario and the shaded area the range of all scenarios together.

The following effects which are estimated for the 21st century in /IPCC 2001b/ do all have a high confidence[14]. Concerning human health, there will be an increase in heat-related deaths and illnesses, a decrease in winter deaths in some temperate regions, an expansion of areas with potential transmission of malaria and dengue, and poor get more and more vulnerable due to increased risk of hunger. Effects on the ecosystem are an extensive coral bleaching and death, an increase in frequency of ecosystem disturbance by fire and insect pests and a substantial loss of ice volume from glaciers. Agricultural effects are reduced frost damage to some crops, increased heat stress damage to some crops and an increased heat stress in livestock. Water resources are substantially affected by decreasing water supply in many wa-

---

[14] The definition of *high confidence* in the context of the IPCC reports means that the chance for the correctness of the predication is 67-95 %.

ter-stressed countries, degrading water quality by higher temperatures and changes in water flow volume. Additionally, there will be an increase of demand due to higher temperatures. The drought frequency will be increased and flood damages will be several-fold higher than in the case of *no climate change scenarios*. There are also other market sector effects in form of decreased energy demand for heating buildings, increased energy demand for cooling buildings and increased insurance prices as well as reduced insurance availability.

The models of the IPCC project that increasing atmospheric concentrations of greenhouse gases will result in changes in daily, seasonal, inter-annual and decadal variability. This will also cause changes in extreme climate phenomena in the 21st century which are very likely. There will be higher maximum temperatures, more hot days and heat waves over nearly all land areas. This change is very likely causing an increased incidence of death and serious illness in older age groups and urban poor, increased electric cooling demand, shift in tourist destinations, increased risk of damage to a number of crops, as well as increased heat stress in livestock and wildlife.

With the shift to higher temperature, there will also be a shift to higher minimum temperatures, fewer cold days, frost days and cold waves over nearly all land areas. In a warmer world the hydrological cycle will become more intense causing more intense precipitation events over many areas. These precipitation events may cause more flood, landslide, avalanche and mudslide damage as well as increased soil erosion.

Key uncertainties about population growth, technological progress, economic growth and governance structures are inherent in the assumptions the quantification of future concentrations is based on. Smaller uncertainties arise from the lack of understanding the carbon cycle and the included effects of climate feedbacks.

Further uncertainties exist about future risks and thus reasons for concern which arise due to global warming. These are illustrated in **Figure 4-9** which depicts the risks of the temperature change. The first risk concerns unique and threatened systems. This risk can occur in form of extinction of species, loss of unique habitats and coastal wetlands, and bleaching and death of coral. The second risk is about extreme climate events. These climate extremes may occur with increased frequency and intensity and thus cause more health, property and environmental impacts at more dangerous levels. The third risk illustrated in **Figure 4-9** is the risk of the distribution of impacts. Cereal crop yield changes vary across regions but they are estimated to decrease in most tropical and subtropical regions. Water availability will decrease in some water-stressed countries but increase in others. There will be larger risks to health in developing countries than in developed countries. Net market sector losses are estimated for many developing countries, mixed effects for developed countries up to a few degrees warming and negative effects for more warming. The fourth risk is about global aggregate impacts. Estimations of the impacts of the globally aggregated net market sector are positive and negative up to a few degrees warming and negative for more warming. However, more people will be adversely affected than beneficially even for little warming. The fifth

and last risk is the risk of large-scale, high-impact events. Examples are a significant slowing of thermohaline circulation (possible by 2100) as well as the melting and collapse of ice sheets, e.g. the West Antarctic ice sheets, which will accelerate the rise of the sea-level.
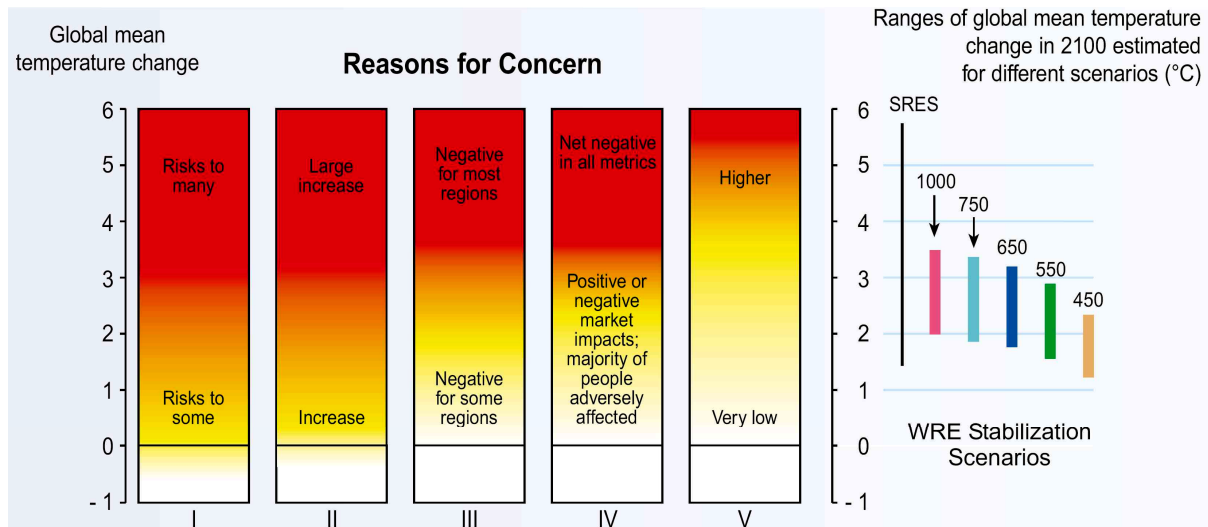
Figure 4-9:   Reasons for concern due to global warming and scenarios for stabilizing CO_2 concentrations at certain levels /IPCC 2001d/

        I.   Unique and threatened systems
        II.   Extreme climate events
        III.   Distribution of impacts
        IV.   Global aggregate impacts
        V.   Large-scale, high-impact events

4.4   Estimation of the damage costs of global warming

The uncertainties described above imply that it is very difficult to estimate the exact damage costs of global warming. Nevertheless, an estimation has to be done and several studies try to do it.

In /European Commission 1999b/ the damage costs are estimated with two different models, on the one hand, with *Climate Framework for Uncertainty, Negotiation and Distribution* (FUND), version 1.6, from the Institute for Environmental Studies at the Vrije Universiteit Amsterdam and, on the other hand, with *Open Framework for Climate Change Impact Assessment* (OF) model, version 2.2, from *Environmental Change Unit* (ECU) at the University of Oxford.

Both models do not consider socially contingent effects of climate change (e.g. migration, hunger, conflict, etc.) because of the high uncertainties inherent in the evaluation of these effects. It is stated that the marginal damages of socially contingent effects may be as high as 10,000 US\$$_{90}$/tC (3,658 €$_{2003}$/t$CO_2$) /European Commission 1999b/. The exclusion probably leads to an underestimation of the total damage costs.

In both models it is assumed that the damages are discounted to 1990, the time horizon is 2100, the scenario is the IS92a from the Second Assessment Report of the IPCC, the model is equity weighted and no socially contingent effects are considered.

With the FUND model, marginal damages of CO_2 emissions are analysed by a Monte Carlo analysis which is shown in **Table 4-4**. Because the uncertainties are asymmetric and relationships are non-linear the mean estimate is higher than the base case. The uncertainty is right-skewed so that median and mode values are smaller than the mean. A high sensitivity of the results exists to the chosen discount rate as can be seen in **Table 4-4**.

Table 4-4: Marginal damages in US\$$_{90}$/tC ($€_{2003}$/t$CO_2$) of CO_2 emissions in the years 1995-2004 for different discount rates simulated with FUND by a Monte Carlo analysis /European Commission 1999b/

Discount rate	0 %	1 %	3 %
Best guess	317 (116)	171 (63)	60 (22)
Mean	465 (170)	244 (89)	82 (30)
Median	405 (148)	210 (77)	70 (26)
Mode	340 (125)	190 (70)	54 (20)
Standard deviation	267 (98)	143 (52)	51 (19)
1-percentile	106 (39)	54 (20)	17 (6)
5-percentile	158 (58)	81 (30)	26 (10)
95-percentile	962 (352)	512 (187)	178 (65)
99-percentile	1,390 (508)	744 (272)	259 (95)

Table 4-5: Marginal damages in US\$$_{90}$/tC ($€_{2003}$/t$CO_2$) of CO_2 emissions in the years 1995-2004 for different discount rates and different scenarios simulated with the Open Framework model /European Commission 1999b/

Discount rate	0 %	1 %	3 %
IS92a-Low	15 (5)	7 (3)	3 (1)
IS92a-Medium	325 (119)	164 (60)	64 (23)
IS92a-High	12,702 (4,651)	6,509 (2,384)	2,677 (980)
IS92d-Low	12 (4)	6 (2)	3 (1)
IS92d-Medium	194 (71)	98 (36)	39 (14)
IS92d-High	7,033 (2,575)	3,405 (1,247)	1,253 (459)
Best guess	**325 (119)**	**164 (60)**	**64 (23)**

Within the Open Framework simulation the uncertainty is illustrated by the use of the two IPCC scenarios IS92a and IS92d from the Second Assessment Report. They are investigated with a range from low to high which is assumed to represent a confidence interval between 80 % and 99 %. The results for the different scenarios and discount rates are presented in **Table 4-5**.

These uncertainty analyses of the two models show large ranges of plausible estimates. The 1-99 percentile range of FUND is 6-95 $€_{2003}/tCO_2$ for a 3 % discount rate and 39-508 $€_{2003}/tCO_2$ for a 0 % discount rate. In the Open Framework model, the uncertainty is even higher. The values have a range of 1-980 $€_{2003}/tCO_2$ for a 3 % discount rate and a range of 4-4,651 $€_{2003}/tCO_2$ for a 0 % discount rate. Altogether the uncertainty is very high and the damage costs may range from a few € to more than thousand € per ton carbon dioxide.

Table 4-6:   The probability characteristics of the marginal costs of carbon dioxide emissions of 88 analysed estimates in US$_{90}/tC ($€_{2003}/tCO_2$) /Tol 2003/

Pure rate of time preference (social discount rate)	3 % (5 %)	1 % (3 %)	0 % (2 %)
Mean	11 (4)	49 (18)	433 (159
Median	7 (3)	23 (8)	134 (49)
Mode	3 (1)	5 (2)	14 (5)
5-percentile	-6 (-2)	-21 (-8)	-103 (-38)
95-percentile	37 (14)	194 (71)	2,244 (822)

/Tol 2003/[15] analyses 88 estimates of the marginal costs of carbon dioxide emissions from 22 published studies. In the study, a sensitivity analysis of different discount rates is performed and displayed in **Table 4-6**. The 5-95 percentile range of the analysed cost estimations is (-38)-822 $€_{2003}/tCO_2$ for a 2 % discount rate and (-2)-14 $€_{2003}/tCO_2$ for a 5 % discount rate. However, /Tol 2003/ concludes that estimations of damage costs are unlikely to exceed 50 US$_{90}/tC (18 $€_{2003}/tCO_2$) for standard assumptions.

In /Tol; Heinzow 2003/, the results of the FUND model, version 2.4, are described. The results are lower than those of version 1.6. For a pure rate of time preference of 1 % the marginal costs of carbon dioxide emissions are ca. 8 US$_{2000}/tC (2 $€_{2003}/tCO_2$) and for a pure rate of time preference of 0 % the marginal costs are ca. 18 US$_{2000}/tC (5 $€_{2003}/tCO_2$).

It is very difficult to determine the external costs by damage costs because of the illustrated ranges and uncertainties. There are several uncertainties regarding future developments because the climate system is very complex. Therefore, it is difficult to simulate its behaviour with present models due to many non-linearities and feedback loops. Additional problems

---

[15]   It is assumed that the prices in /Tol 2003/ are 1990 values because studies of the 1990s are analysed.

arise by long time lags leading to impacts in the distant future which are caused today. A positive discount rate diminishes damage costs in the future and a model time horizon cuts all damage costs behind the horizon so that long term future damages are often inadequately taken into account in present models. Furthermore, many possible effects due to global warming can hardly be quantified, e.g. the loss of biodiversity and certain species, irreversibilities as the collapse of the thermohaline cycle in the North Atlantic, or social effects due to battles for water and soil.

Nevertheless, it is necessary to come to decisions facing the described uncertainties. Therefore, a risk policy is needed. A proposition is given in /WBGU 1998/ (see **Figure 4-10**). The authors distinguish six different classes of risks (Damocles risk, Cyclops risk, Pythia risks, Pandora risks, Cassandra risks and Medusa risks) which are located in three different areas (normal area, transition area, prohibited area). These areas are defined with two dimensions namely the *probability of occurrence* and the *extent of damage*.

If both dimensions are low the risks are in the normal area which demands only standard risk policy that is not considered in the study. Mostly, expected values are used if risks are found in this area.

Risks can not be allocated to this normal area if one of the following conditions is fulfilled:

- High uncertainties in the distribution of damage probabilities
- High potential extent of damage
- High probability of occurrence
- High margins of deviations of damage extent and probability of occurrence
- High persistence, ubiquity and irreversibility
- High potential of conflicts and mobilisation

They are then allocated in the transition area.

Risks are allocated to the prohibited area if a low utility is expected in addition to the high risks or both risk dimensions do have extreme extents. The policy for risks located in the prohibited area demands an imperative risk reduction because the expected consequences are such serious. A possible risk policy may be an immediate prohibition. Risk policy in the transition area is not as obvious as in the other two areas.

A special case is proposed for risks which are located in the prohibited area but policy makers are not aware of them or even repress them because of the delay between the triggering event and the damage occurrence. This class of risk is called Cassandra risk which can be characterised with a high probability of occurrence and a high extent of damage. The estimation of probability of occurrence is uncertain while the estimation of the high extent of damage is sure. An example of the Cassandra risk is global warming because the damage of today's emissions lies in the coming centuries, which are mostly out of perspective of present policy makers.

The second class of risk, which is relevant in the context of global warming, is the Pythia risk. It is characterized by uncertainty in probability of occurrence as well as extent of damage. However, the extent of damage is potentially high. This risk type can be attributed to non-linear effects in climate change, e.g. the instability of the West Antarctic ice sheets.

Finally, the third class of risk, which is relevant in the context of global warming, is the Cyclops risk. It is characterised by uncertainties in the probability of occurrence and a high damage extent which can be estimated with low uncertainties. An example is the collapse of the thermohaline cycle which would cause extreme damages but the probability of occurrence is not known.
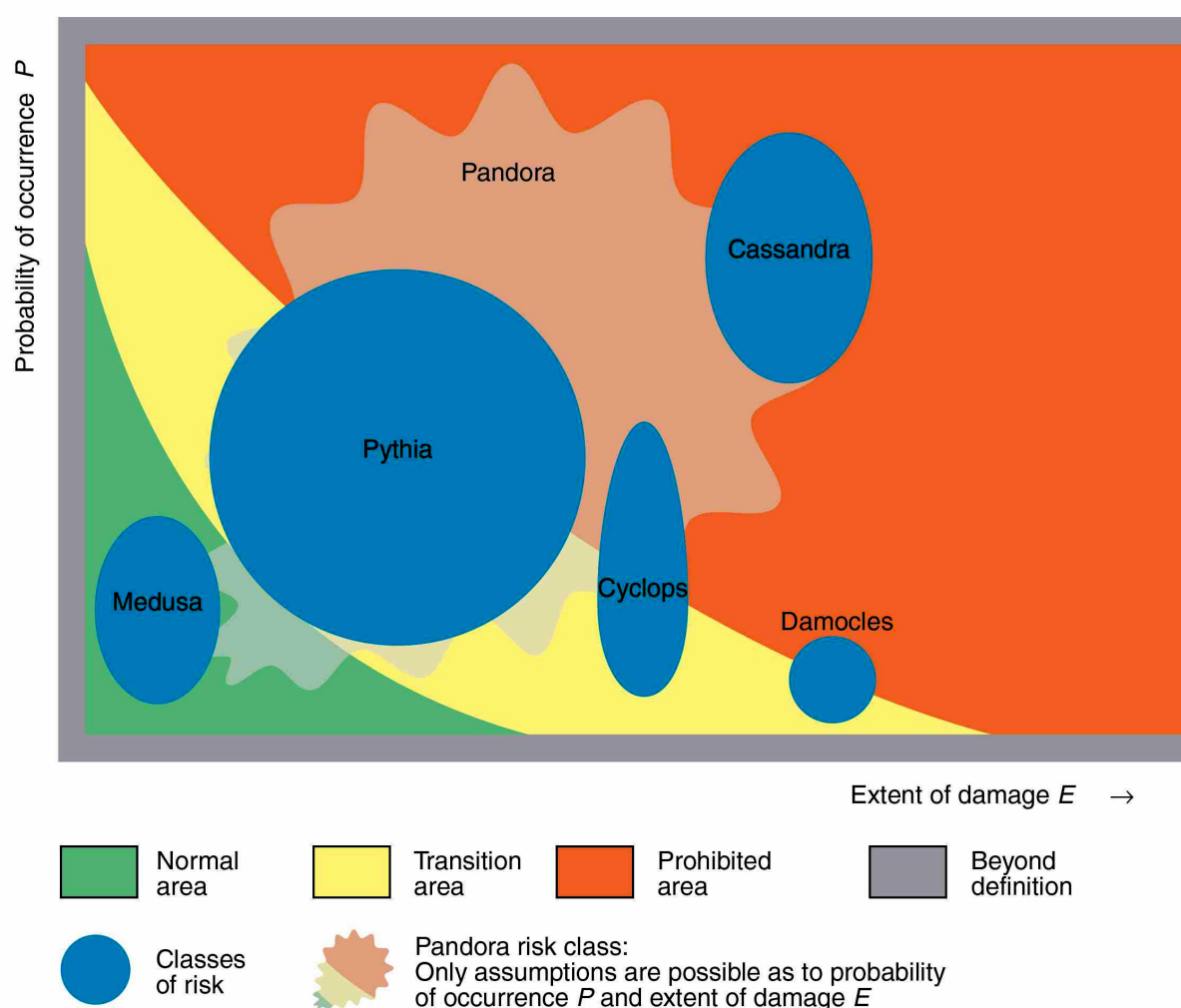
Figure 4-10:   Classes of risk and their location in the normal, transition and prohibited areas defined in /WBGU 1998/[16]

A risk policy for the global warming risks is described in /WBGU 1998/. It is the concept of a tolerance window. This approach is characterised by the normative specification of intolerable risks which define the frame of the tolerance window. The intention of this approach is

---

[16] This figure is derived from *http://www.wbgu.de/wbgu_jg1998_folien_engl.pdf*

the prevention of instabilities which may cause extreme damages. In /WBGU 1998/ it is stated that critical values which exclude potentially high risks should be specified. Examples for these limits are a maximum global mean temperature and a maximum gradient of global warming. However, also the burden on society due to these restrictions has to be taken into account by specifying limits for the burden of society, e.g. maximum emission reduction rates. More critical values defining the frame of the tolerance window should be specified normatively. In a democratic system, these restrictions should be determined in a discourse which is permanently updated with new insights.

An alternative for the estimation of external costs is the use of avoidance costs instead of damage costs which are characterised by high uncertainty. One requirement for the estimation of avoidance costs is a goal of avoidance which should be reached. This goal has to be developed in a scientific and political discourse in order to generate a normative goal on a scientific basis.

One fundamental goal which is ratified by more than 180 countries is the *United Nations Framework Convention on Climate Change* /United Nations 1992/. In Article 2 of the Convention, this goal is postulated in the following way:

"The ultimate objective of this Convention and any related legal instruments that the Conference of the Parties may adopt is to achieve, in accordance with the relevant provisions of the Convention, stabilization of greenhouse gas concentrations in the atmosphere at a level that would prevent dangerous anthropogenic interference with the climate system. Such a level should be achieved within a time-frame sufficient to allow ecosystems to adapt naturally to climate change, to ensure that food production is not threatened and to enable economic development to proceed in a sustainable manner."

The postulated stabilization of greenhouse gas concentrations in the atmosphere is described in the following from a scientific point of view and then analysed considering the applicability for the estimation of external costs.

4.5   The stabilization of global warming

Due to the combined effect of interacting inertias of the various processes of the climate system stabilization of the climate and climate-impacted systems will only be achieved long after anthropogenic CO_2 emissions have been reduced. This interrelationship is illustrated in **Figure 4-11**. This figure is a generic illustration for CO_2 concentration stabilization at any level between 450 and 1,000 ppm. Therefore, it has no units on the ordinate.

The CO_2 emission reduction path in **Figure 4-11** peaks within the next century and is thereafter declining rapidly. After 100-300 years the CO_2 concentration in the atmosphere is stabilized. A few centuries later, the temperature stabilizes so that the incoming solar radiation is balanced with the outgoing infrared radiation. Due to their large mass, thickness, thermal capacity and the slow heat transport process, the oceans and the cryosphere are the

main sources of physical inertia in the climate system. They need millennia to melt and expand thermally in order to adapt to the ambient temperature. Ice sheet models project that a local warming of larger than 3°C, if sustained for thousands of years, would lead to virtually a complete melting of the Greenland ice sheet with a resulting sea-level rise of about seven metres.
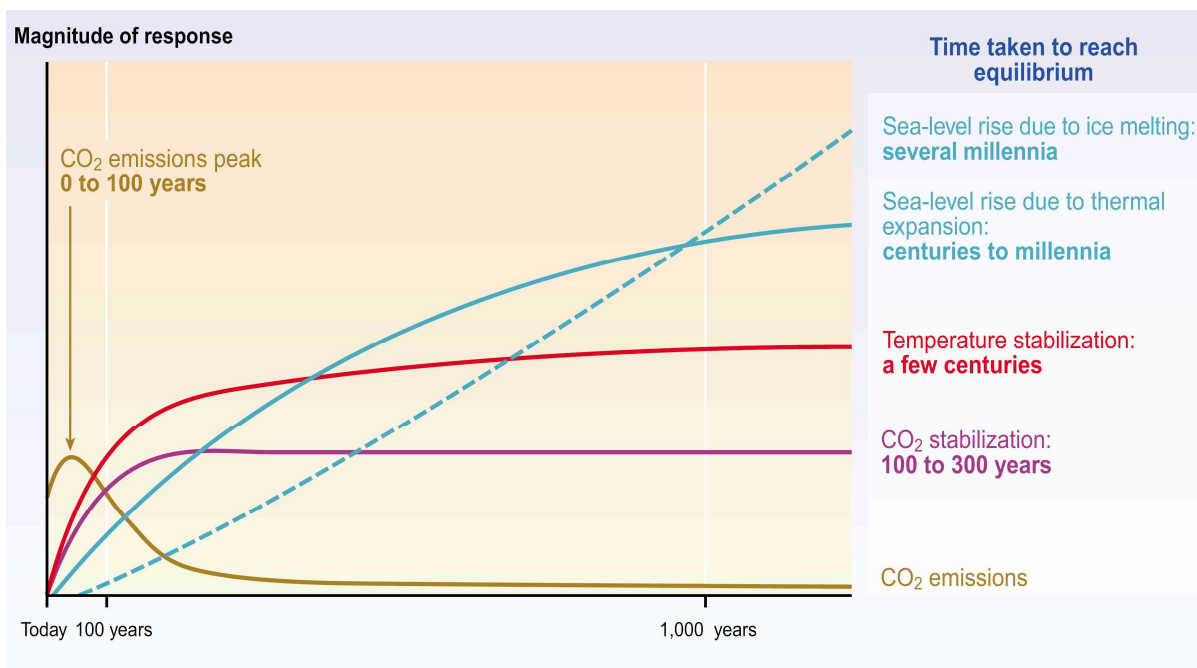
Figure 4-11:   Dynamics of global warming /IPCC 2001d/

The inertia and the possibility of irreversibility in the interacting climate, ecological and socio-economic systems are major reasons why anticipatory adaptation and mitigation actions are beneficial. A number of opportunities to exercise adaptation and mitigation options may be lost if action is delayed.

Stabilization of CO_2 concentrations at any considered level requires a significant reduction of global net emissions to a small fraction of the current ones. This can be derived from the stabilization scenarios of IPCC presented in **Figure 4-12**. The stabilization of atmospheric CO_2 concentrations at 450 ppm, 650 ppm, or 1,000 ppm requires global anthropogenic CO_2 emissions to drop below the year 1990 level within a few decades, about a century or about two centuries, respectively. Afterwards, the concentrations should continue to decrease.

In the stabilization scenarios of IPCC it is assumed that emissions of gases other than CO_2 follow the SRES A1B scenario until the year 2100 and are constant thereafter. The dashed lines in **Figure 4-12** show the temperature changes projected for S profiles, an alternate set of CO_2 reduction paths. With the shaded area the effect of a range of climate sensitivity across the five stabilization cases is illustrated and the coloured bars on the right hand side show the range at the year 2300 for each WRE[17] profile. The range is caused by different climate

---

[17]   WRE scenarios are those that are proposed by Wigley, Richels and Edmonds in /IPCC 2001a/.

model tunings. The diamonds on the bars show the equilibrium warming for the respective stabilization level using average model results. For comparison the estimated results for the SRES emission scenarios in the year 2100 are included.
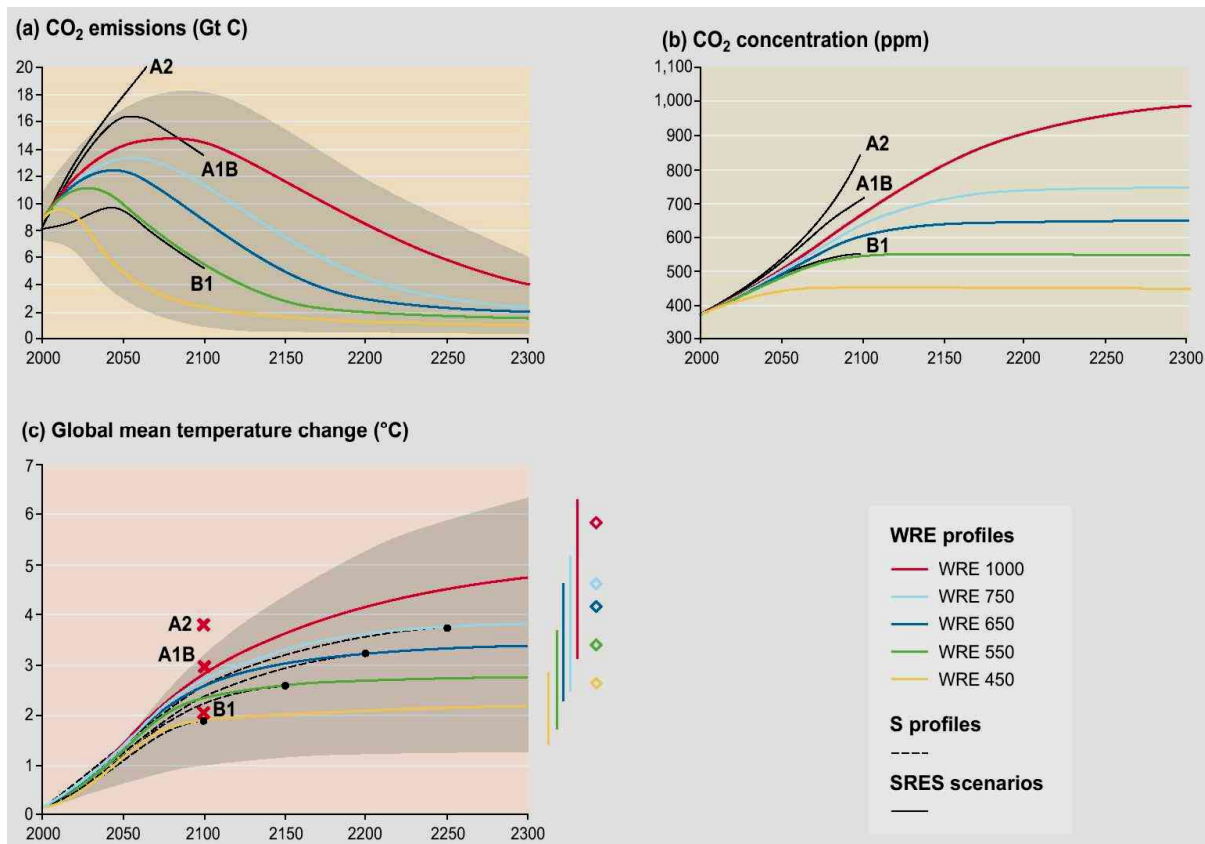
Figure 4-12:   Stabilization scenarios /IPCC 2100d/

The global average surface temperature is estimated to increase 1.2-3.5 °C by the year 2100 relative to 1990 for CO_2 reduction paths which would eventually stabilize the concentration of CO_2 at a level of 450-1,000 ppm. The equilibrium temperature rise would take many centuries to be reached and it ranges from 1.5 to 3.9°C above the year 1990 levels for stabilization at 450 ppm and 3.5 to 8.7°C above the year 1990 levels for stabilization at 1,000 ppm. This range of uncertainty is displayed in **Figure 4-13** for different CO_2 stabilization levels.

The projected range of sea-level rise due to thermal expansion at equilibrium after several millennia is 0.5-2 m for an increase in CO_2 concentration to 560 ppm and 1-4 m for an increase to 1,120 ppm. Besides thermal expansion, there are other contributions to sea-level rise, e.g. from the melting of polar ice sheets and land ice. Even for stabilization levels of 550 ppm the sea-level would rise several metres.

For a lower stabilization level the severity of impacts from climate extremes is expected to be less, fewer regions would suffer adverse net market sector impacts, global aggregate impacts would be smaller, and risks of large-scale high-impact events would be reduced.

Temperature change relative to 1990 (°C)

Temperature
change at
equilibrium

Temperature
change
in year 2100

Eventual CO₂ stabilization level (ppm)
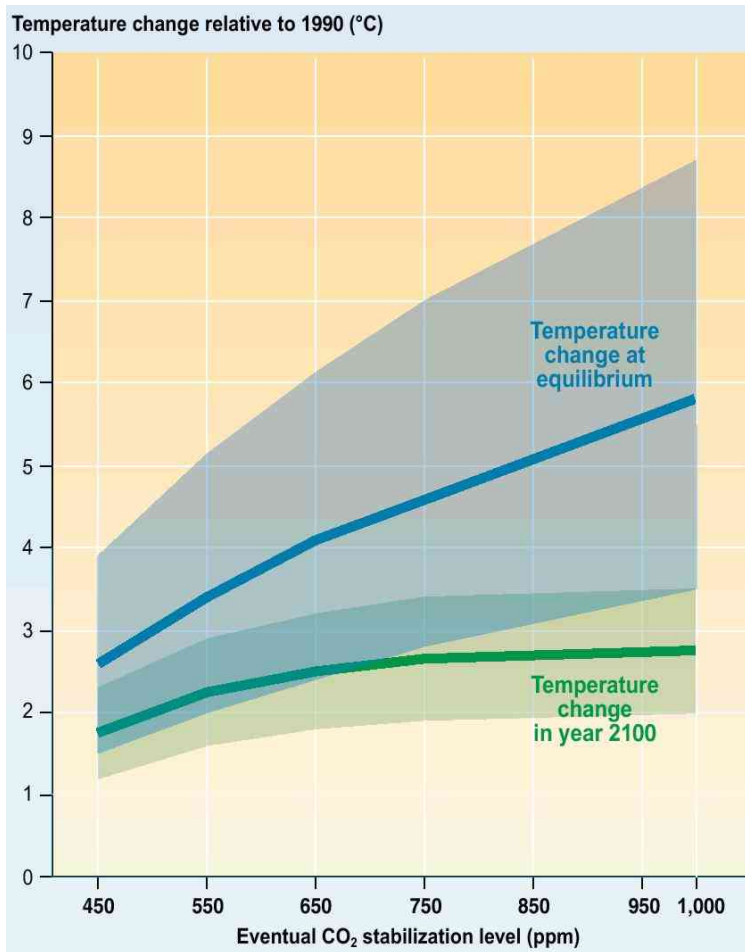
Figure 4-13:   Range of uncertainty in temperature changes related to the year 1990 for different
stabilization levels /IPCC 2001d/

4.6   Estimation of the avoidance costs of global warming

The fundamental question for the estimation of the avoidance costs is which generally ac-
cepted goal has to be achieved. This is essential since the marginal damage costs are not
available and thus an interception of the marginal damage costs curve and the marginal
avoidance costs curve is not available. The original way, described in chapter 2, is that this
interception determines the necessary reduction of the emissions and the corresponding emis-
sions tax which leads to a Pareto optimum from the environmental economics' point of view.

    Another approach is that an emission reduction goal is defined which should be achieved.
With knowledge about the marginal avoidance costs curve, the intersection should determine
the emissions tax which is as high as the marginal external costs at the aimed emission level.
This is necessary if one wants to apply the precautionary principle because of large uncertain-
ties and risks in the case of global warming. The estimations described in chapter 4.4 have a
large range and uncertainties, and do not consider effects which can not be quantified such as
social contingent effects. In order to get as near as possible to the Pareto optimum the precau-
tionary principle seems to be the better way for the provision of sustainability criteria.

/Azar; Rodhe 1997/ state that "*until it has been proven that a temperature increase above 2°C is safe or that the climate sensitivity is lower than the central estimate,* […] *the global community should* […] *make stabilization in the range 350 to 400 ppm*".

At a comparably level, /WBGU 2003/ stresses that there are high risks if the global average temperature exceeds 2°C above pre-industrial levels. /WBGU 2003/ also limits the warming rate that should not be more than 0.2 °C per decade. In comparison with **Figure 4-13** the stabilized CO_2 concentration should be less than 450 ppm as even the lower end of the temperature warming range passes over the limit. It should be noted that **Figure 4-13** illustrates the temperature change from 1990 figures and not from pre-industrial figures.

This temperature limit of 2 °C above pre-industrial levels is supported by studies which conclude that at a level of approximately 3 °C the Greenland ice sheets will vanish and increase the sea-level by approximately seven metres. **Figure 4-9** and its interpretation give additional support for a temperature limit at this level.

/Nakicenovic; Riahi 2003/ model the carbon permit price for stabilization scenarios with constraints of the *Wissenschaftlicher Beirat der Bundesregierung globale Umweltveränderungen* (WBGU). The stabilization scenarios stabilize the atmospheric CO_2 concentration at 400 ppm in the case of the B2-400 and B1-400 as well as at 450 ppm in the case of the A1T-450 (see **Figure 4-15**). The stabilization is achieved by corresponding emission reduction paths (see **Figure 4-14**) which are compared to their respective baseline scenarios. The baseline scenarios portray very optimistic baselines compared to the scenarios in **Figure 4-7**. Additional optimistic assumptions are made for the stabilization scenarios: a global social planner with perfect foresight, cost minimisation, existence of an agreement on emission entitlements and a perfectly functioning market in emission permits trade.

A further assumption is the use of *contraction and convergence* (c&c). It means that all regions should converge to a common per capita emission entitlement by a given pre-specified date. This pre-specified date is in the case of c&c2050 the year 2050 and in the case of c&c2100 the year 2100. There is comparatively little difference between the both convergence schemes as can be derived from **Figure 4-17**. Furthermore, WBGU constraints include the assumption that CO_2 capture and storage is a tentative solution for the next decades but phased out in 2100. CO_2 capture and storage contributes the main part of the reductions. Another assumption is that all nuclear plants are phased out globally until the year 2050. The calculation is performed with a discount rate of 5 % (cf. chapter 3.1). All these very restrictive constraints and the few scenarios make this study an illustrative one demanding for further research.
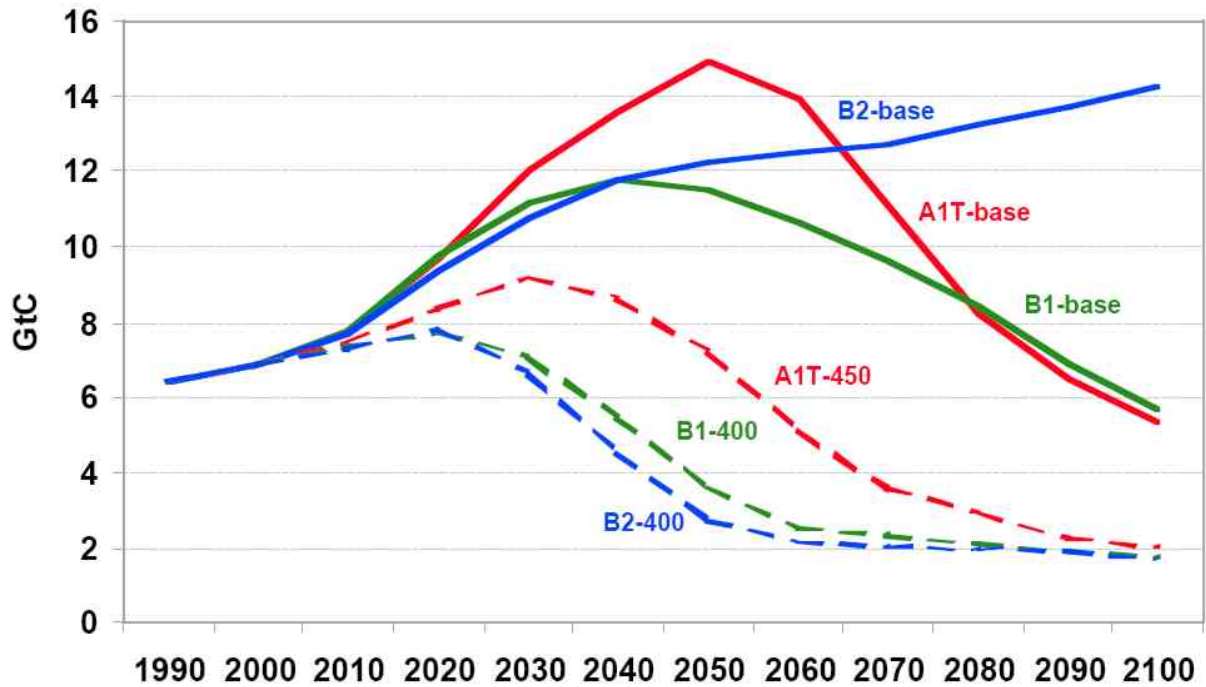
Figure 4-14: Global CO2 emissions of three alternative baseline scenarios A1T-base, B1-base and B2-base as well as corresponding emission profiles consistent with stabilization at 400 ppm (B1-400 and B2-400) and 450 ppm (A1T-450), respectively /Nakicenovic; Riahi 2003/
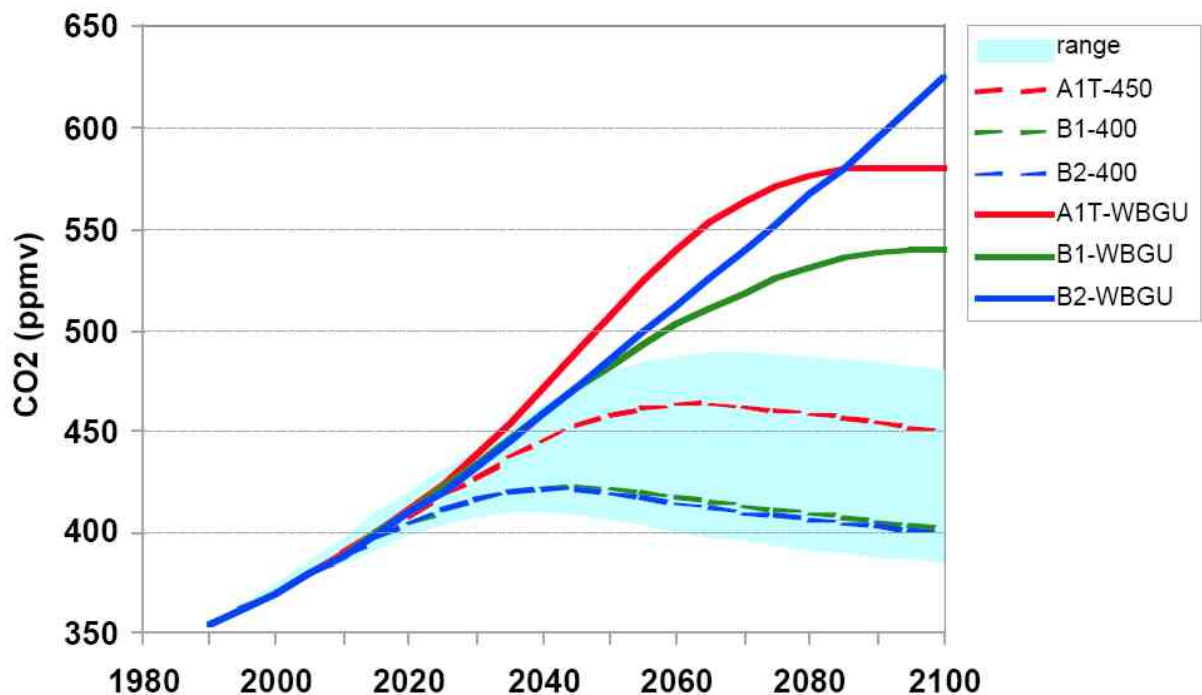
Figure 4-15: Atmospheric CO_2 concentration /Nakicenovic; Riahi 2003/

The shaded area indicates the model uncertainty for the three stabilization scenarios.
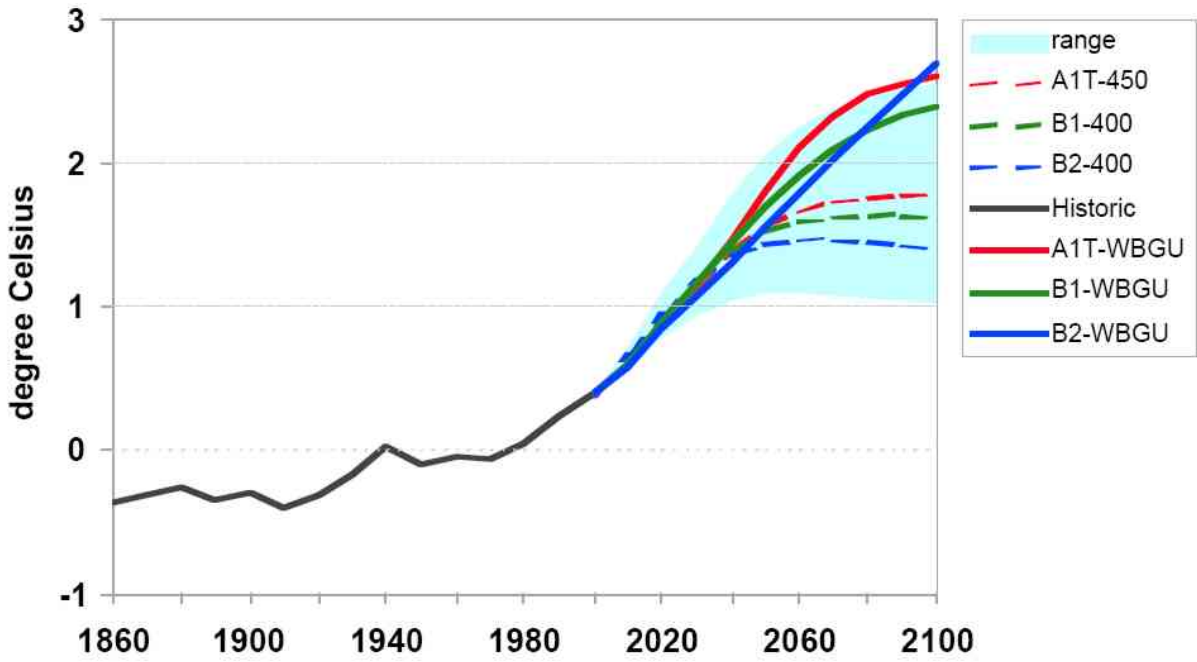
Figure 4-16:   Global mean temperature change, compared to the 1961 to 1990 mean /Nakicenovic; Riahi 2003/

The shaded area indicates the model uncertainty for the three stabilization scenarios.
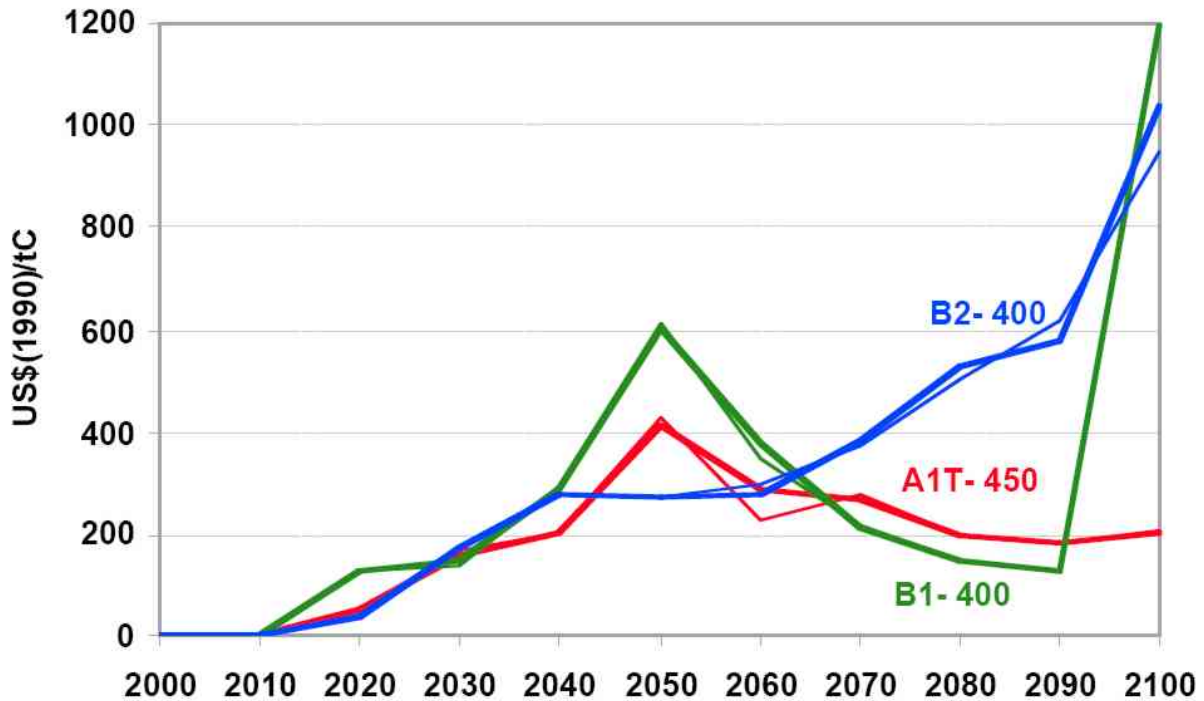
Figure 4-17:   Carbon permit price for six climate stabilization policy scenarios /Nakicenovic; Riahi 2003/

Bold lines refer to the c&c2050 emission permit allocation scheme, thin lines to the c&c2100 allocation model.

The global mean temperature change within the considered scenarios is displayed in **Figure 4-16**. It is in the range of 1.5-3.0 °C compared to pre-industrial figures and thus approximately 2 °C with a little chance of less and a higher risk of more global warming.

Finally, **Figure 4-17** illustrates the carbon permit price or the globally equalised marginal carbon abatement costs. The difference between the two emission permit allocation regimes is small so that it is not analysed in the study at hand. Main differences arise from the type of base scenario. The robust finding of /Nakicenovic; Riahi 2003/ is that the marginal carbon abatement costs are quite close until 2040. Some differences arise around 2050 when the nuclear power plants are phased out as well as around 2100 when the sequestration is phased out. While the scenario A1T-450 remains at approximately 200 US\$$_{90}$/tC (73 €$_{2003}$/tCO$_2$), B1-400 is fluctuating considerably in the range of 100-1,200 US\$$_{90}$/tC (37-439 €$_{2003}$/tCO$_2$) and B2-400 is more or less increasing steadily up to 1,000 US\$$_{90}$/tC (366 €$_{2003}$/tCO$_2$) in 2100. These costs of meeting the climate stabilization target will increase if any assumption is relaxed. Therefore, the displayed costs should be interpreted as minimum costs.

In another study, /Tol; Heinzow 2003/ estimate the avoidance costs with FUND (Climate Framework for Uncertainty, Negotiation and Distribution), version 2.4, which is also used for the estimation of damage costs (cf. chapter 4.4). /Tol; Heinzow 2003/ model the avoidance costs as minimum costs to achieve the target of a limited CO$_2$ concentration of 450 ppm. Therefore, the marginal costs are equalised everywhere. This corresponds, for instance, to a perfect competitive global market in emission permits or a uniform tax. Another assumption is a perfect capital market which enables the marginal costs to grow with the discount rate. This discount rate is assumed to be 3 % per year with a rate of time preference of 1 %. A discussion about the discount rate is performed in chapter 3.1. Furthermore, the costs are presented as average costs per decade which are total costs over total emission reduction and not as marginal costs. With a 3 % discount rate, the avoidance costs will double every 23.45 years so that in 2095 (average over 2090-2100) the avoidance costs will reach the 14.3-fold of the avoidance costs in 2005 (average over 2001-2010). /Tol; Heinzow 2003/ estimate the average avoidance costs over the years 2001-2010 to be 495 US\$$_{2000}$/tC[18] (144 €$_{2003}$/tCO$_2$). These estimations are based on minimal costs assumptions due to perfect markets and a discount rate which includes time preference of 1 % which is not based on sustainability criteria. Therefore, it should not be used as the upper end of the range of CO$_2$ avoidance costs.

In the study at hand, the range of CO$_2$ avoidance costs for the next decades is based on /Nakicenovic; Riahi 2003/ and /Tol; Heinzow 2003/. It is assumed that /Nakicenovic; Riahi 2003/ represent the lower end and /Tol; Heinzow 2003/ the middle value. With the uncertainties of the estimations, the avoidance costs of these studies are assumed to be 75 €$_{2003}$/tCO$_2$ and 150 €$_{2003}$/tCO$_2$, respectively. Symmetrically, the upper end of the range is assumed to be

---

[18] It is assumed that prices of 2000 are used.

225 $€_{2003}$/tCO_2 with the assumptions of political lags and market imperfections. The range is displayed in **Table 4-7**.

This range is within the range of the estimations of the FUND model in **Table 4-4** for 0 % and 1 % discount rate, in the range of the estimations of the OF in **Table 4-5** for all considered discount rates as well as in the range of 22 published studied in **Table 4-6** for 2 % discount rate.

Table 4-7:   External costs of global warming

Estimations	$€_{2003}$/tCO_2
Low	75
Medium	150
High	225

4.7   Global Warming Potential

The *Global Warming Potential* (GWP) is an index based on radiative forcing. It is used in order to estimate the potential future impacts of greenhouse gas emissions relative to CO_2. The GWP is defined as the ratio of the time-integrated radiative forcing from the instantaneous release of 1 kg of a greenhouse gas relative to that of 1 kg of a CO_2 /IPCC 2001a/:

$$GWP(x) = \frac{\int_0^{TH} a_x \cdot [x(t)] dt}{\int_0^{TH} a_r \cdot [r(t)] dt} = \frac{\int_0^{TH} a_x \cdot [x(t)] dt}{AGWP} \qquad (4\text{-}2)$$

In this equation, TH is the *time horizon* of the calculation, a_x the *radiative efficiency* due to a unit increase in atmospheric abundance of the considered substance ($[a_x]$ = Wm^{-2}kg^{-1}) and x(t) is the time-dependent *decay* in abundance of the instantaneous release of the considered substance. The corresponding variables of the reference substance CO_2 are in the denominator which is called the *Absolute GWP* (AGWP). If the lifetimes (represented by the decay of the considered substance and the reference substance CO_2) differ significantly the GWP becomes sensitive to the choice of time horizon. With longer time horizons the GWP decreases if the considered substances decay more rapidly than the reference substance. The GWP increases if the considered substances decay more slowly than the reference substance.

/IPCC 2001a/ calculates with a background CO_2 mixing ratio of 364 ppm and a radiative efficiency for small perturbation from this level of 0.01548 Wm^{-2}ppm^{-1}. Thus the AGWP of CO_2 is 0.207, 0.696 and 2.241 Wm^{-2}ppm^{-1} for 20, 100 and 500 year time horizons, respec-

tively. With an uncertainty range of +/- 35 % **Table 4-8** shows the GWP of the three main contributors to the greenhouse gas effect. There are many other greenhouse gases (e.g. chlorofluorocarbons, hydro chlorofluorocarbons, hydro fluorocarbons, chlorocarbons and bromocarbons) but they are not listed as their contribution to the greenhouse effect is assumed to be negligible compared to CO_2. In this study even N_2O is not considered because its contribution to the total GWP is less than 1 % in case of the considered technologies.

$CO_{2,equ}$ is used as a unit to describe the global warming potential of the other greenhouse gases. Thus 1 kg CH_4 corresponds to 23 kg $CO_{2,equ}$ as CH_4 has a GWP-100a of 23. Equivalently 1 kg N_2O corresponds to 296 kg $CO_{2,equ}$. The sum over all emitted greenhouse gases in $CO_{2,equ}$ can be used to determine the damage of them if the damage of CO_2 is known.

Table 4-8:   GWP /IPCC 2001a/

Gas	GWP-20a	GWP-100a	GWP-500a
CO_2	1	1	1
CH_4	62	23	7
N_2O	275	296	156

5   Life Cycle Analysis

In the study at hand, the *life cycle inventory* (LCI) of *Environmental and Ecological Life Cycle Inventories for present and future Power Systems in Europe* (ECLIPSE) is used because one of the goal of this study is to provide a harmonised set of public, coherent, transparent and updated LCI data on new and decentralised power systems.

Its public availability is ensured by internet (*http://www.ECLIPSE-eu.org*). The transparency is achieved with methodological guidelines in /Setterwall et al. 2004/. They should be used in all ECLIPSE studies and will be described below in more detail. Examples are used in order to increase the comprehensibility. The up-to-dateness is ensured with actual data for the recent years. Up-to-dateness is very important in the case of many considered technologies (e.g. photovoltaic systems, wind turbines and fuel cells) because they have been rapidly improving over the last years (cf. chapters about the market development).

The methodological guidelines in /Setterwall et al. 2004/ focus on system boundaries, the functional unit, input and output flows, data format, the end-of-life phase and LCI background data. Following /Setterwall et al. 2004/, some of these issues are described below. They have been consistently applied in the modelling activities and in the database of ECLIPSE. The methodological guidelines are complementary to the ISO 14040-41 which gives specific guidance on how to conduct LCA on electricity generation systems.

Boundaries:

The general life cycle scope of electricity generation systems is illustrated in **Figure 5-1**. Generally, there are two different electricity generation technologies, those using fuel and those using flowing energy resources, e.g. solar insulation or wind. For the fuel-based plants, operation and fuel preparation is most important for the environmental profile in LCA terms whereas the construction of the plants is crucial for the technologies using flowing energy resources.

The life cycle scope of electricity generation systems includes the following main phases:
- Fuel preparation (exploration and prospecting of fuel resources, fuel resource extraction and processing, and fuel transports)
- Infrastructure (construction of power plant including exploration, prospecting and extraction of ores, minerals, etc., material manufacture, production of components and transports)
- Operation (normal malfunctions, production of operational chemicals, incineration of operational waste, disposal processes, handling of fuel residues, reinvestments in machines and transports)
- End-of-life processes (incineration of waste and disposal processes)

The following items in the main life cycle phases are excluded in the ECLIPSE studies:

- Construction and deconstruction of suppliers facilities
- Construction and deconstruction of vehicles and roads outside the studied site of power plant
- Construction, deconstruction and maintenance of transmission and distribution networks
- Transmission and distribution to the customer (the electricity produced is just delivered to the power network)
- Environmental impacts caused by bigger accidents, e.g. averages of oil tankers, which occur very seldom
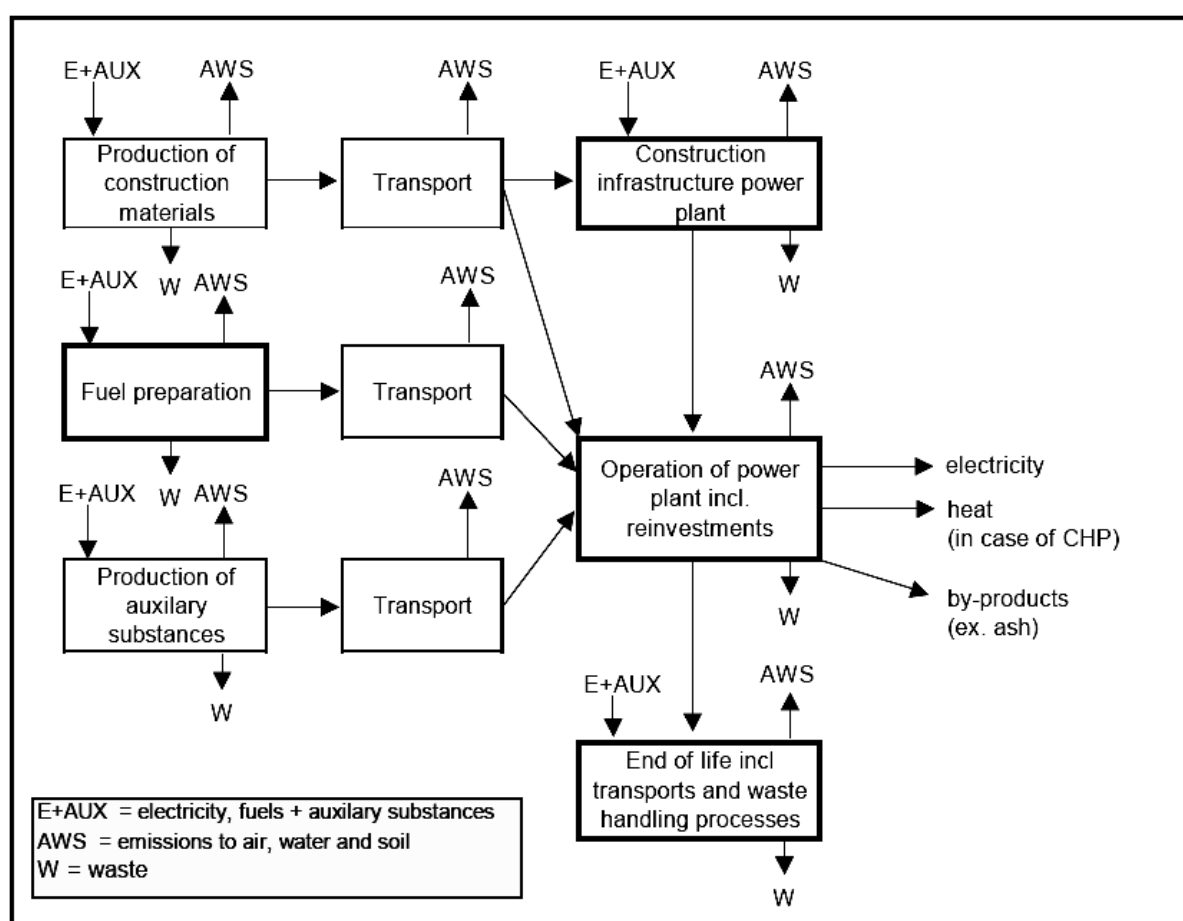
Figure 5-1:   The general life cycle scope of electricity generation systems /Setterwall et al. 2004/

EU-15 plus Switzerland and Norway is the geographical scope of most processes and the temporal scope spans existing, mature technologies considering data up to about 10 years old but also newer technologies like wind turbines and coming technologies like fuel cells. Also some examples are calculated representing the conditions in 5 or 10 years.

Functional unit:

The functional unit used in ECLIPSE is *kWh generated electricity at specified voltage level delivered to the power network* (kWh_{el}).

In the case of *combined heat and power generation* (CHP), the functional unit is *kWh generated electricity at specified voltage level delivered to the power network* (kWh_{el}) and *kWh produced heat with specified temperature delivered to the heat distribution network* (kWh_{th}).

The allocation between electricity and heat in CHP is based on the exergy content. Exergy measures which part of a quantity of energy can be made available in the form of work. This definition assumes that mechanical work as well as electrical energy is pure exergy. The *electrical exergy content* ex_{el} of an electricity unit is represented by the ratio of the *exergy of electrical energy* Ex_{el} and the *electrical energy* E:

$$ex_{el} = \frac{Ex_{el}}{E} = 1 \qquad (5\text{-}1)$$

The second fundamental theorem of thermodynamics describes the losses connected with transformation of heat into another form of energy. Hence, the *exergy content* ex_{th} of a unit of heat (which is available at a temperature T_m in an *ambient temperature* of T_0) is represented with the ratio of the *exergy of the heat* Ex_{th} and the *heat* Q:

$$ex_{th} = \frac{Ex_{th}}{Q} = \left(1 - \frac{T_0}{T_m}\right) \qquad (5\text{-}2)$$

Normally, the heat is used in a local heat network. A circulating medium is heated to the outgoing temperature T_{in}. This medium is fed into the local heat network (index *in*). With a lower returning temperature T_{out} this medium returns to the plant leaving the local heat network (index *out*). For this reason the *thermodynamic mean temperature* T_m is chosen:

$$T_m = \frac{T_{in} - T_{out}}{\ln\left(\dfrac{T_{in}}{T_{out}}\right)} \qquad (5\text{-}3)$$

Following the allocation based on exergy content, heat production only bears that part of the environmental impact that corresponds to the ratio of the exergy content of the heat over the total exergy which consists of the exergy of the electricity and the exergy of the heat. The allocation factors all_{el} for electricity and all_{th} for heat are defined with the *efficiency of gener-*

ating electricity η_{el} = E/W and the *efficiency of generating heat* η_{th} = Q/W with the relation to *energy input* W in form of fuel as:

$$all_{el} = \frac{ex_{el} \cdot \eta_{el}}{ex_{el} \cdot \eta_{el} + ex_{th} \cdot \eta_{th}} = \frac{\eta_{el}}{\eta_{el} + ex_{th} \cdot \eta_{th}} = \frac{1}{1 + \left(1 - \frac{T_0}{T_m}\right) \cdot \frac{\eta_{th}}{\eta_{el}}} \qquad (5\text{-}4)$$

$$all_{th} = \frac{ex_{th} \cdot \eta_{th}}{ex_{el} \cdot \eta_{el} + ex_{th} \cdot \eta_{th}} = \frac{ex_{th} \cdot \eta_{th}}{\eta_{el} + ex_{th} \cdot \eta_{th}} \qquad (5\text{-}5)$$

Total life cycle impacts are then allocated with all_{el} and all_{th} to the electricity and the heat production. In the case that efficiencies η_{el} and η_{th} are not available, the allocation factors can also be calculated with:

$$all_{el} = \frac{ex_{el} \cdot E}{ex_{el} \cdot E + ex_{th} \cdot Q} = \frac{E}{E + ex_{th} \cdot Q} = \frac{1}{1 + ex_{th} \cdot \frac{Q}{E}} = \frac{1}{1 + \left(1 - \frac{T_0}{T_m}\right) \cdot \frac{Q}{E}} \qquad (5\text{-}6)$$

$$all_{th} = \frac{ex_{th} \cdot Q}{ex_{el} \cdot E + ex_{th} \cdot Q} = \frac{ex_{th} \cdot Q}{E + ex_{th} \cdot Q} \qquad (5\text{-}7)$$

Both alternatives have the characteristic that the sum of all_{el} and all_{th} should be one because all impacts are distributed to electricity and heat.

One of the difficulties associated with this allocation method is that the exergy content is highly dependent on the ambient temperature, which varies both geographically and over time. Moreover, it depends on the temperature at which the produced heat should be available. The allocation method based on exergy content is one of several different ones all having their advantages and disadvantages. In comparison, the allocation method based on exergy content tends to allocate less environmental load to the heat and, hence, more to electricity but seems to be the best choice because of the following reasons. Allocation methods which are based on material flows with allocation based on mass or mole quantities are not appropriate for energy flows which are considered in the context of this study. Monetary allocation is difficult as prices of electricity and heat are volatile and need to be estimated over the life time of the considered systems. The uncertainty of monetary allocation is not appropriate in this context. Another allocation method is the allocation based on energy. This is possible for power and heat generating systems but neglects the quality of the products which can better be expressed in terms of exergy.

A sensitivity analysis of the different parameters influencing the allocation factor for electricity shows that it is highly sensitive to the ambient temperature, the heating temperature and the electrical efficiency. The CHP plant for this example is assumed to have an ambient

temperature of 15 °C, a heating temperature of 60 °C, an electrical efficiency of 30 % and a thermal efficiency of 65 %.

Figure 5-2 shows that a higher ambient temperature and **Figure 5-3** shows that a lower heating temperature will generate a higher allocation factor for electricity. Within the temperature ranges used in the figures the highest allocation factor for electricity is ca. 15 % higher than the lowest. Thus the allocated emissions per kWh_{el} may change by 15 % within the investigated temperature ranges. **Figure 5-4** shows that an increasing electrical efficiency will increase the allocation factor for electricity.

The method of allocation between electricity and heat in CHP plants is of high importance for the results. If the exergy method is used the choice of ambient temperature and the temperature for the district heating system are critical parameters which should be adjusted in direct comparisons. However, this is not consistently performed in the ECLIPSE reports.
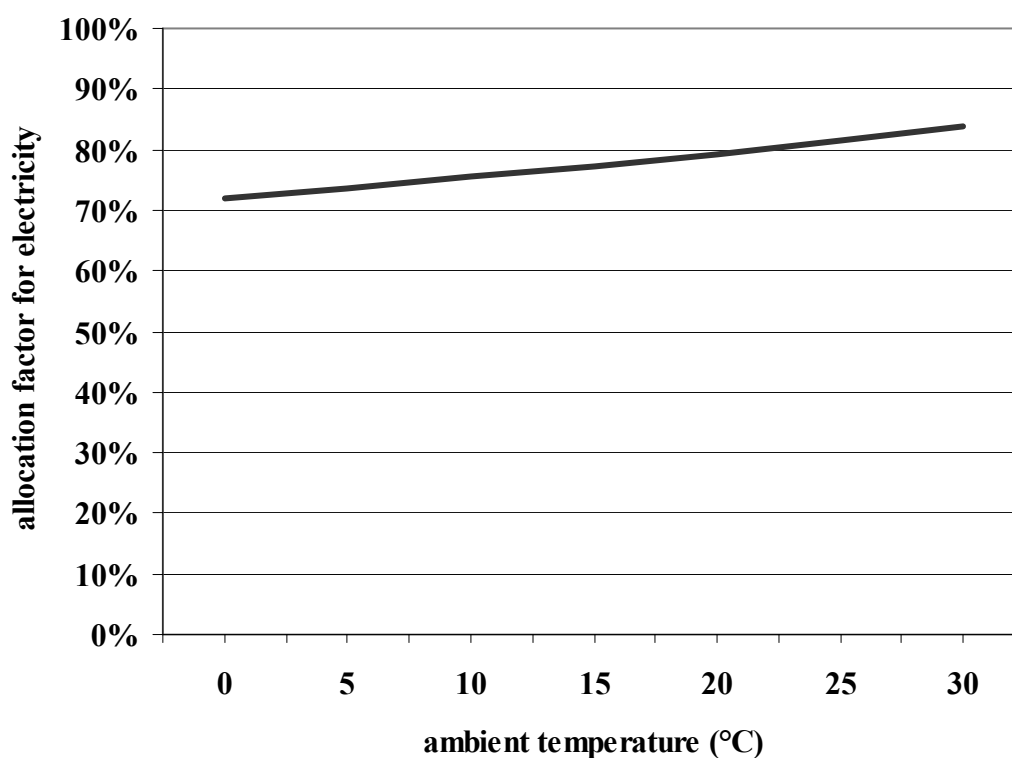
Figure 5-2:   Sensitivity of the allocation factor for electricity to the ambient temperature
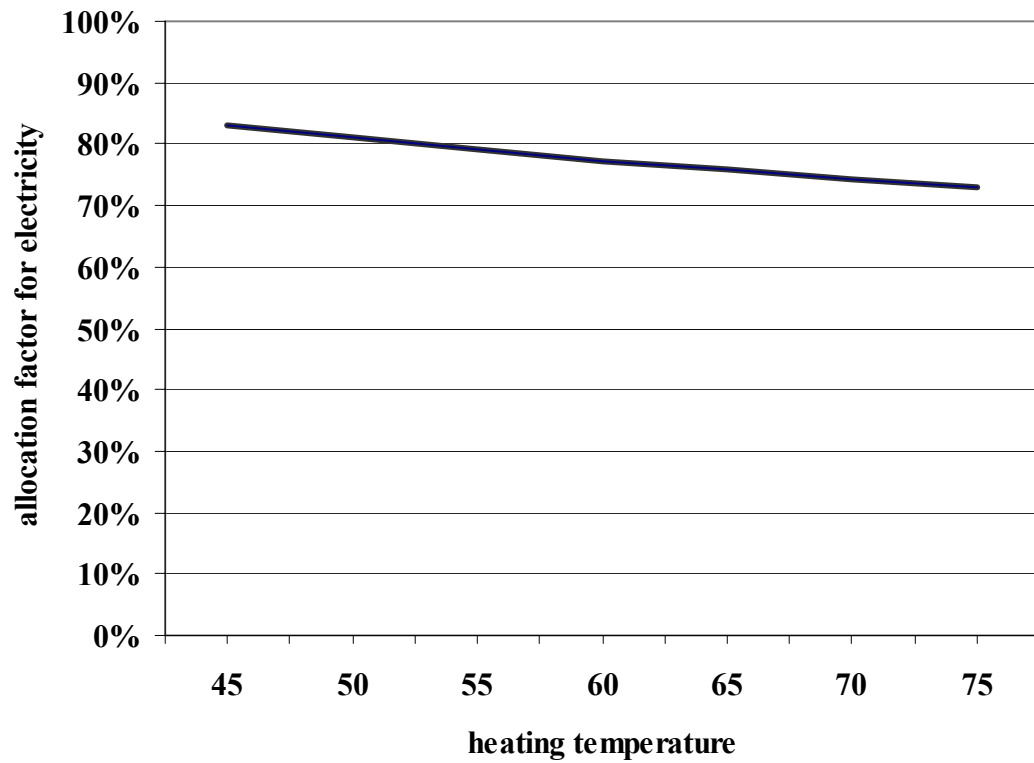
Figure 5-3: Sensitivity of the allocation factor for electricity to the heating temperature
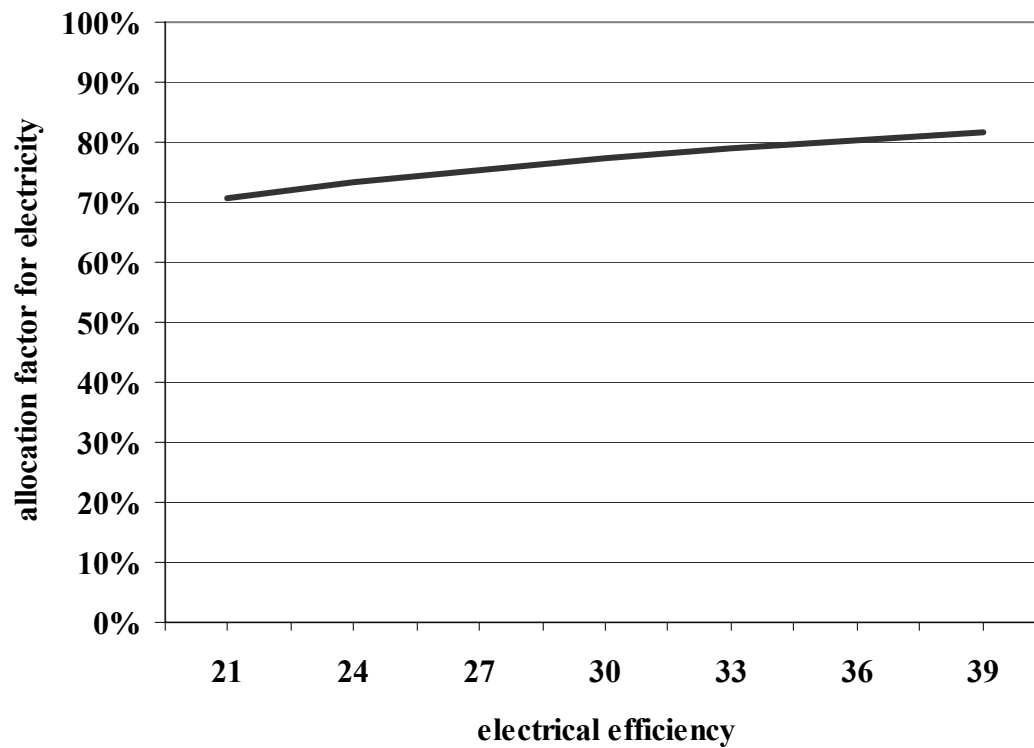
Figure 5-4: Sensitivity of the allocation factor for electricity to the electrical efficiency

Input and output flows:

The same generic data for upstream processes regarding manufacturing of raw material, electricity production, transports etc. have been used in all ECLIPSE studies. In **Table 5-1** sources of some upstream data are listed.

Table 5-1:   Sources of upstream data in ECLIPSE

Upstream data	Source
Steel	/IISI 2000/
Aluminium	/EAA 2002/
Cement	/Frischknecht et al. 1996/
Chemicals	/Frischknecht et al. 1996/
Concrete	/Frischknecht et al. 1996/
Copper and other metals	/Frischknecht et al. 1996/
Electricity generation	/Frischknecht et al. 1996/
Electricity generation mix	IEA-Statistics, mean value 1998-2000 for the EU-countries plus Norway and Switzerland
Glass	/Frischknecht et al. 1996/
Natural gas	/Frischknecht et al. 1996/
Oil, diesel	/Frischknecht et al. 1996/
Plastics	Association of Plastics Manufacturers in Europe[19]
Transports, lorries	EU emission standards for Euro3-motors and /NTM 2000/
Transports, ships	/Borken et al. 1999/

In late 2003, updated LCA data on background processes have been published in /Dones et al. 2003/. However, these data have not been included in the ECLIPSE studies. The change in LCA data compared to /Frischknecht et al. 1996/ is illustrated in **Table 5-2** showing the difference between the updated and the old LCA data for selected products, e.g. natural gas, concrete and copper, using different indicators. **Table 5-2** displays that the LCA data for CO_2, CH_4 and N_2O of ECLIPSE tend to be lower using the updated data because the GWP-100a is lower (with the exception of hard coal). The other indicators, UBP97 and EI99, are not further explained in this study as they are just for illustration but further literature is quoted.

---

[19] http://www.apme.org/

Table 5-2:   Difference in LCA data between /Frischknecht et al. 1996/ and /Dones et al. 2003/ following /Frischknecht 2003/ by means of Umweltbelastungspunkte 97 (UBP97)[20], Eco-Indicator 99 (EI99)[21] and Global Warming Potential (GWP-100a)[22]

Product	UBP97	EI99	GWP-100a
Electricity UCTE	3.9 %	- 11.5 %	-9.1 %
Light fuel oil	- 16 %	3.1 %	-0.9 %
Petrol	- 23.5 %	- 1.4 %	- 17.5 %
Natural gas	- 23.4 %	- 4 %	- 33.8 %
Hard coal	- 1 %	- 42.9 %	2.1 %
Steel low alloyed	74.7 %	84.1 %	- 39.5 %
Concrete	152.3 %	343 %	- 11.1 %
Copper	56.5 %	97.2 %	- 70.1 %
Organic chemicals	- 16.7 %	126.1 %	- 8.5 %

Data quality:

In the ECLIPSE studies, data concerning particulates use different classes and often they can not be valued by the impact pathway approach at the present state of the methodology. Some processes included a distinction of PM2.5, PM10 and particulates larger than PM10 but there are too many unspecified particulates so that a classification is not achieved. This is especially critical because different exposure-response functions for PM2.5 and PM10 do exist for the calculation of external costs and particulates larger than PM10 are generally not considered in the calculations. Thus, the particulates emissions in the ECLIPSE studies do not have the data quality which is required for the estimation of external costs. However, since particulates are very important emissions they are reported in the description of the studies without any classification. Despite arising inconsistencies the external costs of all quantified particulates are estimated with the damage factor of PM10.

---

[20]   More information is available in /BUWAL 1998/.

[21]   Description of the methodology is available in *http://www.pre.nl/eco-indicator99/default.htm*

[22]   See chapter 4.7

Comparison with other topical German studies:

Besides ECLIPSE, two further topical studies are published in 2004 which analyse life cycles of future electricity generation systems. They are referred to as /BMWA 2004/ and /BMU 2004/. Both studies are described below and their results are taken for comparison in the following chapters. It should be noted that a comparison between the studies lacks of consistency because the assumptions differ from study to study. Nevertheless it seems necessary to compare the LCIs of different studies in order to show that the respective data should not be considered as definite. All LCIs should be regarded as data under specific assumptions which, actually, can not be generalised.

/BMWA 2004/:

The goal of /BMWA 2004/ is to provide a LCI for power generation systems projected to the year 2010. In /BMWA 2004/, fossil power plants, bio-fuelled CHP plants, fuel cells, photovoltaic systems and wind turbines are analysed. The determination of the LCI is performed with the software BALANCE which combines classical process chain analysis with Input-Output-Analysis forming a hybrid approach.

/Frischknecht et al. 1996/ deliver the basis for the process chain analysis. Since it is especially developed for Switzerland and contains data for the early 1990s the database is optimized for Germany and the year 2010, mainly in processes of fuel supply and electricity. The projections include significant reductions of methane for natural gas supply and coal supply in an order of 50 % compared to the situation in 1997. However, particulates emissions double in the case of coal supply.

/BMU 2004/:

Another topical study is /BMU 2004/. It aims to describe and evaluate environmental impacts of renewable energies inter alia. The regional scope is Germany and the temporal scope is the year 2010 as in /BMWA 2004/. It is additionally taken into account because it is up to date and analyses technologies which are not studied in ECLIPSE and /BMWA 2004/. Additional technologies are river power plants (cf. chapter 5.6), solar thermal power plants (cf. chapter 5.7) and geothermal power plants (cf. chapter 5.8). They are described in this chapter but it should be noted that the results are not consistent to the ECLIPSE results due to different assumptions concerning the upstream chains.

In the following chapters the considered technologies are described in detail based on the ECLIPSE reports. The results are always examples for the given assumptions as every application depends on the site of the plant and many other conditions, e.g. weather conditions in the case of photovoltaic and wind.

5.1   Photovoltaic systems

5.1.1   Technology

Photovoltaic (PV) cells are semiconductor devices which directly convert solar energy into *direct current* (DC) electricity. PV modules consist of PV cells which are connected. A connection of several PV modules is a string and all strings are a PV generator. Due to this modularity the installation possibilities concerning the installed power, the arrangement, or the location have a wide range.

Technologies:

There exists a large variety of PV technologies. Three generations can be distinguished /Werner 2004/:

The first generation is based on wafered crystalline silicon and can be differentiated into *single crystalline silicon* (sc-Si) and *multi-crystalline silicon* (mc-Si). Mc-Si has less crystal purity than sc-Si and thus less efficiency. For the first generation, the production process is described in chapter 5.1.3.

Thin films are assigned to the second generation. In this generation *amorphous silicon* (a-Si), *cadmium telluride* (CdTe), the alloys of *Cu(In,Ga)(S,Se)$_2$* (CIGS), e.g. copper indium diselenide, and crystalline silicon (c-Si) can be distinguished. In the case of thin films the semiconductor layer is directly deposited on a substrate, e.g. glass. The production is assumed to be cheaper than for first generation PV as less semiconducting materials are consumed and integrated manufacturing possibilities without wafer fabrication exist which seem to be easier than wafer production. This calculation does not work out as first generation PV is proceeding on the learning curve much faster than the second generation. Additional problems within the second generations are the low efficiencies of a-Si and CdTe, the low yield of the integrated manufacturing process, the toxicity of cadmium (used in CdTe and Cu(In,Ga)(S,Se)$_2$ production) and the lack of indium for Cu(In,Ga)(S,Se)$_2$ alloys limiting the possible capacity to approximately 90 GW. However, there are a lot of advantages of the second generation PV resulting in possible successes in niche markets, e.g. for applications in flexible modules, under low illumination conditions and at high temperatures. /Werner 2004/ emphasises that apart from the other three technologies c-Si has the potential to combine the advantages of crystalline silicon, e.g. material availability, non-toxicity and high efficiencies, with the advantages of thin films, e.g. less material consumption and large-area deposition.

The third generation aims to overcome the maximum efficiency limit of around 30 %. According to /Werner 2004/, five main concepts can be differentiated:

-    stacks of multiple cells (using different band gaps)
-    concentrator cells

- utilization of low-energy photons which are normally not absorbed
- hot electron cells generating additional electron/hole pairs for energies above the band gap
- photon conversion to adjust the spectrum of the sunlight to the characteristics of the semiconductor

However, all these concepts are still in the state of basic research.

Applications:

The ensemble of additional components for a PV system besides the modules is called *Balance of System* (BOS). The components vary depending on the type of electrical connection (grid-connected or off-grid) and the type of mounting structure (e.g. ground-mounted or building-integrated).

With grid connected systems the generated electricity is fed into an electricity grid. For this purpose a DC-AC inverter is required. A typical circuit diagram is shown in **Figure 5-5**. It shows the PV generator on a mounting construction. The modules are connected in serial to so-called strings. Several strings are connected in parallel in the junction box which has an overload protection. The strings have diodes which ensure that the direct current only flows in the right direction. Another protection device is the DC circuit breaker which breaks the connection between inverter and the junction box in order to ensure zero potential, e.g. in the case of maintenance in the downstream devices. The inverter converts the direct current into alternating current and feeds the power into the grid measured with electricity meters.
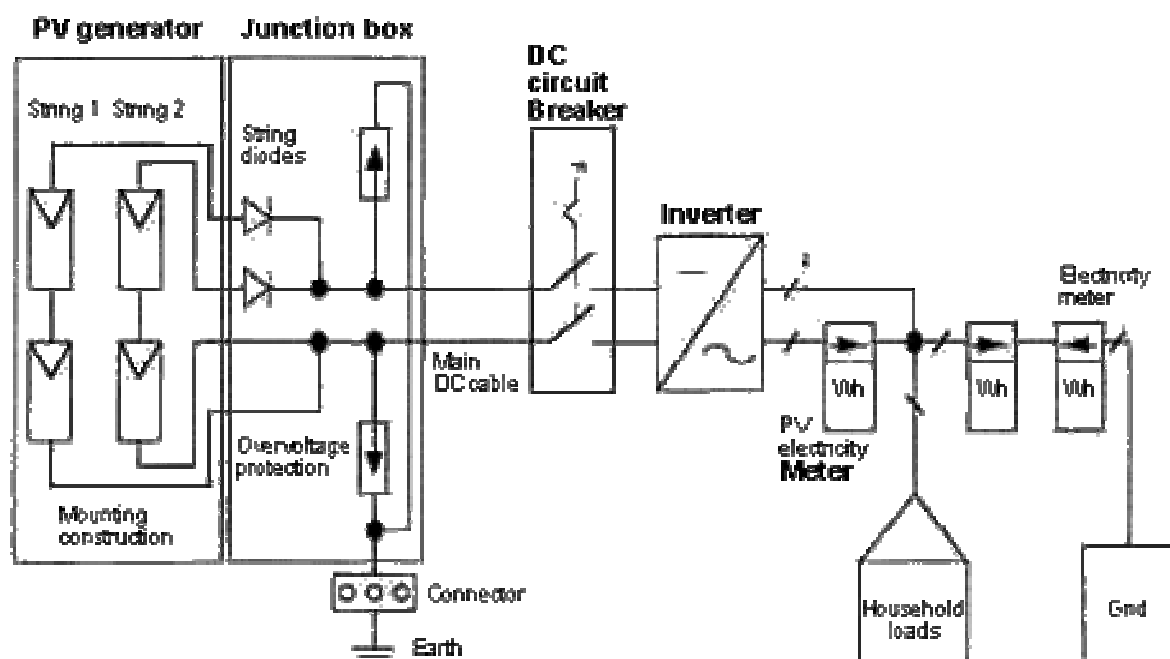
Figure 5-5:   Grid connected PV system /IEA-PVPS 2002/

Generally, an off-grid (stand-alone) system needs storage devices, e.g. lead-acid batteries, for stationary use. They are not considered further in this context. The focus is laid on grid-connected systems.

Ground-mounted power plants for more centralized electricity generation do need a large amount of surface. Their main potentials may be expected in deserted areas /Ito et al. 2004/. Building-integrated systems for more distributed generation can be differentiated into many different types. Further distinctions can be made between retrofit installation and integrated systems as well as for the type of surface between roofs and facades. At last one can distinguish between opaque PV cladding (e.g. roofs) and semi-transparent systems (e.g. skylights, facade windows, etc.). Chapter 5.1.3 gives more details.

Potentials:
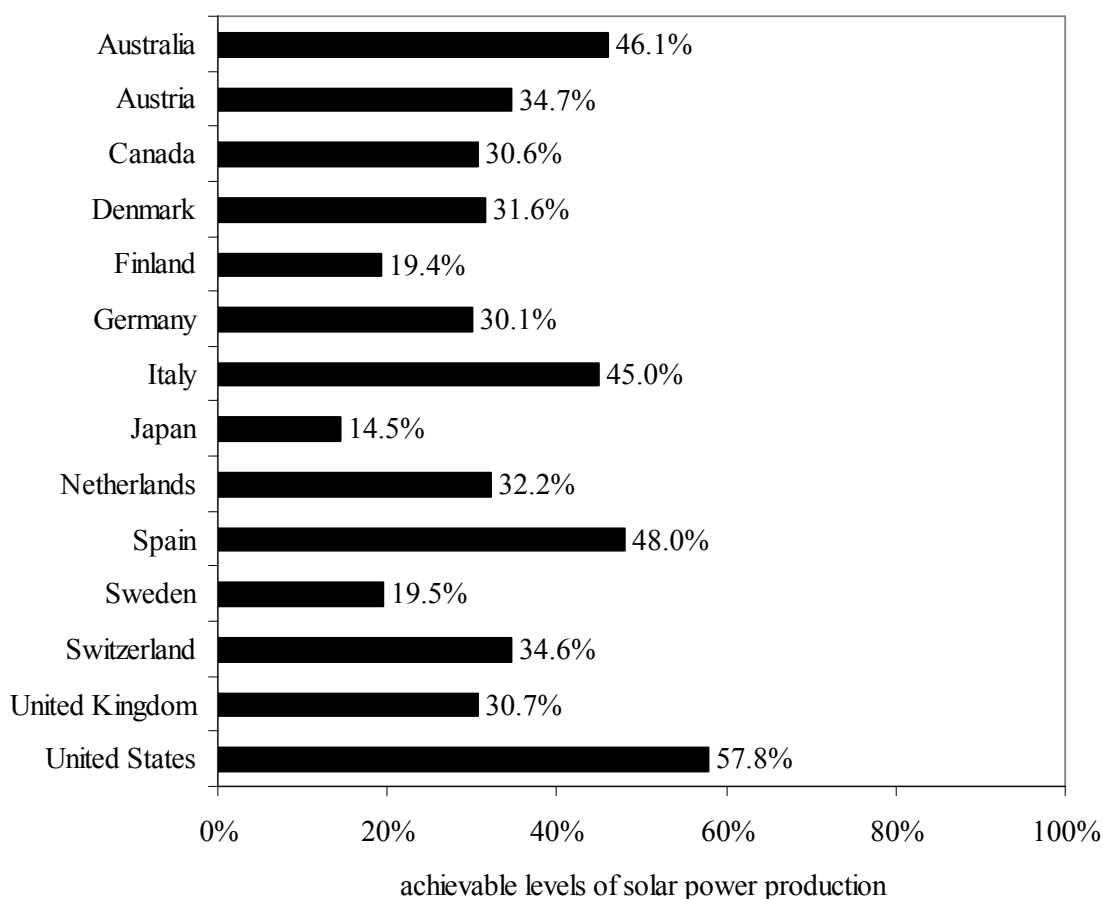
Figure 5-6: Achievable levels of solar power production from PV roofs and facades in the respective IEA country /IEA-PVPS 2001/

The sun irradiates annually an energy quantity of ca. 5,600,000 EJ to the earth. For comparison, the global primary energy consumption was ca. 357 EJ in the year 2001. With this energy balance it can be stated that theoretically 0.0065 % of the incoming solar energy may meet the present global primary energy demand. Unfortunately, the solar energy is distributed unevenly on the earth. The mean daily horizontal radiation in Europe is displayed in **Figure**

5-7 showing that there is an approximate factor of three between Northern and Southern parts of Europe.
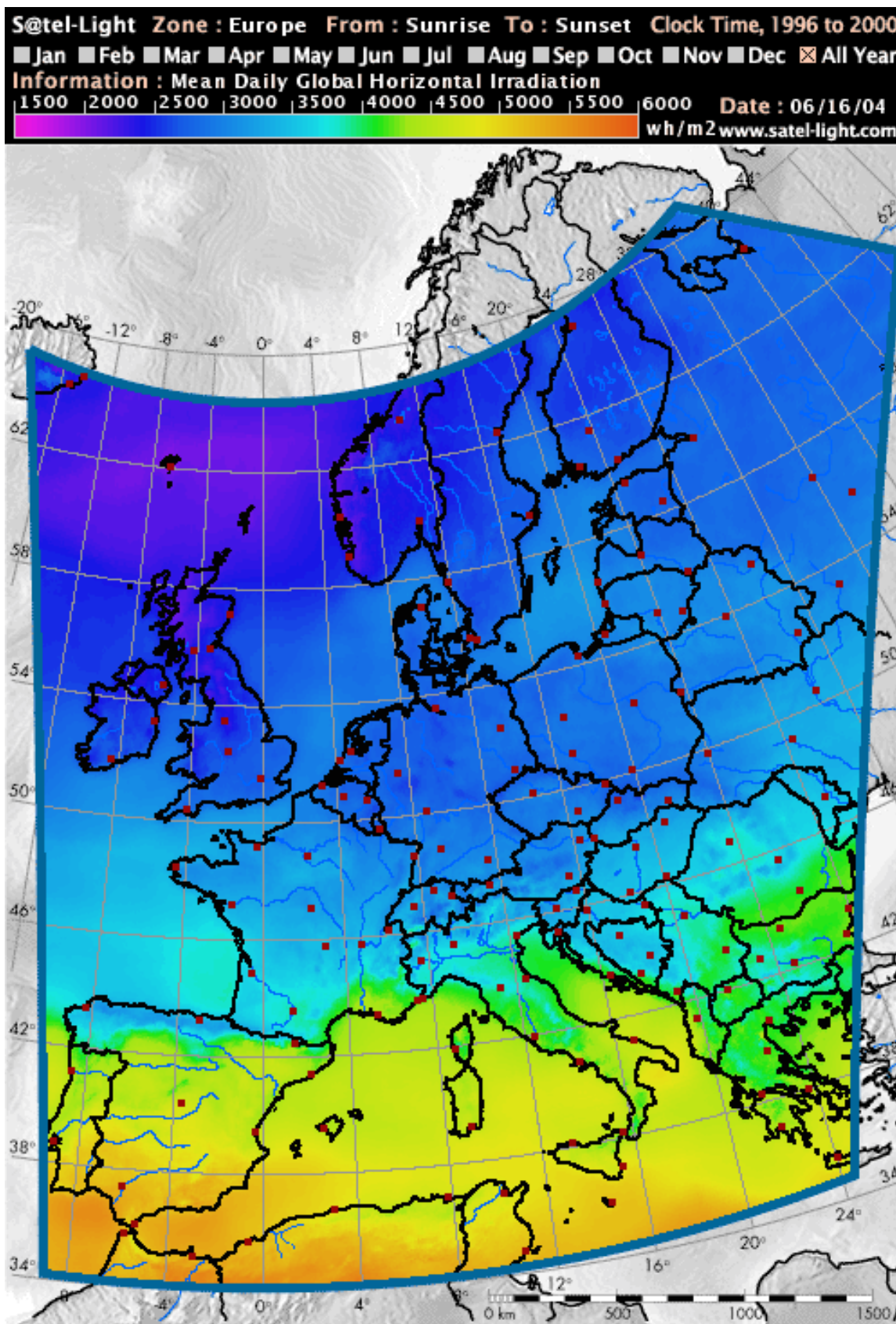
Figure 5-7:   Mean daily horizontal radiation in Europe (generated with *http://www.satel-light.com*)

Besides huge potentials in worldwide deserts (/Ito et al. 2004/ estimate that the recent world wide primary energy demand can be met with PV in the desert Gobi), /IEA-PVPS 2001/ determines large *achievable levels of solar power production* by PV roofs and facades in IEA countries. The *achievable level of solar power production* is the ratio of *building integrated PV solar electricity production potential* over *current electricity consumption* for the respective country. For the assumptions of a minimal solar yield of 80 % and an overall PV system efficiency of 10 %, the results are shown in **Figure 5-6**. European countries as Denmark, Germany and the United Kingdom have an achievable level of solar power production of ca. 30%.

5.1.2   Market development
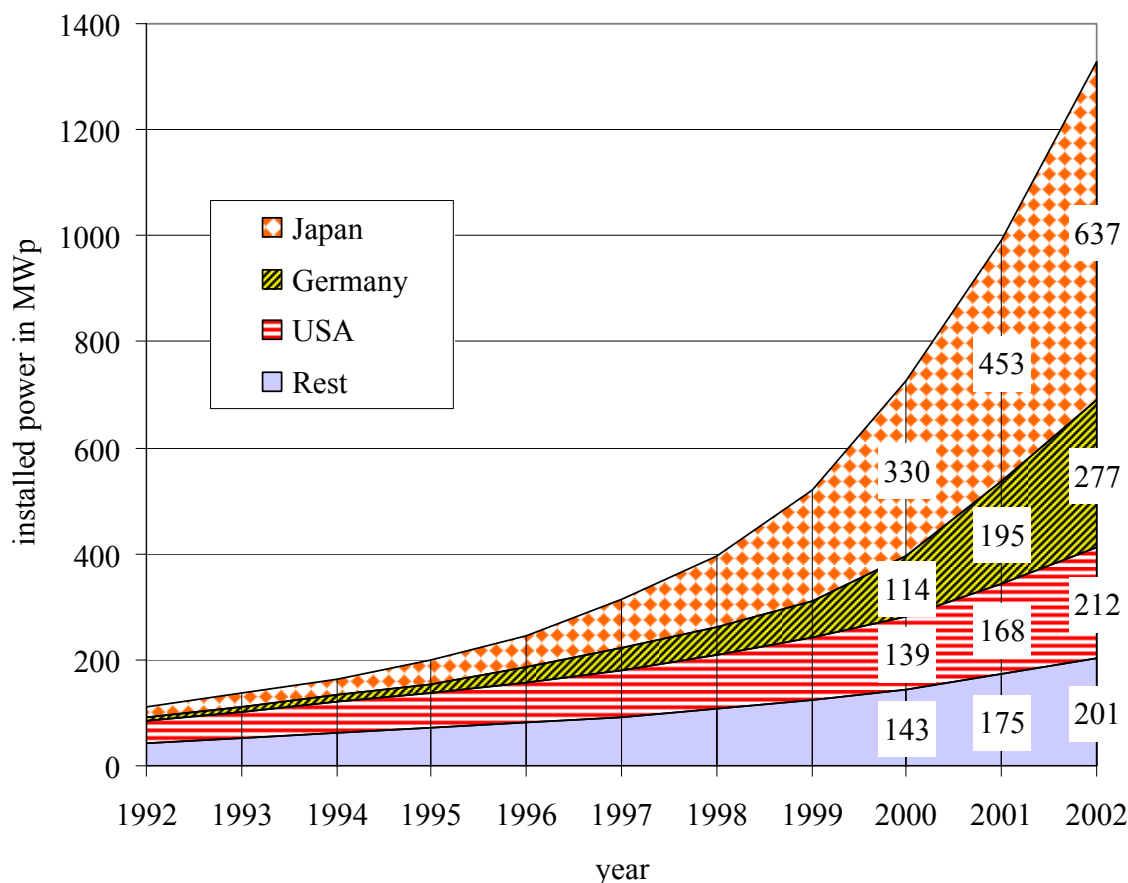
Figure 5-8:   Installed PV capacity world wide 1992-2002 in MWp /IEA-PVPS 2003/

In the *International Energy Agency's Photovoltaics Power Systems Programme* (IEA PVPS)[23] a yearly survey on trends in PV applications is carried out. The last published one is /IEA-PVPS 2003/. The main results are that the PV market world wide is booming with a

---

[23]   http://www.oja-services.nl/iea-pvps/index.html

yearly growth rate of approximately 30 % over the last 10 years (see **Figure 5-8**). The term peak power expressed in Watt peak (Wp) indicates the maximum power produced by a PV device when exposed to sun radiation with standard test conditions (solar radiation of 1,000 W/m², ambient temperature of 25 °C and an Air Mass of 1.5).

The proportion of capacity which is connected to the grid has been risen from 40 % in 1997 to 74 % in 2002 /IEA-PVPS 2003/. **Figure 5-9** shows the development of the proportion of different cell technologies on world markets. It displays that an increasing proportion of first generation cells dominates world markets with ca. 94 % and that second generation cells loose market shares mainly due to a-Si.

/Schmela 2004/ illustrates the shares on cell markets of different world regions. Japan has a share of 48.7 % (44.2 %), Europe 27.0 % (25.2 %), USA 12.0 % (20.7 %) and Australia, India as well as other Asian countries 11.5 % (10.0 %) in the year 2003 (2002). The world biggest PV cell producers are Sharp with a market share of 26.4 % (22.0 %), Kyocera 9.6 % (10.7 %), BP Solar 9.2 % (12.8 %) and Shell Solar 8.3 % (9.9 %).
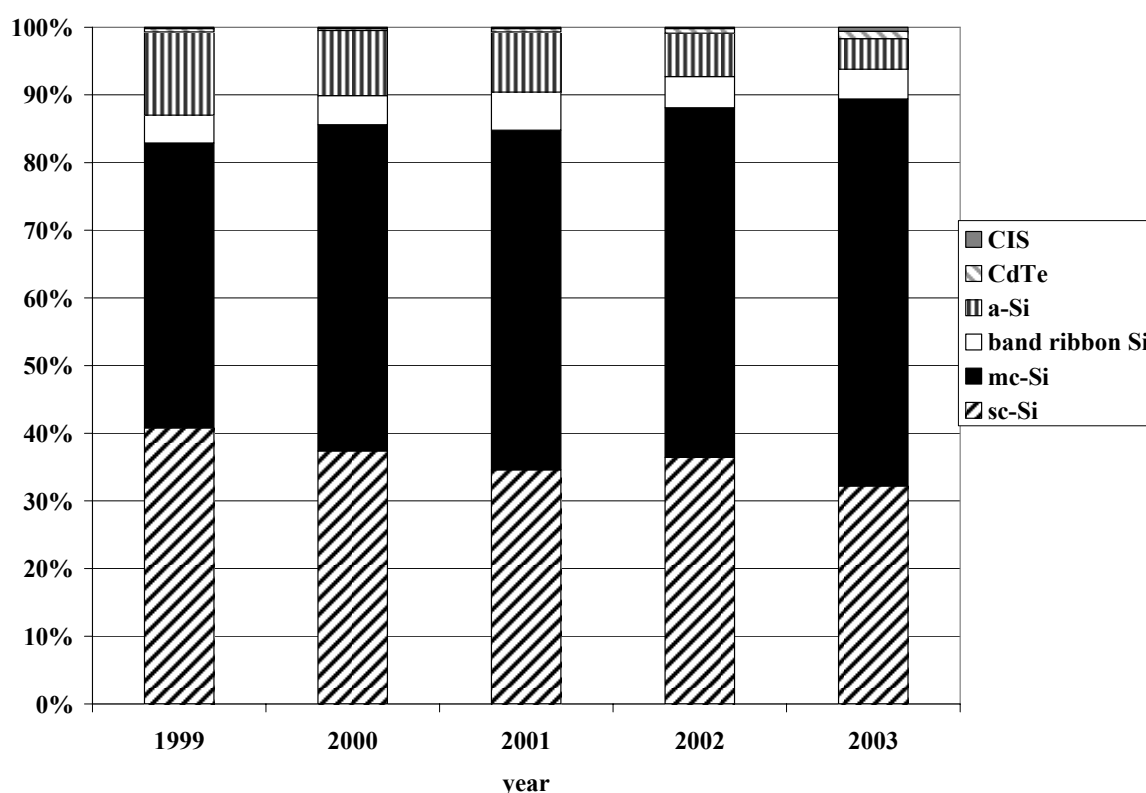
Figure 5-9: Shares of different cell technologies on world markets capacities /Schmela 2004/

Europe imports a large proportion of the demanded PV cells and modules above all from Japan and the USA. This market situation causes problems in representative life cycle analysis. /Frankl et al. 2004/ only consider a European life cycle which can not be used for detail LCA in the case of PV systems whose components are not made in Europe. An additional problem for LCA results from the high dynamics on the PV market where market shares decline (e.g. USA) or increase (e.g. Japan) with a high rate. Therefore, the presented LCI is just

an example of an assumed life cycle for European conditions and can not be used for gener-
alization because the European market only has a share of about a quarter of global markets.

5.1.3   LCA results in ECLIPSE

Thin film technologies are not analysed in this context because according to /Werner 2004/ a
large market penetration is not expected and the difference in LCI data is not significant as
illustrated exemplarily in **Figure 5-10**. The figure shows the comparison of the emissions of
the different technologies. CIGS and a-Si are within the range of sc-Si and mc-Si for CO_2,
SO_2 and NO_x emissions. Particulates emissions of the second generation technology are
higher and NMVOC emissions are lower than the emissions of the first generation technol-
ogy. Altogether it can be stated that external costs of the second generation are in the range of
the first generation technology. Thus it is not further analysed in this study.
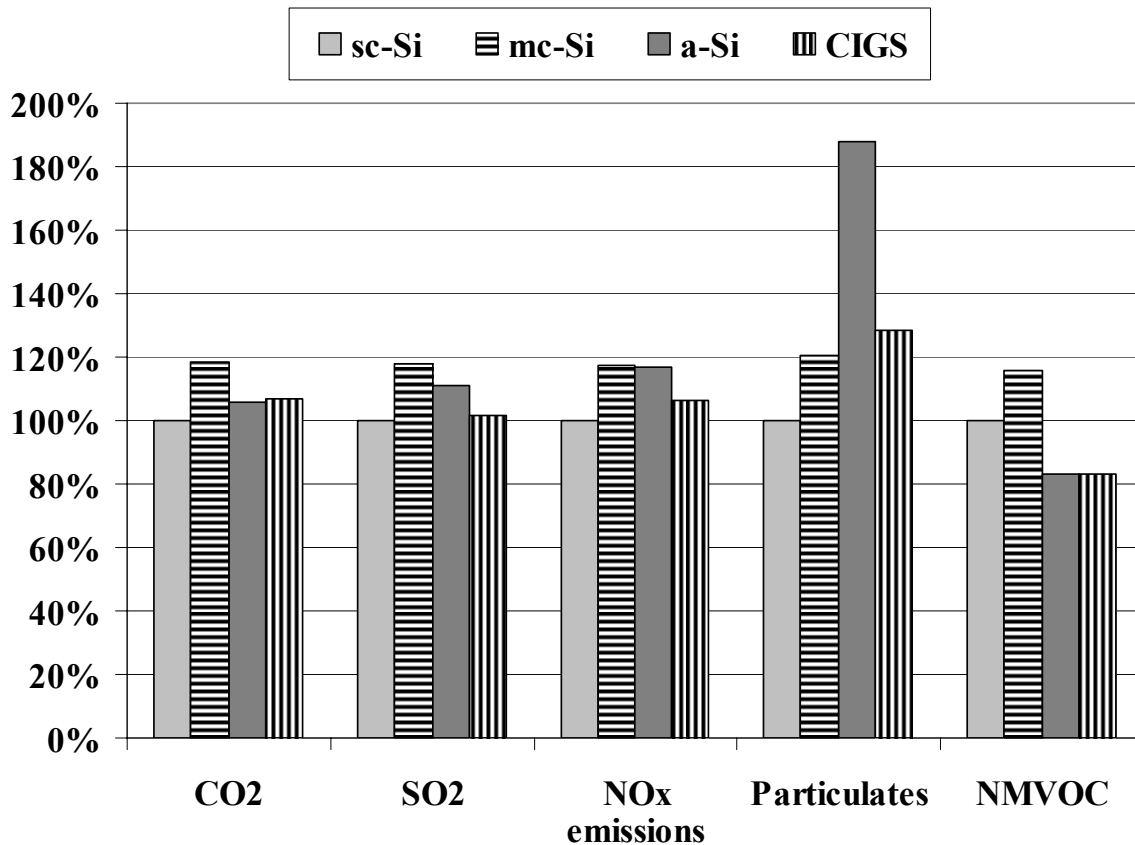
Figure 5-10:   Comparison of emissions of the different PV technologies in relation to sc-Si at the
reference site Italy (in kg/kWh_{el})

For the study at hand the emissions results of the common minimum lists of /Frankl et al.
2004/ are changed. In the total result list of the SimaPro software there are different indica-
tors concerning particulates: dust, dust (coarse), dust (coarse) process, dust (PM10) mobile,
dust (PM10) stationary, dust (SPM) and particulates (unspecified). /Frankl et al. 2004/ only
consider particulates (unspecified). For the calculations of external costs it is required to have

the classification of different sizes (i.e. PM2.5 and PM10) in order to be able to use the appropriate exposure-response functions. It was not possible to get any detailed specifications which allowed classifying the different indicators in the total result list. Therefore, it is assumed that the coarse particulates are larger than PM10 so that the particulates in the following tables are the sum of dust, dust (PM10) mobile, dust (PM10) stationary, dust (SPM) and particulates unspecified.

A similar problem arises with the sulphur dioxide. The total result list includes the indicators SO_2, SO_x and SO_x (as SO_2). It was not possible to get further background information. Therefore, it is considered that sulphur dioxide is calculated with the sum of all three indicators. However, in some examples /Frankl et al. 2004/ only sum SO_x and SO_x (as SO_2) but not SO_2. In this study it is assumed that sulphur dioxide is calculated as the sum of all three indicators.

Assumptions:

/Frankl et al. 2004/ take three geographic locations for operation: Central Italy as the reference case, Spain as a case with maximum insulation and Northern Europe for minimal insulation. They use direct manufacturing and efficiency data from a specific process and company typical for the year 2001 and literature data from /Dones et al. 2003/. For the forecast 2005-2010 no technological breakthroughs and only marginal changes in key influencing parameters are considered. There are no direct data on module recycling available. Therefore, only recycling of metals is taken into account and all the rest of materials are assumed to be disposed via landfill. This is a correct approach because for actual PV systems no recycled modules are used. In future systems this may change because recycling technologies are developed to close the material flow. In the coming years this may only be a very small proportion because of the high growth rate of PV systems and their long life times.

Life Cycle:

The main life cycle phases of a PV system are the manufacturing of modules, the production of Balance of System (BOS), the operation and the end-of-life. They are illustrated in **Figure 5-11**.

Silicon feedstock production:
The first unit process for crystalline silicon modules is the production of the silicon feedstock. *Metallurgical-grade silicon* (MG-Si) is prepared from quartz sand within an arc furnace at temperatures higher than 1550 °C. The silicon dioxide (SiO_2) is reduced with carbon to MG-Si and CO.

$$SiO_2 + 2C \rightarrow Si + 2\,CO$$
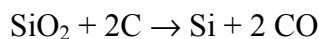
This MG-Si has to be purified further into *electronic-grade silicon* (EG-Si). Firstly, the MG-Si has to be cleaned. For this process the MG-Si reacts at temperatures of 300-400 °C with *hydrochloride acid* (HCl) forming liquid *trichlorosilane* ($SiHCl_3$) and hydrogen with the reaction

$$Si + 3HCl \rightarrow SiHCl_3 + H_2$$
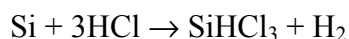
The trichlorosilane is distilled many times resulting in higher purity. In the next step the Si has to be extracted with chemical vapour deposition at temperatures of ca. 1,000 °C. In this process the trichlorosilane reacts with hydrogen on the surface of a hot silicon rod serving as a nucleus for condensation of silicon with the reaction

$$4SiHCl_3 + 2H_2 \rightarrow 3Si + SiCl_4 + 8HCl$$
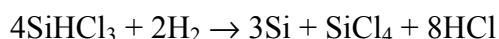
By-products of this reaction besides the high-purity silicon are hydrochloride acid (HCl) and *silicon tetrachloride* ($SiCl_4$). The result is a polycrystalline silicon rod with high-purity EG-Si. In order to get single-crystalline silicon Czochralsky-growth is performed (see **Figure 5-12**). In this process a small silicon single crystal serves as a seed for the condensation of liquid polycrystalline silicon needing temperatures above 1,415 °C (melting point of Si). The growing sc-Si rod (ingot) is slowly drilled and drawn out of the melt. Another possibility to get sc-Si out of mc-Si besides the Czochralsky-growth is the float-zone growth which is not analyzed in /Frankl et al. 2004/.

For the present scenario of PV silicon feedstock the assumption of 50 % off-spec EG-Si scraps and 50 % non-prime direct poly-Si production is considered based on the situation in 2001.

Off-spec EG-Si scraps originate in the purification as well as in the Czochralsky crystallization process. This route is very inefficient because a second crystallization step has to be performed for the PV industry. Economic allocation is used because the scraps (11 % of the total EG-Si mass) would be produced anyway resulting in an allocation factor of 3.2 % due to less economic value of the scraps (20 €/kg instead of 75 €/kg for the electronic industry).

Poly-crystalline silicon produced by the silicon industry is directly sold as feedstock to the PV industry. It is called *non-prime direct poly-crystalline silicon* (poly-Si). The energy need is expected to be lower because the PV industry requires a lower purity than the microelectronics industry enabling a faster purification process. However, /Frankl et al. 2004/ assume the same inventory data as for EG-Si excluding the ones referred to the Czochralsky-growth because no reliable data were available. Since the production is made on purpose for the PV industry the allocation factor is 100 %.
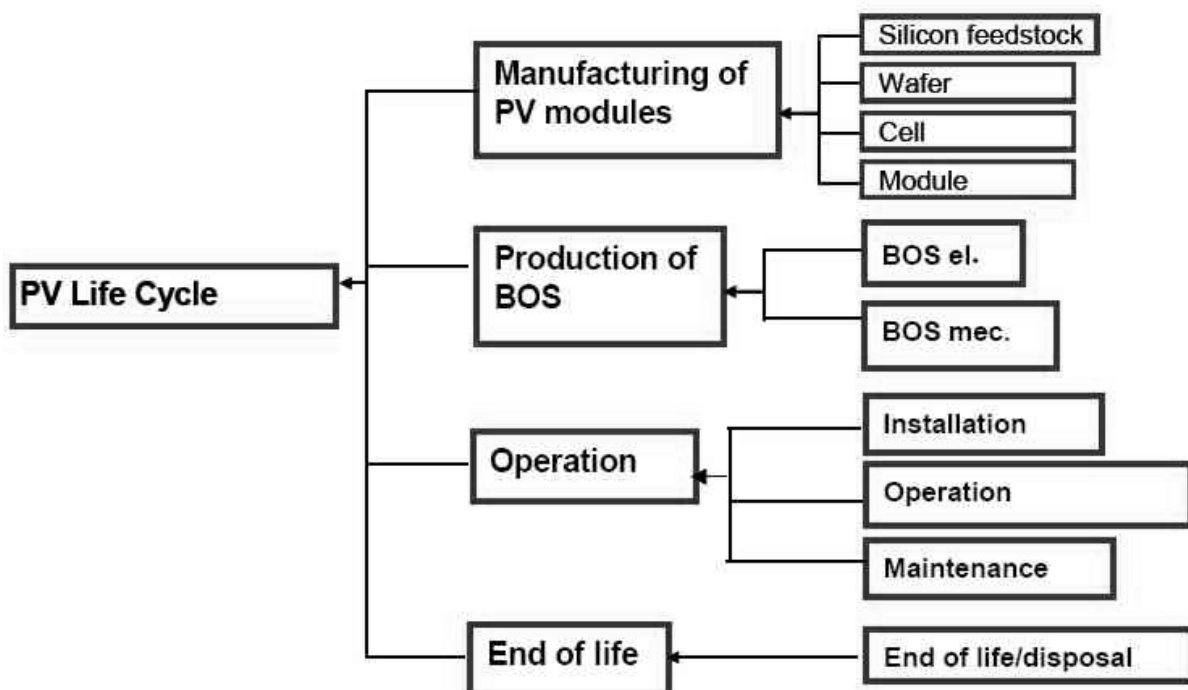
Figure 5-11: PV Life cycle phases /Frankl et al. 2004/
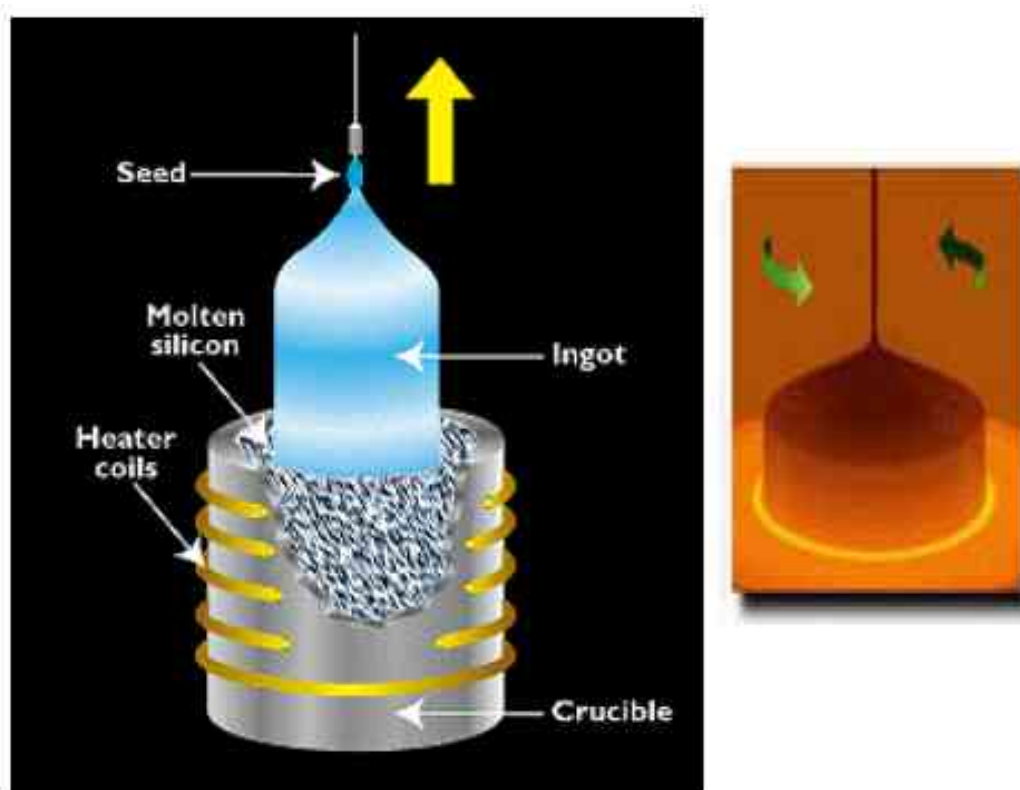
Figure 5-12: Czochralsky-growth /Carter 2001/

In the future, other processes for *solar-grade silicon* (SG-Si) production are likely to be used. In all cases energy consumption and other emissions are expected to be considerably lower than at present. However, reliable primary data are still not available so far, so that

/Frankl et al. 2004/ assume the future Si feedstock to be 25 % EG-Si scraps based on economic allocation and 75 % direct poly-crystalline silicon. /Willeke 2004/ describes that there is expected to be a operational plant for SG-Si in the year 2005 and an increasing production to meet the demand of the PV industry.

Wafer production:

The production of sc-Si wafers includes five steps: scraps washing, ingot growth with Czochralsky process, ingot squaring, ingot cutting, wafer washing and testing.

As a first step, the silicon feedstock is washed chemically to eliminate surface impurities. Then it is crushed in order to make it more homogeneous. /Frankl et al. 2004/ consider losses of 1 % of non re-usable contaminated silicon waste.

In the next step for sc-Si, the ingot growth is made with the Czochralsky casting process described above. Adding *boron* (B) to the melt, p-dopes the ingot. Instead of the Czochralsky process, for mc-Si a directional solidification casting process is used which is much less energy-intensive and cheaper. However, mc-Si is a less pure and more fragile material than sc-Si. This results in lower cell efficiencies and the need for thicker wafers. The product of directional solidification process with a Si-mass yield of 99 % is a block. The material losses cannot be recycled. A technology which is not considered in /Frankl et al. 2004/ is the crystalline growth on ribbons.

The ingot is contoured and squared in order to optimize the area of PV cells in the third step. For the case of sc-Si, /Frankl et al. 2004/ assess quasi-squared wafers of 156 cm² area as well as a mass efficiency of 65 % due to material losses. They also assume a specific electricity consumption of 123 kWh/kg wafer material based on /Frischknecht 2003/ referring to the production data from Wacker. Up to 80 % of the silicon losses can be recycled and re-used as Si feedstock input. In the case of mc-Si, a large part of the ingot is not pure enough and should be cut away during the contouring and portioning step resulting in a mass yield of 66 %. Only 50 % of the silicon waste generated in this step can be re-used for internal feedstock recycling. All inventory data for this unit process are taken from /Cherubini 2001/.

In the forth step the ingot is cut into wafers. The most common technology is the multi-wire saw presently producing sc-Si wafers with a thickness of 220-350 µm. Since sc-Si is more homogeneous and thus less fragile than mc-Si the lower figures of present commercial wafer and wire thickness are chosen. The cutting parameters and mass yield for sc-Si as well as mc-Si are listed in **Table 5-3**.

Mc-Si re-used wafers are considered for a future scenario which is described in a sensitivity analysis below. In this case, after their end of life the dismantled cells are chemically and thermally treated and converted into new wafers. Due to the lack of detailed data only the energy consumption of the process is analyzed.

/Willeke 2004/ expects that the wafer thickness will be reduced to 180 µm in 2010 and 100 µm in 2020. Kerf losses in /Willeke 2004/ do not comply with the kerf losses in /Frankl

et al. 2004/ because /Willeke 2004/ assumes a reduction from 250 μm at present to 160 μm in 2010 and 150 μm in 2020. Thus, /Frankl et al. 2004/ probably make an underestimation.

In the fifth step the wafer is washed and tested.

Table 5-3: Cutting parameters and mass yield for sc-Si and mc-Si wafers /Frankl et al. 2004/

Wafer	Wafer thickness	Wire thickness / cutting losses	Cut yield	Process yield due to broken wafers	Total Si-mass yield
sc-Si present	250 μm	150 μm	62.5 %	95 %	59.4 %
sc-Si future	180 μm	120 μm	60.0 %	95 %	57.0 %
mc-Si present	300 μm	200 μm	60.0 %	95 %	57.0 %
mc-Si future	180 μm	120 μm	60.0 %	95 %	57.0 %

Cell manufacturing:

The production of standard cells proceeds the following steps:

In the first step, wafers are put in several chemical baths in order to obtain a perfectly clean wafer surface. The second step is the n-doping of the front surface with *phosphor* (P) atoms. Temperatures of 800°-900°C ensures the diffusion of P atoms to the p-n junction zone. In this step, a coat of phosphor glass is formed which must be etched. In order to decrease surface reflection a *titanium dioxide* (TiO_2) coating is applied with chemical vapour deposition. For the front contacts a very thin metallic grid with silver paste and for the back contacts a thin aluminium-silver paste layer is applied. Then, the anti reflection coating and the contacts are sinterized. Finally, the quality of cells in terms of light conversion efficiency is tested with the help of a sun simulator. The process yield of 92 % is taken as a conservative assumption. Non qualified or broken cells are sent to internal recycling. For the present sc-Si cells, an efficiency of 15 % is used and 18 % efficiency for future cells. However, due to the lower performances of mc-Si cells, an efficiency of 12 % is used for present and 15 % efficiency for future cells.

/Frankl et al. 2004/ state that the environmental hot-spots of PV cell manufacturing are electricity consumption and emission of chemicals into the water. In the study at hand, only the first hot-spot is taken into account. The last one is not considered any further.

In the wafer production as well as in the cell manufacturing silicon waste is produced. A part of it can be recycled as internal feedstock. This results in a net decrease of the input of external feedstock. In the case of sc-Si for present configurations, the recycled and re-used silicon is assumed to be 36 % of the total silicon feedstock input. The scraps coming from ingot shaping are the main source of recycled feedstock. Recycling from contaminated Si waste of the cutting process is not yet achieved. /Frankl et al. 2004/ assume for future configuration that about 50 % of the silicon powder from the wire-saw slurries will be recovered.

In the case of mc-Si at present, about 50 % of the silicon waste generated during ingot contouring and portioning can be recycled. A future recycling rate of silicon waste generated in the cutting phase of about 58 % is considered. Altogether, the internal recycled feedstock for present mc-Si production is 22 % of the total silicon feedstock input. For improved future mc-Si module production, the internal recycled feedstock is 50 % of the total silicon feedstock input.

Module assembling:

The assembling of sc-Si modules includes the unit processes electric contacts formation, production of encapsulation materials, lamination, frame production and mounting, junction box production and mounting as well as module testing.

In the first step, electric contacts made from small copper tapes are created and welded in order to connect the cells. The lamination as the second step is the sealing of the cells in an encapsulation. For electrical insulation the cells are encapsulated by an *ethyl-vinyl-acetate* (EVA) layer. At the front, a tempered glass sheet with high light transmittance and good mechanical resistance is applied. On the back, an opaque substrate, e.g. tedlar, or a transparent substrate, e.g. glass, is applied. This sandwich is put in an oven, in which the EVA foils polymerize, become transparent and guarantee the sealing. The next step is the production and mounting of the junction box, usually made of *polyvinyl chloride* (PVC). Finally, the last step is the module testing.

Hot spots of environmental impacts in the module assembling process are the mass-efficiency of the process and the efficiency of the modules. For present sc-Si modules, 13 % efficiency are taken into account. Future sc-Si modules are expected to reach 16 %. This is a realistic and conservative estimation because the SunPower Corp. completed a 25 MW/year factory in May 2004 where cells with 19.9 % efficiency have been produced /Mulligan et al. 2004/. With the same technology cells with 21.5 % efficiency have been produced in a pilot line which were assembled to a module with a record efficiency of 18.2 %. Future efficiencies of some modules may thus surpass 16 % but the average efficiency of all modules on the markets may be in this region. In the case of semi-transparent sc-Si modules, cells are usually placed slightly more distantly, thus leading to lower module efficiencies of 12 % at present and 15 % in the future. For present mc-Si modules 10.7 % efficiency has been taken into account and 13.5 % for future ones. In the case of semi-transparent mc-Si modules lower module efficiencies of 9.5 % at present and 12.5 % for the future are assumed.

Life times of present modules are assumed to be 25 years which is mostly guaranteed by module manufacturers. The assumption for future modules is that their life time will be 30 years. This is surpassed with the expectations of /Willeke 2004/ with an assumed life time of 35 years in the year 2010.

/Frankl et al. 2004/ use the inventory data from studies of 1996 and 2001. The assumed electricity mix is the European one as described in the methodological guidelines of

ECLIPSE. However, several PV firms today use renewable energy. This scenario is covered in a sensitivity analysis in the text below.

Mechanical BOS:

The impact share of mechanical BOS over the whole life cycle of PV systems is mainly caused by indirect impacts related to the production processes of materials used for the mounting structures of the PV modules (steel, concrete, aluminium etc.).

In /Frankl et al. 2004/ the following cases are considered:

- *Tilted roof retrofit*: This structure supports PV modules fixed to the roof without substitution of cover material.
- *Flat roof*: PV modules are mounted on a tilted structure fixed to the flat roof through concrete blocks.
- *Integrated tilted roof*: PV modules are integrated in the roof substituting cover tiles.
- *Solar roof tiles*: They are a particular roof integrated installation replacing the conventional clay tiles and substituting a part of the roof.
- *Sun shading façade retrofit*: PV modules are integrated in a sun shading system.
- *Skylight integrated*: It is a partly see-through photovoltaic roof completely replacing the original roof materials. No specific supporting structures are needed and, therefore, no material demand is considered for the BOS.
- *Vertical façade integrated*: The PV modules completely replace the original materials and no specific PV supporting structure is used. Therefore, no BOS is considered.
- *Aluminium reflector in a flat roof*: It is an integration structure installed on a flat roof PV system in order to increase the net solar radiation on PV modules. It is placed between two PV module rows. The reflector is mainly composed of steel and aluminium.
- *Ground-mounted*: It needs a foundation and, thus, has a significant demand of materials.
- *Solar roof tiles with heat recovery*: An integrated system with solar roof tiles is complemented with a heat recovery unit. The heat recovery unit collects the heat dissipated by the photovoltaic modules. This application is taken into account for future configurations.

Electrical BOS:

/Frankl et al. 2004/ consider two kinds of inverters: one for small PV systems (< 5 kWp) with an efficiency of 95 % and one for large PV systems (> 100 kWp) with an efficiency of 96 %. Both inverters are considered to have a lifetime of 12 years. Therefore, more than one inverter is needed over the whole lifetime of a PV system.

Installation:

The installation of the PV system depends on the different configurations. The transport of materials is included in the assessment. It is assumed that a medium regional lorry drives an average distance of 300 km for the transport of modules from the production company to the installer and 100 km for the transport of modules and BOS materials from the installer to the installation site.

Operation:

The most important parameter for the operation is the solar radiation depending on the plant site (see **Figure 5-7**). In the Southern part of Europe the same PV systems produces the three fold amount of energy compared to the same system in the Northern part.

The optimal insolation can only be obtained in the cases of flat roofs and ground-mounted power plants whose orientation is optimized. In all other cases there are energy losses due to possible disorientation because average systems are not oriented optimal. For this disorientation losses, /Frankl et al. 2004/ use correction factors in order to represent average, suboptimal figures. Additional losses occur due to high temperatures in installations with low ventilation as the voltage output of modules decreases with increasing temperatures. A general correlation is that the more southern the location, the less energy is collected on a vertical façade and the higher are temperature losses.

The correlation between the different efficiencies can be formalized. The *annual energy production* E is the product of the *average annual solar radiation on optimal tilt angle* I and the *total PV efficiency* η_{PV} which is in the considered examples between 50 % for a vertical façade in Southern Spain and 91 % for a flat roof in Central Europe. The *total PV efficiency* η_{PV} is the product of the *BOS total efficiency* η_{tot} and the *module efficiency* η_{mod} whereas the BOS total efficiency is the product of the *BOS position efficiency* η_{pos} and the *BOS efficiency* $\eta_{BOS,el}$ which is the product of the *BOS inverter efficiency* η_{inv} and the *BOS losses efficiency* η_{loss} (mismatching, temperature effect etc.):

$$E = I \cdot \eta_{PV} = I \cdot \eta_{tot} \cdot \eta_{\mathrm{mod}} = I \cdot \eta_{pos} \cdot \eta_{BOS,el} \cdot \eta_{\mathrm{mod}} = I \cdot \eta_{pos} \cdot \eta_{inv} \cdot \eta_{loss} \cdot \eta_{\mathrm{mod}} \quad (5\text{-}8)$$

Maintenance:

Labour and the electricity consumption for the dismounting of defect modules is considered to be negligible. The only important maintenance operation over the life time is the replacement of the inverter which is thus counted twice in the life cycle phase installation.

End-of-life:

Direct data for end-of-life of dismantled PV systems are not available. The assumptions for the present scenario are that 80 % of disassembled aluminium and ferro-metals components are recycled and the other parts are disposed to landfill. For the future scenario, it is assumed

that 80 % of disassembled aluminium and ferro-metals components as well as 100 % of modules are recycled and the other parts are disposed on a landfill. The transports to recycling facilities and to landfills are taken into account with a medium distance of 50 km to separate collection facilities, 50 km to landfill and 200 km to inert landfill.

The data sources of the PV life cycle follow the methodological guidelines in /Setterwall et al. 2004/ with the exception of the data for Si feedstock production from /Frischknecht 2003/, the data for PV modules production from /Frischknecht 2003/, /Cherubini 2001/ and /Frankl 1996/ as well as the data for the BOS materials from /Frankl 1996/ and /Frankl; Gamberale 1998/.

Results of the examples:

Sc-Si:

Table 5-4 lists the technical data for a sc-Si PV system in Central Italy as reference case. The PV system is retrofit installed on a tilted roof and has a peak power of 1 kWp. A system representing the present case and a system representing a future case (around 2010) are compared.

Over the whole life cycle of a PV system the module manufacturing causes the main part of the emissions. This is displayed in **Figure 5-13**. 60 % of particulates and 75-90 % of the other emissions are caused by the module manufacturing. Most of the remaining contribution is caused by the production of the BOS.

In the life cycle phase module manufacturing, the module assembling, wafer production and the silicon feedstock are responsible for similar parts of the emissions with the exception of particulates which are mainly caused by module assembling (see **Figure 5-14**). /Frankl et al. 2004/ point out that the high share of the module assembling unit is due to the high energy content of the aluminium frame mounted. Furthermore, they point out that in the silicon feedstock unit the highest share comes from the direct poly-Si because economic allocation is considered for the LCI flows of off-spec EG-Si scraps. Finally, they explain that the impacts from BOS production are mainly caused by the production of aluminium and steel components.

Three locations are considered in /Frankl et al. 2004/. Central Europe with a radiation of 1,200 kWhm^{-2}a^{-1} on a south-oriented 35° tilted surface, Central Italy with an radiation of 1,740 kWhm^{-2}a^{-1} on a south-oriented 30° tilted surface and Southern Spain with an radiation of 2,000 kWhm^{-2}a^{-1} on a south-oriented 27° tilted surface.

Table 5-5 shows the parameters of different plant sites. The correlations between these parameters can be derived from this table. The more southern the site the higher the radiation as the insolation angle is steeper. Therefore, the optimal tilt angle for fixed PV systems should be flatter. With increasing insolation the average temperature increases resulting in more losses due to the temperature effect and thus decreasing η_{loss}. PV modules have the character-

istic that the voltage drops with increasing temperature (temperature effect). The increasing radiation compensates the decreasing efficiency resulting in more energy yield for the same PV system the more southern the site. Since the emissions of the life cycle are assumed to be independent from the site, the amount of emission of the considered systems stays constant. This results in the correlation that the more southern the site the less emissions per energy unit occur as displayed in the last row of **Table 5-5**. For the same PV system in Germany instead of Southern Spain, 83 % more emissions are contributed to each energy unit. Or the other way around, the same PV system in Southern Spain cause 46 % less emissions than in Germany. The latter correlation is displayed in **Figure 5-15**. Germany is an additional consideration in the study at hand and not regarded by /Frankl et al. 2004/. The radiation for Germany has a lower average value because it ranges from 950 $kWhm^{-2}a^{-1}$ in Northern Germany to 1150 $kWhm^{-2}a^{-1}$ in Southern Germany. The figures in brackets added in the rows of tilt and azimuth angle show the possibilities of variation for the angles in order to achieve a position efficiency of 95 %. Therefore, the tilt angle in Germany can be in the range of about 6-46° and the azimuth angle in the range from -60° to +60° /PHOTON 2004/. These possible ranges illustrate that the position efficiency of 95 % covers a very large part of roof orientations.

Table 5-4:   Technical data for a sc-Si PV system in Central Italy retrofit installed on a tilted roof with a peak power of 1kWp /Frankl et al. 2004/

Technical data	Present sc-Si system	Future sc-Si system
Internal recycled feedstock	36 %	35 %
External silicon feedstock	64 % (50 % EG-Si scraps and 50 % direct poly-Si)	65 % (25 % EG-Si scraps and 75 % direct poly-Si)
Wafer thickness	250 μm	180 μm
Wire thickness	150 μm	120 μm
Module efficiency	13 %	16 %
Module equipment	glass-tedlar, aluminium frame	solar roof tiles
Installation	30° tilt angle, 0° azimuth angle	30° tilt angle, 0° azimuth angle
η_{pos}	95 %	97 %
η_{loss}	90 %	92 %
η_{inv}	95 %	95 %
η_{tot}	81 %	85 %
Radiation	1740 kWh/m² a	1740 kWh/m² a
Annual electricity production	1413 kWh/kWp a	1475 kWh/kWp a

Figure 5-13: Contribution of life cycle phases to the emissions of a present sc-Si PV system that is installed on tilted roof retrofit (in kg/kWh$_{el}$)
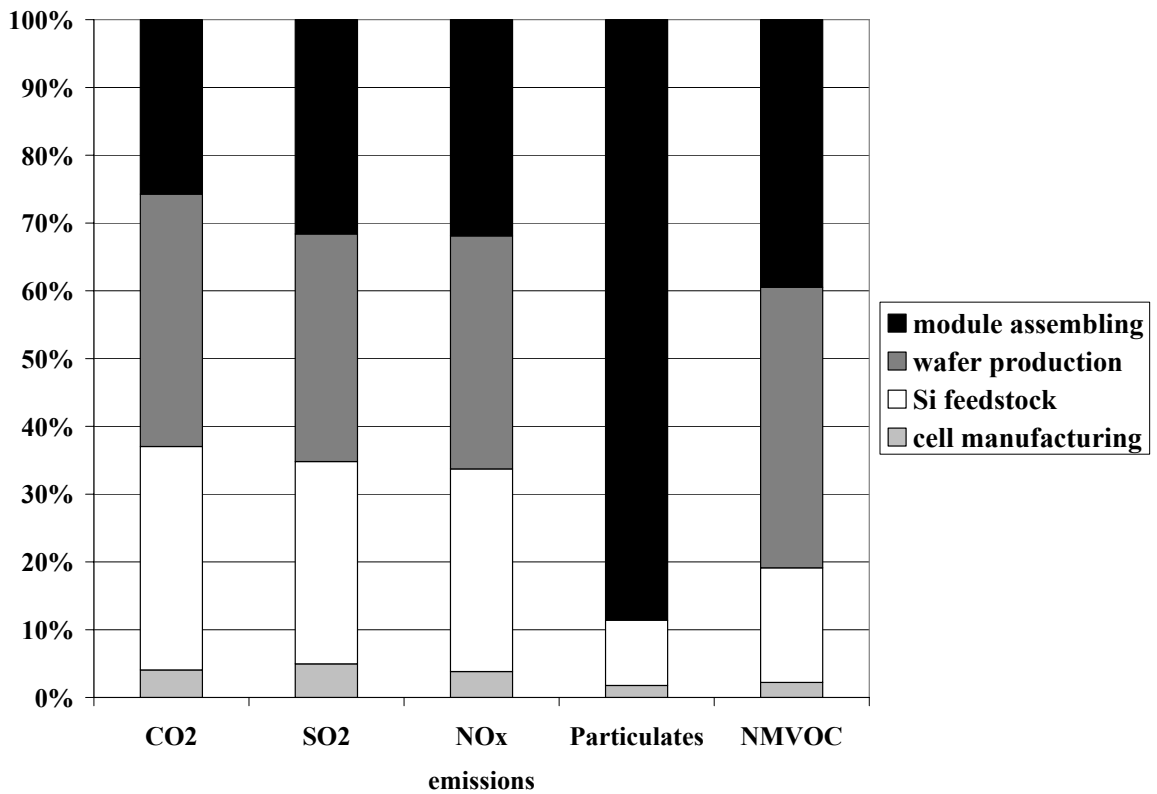
Figure 5-14: Contribution of the module manufacturing units to the emissions in the case of sc-Si (in kg/kWh$_{el}$)

Table 5-5:   Parameters of different plant sites /Frankl et al. 2004/

Parameters	Southern Spain	Central Italy	Central Europe	Germany
Radiation	2000 kWh m^{-2}a^{-1}	1740 kWh m^{-2}a^{-1}	1200 kWh m^{-2}a^{-1}	1000 kWh m^{-2}a^{-1}
Tilt angle	27°	30°	35°	36° (+10°,-30°)
Azimuth angle	0°	0°	0°	0° (+-60°)
η_{pos}, η_{inv}	95 %	95 %	95 %	95 %
η_{loss}	88 %	90 %	96 %	96 %
η_{tot}	79 %	81 %	87 %	87 %
Relative emissions/kWh$_{el}$	0.89	1.00 (reference)	1.36	1.63
	1.00 (reference)	1.12	1.53	1.83
	0.65	0.74	1.00 (reference)	1.20
	0.54	0.62	0.83	1.00 (reference)
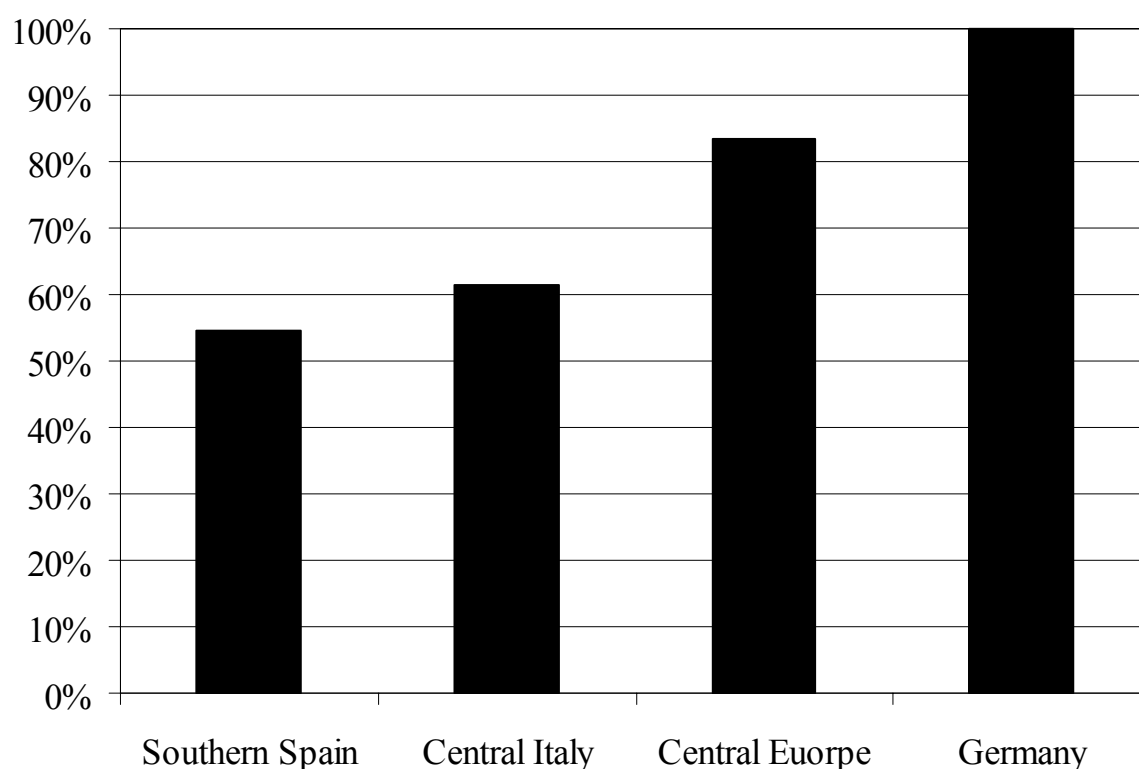
Figure 5-15:   Comparison of the emissions at different sites for the same PV system (in kg/kWh$_{el}$)

Figure 5-16 illustrates the influence of different Si feedstock combinations on the emissions per kWh in the case of a sc-Si PV system on tilted roof. It shows that the direct poly-Si feedstock is responsible for more specific emissions than EG-Si scraps based on economic

allocation. With the third bar it is shown that EG-Si scraps based on mass allocation are responsible for more specific emissions than direct poly-Si.
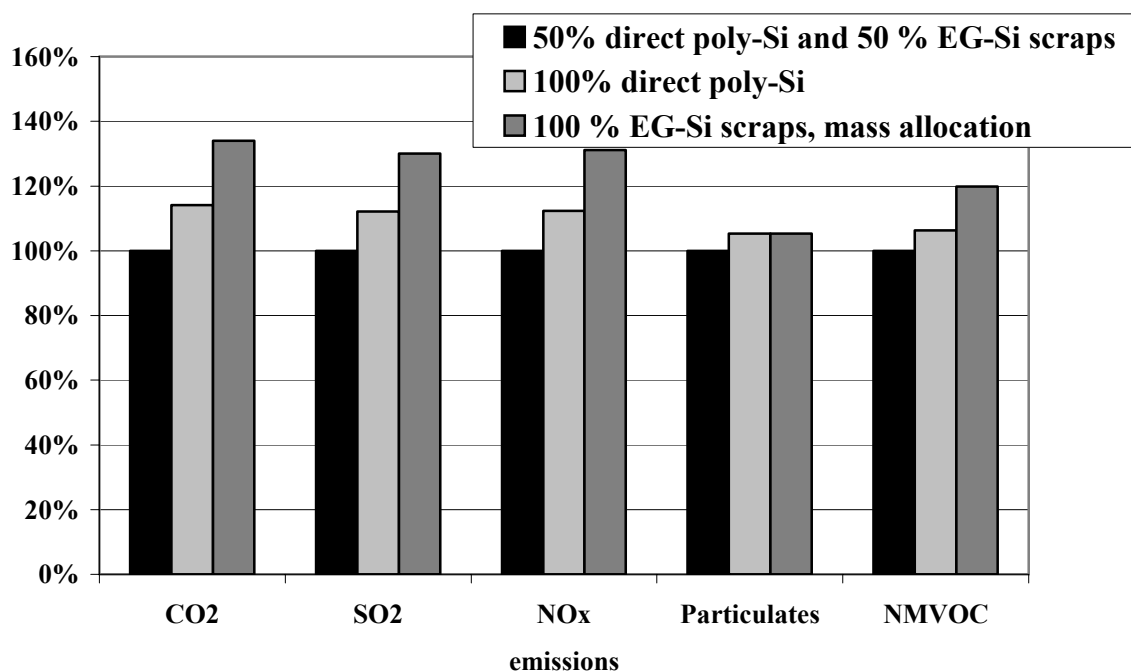
Figure 5-16: Comparison of the emissions for different Si feedstock combinations in the case of sc-Si on tilted roof (in kg/kWh_{el})

For the future case the results are significantly better than for the present case. This results from several improvements (see **Table 5-4**): The modules do have a higher efficiency. Thinner wafers and less cutting losses are responsible for a better Si mass efficiency. Higher total BOS efficiency results from a better control of thermal losses and a better positioning which can be achieved with improved planning. Lastly, a lower amount of aluminium due to frameless modules and less aluminium for mounting structure reduce the amount of aluminium which is very energy intensive. The result of the improvements on the emissions per kWh_{el} is shown in **Figure 5-23**.

Mc-Si:

Table 5-6 lists the technical data for a mc-Si PV system in Central Italy as reference case. The PV system is retrofit installed on a tilted roof and has a peak power of 1 kWp. A system representing the present case and a system representing a future case (about 2010) are compared.

The distribution of the contribution to the emission of the life cycle phases module manufacturing, BOS production and the others is quite similar to the case of sc-Si. Thus it is not displayed. In contrast, within the life cycle phase module manufacturing the distribution is different as can be seen in **Figure 5-17**. The Si feedstock is responsible for a larger share than in the case of sc-Si because of the lower internal feedstock of only 20 % compared to 36 % in

the case of mc-Si. The wafer production contributes less in the case of mc-Si compared to sc-Si as less energy is consumed for wafers with less purity.

Table 5-6:   Technical data for a mc-Si PV system in Central Italy installed on a tilted roof with a peak power of 1 kWp /Frankl et al. 2004/

Technical data	present mc-Si system	future mc-Si system
Internal recycled feedstock	22 %	50 %
External silicon feedstock	78 % (50 % EG-Si scraps and 50 % direct poly-Si)	50 % (25 % EG-Si scraps and 75 % direct poly-Si)
Wafer thickness	300 μm	180 μm
Wire thickness	150 μm	120 μm
Module efficiency	10.7 %	13.5 %
Module equipment	tilted roof retrofit glass-tedlar, aluminium frame	solar roof tiles glass-tedlar, frameless
Installation	30° tilt angle, 0° azimuth angle	30° tilt angle, 0° azimuth angle
η_{pos}	95 %	97 %
η_{loss}	90 %	92 %
η_{inv}	95 %	95 %
η_{tot}	81 %	85 %
Radiation	1740 kWh/m² a	1740 kWh/m² a
Annual electricity production	1413 kWh/kWp a	1475 kWh/kWp a
Life time	25 years	30 years

Results are slightly worse for mc-Si than for sc-Si. This is mainly caused by the lower module efficiency (see **Figure 5-23**).

An increase of internal feedstock from 22 % to 50 % results in significant lower emissions with a reduction up to 20 % for CO_2 and SO_2. This is shown in **Figure 5-18**.

Figure 5-19 shows the change in emissions due to an improvement of wafer cutting. This improvement is achieved due to lower wafer thickness and lower cutting losses resulting in a higher mass efficiency of the production process. This results in a reduction of nearly 20 % of overall emissions with an improvement of wafer thickness from 300 μm to 250 μm and with an improvement of cutting losses from 200 μm to 150 μm. Only particulates emissions do not change significantly.
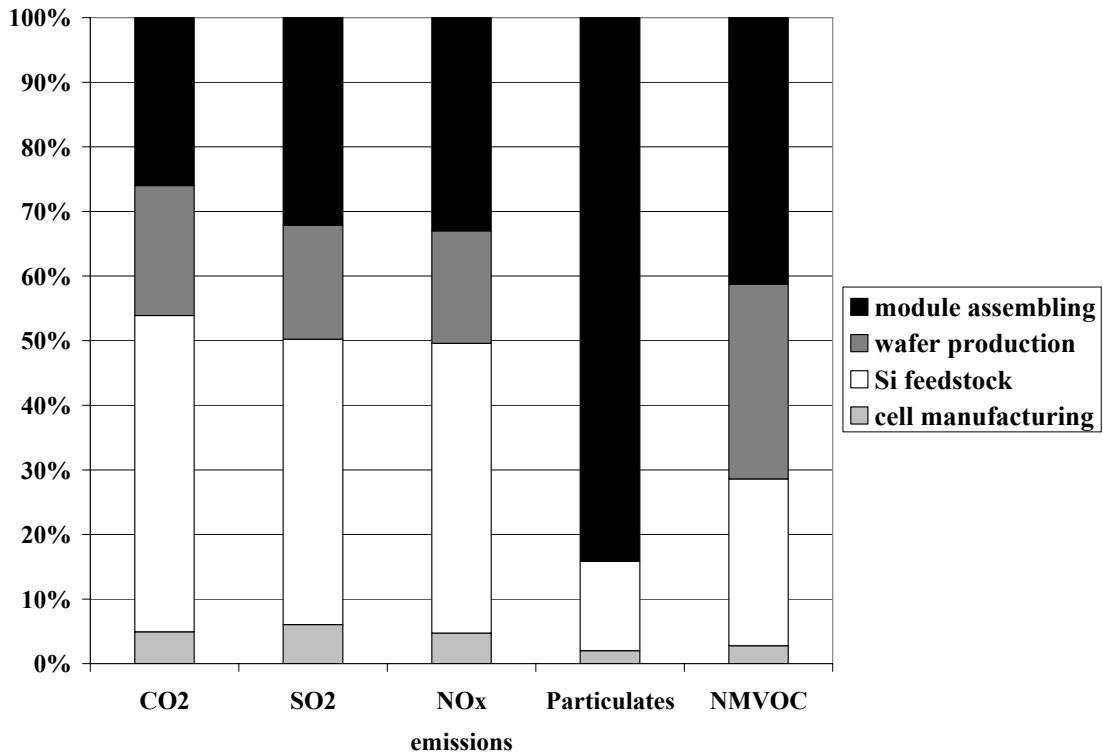
Figure 5-17:   Contribution of the module manufacturing units to the emissions in the case of mc-Si (in kg/kWh$_{el}$)
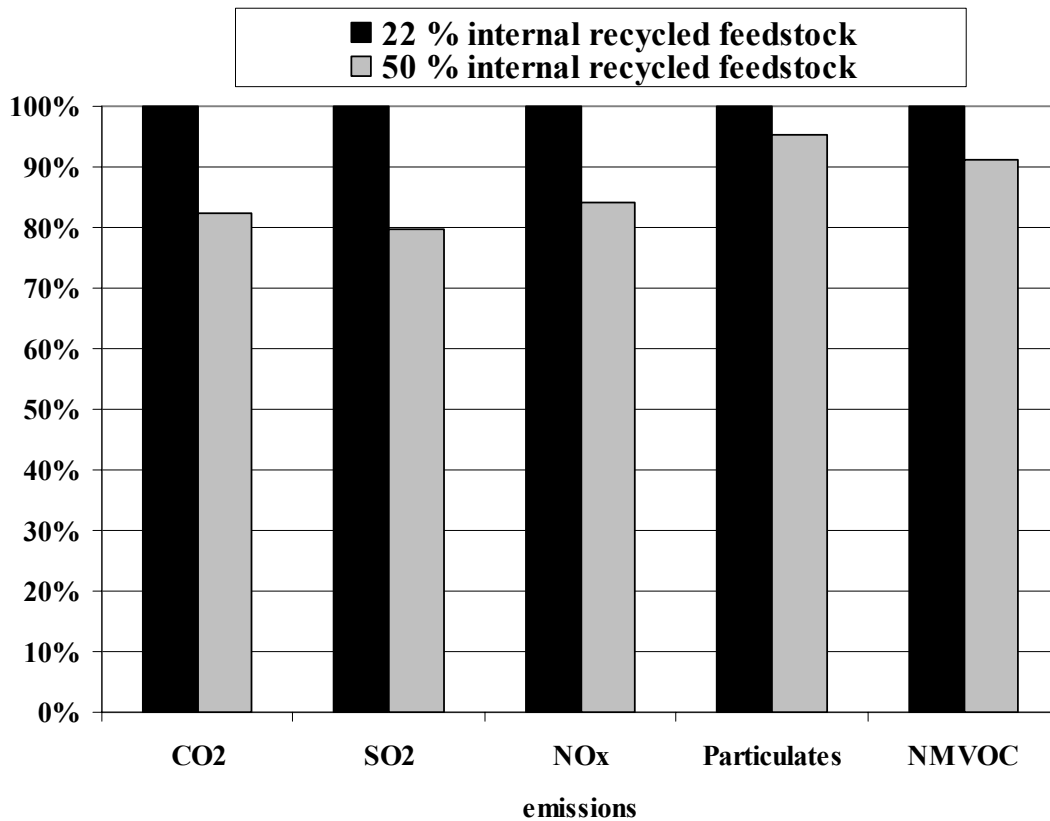
Figure 5-18:   Emissions with a higher share of internal recycled feedstock in the case of mc-Si (in kg/kWh$_{el}$)
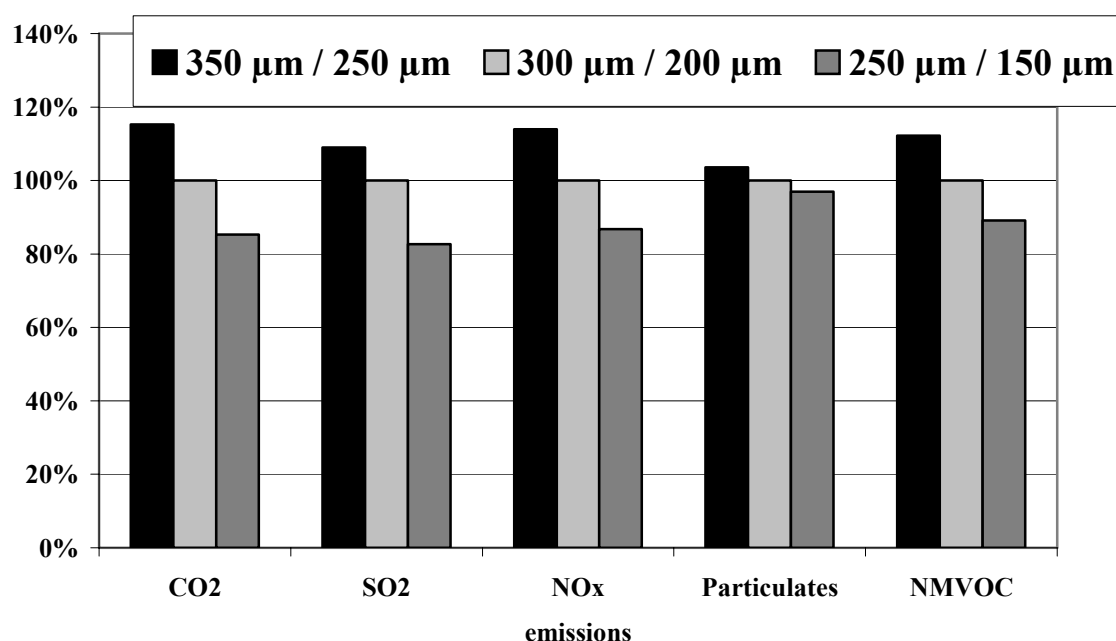
Figure 5-19:   Change in emissions with different wafer thickness / cutting losses with relation to 300 µm wafer thickness and 200 µm cutting losses (in kg/kWh$_{el}$)

Table 5-7:   Parameters of different types of building integration for mc-Si with η_{inv} = 95 % for Central Italy /Frankl et al. 2004/

Application	Module equipment	η_{pos}	η_{loss}	η_{tot}	η_{mod}
Tilted roof retrofit	with frame	95 %	90 %	81 %	10.7 %
Flat roof	with frame	100 %	93 %	88 %	10.7 %
Tilted roof integrated	frameless	97 %	92 %	85 %	10.7 %
Solar roof tiles	frameless	97 %	92 %	85 %	10.7 %
Skylight integrated	frameless	95 %	90 %	81 %	9.5 %
Sun shading façade retrofit[24]	with frame			75 %	10.7 %
Vertical façade integrated	frameless	62 %	92 %	54 %	10.7 %
Flat roof with aluminium reflector	with frame	100 %	93 %	88 %	10.7 %
Ground mounted power plant[25]	with frame	100 %	93 %	89 %	10.7 %

In order to compare the different types of building integration and their influence to the emissions per kWh$_{el}$ the most important parameters are listed in **Table 5-7**. The emissions per

---

[24]   Data for η_{pos} and η_{loss} are not given.

[25]   In the case of a ground mounted power plant the inverter efficiency is η_{inv} = 96 % instead of 95 %

kWh_{el} are illustrated in **Figure 5-20** with the tilted roof retrofit building integration as the reference case (100 %).

In the case of the tilted roof retrofit system the sun exposure cannot always be optimal, as it is a retrofit system. The electric system losses can be higher due to overheating and module mismatching problems.

The exposure is optimized on flat roofs and the modules are usually retro-ventilated. PV module rows should keep a certain distance from each other because of self-shading problems. Altogether PV systems on flat roofs do have the highest total BOS efficiency.

Tilted roof integrated mounting structures and solar roof tiles substitute the construction materials. The possibility of planning a better exposure of the panels and of using cell cooling systems leads to less losses than for tilted roof retrofit systems. However, the author of the study at hand has to note that this is an across-the-board assumption which should be fulfilled in all cases. There are also many integrated structures which are not cooled enough to reduce losses more than those of a retrofit structure which is cooled due to heat convection between the roof and the modules.

PV modules of skylight integrated mounting structures replace the original glass skylight of the same thickness. In order to optimize solar gain of a sun shading façade, it is necessary to optimize the width between the PV modules and their orientation.

The PV system integrated in a vertical façade and the building are planned and designed together. However, significant losses are due to the vertical orientation depending on the latitude. PV modules replace conventional glass windows of the same thickness.

The net incident solar energy in the case of a flat roof with aluminium reflector is higher (+ 523 kWh). In other respects the losses are the same as for a flat roof PV system.

Ground-mounted PV plants have an optimized exposure of panels to the solar radiation. Thus, the total BOS efficiency is the maximum one compared to the other mounting structure. It even surpasses the total BOS efficiency of flat roof systems as the inverter efficiency is assumed to be 96 % instead of 95 % for the others.

The comparison of the emissions of different mounting structures is illustrated in **Figure 5-20** and based on the reference system which is on a tilted roof retrofit and sited in Central Italy. A flat roof has a much higher BOS material demand of concrete and steel. However, the CO_2, SO_2 and particulates emissions are lower than for the tilted roof retrofit due to the higher system efficiency. The results of tilted roof integrated are better for all surveyed emissions due to frameless modules and the assumptions of better positioning. Solar roof tiles still have less emission than tilted roof integrated systems because they have the same efficiency parameters but do not have a frame. This leads to ca. 20 % less CO_2, SO_2 and NO_x emissions for the whole life cycle compared to a tilted roof retrofit system. NMVOC emissions are only reduced by ca. 10 % but particulates emissions even by ca. 50 %. With these results this building integration system seems appropriate for future configurations from the emission's point of view.

In the case of skylight integrated PV systems, the efficiency of the module is lower due to a larger distance between the cells to make it more transparent for sunlight. The total BOS efficiency is the same. Very special for this building integration system is the replacement of conventional glass and no need for mounting structures. Therefore, no material demand for BOS (e.g. aluminium) is considered. This emission reduction is partially compensated by the thicker glass used in the module (5+5 mm) compared to the tilted roof retrofit modules (tedlar + 3mm glass). With the substitution of conventional window glass the CO_2 emissions are reduced by 20 %, the SO_2 emissions by 27 %, the NO_x emissions by 8 % and particulates emissions by 77 % compared to a tilted roof retrofit system.

The emissions of a sun shading façade retrofit are significantly the worst with the exception of NMVOC because of the low system efficiency and a very high material demand for the retrofit external mounting structure. However, these results can be improved by optimizing the position and by using a lighter mounting structure and frameless modules. Additionally the sun shading effect of the modules reduces the energy demand for cooling or alternatively substitutes another sunshading system. These improvements which are not considered in the regarded case would reduce the emissions significantly.

A building integration system for a vertical facade differs from that for a tilted roof retrofit in its module equipment that is glass-glass, semi-transparent and frameless as well as in its position and losses efficiencies. The modules replace conventional glass and they do not need a mounting structure. Therefore, no material demand for the BOS is considered. The reduction of materials is compensated by the lower efficiency resulting in higher emissions compared to a system on tilted roof retrofit. Despite the smaller overall efficiency these systems increase the amount of available surfaces suitable to PV cladding significantly. The position efficiency differs significantly from the site. /Frankl et al. 2004/ assume a position efficiency for Central Italy of 62 % whereas this value would be 75 % for Germany /PHOTON 2004/ due to a lower tilt angle of the sun.

An installation on a flat roof with an aluminium reflector increases the amount of collected diffused light. Due to additional optimal positioning the system has lower emissions than a system on tilted roof retrofit.

Despite the higher inverter efficiency a ground mounted power plant is responsible for more emissions, with the exception of particulates, than a tilted roof retrofit because of the need for foundation and larger mounting structures.

The contribution of the mechanical BOS to the LCI varies significantly with ground mounted plants having the most impacts, followed by the tilted roofs, frameless modules and eventually vertical facades with the absence of mechanical BOS materials.
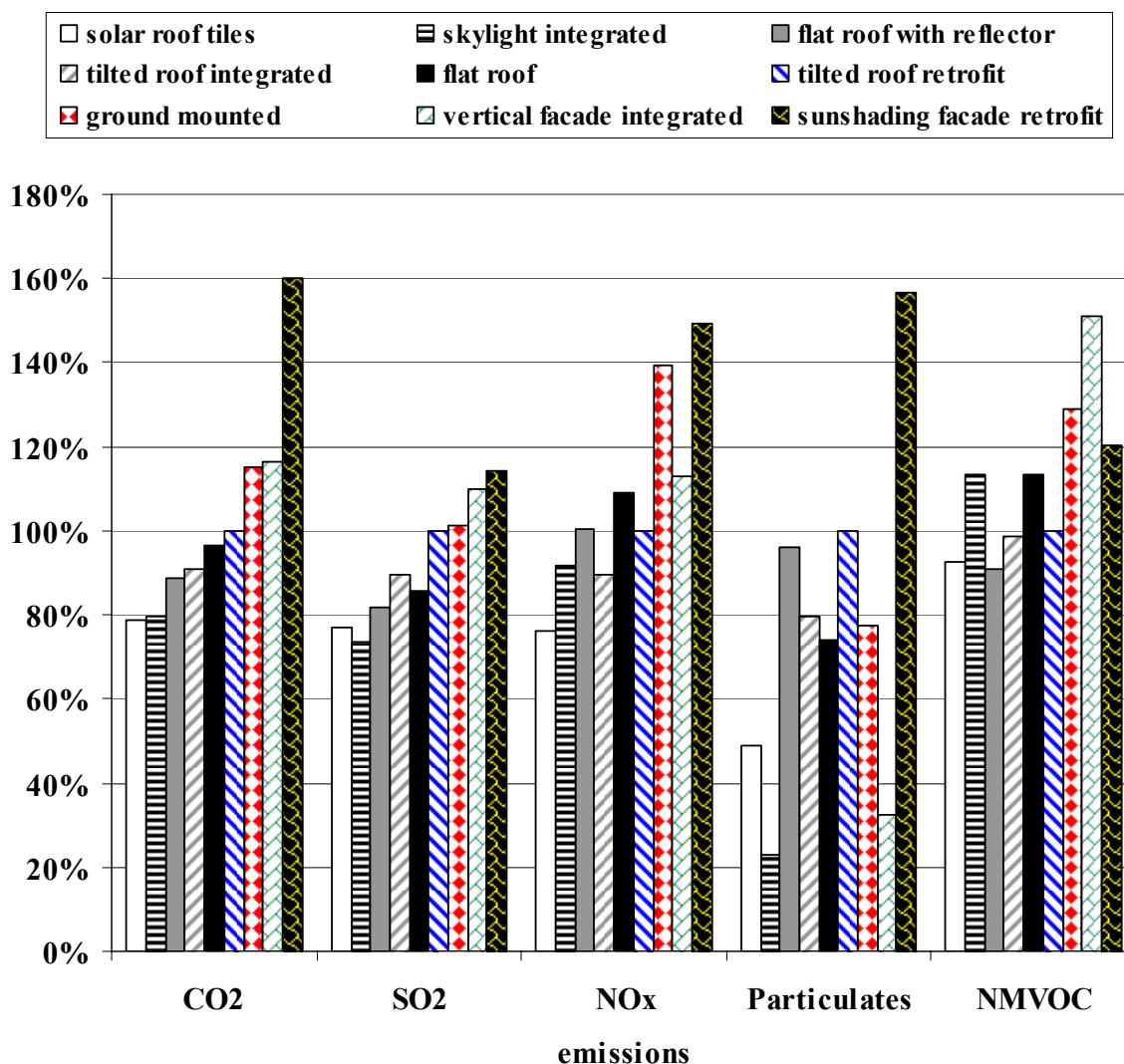
Figure 5-20: Comparison of the emissions due to different types of building integration with relation to tilted roof retrofit (in kg/kWh$_{el}$)

The combination of several technological improvements (cf. **Table 5-6**), i.e. higher module efficiency, better use of silicon mass in the manufacturing process, higher internal recycling, longer lifetime and optimized BOS with solar tiles, results in significant reductions of emissions in the order of 60 % (see **Figure 5-21**).

This future scenario can be alternated with the use of 100 % direct poly-Si resulting in relative small amounts of additional emission compared to the original future scenario because direct poly-Si has more impacts than the EG-Si scraps. This is shown in **Figure 5-16**.

Another future scenario is the reduction of Si feedstock due to 50 % reused wafers after their end of life together with the other future improvements. The emissions are the lowest compared to the other three scenarios.
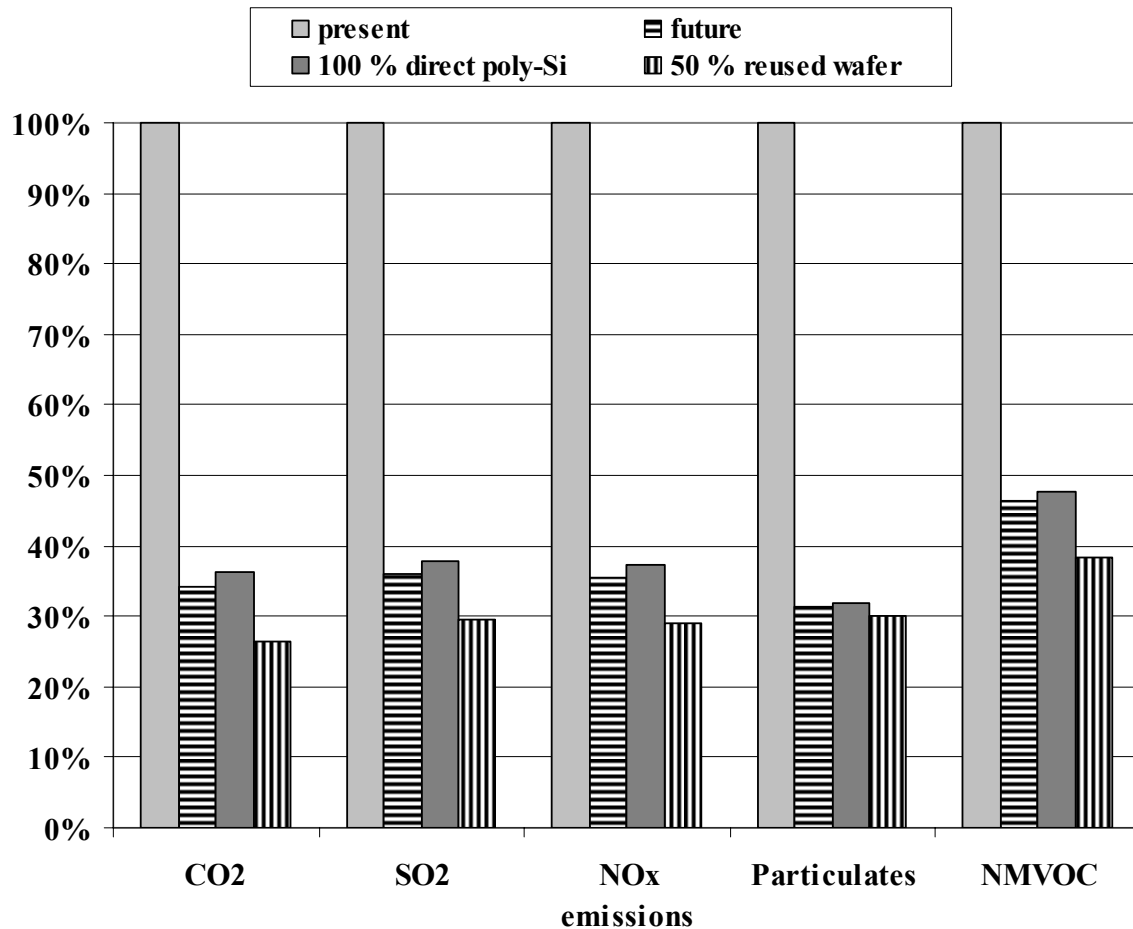
Figure 5-21:   Future developments in the case of mc-Si in relation to the present case (in kg/kWh$_{el}$)

/Frankl et al. 2004/ use the electricity mix of Europe for their calculations because it is required by the methodological guidelines of ECLIPSE. The main reason for this choice is the achievement of comparableness. In the case of renewable energies, many companies use electricity from renewable energies in order to meet their image of environmental friendly products. This results in fewer emissions than displayed in this study.

Thus, /Frankl et al. 2004/ perform a sensitivity analysis with three different scenarios of the electricity mix for mc-Si systems. The first scenario uses the electricity mix of Norway with 99.5 % hydropower and 0.5 % thermo-power for MG-grade Si production. The second scenario expands the first one with the use of an electricity mix of Wacker, the main EG-Si producer in Europe with 24 % hydropower and 76 % gas-fired CHP for the silicon purification process. The third scenario uses 100 % hydropower electricity in all module production unit processes. It is shown in **Figure 5-22** that the greenhouse gas emissions are reduced by 2.5 % in the first, 12 % in the second and 50 % in the third scenario.
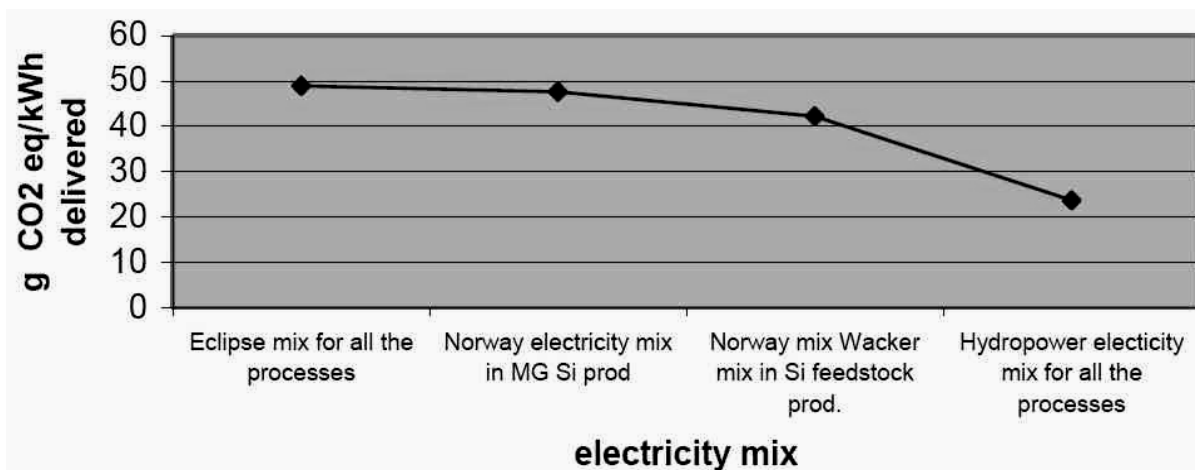
Figure 5-22: Sensitivity analysis for mc-Si technology with different electricity mix /Frankl et al. 2004/

Summarizing the two sensitivity analyses for the future and the electricity mix, it can be stated that the LCI results are very conservative. Today, it may be achievable to produce PV modules were most of the production steps use electricity from renewable energies. This would result in much less emission, i.e. approximately 50 % compared to the results used for the ECLIPSE electricity mix. Additional improvements in the coming years may decrease the results by another 50 %. Altogether, approximately 25 % of the emissions stated in /Frankl et al. 2004/ may be caused by future production.

The key hotspots of LCI results of PV systems are the electricity mix, module efficiency, module lifetime, silicon feedstock production and the kind of allocation as well as the silicon mass yield which mainly depends on wafer cutting, mass efficiency and on internal recycling of Si waste. Since the most important impacts are related to energy and material consumption in upstream or early production phases, each improvement either in energy consumption or mass yield will determine an improvement in the overall results. Other very important parameters are the plant site with its radiation conditions, the type of building-integration and the BOS efficiency.

Feedstock production is based on literature published in 2003. However, there are still significant uncertainties regarding inventory data from electronic industry. The data regarding wafer production come from the PV industry, which of course has an interest in data with a high degree of accuracy. The module assembling data and BOS data come from both literature and primary sources. Due to the lack of detailed and reliable data the end of life processes for PV module recycling are not considered but should be as soon as possible in future research. Altogether the data can be considered as up-to-date and representative for the European market.

5.1.4   Emissions of PV systems

In the paragraphs above, extensive sensitivity analyses are performed. For further calculations of external costs, representative PV systems are chosen. The site of the PV system is considered to be Germany. If other sites are analysed **Table 5-5** can be used to adjust the emissions. Four different PV systems are selected whose parameters are listed in **Table 5-4** and **Table 5-6**. The emissions in kg/kWh_{el} are shown in **Table 5-8** and are compared in **Figure 5-23**.

Table 5-8:   Emissions of PV systems installed in Germany in kg/kWh_{el} derived from /Frankl et al. 2004/

Emissions	Sc-Si present Germany	Sc-Si future Germany	Mc-Si present Germany	Mc-Si future Germany
CO_2	6.54E-02	3.50E-02	7.75E-02	2.65E-02
CH_4	1.73E-04	9.89E-05	1.85E-04	6.57E-05
SO_2	2.97E-04	1.63E-04	3.50E-04	1.27E-04
NO_x	1.38E-04	7.41E-05	1.62E-04	5.75E-05
Particulates	5.16E-05	2.33E-05	6.23E-05	2.04E-05
NMVOC	2.30E-05	1.49E-05	2.66E-05	1.23E-05

These emissions can be compared with the results of /BMWA 2004/. The emission figures of CO_2, CH_4, NO_x and NMVOC in the BMWA study projecting 2010 are in-between the present and future cases of the ECLIPSE study. SO_2 emissions in the ECLIPSE study are ca. two-fold and particulates emissions ca. three-fold higher than in the BMWA study. In the case of particulates emissions it should be noted that the data quality is not very good as mentioned above. Altogether, it should be noted that different assumptions and databases of the upstream processes, e.g. a different electricity mix, may lead to significant different results. Therefore, the ECLIPSE results can be regarded as supported by the results of the BMWA study.

Another comparison can be performed with /BMU 2004/. The PV system analysed in /BMU 2004/ is assumed to have a capacity of 3 kW, to be based on mc-Si, to be manufactured with a progressive solar silicon process and to be integrated into a roof. Further assumptions are a module efficiency of 13.4 %, an radiation of 1000 $kWhm^{-2}a^{-1}$, a wafer thickness of 300 μm, sawing losses of 200 μm and a life time of 25 years. The results are listed in **Table 5-9** including a comparison of a similar system analysed in ECLIPSE. It can be seen that the CO_2 emissions are 28 % and the CH_4 emissions 19 % higher. The SO_2 emissions are 18 %

lower but NO_x and particulates emissions are nearly the double. Since the calculation is not explicated in /BMU 2004/ it is not possible to explain this variation.
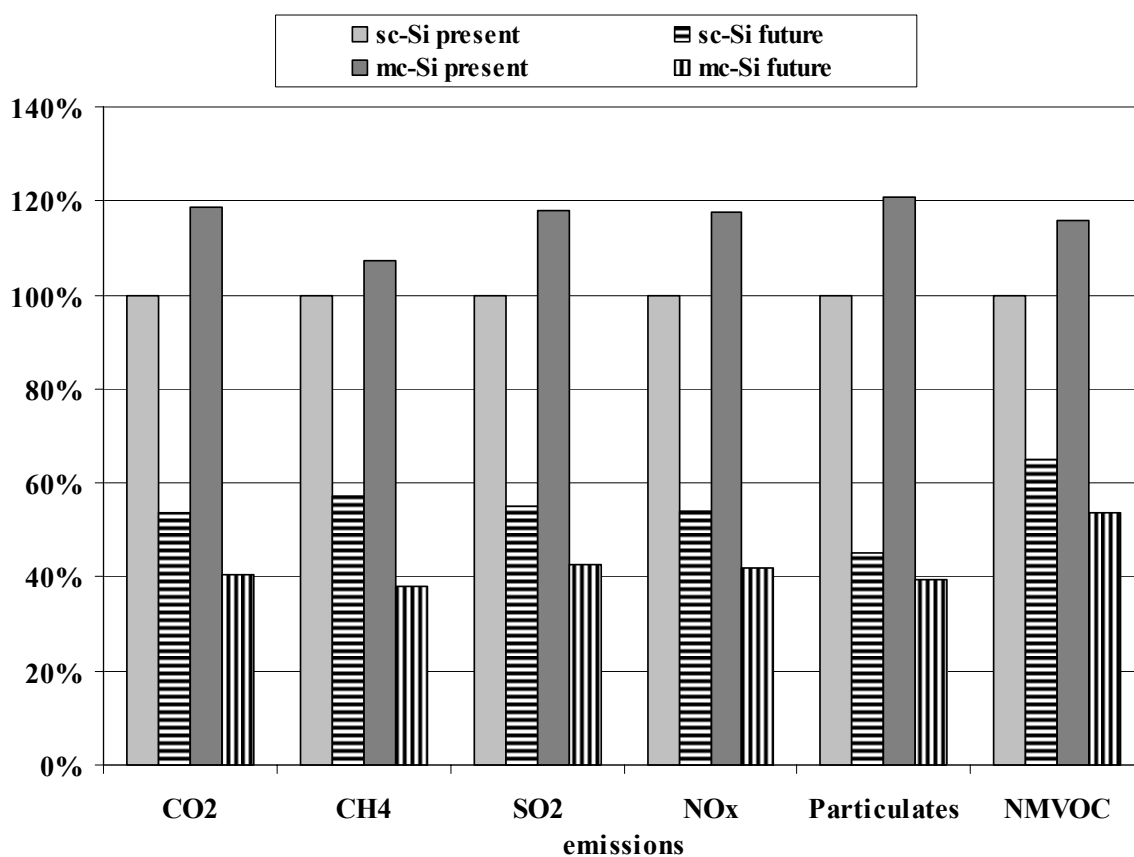
Figure 5-23:   Comparison of the emissions of sc-Si and mc-Si PV systems for the present and the future (in kg/kWh$_{el}$)

Table 5-9:   Comparison of the emissions (in kg/kWh$_{el}$) of a mc-Si PV system in Germany from /BMU 2004/ and from /Frankl et al. 2004/

Emissions	/BMU 2004/	Compared to mc-Si present
CO_2	9.90E-02	128 %
CH_4	2.20E-04	119 %
SO_2	2.88E-04	82 %
NO_x	3.40E-04	210 %
Particulates	1.19E-04	191 %

5.2   Wind Turbine Systems

5.2.1   Technology

The following description of the wind power technology is based on the internet publication /Danish Wind Industry Association 2003/.

Wind power:

About one or two percent of the annual radiation of the sun to the earth (with an energy of 5.6 * 10^{24} J) is transformed into wind energy. Wind is generated by different heating of the earth due to different thermal capacities leading to different pressures which tend to balance. At a site where the air is heated faster (e.g. shore, mountains) the air rises and creates a lower pressure at ground level attracting the cooler air from the site where the air is heated slower (e.g. offshore, valleys). This balancing of the pressure differences is responsible for the wind consisting of moving air with a certain mass. Its energy content which drives the wind turbines varies with the speed by the third power (see **Figure 5-24**). The *power* P_{wind} of the wind with a *velocity* v and a *mass* m which passes through a circular *area* A with the *radius* r in a certain *time* t is calculated with the following formula:

$$P_{wind} = \frac{\frac{1}{2} \cdot m \cdot v^2}{t} = \frac{\frac{1}{2} \cdot \rho \cdot A \cdot dis \cdot v^2}{t} = \frac{1}{2} \cdot \rho \cdot A \cdot v^3 \cdot = \frac{1}{2} \cdot \rho \cdot \pi \cdot r^2 \cdot v^3 \qquad (5\text{-}9)$$

Within this relation the *density* ρ and the *distance* dis are used as derived variables.

   Figure 5-24 illustrates that it is very important for high energy yields of wind turbines to have a plant site with high wind velocities.

   Due to the topography of the surface the wind speed is slowed down. On the surface the wind speed is zero. It increases with the height in a logarithmic way. The fewer the obstacles and the less the roughness of the surface the faster the wind speed increases with the height. This is an advantage for wind turbines on the sea, so-called offshore wind power. Another advantage is the low turbulence intensity because of less temperature variances than on land which enables longer life times of the wind turbines.

   With the mathematical approach of a Weibull distribution (see **Figure 5-25**) the probability density of a certain wind speed can be illustrated at a specific location. The higher the mean wind speed the lower the probability density of low wind speeds and the higher the probability density of high wind speeds.
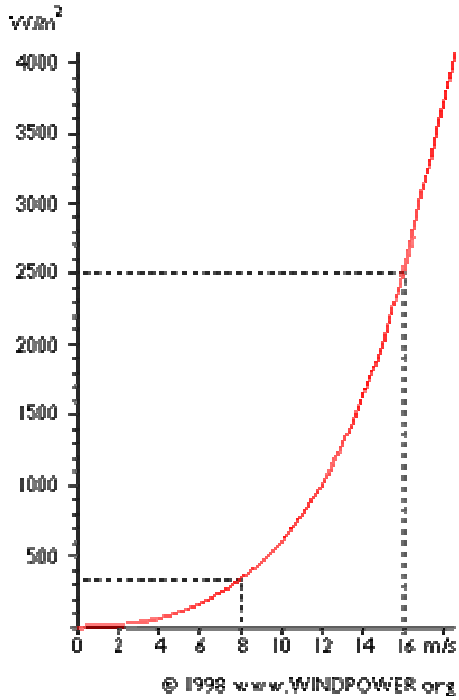
Figure 5-24:   Wind power (in W/m²) in relation to its speed (in m/s) /Danish Wind Industry Association 2003/
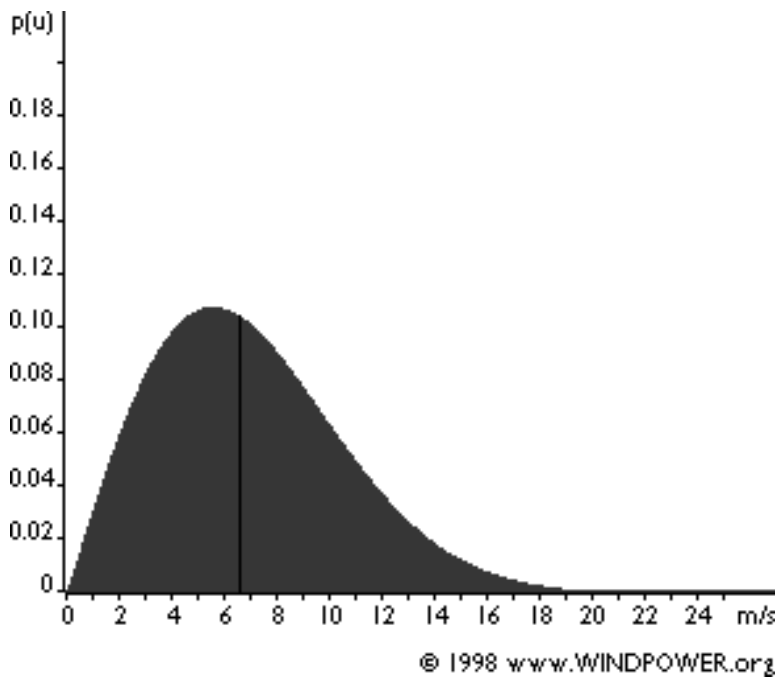
Figure 5-25:   Weibull distribution (probability density over wind speed in m/s) /Danish Wind Industry Association 2003/

It is not possible to use the whole kinetic energy content of the wind because the wind speed would then get zero. In such a case without wind no wind turbine moves and generates electricity. The Betz' Law proves that at maximum of 16/27 or ca. 59 % of the kinetic energy of the wind can be converted into mechanical energy by a wind turbine.
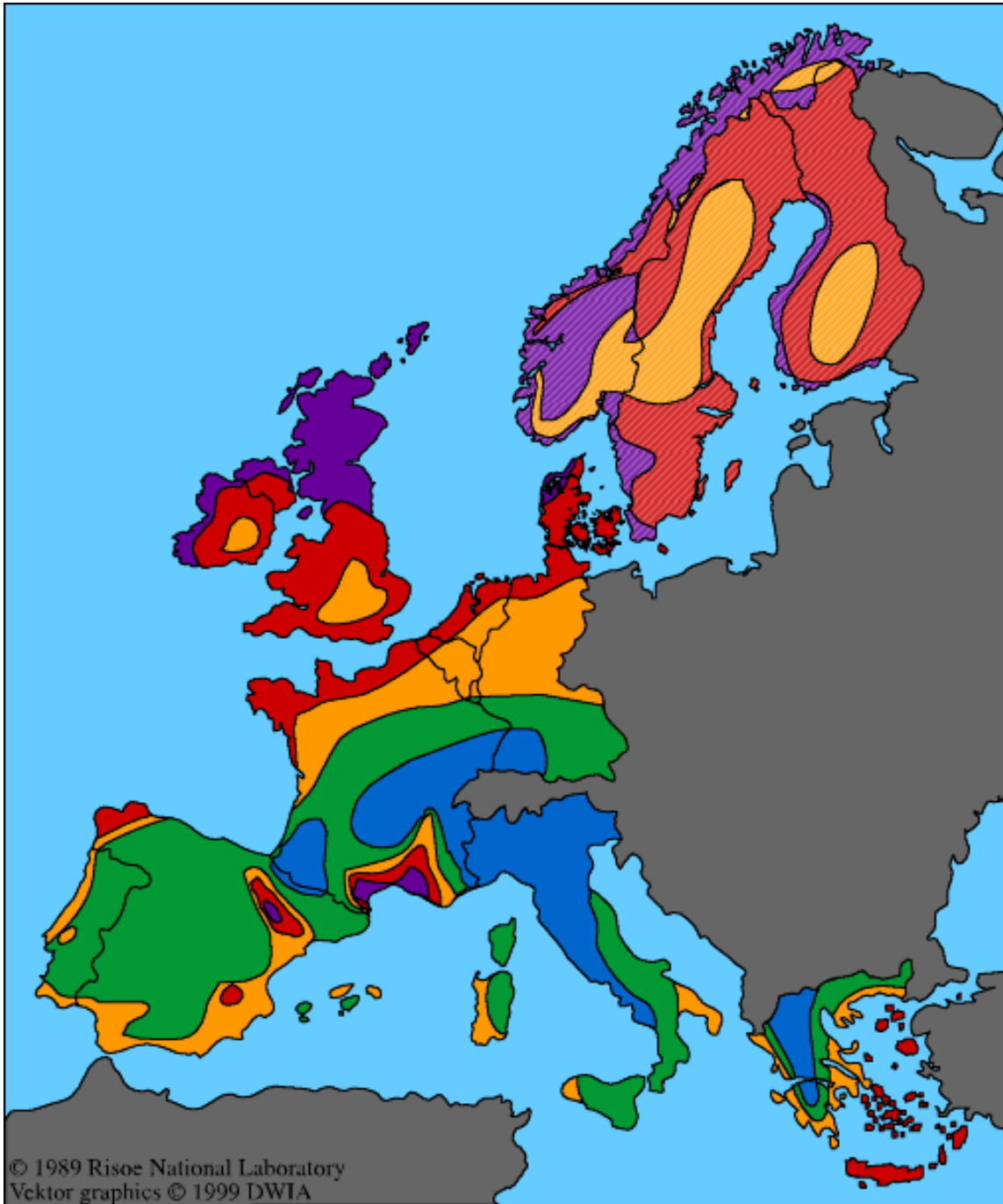
Wind resources at 50 (45) m above ground level

Colour	sheltered terrain		open plain		at a sea coast		open sea		hills and ridges	
	m/s	W/m²	m/s	W/m²	m/s	W/m²	m/s	W/m²	m/s	W/m²
	>6.0	>250	>7.5	>500	>8.5	>700	>9.0	>800	>11.5	>1800
	5.0-6.0	150-250	6.5-7.5	300-500	7.0-8.5	400-700	8.0-9.0	600-800	10.0-11.5	1200-1800
	4.5-5.0	100-150	5.5-6.5	200-300	6.0-7.0	250-400	7.0-8.0	400-600	8.5-10.0	700-1200
	3.5-4.5	50-100	4.5-5.5	100-200	5.0-6.0	150-250	5.5-7.0	200-400	7.0-8.5	400-700
	<3.5	<50	<4.5	<100	<5.0	<150	<5.5	<200	<7.0	<400
			>7.5							
			5.5-7.5							
			<5.5							

Figure 5-26:   Wind map Europe /Danish Wind Industry Association 2003/

The distribution of regions with specific wind velocities is illustrated in **Figure 5-26** which shows a wind map of Europe. The data for Norway, Sweden and Finland are from a later study and calculated for 45 m above ground level in the open plain whereas the other regions are calculated for 50 m above ground level and for different terrains. Purple areas have the strongest winds whereas blue ones have the weakest. The legend below the map gives the wind speed as well as the power of the wind for the different regions and different terrains. It should be noted that the given figures are just mean values so that there may be also sites with high wind velocity in zones with weak winds, e.g. on hills. The map is intended to give an impression about the distribution of the wind speeds in Europe. Investment decisions for specific sites should generally be based on local measurements which are representative for average conditions.

/EWEA 2004a/ refers to a study from 1993 which investigated that the technical onshore potential of wind power in EU-15 and Norway is 640 TWh/a. The offshore potential in EU-15 without Sweden and Finland is referred to a study from 1995 which estimates 3,030 TWh/a. Altogether, the potential is larger than the total electricity generation of 2,841 TWh in the ECLIPSE region in the year 2001 /IEA 2003/.

Wind turbines:

According to /Slootweg; de Vries 2003/, the power curve in **Figure 5-27** displays different areas of the operation of a wind turbine. On the one hand, below a certain wind speed, the so-called *cut in wind speed*, normally between 1.5 m/s and 5 m/s, the wind turbine does not generate any energy due to mechanical resistance and other losses. On the other hand, the wind turbine stops its generation above the *cut out wind speed* at about 25 m/s to avoid damages. In between, the generated power increases with increasing wind speed until the wind turbine reaches its nominal output with the *nominal wind speed* which is between 12 and 15 m/s. The curve progression is achieved by maximising the rotor efficiency. Above the nominal wind speed this procedure would result in a overload of the electrical systems. Therefore, the mechanical power has to remain constant above the nominal wind speed. This is achieved by a reduction of efficiency with increasing wind speed.

The reduction of efficiency is controlled either by *stall power limitation* or by *pitch control*. In case of the former strategy, the blades are designed in a way that at high wind speeds the aerodynamic efficiency of the rotor decreases. In contrast, the pitch control actively turns the blades out of the wind with increasing wind speed. According to /ISET 2004/, 81 % of the wind turbines in Germany in 2002 have been installed with pitch control compared to 30 % in 1993.
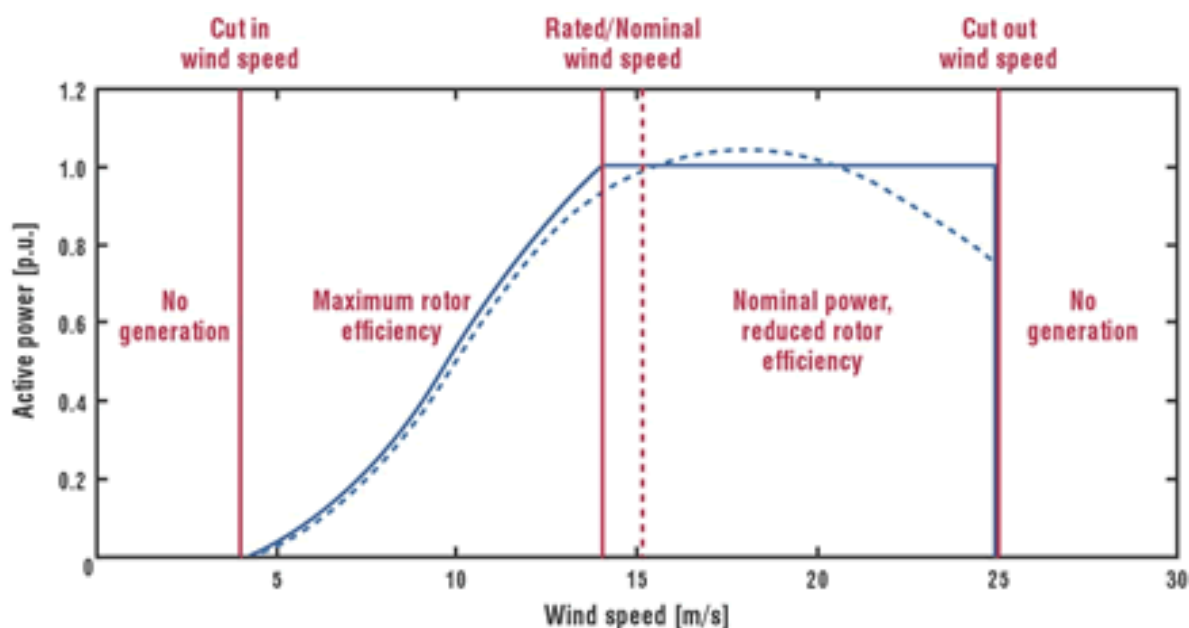
Figure 5-27: Power curve and areas of operation of a stall limited (dashed line) and a pitch controlled (solid line) wind turbine /Slootweg; de Vries 2003/

Wind turbines can be characterized by different technological choices. The axis of the turbine may be horizontal or vertical but vertical axes are quite rare. Wind turbines with different numbers of blades do exist, but all newly installed wind turbines consist of three blades /ISET 2004/. Most modern rotor blades on large wind turbines are made of glass fibre reinforced polyester or epoxy.

Considerations for the choice of tower techniques are cost, mechanical attributes, aesthetical perception and transport considerations. Lattice towers are cheap but often considered as not aesthetic. Therefore, they can be seen as an option for off-shore farms. Tubular steel towers are more expensive but felt as more aesthetic. They are widely used for large on-shore and off-shore wind turbines. For very large wind turbines, tubular tower dimensions may create transport problems. Therefore, concrete and hybrid towers are considered with the lower part of concrete and the upper part of steel. The higher the tower the higher the wind speed. Therefore, an optimisation should be done depending on the cost of the tower and the energy output.

Mostly a gearbox is necessary (see **Figure 5-28**) to connect the low-speed shaft of the wind turbine rotor (30 to 60 rpm) to the high-speed shaft of the generator (1200 to 1500 rpm). Generators with many poles can rotate at a very low speed so that the rotor of the turbine can be directly connected to the generator. These generators are heavier than common generators.

Direct grid connection means that the generator is connected directly to the (usually 3-phase) alternating current grid. Therefore, a gearbox is necessary. With an indirect grid connection some devices are needed to adapt the fluctuating internal AC current to the fixed frequency AC current. These devices are rectifiers and two inverters to control the stator current and the output current. The wind turbine can then be driven at a variable speed which implies

less load on the blades and the tower, a better power quality, and an improved electricity yield.
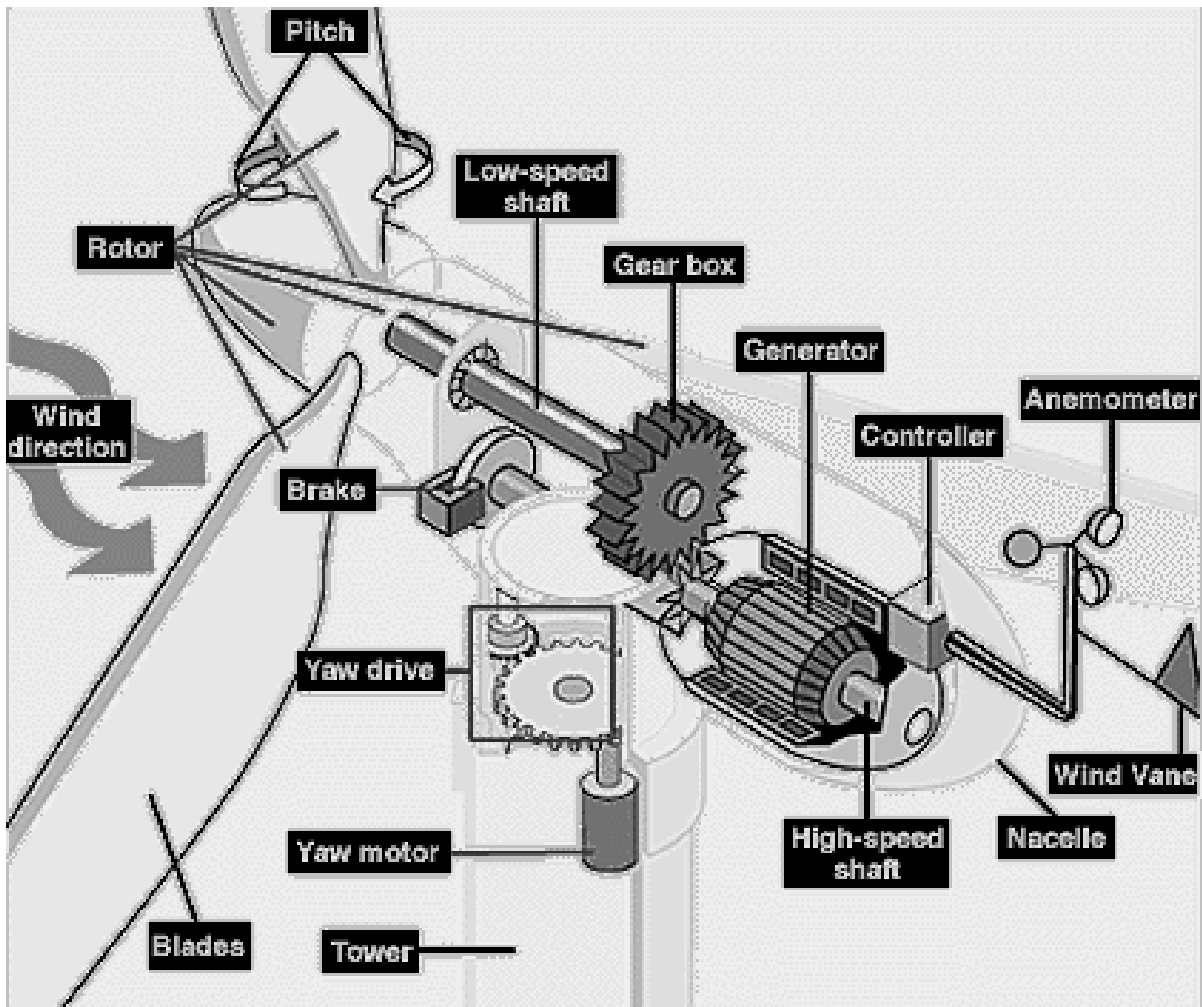
Figure 5-28: Wind turbine components /U.S. Department of Energy 2004/

Figure 5-28 gives an impression of standard components of a wind turbine with gearbox. The rotor consists of the blades (pitch controlled) and the hub. Wind power is converted into rotating energy of the rotor. The energy is transmitted to the gear box over the low-speed shaft. In the gear box, the speed is transformed. The high speed shaft drives the generator and the generator transforms the rotating energy into electricity which is fed into the electricity grid. Other components of a wind turbine are

- the brake which can stop the rotor in emergencies
- the yaw drive driven by the yaw motor which is used to keep the rotor facing into the wind with information from the wind vane
- the wind vane which gives data about the current wind direction
- the controller which controls the operating conditions as displayed in **Figure 5-27** with information from an anemometer
- an anemometer which gives data about the current wind speed

In order to reach a certain height with higher wind speeds the rotor is installed on a tower which holds the rotor and the nacelle. Within the nacelle most of the components described are installed in order to protect them from weather influences.

/Slootweg; de Vries 2003/ state that virtually all wind turbines installed are based on one of the three main wind turbine types illustrated in **Figure 5-29** and described in more detail below.
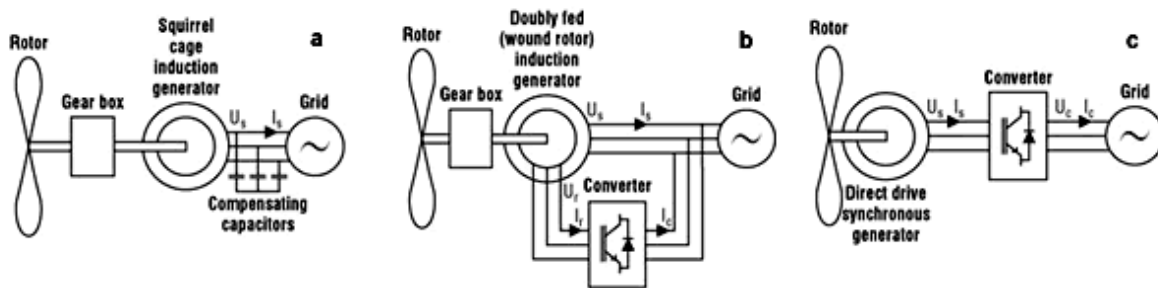
Figure 5-29:   Wind turbine types /Slootweg; de Vries 2003/

a) Fixed speed turbine with squirrel cage induction generator
b) Variable speed turbine with doubly fed induction generator
c) Variable speed turbine with direct drive synchronous generator

In a fixed speed turbine the rotor is connected with a squirrel cage (asynchronous) induction generator via a gearbox and the generator stator winding is connected to the grid. The speed varies around 1-2 % as the generator slip varies with the generated power but it is commonly referred to as a *fixed speed* turbine as the variation is relatively small. The squirrel cage generator draws reactive power from the grid which needs to be compensated by capacitors. Advantageous is its relative simplicity which benefits the price. Disadvantageous is the need of more mechanically robustness as fluctuations in wind speed are translated directly into drive train torque fluctuations resulting in grid voltage fluctuations.

In a variable speed turbine with a doubly fed (asynchronous) induction generator the required decoupling of mechanical and electrical frequency is achieved with a converter feeding the rotor winding, while the stator winding is connected directly to the grid. However, this configuration still needs a gearbox.

In a variable speed turbine with a direct drive synchronous generator, the generator and the grid are completely decoupled by means of a power electronic converter such as an AC-DC-AC converter allowing variable speed operation. Compared to a doubly fed induction generator, the power electronic must be able to handle much more power. One advantage of a variable speed turbine is that the generated reactive power and the grid voltage are easily controllable by the power electronics. Another advantage is that rapid power fluctuation (flicker) is scarce because the rotor behaves like a flywheel, which stores energy temporarily. However, the built-in power electronics are sensitive to voltage dips caused by faults and switching and additional costs arise due to the converter.

For the year 2002, /ISET 2004/ determine a share of 24 % of all installed wind turbines in Germany for asynchronous generators, 42 % for doubly fed induction generators and 35 % for synchronous generators.

5.2.2   Market development

	1996	1997	1998	1999	2000	2001	2002	2003
Germany	1545	2080	2874	4443	6113	8754	12001	14609
Spain	249	512	834	1225	2538	3337	4830	6202
Denmark	857	1116	1450	1761	2364	2534	2880	3110
rest of EU15	465	606	725	904	1308	1637	1875	2703
Italy	71	100	180	283	427	697	785	904
Netherlands	299	325	363	411	449	483	686	873

installed wind power in MW in the respective year
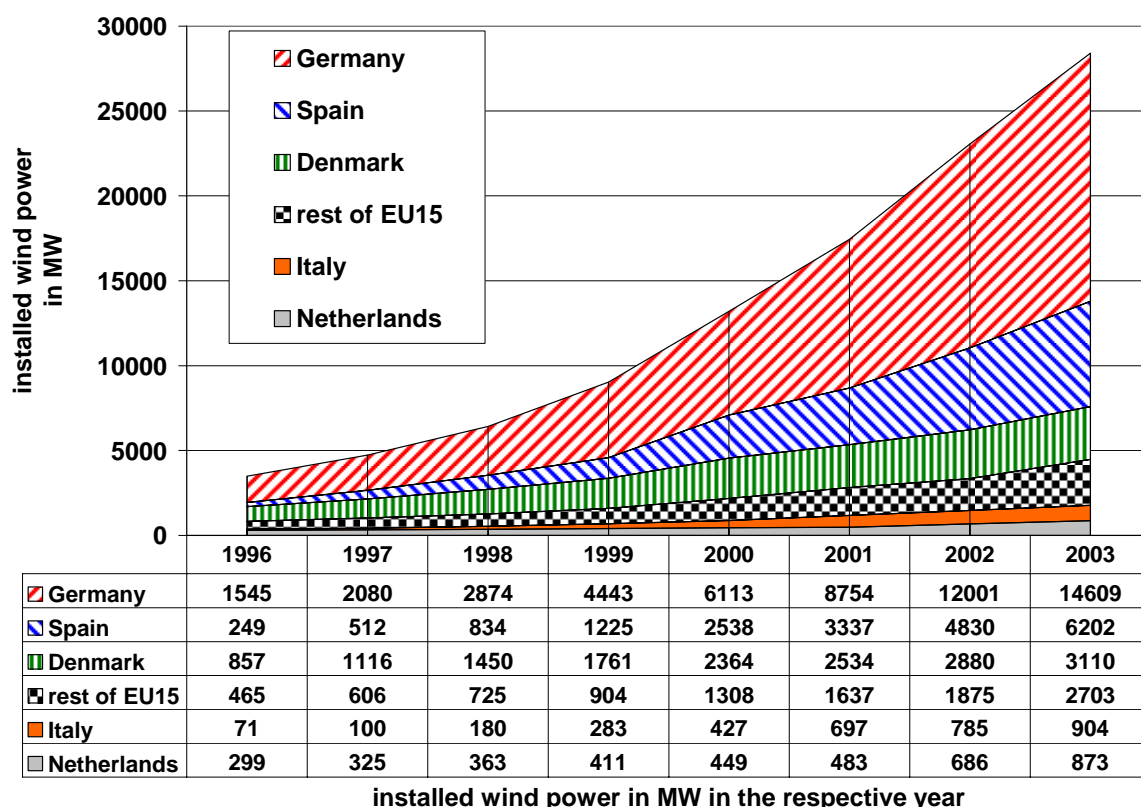
Figure 5-30:   Development of the installed wind power in EU-15 in the years 1996-2003 /Bundesverband Windenergie 2004/

In the EU-15, there has been a boom of wind power over the last years as displayed in **Figure 5-30**. The average growth rate of the installed wind power has been 35 % per year between 1996 and 2003. This rapid growth resulted in a total installed wind power at the end of 2003 of 28,401 MW compared to 3,486 MW seven years before. The distribution in 2003 is illustrated in **Figure 5-31**[26]. Germany is the world leader with an installed wind power of 14,609 MW in the end of 2003 which is more than a third of 39,294 MW worldwide /EWEA 2004a/. In EU-15, Germany has half of all installed power within its boundaries resulting in more than 3 % of the German electricity consumption in 2003. A lot of data can be looked up in the database *Renewable Energy Information System on Internet* (REISI) /ISET 2004/ and the web pages of /Bundesverband Windenergie 2004/. /EWEA 2004a/ predicts that there could be as

---

[26]   There is little difference between the data of **Figure 5-30** and **Figure 5-31**. The difference is not analysed in this study because data of different data sources often differ.

much as 75,000 MW (ca. 5.1 % contribution to energy consumption) installed in 2010 in EU-15 and 180,000 MW (ca. 12.1 % contribution to energy consumption) in 2020.
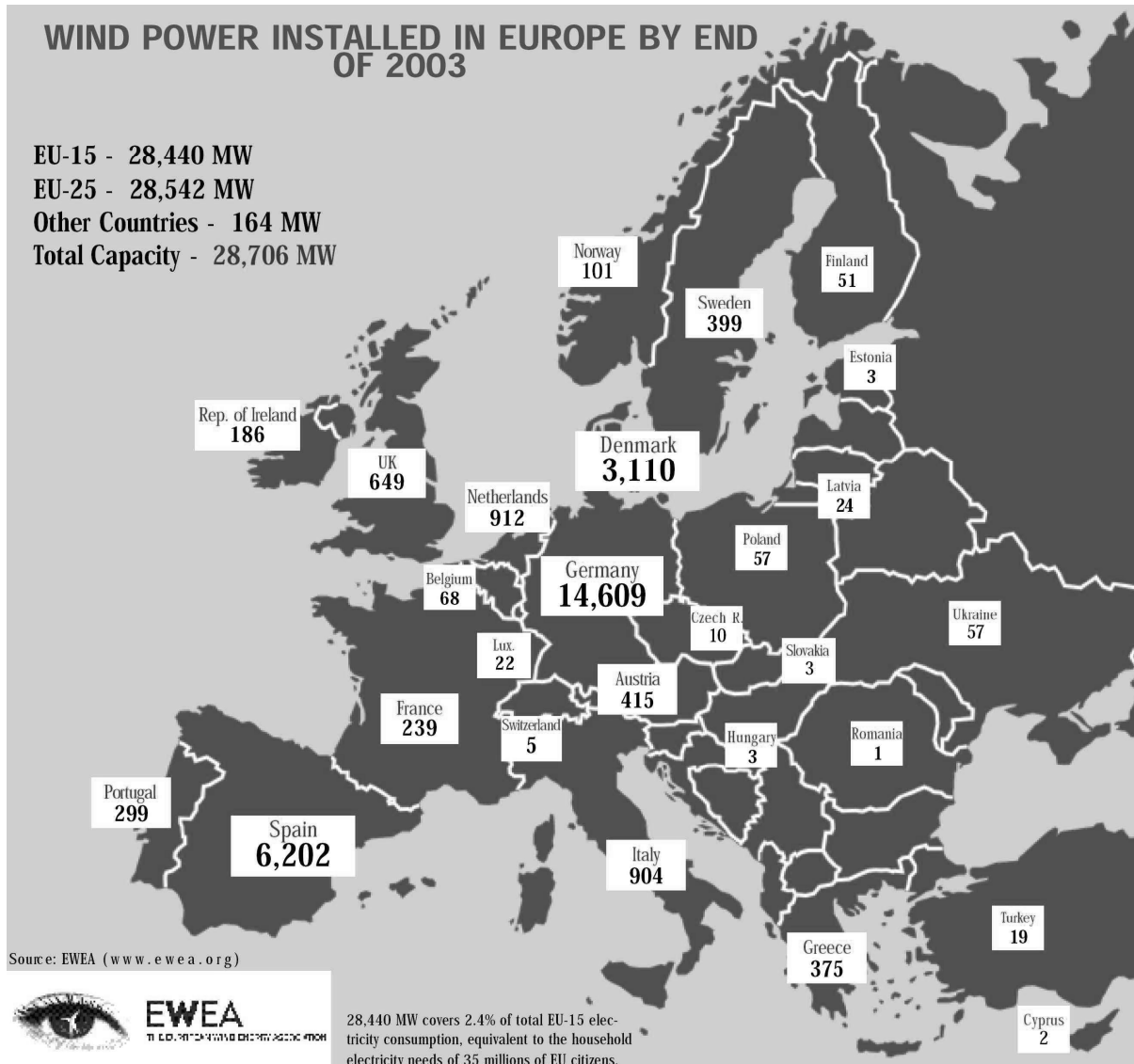
Figure 5-31:   Wind power installed in Europe by end of 2003 /EWEA 2004b/

According to this dynamic development the size of the wind turbines is steadily increasing. In 2002 59 % of the installed power in Germany originated from wind turbines with a power between one and two MW, 29 % between a half and one megawatt and the remaining 12 % from turbines with less than a half and more than two megawatt /ISET 2004/. The shift to larger sizes is continuing, e.g. because of offshore developments.

5.2.3   LCA results in ECLIPSE

/Chataignere; Le Boulch 2003/ selected four different sizes of wind turbines for their study. Firstly, they investigate a 600 kW wind turbine which has been installed in the early nineties. However, it is still used in turbulent wind conditions or in locations with a weak grid. Sec-

ondly, they analyse an example of a 1.5 MW wind turbine which is used at present for many installations. Thirdly, they study a 2.5 MW wind turbine representing a system already present on the market with interesting opportunities for off-shore projects. Lastly, they also provided a very rough example of a 4.5 MW wind turbine in prototype stage.

Life Cycle of wind turbines:

/Chataignere; Le Boulch 2003/ meet the assumptions for the life cycle of wind turbines given in **Figure 5-32**. The life cycle consists of the life cycle phases building, operation and end of life. They are described in the following in more detail.

For all life cycle phases, data are taken from the literature or expert knowledge. In case of the maintenance and end-of life phases as well as the 4.5 MW prototype estimations are taken from expert knowledge because few data are available.

Building:

For the elements of the wind turbine, i.e. tower, nacelle, blade, grid connection and foundation, the calculations in /Chataignere; Le Boulch 2003/ only encompass the material consumption.

The steel of the tower of the 600 kW wind turbine (Vestas V44) is assumed to be galvanized steel whereas the steel for the foundation is assumed to be secondary steel. For the grid connection, only the transformer with its steel consumption is taken into account and no cables are considered. Uncertainties exist whether the amount of material includes losses during the manufacturing process. Data are mainly taken from /McCulloch et al. 2000/.

Data of the 1,500 kW wind turbine (Enercon E66) are mainly taken from /Pick et al. 1998/ and /Gürzenich et al. 1998/.

For the 2,500 kW wind turbine (Nordex N80), the material amounts neglect the losses of material during the production process. The data are from N80 specifications and average turbine composition which leads to a low data quality for the nacelle. Data of the tower, the-foundations and the grid connection are estimated to be quite good because they are based on a real study.

Being a prototype the materials of the 4,500 kW turbine (Enercon E112) are estimated with a detailed mass balance corresponding to the 1,500 kW wind turbine (Enercon E66) for the nacelle, blades, tower and foundations, whereas the grid connection is calculated with the ratio on power of 4,500 kW / 1,500 kW.

The assembling module includes the direct input (energy and water consumption but no raw materials) and output (emissions to air, waste and water used) of the tower factory, the blade factory, the machine and controller factory, and the assembling factory.

For the transport module, the transport from the sub-contractors to the wind turbine factory and further to the erection site are assumed to be 600 km for the transport of the nacelle

and blades, 400 km for the transport of the tower and transformer, and 50 km for the transport of material for the foundations. These data are considered to be one-way distance. For off-shore cases also transport by cargo ship with a distance of 25 km or 40 km according to the example is included.

By lack of data for the on-site erection step, /Chataignere; Le Boulch 2003/ use data for wind turbines analysed in /Pick et al. 1998/. They consider an on-site energy consumption of 110 MJ for the 600 kW wind turbine. The energy consumption is assumed to be diesel oil consumed by cranes. For the 1,500 kW wind turbine, the energy consumption is assumed to be 556 MJ which is also used in the case of the 2,500 kW wind turbine multiplied with the ratio of the power. However, it is not taken into account for the 4,500 kW wind turbine.
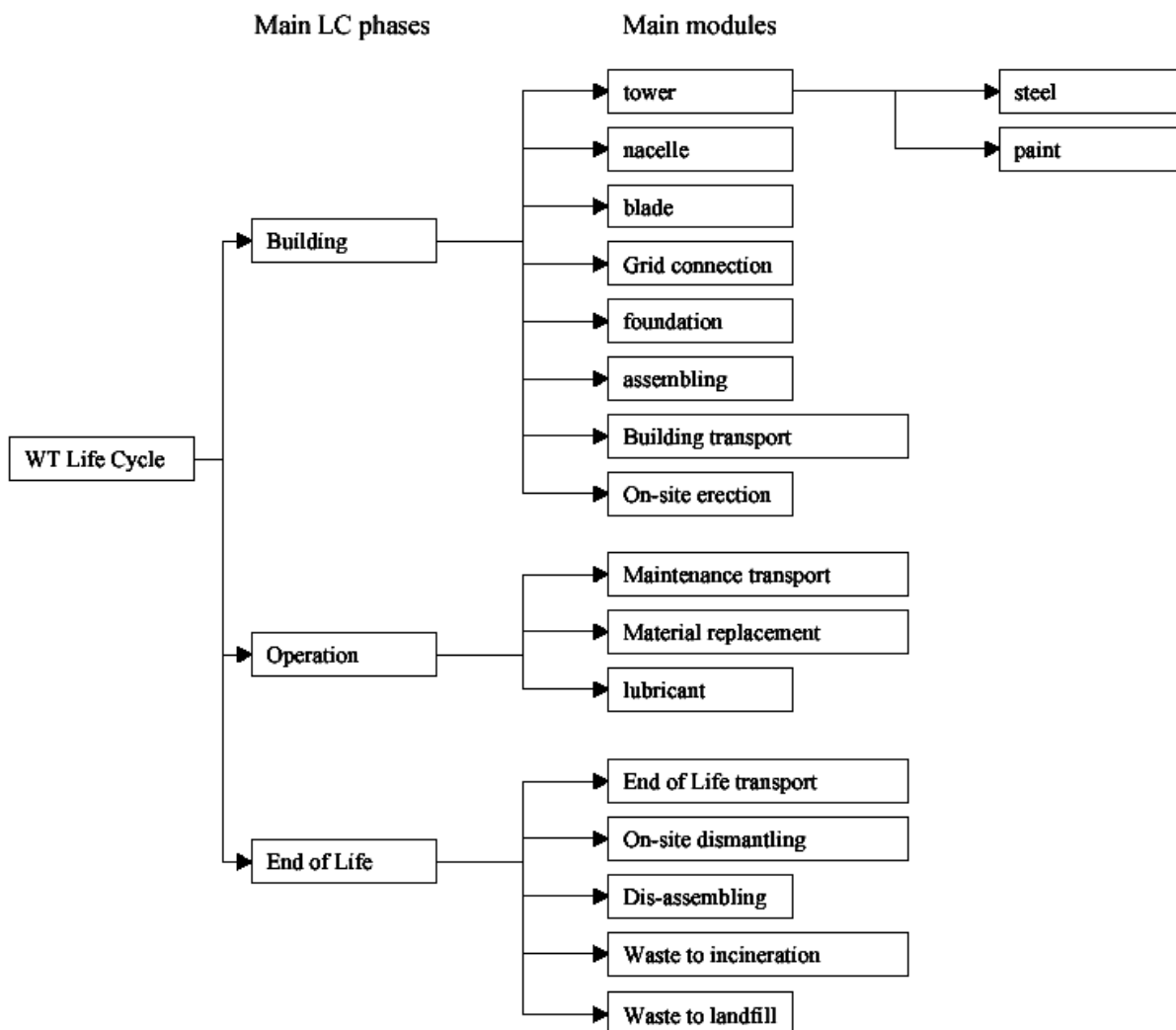
Figure 5-32:   Life cycle of wind turbines /Chataignere; Le Boulch 2003/

The quality of the data differs significantly. It is very high for the 1,500 kW wind turbine whereas it is very rough for the 4,500 kW wind turbine because only a mass balance is used in case of the nacelle and the blades. For the 600 kW and the 2,500 kW wind turbines, the quality of the data is less good than for the Enercon model because the study on Vestas wind

turbines is less precise and for the Nordex wind turbine some statistical assumptions on material demand are taken into account.

The quality of the operation phase and the end of life phasee is even less good than the building phase but they are not predominantly for the whole life cycle emissions (cf. **Figure 5-33** and **Figure 5-34**). Thus, it is important to have good data quality for the building phase, at least.

Operation:

For the lubricant consumption /Chataignere; Le Boulch 2003/ considered that the amount of oil for the gearbox is proportional with the power ratio to the Nordex N-80 2.5 MW wind turbine and that it is changed totally every 8 years.

The material replacement is considered to be 15 % of the nacelle and one third of the blades during the considered life cycle. Therefore, 15 % of the assembling module is taken into account for material replacement. Actually, 15 % of the building on-site erection energy should be taken into account but /Chataignere; Le Boulch 2003/ just list it in the material replacement module of the 2.5 MW wind turbine.

For the maintenance transport of the replaced material, the same assumptions as for the building phase are taken into account. Additionally, visits for one isolated onshore wind turbine are considered to consist of five travels each year by car consuming unleaded gasoline over a one-way distance of 50 km, whereas for a wind farm one intervention per wind turbine and year is assumed consuming 40 kg of heavy fuel oil.

End of life:

Most of the impacts are related to the building of the wind turbine. However, the end of life should also be taken into account. An optimistic situation for end of life phases is modelled assuming that 90 % of the metal is recovered and the remaining 10 % deposited on a landfill while 80 % of the blades are considered to be deposited on a landfill and 20 % shredded and used for certain plastics or concrete. /Chataignere; Le Boulch 2003/ assume that on-site dismantling energy consumption is the same as the energy necessary for the erection.

A 50 km distance from the wind turbine location to the treatment places disassembling, incineration and landfill is included as end of life transport. The flows of the recycling processes are not included but recovered matter is counted and replaced elements are not taken into account.

Technical data for wind turbines:

The technical data for the considered wind turbines is given in **Table 5-10**. Only the Nordex N80 wind turbine is also considered in offshore context in a wind farm with 100 wind turbines. All other wind turbines are considered to be stand alone wind turbines (not included in

a wind farm). The life time is assumed to be 20 years and they are all pitch controlled. All three different types of generators which are described above are considered. With the exception of the Enercon E112, all towers are tubular and made of steel. The Enercon E112 tower is also tubular but made of concrete because steel towers of this height are hardly transportable. /Chataignere; Le Boulch 2003/ distinguish deep foundations from shallow foundations for onshore applications. In the study at hand, only deep foundations are analysed because there are only marginal differences in the overall life cycle results. The Nordex N80 offshore wind turbine is assumed to have a caisson foundation which is specified in more detail below. It is also the only wind turbine in a wind farm so that losses of the internal grid are considered. The other wind turbines do not have an internal grid so that only electricity losses in the transformator occur. Full load hours are considered to be representative for site-specific weather conditions. With higher turbines and less obstacles the full load hours increase.

Table 5-10:   Technical data for the wind turbines considered in this study derived from the examples in /Chataignere; Le Boulch 2003/

Technical data	Vestas V44[27]	Enercon E66[28]	Nordex N80 onshore[29]	Nordex N80 offshore[30]	Enercon E112[31]
Power	600 kW	1,500 kW	2,500 kW	2,500 kW	4,500 kW
Rotor diameter	44 m	66 m	80 m	80 m	114 m
Hub height	35 m	67 m	60 m	60 m	124 m
Type of tower	tubular, steel	tubular, steel	tubular, steel	tubular, steel	tubular, concrete
Variable speed	no	yes	yes	yes	yes
Generator	asynchronous	synchronous	asynchronous	asynchronous	synchronous
Foundation	not specified	deep	deep	caisson	not specified
Full load hours	2,500 h/y	2,500 h/y	3,000 h/y	4,000 h/y	4,000 h/y
Losses	1 % (transformer)	1 % (transformer)	1 % (transformer)	3 % (internal grid)	1 % (transformer)

---

[27] http://www.windturbines.ca/vestas_v44.htm

[28] http://www.enercon.de/deutsch/produkte/e_66_daten.html

[29] http://www.nordex-online.com/produkte_und_service/onshore/n80/ueberblick.html

[30] http://www.nordex-online.com/produkte_und_service/offshore/n80/ueberblick.html

[31] http://www.enercon.de/deutsch/produkte/e_112_daten.html

Results of the examples:

/Chataignere; Le Boulch 2003/ identify that the main part of the emissions considered in this study is caused by the building phase. This part is 60-80 % for the 600 kW wind turbine. For the larger turbines it is even higher, i.e. 80-90 % for the 1.5 MW and 2.5 MW turbine and 85-90 % for the 4.5 MW turbine. This can be compared in **Figure 5-33** and **Figure 5-34**.

In the building phase of the 600 kW wind turbine, ca. 80 % of the CO_2, SO_2 and particulates emissions, and ca. 50 % of the NO_x emissions are caused by the tower and nacelle materials each contribution a half (see **Figure 5-35**).

In the case of the 1,500 kW wind turbine, the tower and the nacelle materials contribute 60 % of the building phase to SO_2 emissions, 70 % to CO_2 emissions and 80 % to particulates emission (see **Figure 5-36**).

In offshore context (N80 offshore), the foundation causes most of the emissions. Approximately 50 % of the CO_2, NO_x and NMVOC emissions are caused by the materials for the foundation and approximately 30 % of the SO_2 and particulates emissions. The second significant part has the material for the nacelle (see **Figure 5-37**).

In the operation phase, nearly all emissions are caused by the material which has to be replaced. In the end of life phase nearly all emissions result from the disassembling.
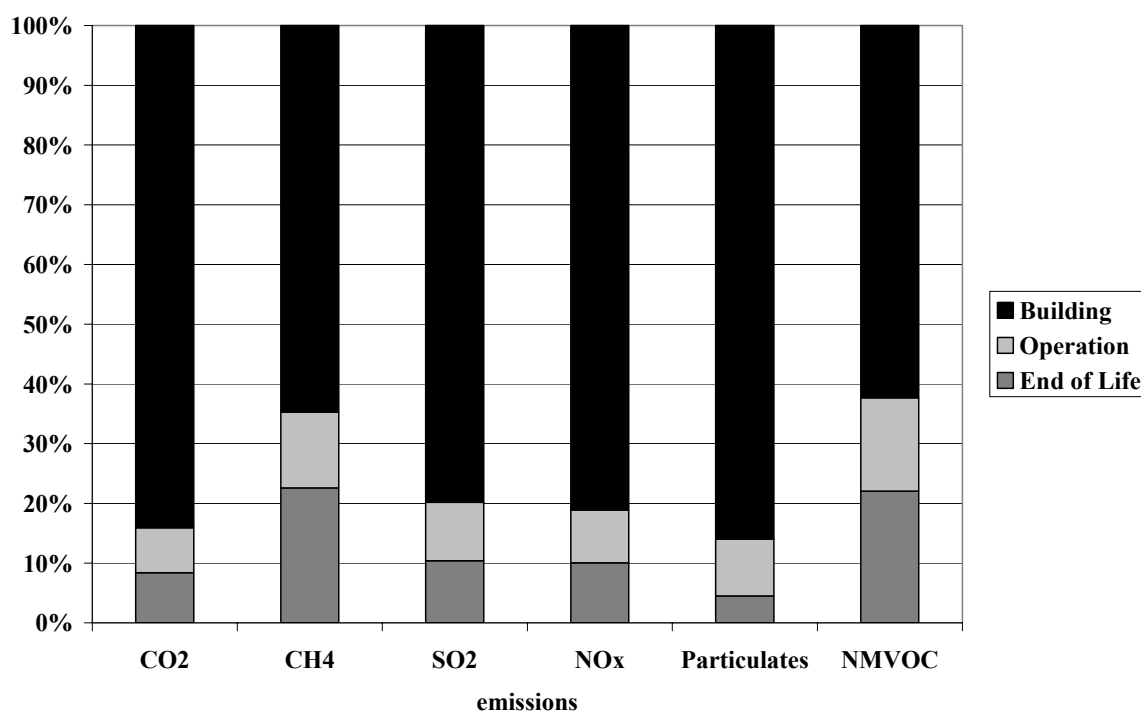
Figure 5-33:   Contribution of the life cycle phases to the emissions of the Vestas V44 wind turbine (in kg/kWh$_{el}$)
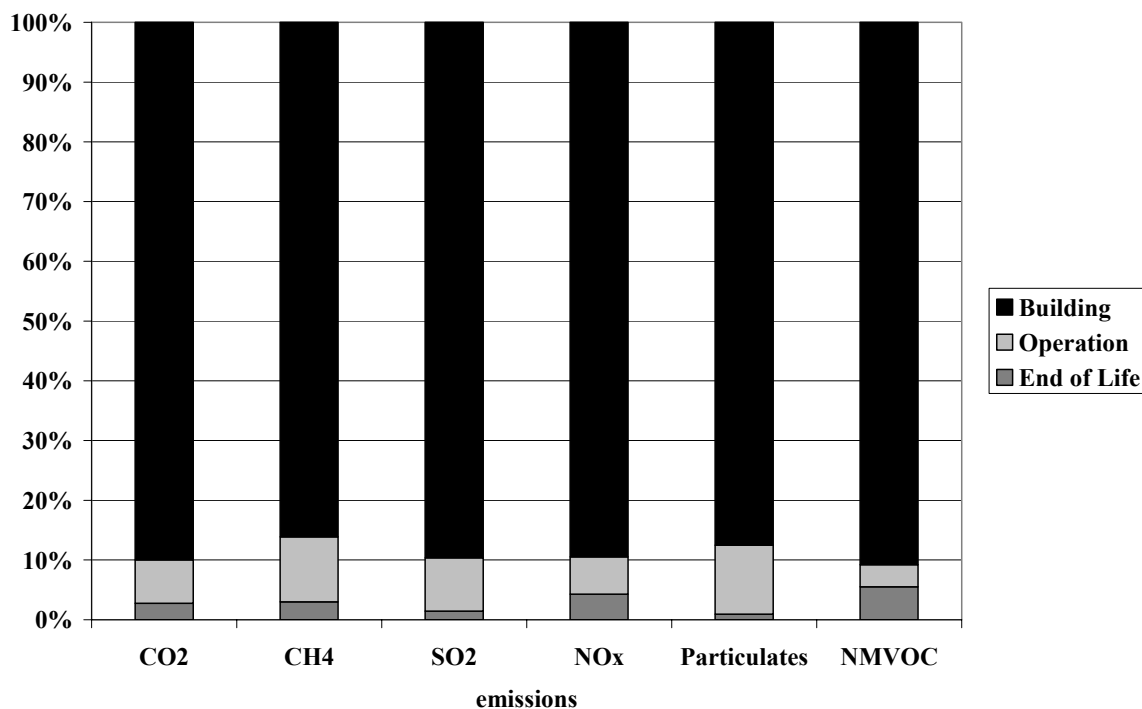
Figure 5-34:   Contribution of the different life cycle phases to the emissions of the E112 wind tur-
                     bine (in kg/kWh_el)
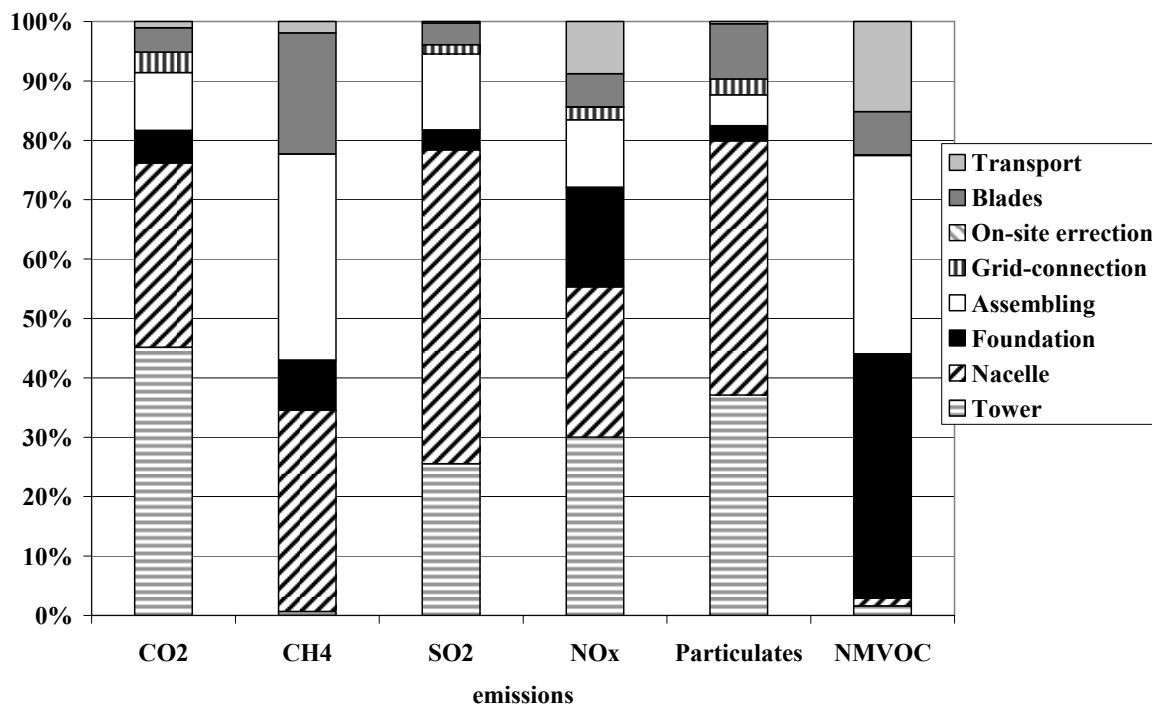
Figure 5-35:   Contribution of the life cycle units of the building phase to the emissions from the
                     building phase of the Vestas V44 wind turbine (in kg/kWh_el)
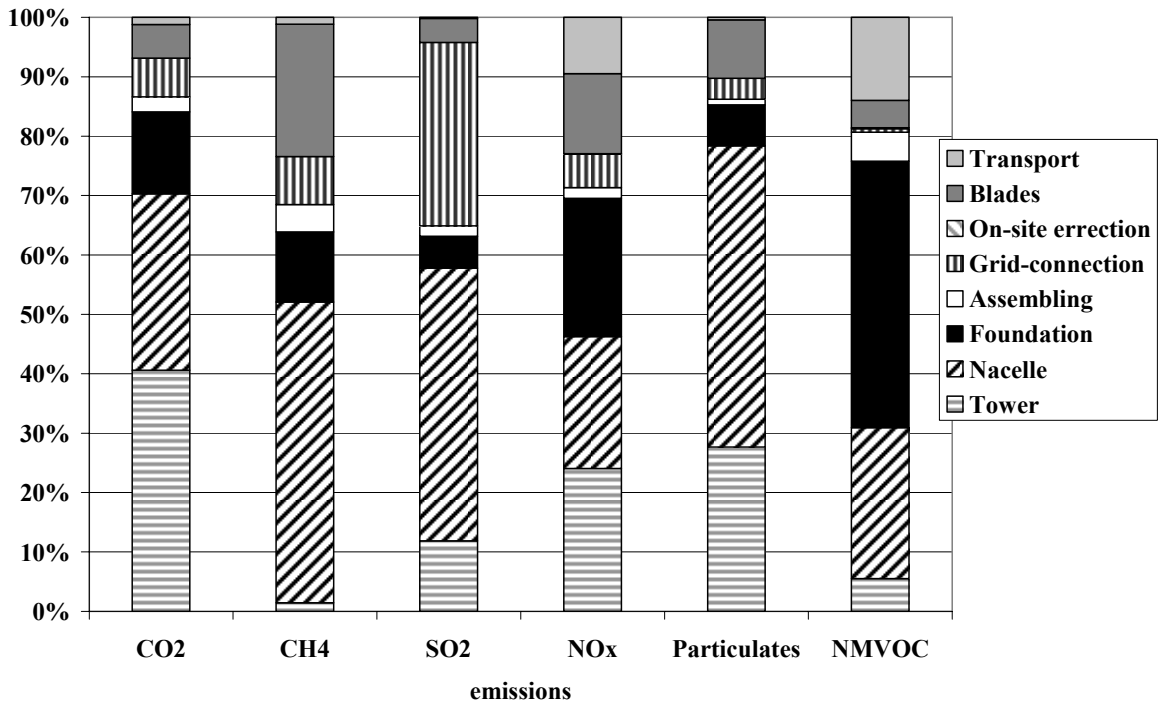
Figure 5-36: Contribution of the life cycle units of the building phase to the emissions from the building phase of the Enercon E66 wind turbine (in kg/kWh$_{el}$)
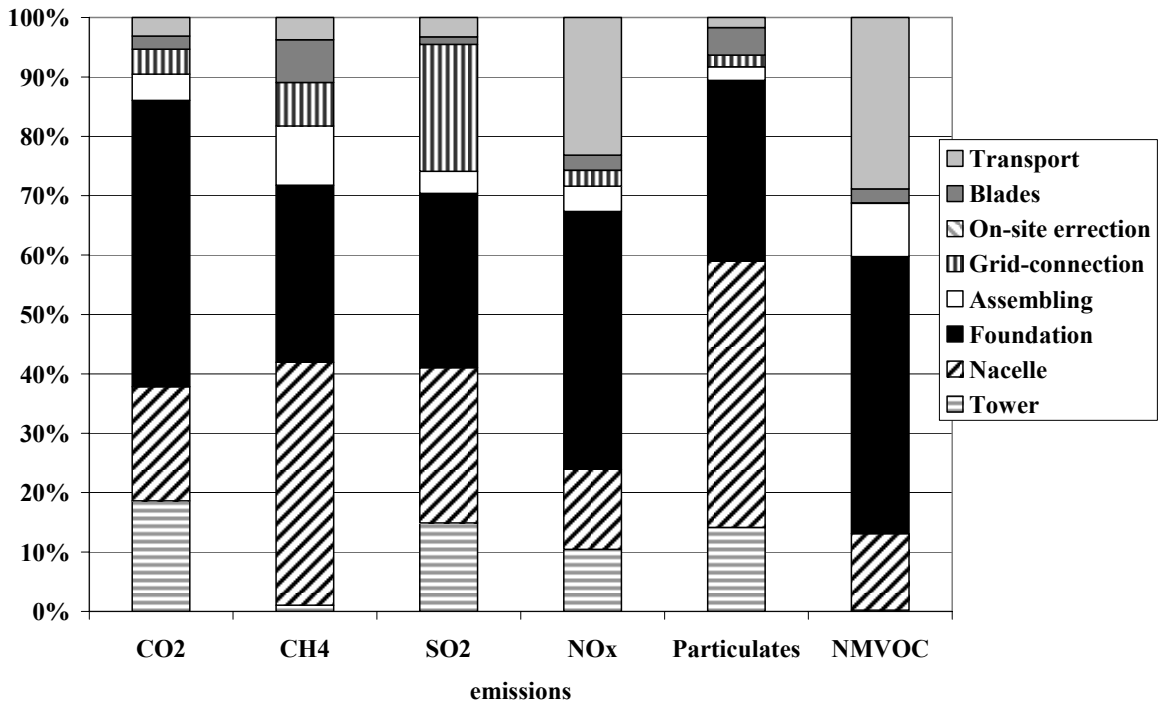
Figure 5-37: Contribution of the life cycle units of the building phase to the emissions from the building phase of the Nordex N80 offshore wind turbine (in kg/kWh$_{el}$)
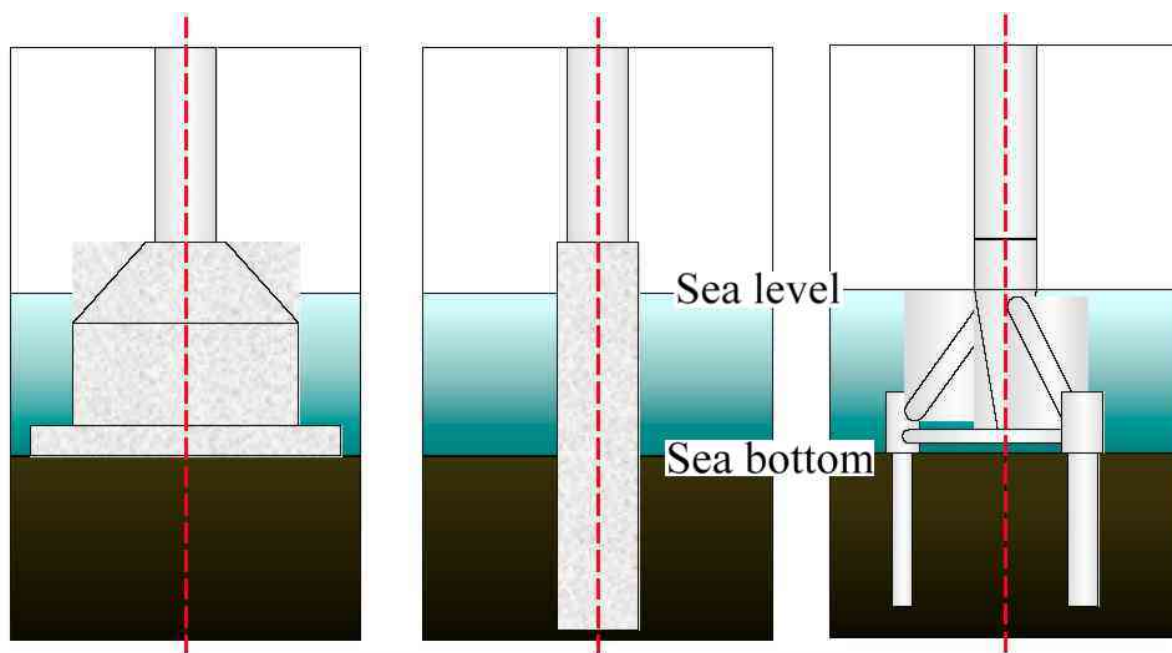
Figure 5-38: Foundations: on the left caisson, in the middle monopile and on the right tripod /Eckhardt et al. 2002/
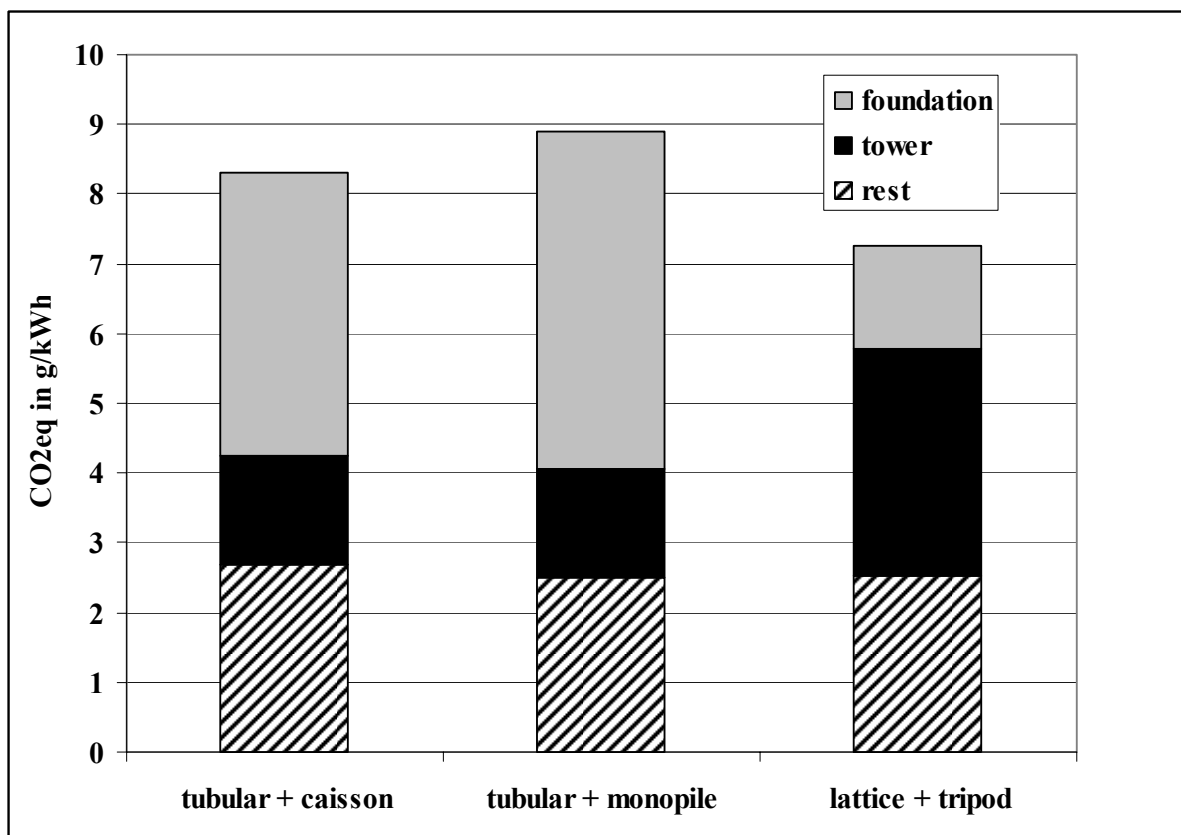
Figure 5-39: Comparison of the greenhouse gas emissions in the life cycle phase building from different tower and foundation configurations

Considering different constructions in the offshore context, three different combinations of tower and foundation are investigated. The tower can be tubular or lattice and the foundation caisson, monopile or tripod. An illustration of the foundations shows **Figure 5-38**. In order to give an impression of the difference between these configurations **Figure 5-39** shows a comparison of the greenhouse gas emissions which are caused in the building phase. The figure illustrates that for the materials of a lattice tower approximately twice as much greenhouse gases are emitted than in case of a tubular tower. Considering the foundation, the tripod foundation causes by far the fewest greenhouse gas emissions compared to a caisson foundation which is responsible for less greenhouse gas emissions than the monopile foundation.

It can be stated that the use of a tubular tower together with a tripod foundation may cause the fewest greenhouse gas emissions compared to the other possible combination of the considered towers and foundations.

5.2.4 Emissions of wind turbine systems

The emissions of the considered wind turbines for the whole life cycle are listed in **Table 5-11** and compared in **Figure 5-40**. In order to adapt the results to different wind conditions the figures can be multiplied with the coefficient f*ull load hours of the study at hand / full load hours of investigated wind conditions*.

Table 5-11:   Emissions of wind turbines (in kg/kWh_{el}) derived from /Chataignere; Le Boulch 2003/

Emissions	Vestas V44	Enercon E66	Nordex N80 onshore	Nordex N80 offshore[32]	Enercon E112
CO_2	7.32E-03	1.17E-02	7.59E-03	9.16E-03	8.37E-03
CH_4	6.05E-06	1.43E-05	1.08E-05	1.02E-05	1.51E-05
SO_2	2.24E-05	5.78E-05	4.16E-05	4.16E-05	4.38E-05
NO_x	1.50E-05	2.32E-05	1.54E-05	2.17E-05	2.63E-05
Particulates	7.81E-06	1.35E-05	1.10E-05	1.10E-05	1.13E-05
NMVOC	1.49E-06	2.18E-06	2.00E-06	2.46E-06	3.29E-06

The 1.5 MW wind turbine Enercon E66 has the highest emissions per kWh_{el} with the exception of NMVOC. Nevertheless, it is taken as the representative wind turbine because data quality is the best as discussed above.

---

[32] Wind farm with 100 wind turbines, 40 km away from shore, tubular tower and caisson foundation

☒ **Vestas V44**   ☐ **Enercon E66**   ☒ **Nordex N80 onshore**   ☐ **Nordex N80 offshore**   ☒ **Enercon E112**
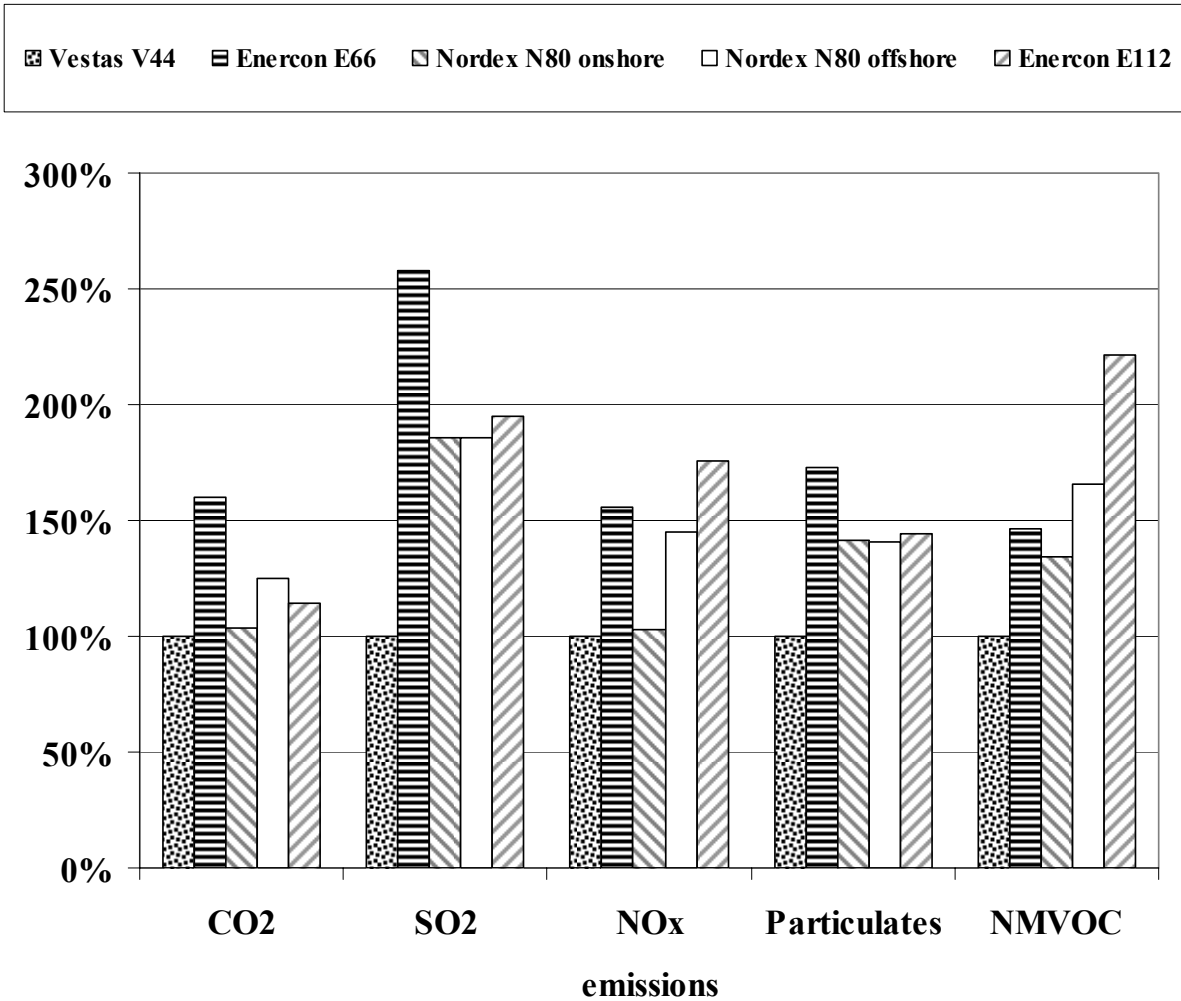
Figure 5-40:   Comparison of the emissions of the considered wind turbines related to Vestas V44 (in kg/kWh$_{el}$)

Another actual study performed a LCA for an offshore wind farm with 40 wind turbines 100 km away from coast in a water depth of 20-30 m /BMWA 2004/. They calculate with full load hours of 4,400 h/a and they analyse the REpower 5M wind turbine which is installed in 2004 for test operations near Brunsbüttel, Germany. The wind turbines with tubular tower have tripod foundations. About 80 % of the CO_2, SO_2, CH_4 and particulates emissions are caused by the building phase. Thus, the contribution of the different life cycle phases to the life cycle emissions are similar to those presented in **Figure 5-33**. The emissions per kWh$_{el}$ are higher than those of the Nordex N80 offshore wind turbine analysed in /Chataignere; Le Boulch 2003/ (see **Table 5-12**). This may be attributed to different upstream processes, e.g. German electricity mix instead of the European one. However, it may also be that the assumptions in /Chataignere; Le Boulch 2003/ are too optimistic or those of /BMWA 2004/ too pessimistic.

Table 5-12: Comparison of the emissions of an offshore wind turbine from /BMWA 2004/ and from /Chataignere; Le Boulch 2003/ (in kg/kWh$_{el}$)

Emissions	/BMWA 2004/	Compared to Nordex N80 offshore
CO_2	1.86E-02	203 %
CH_4	6.71E-05	658 %
SO_2	1.78E-04	428 %
NO_x	6.19E-05	285 %
Particulates	5.90E-05	536 %
NMVOC	9.02E-05	3667 %
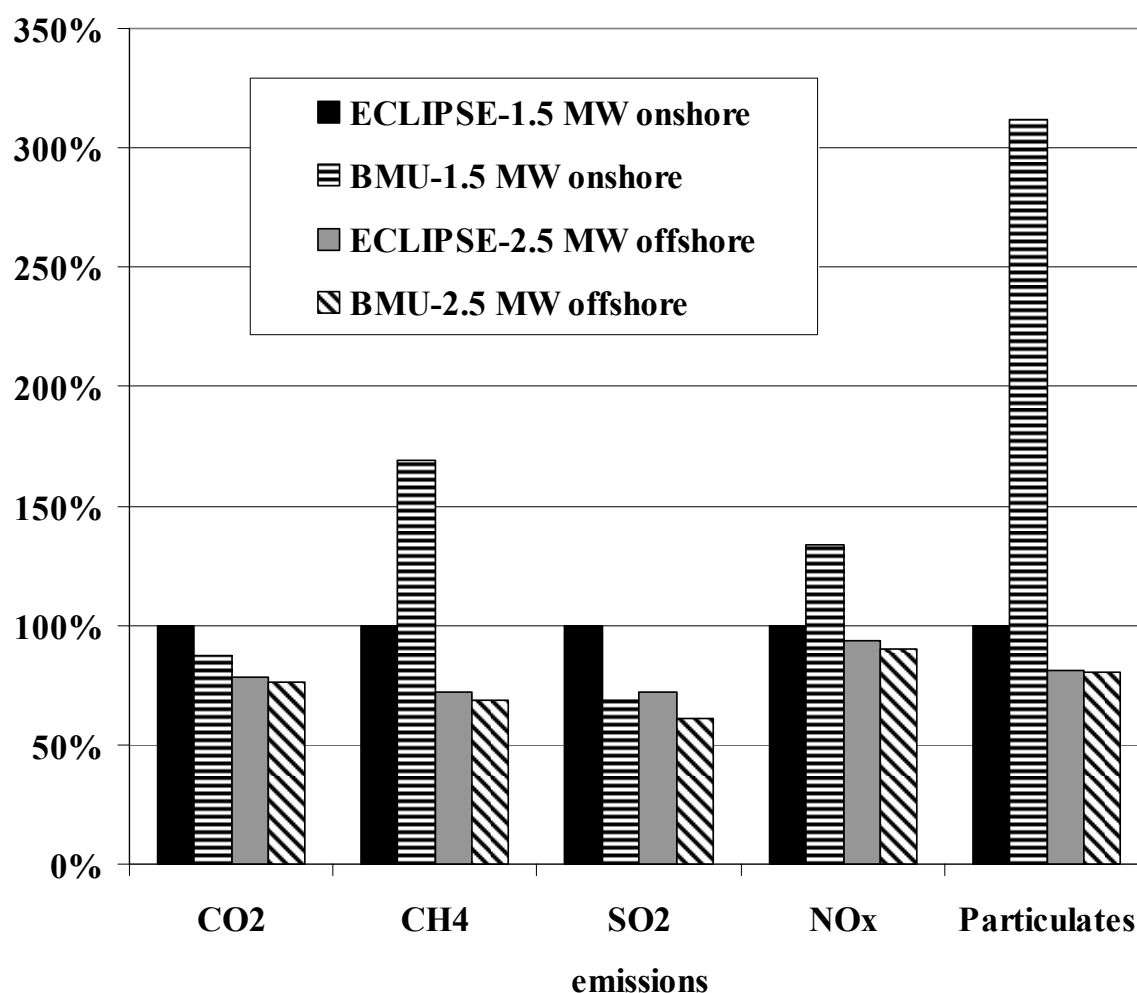
Figure 5-41: Comparison of the emissions of the wind turbines analysed in /BMWA 2004/ and /Chataignere; Le Boulch 2003/ (in kg/kWh$_{el}$)

In /BMU 2004/ wind turbines are analysed. The study performs a detailed balance of a 1.5 MW wind turbine near the coast with a life time of 20 years. Material and energy demand for this wind turbine are derived from /Pick et al. 1998/. **Figure 5-41** shows that the CO_2 and SO_2 emissions are 13 % and 32 %, respectively, lower but that the CH_4 emissions 69 %, the NO_x emissions 34 %, and the particulates emissions even 212 % higher compared to the LCI data from /Chataignere; Le Boulch 2003/. Due to the low data quality for particulates the variation of particulates emissions may be attributed to data quality problems. The variations of the other emissions may be attributed to different assumptions.

/BMU 2004/ analyse a wind turbine whose data are derived from /Chataignere; Le Boulch 2003/. Therefore, the differences between BMU and ECLIPSE should not be very significant. The similarity is displayed in **Figure 5-41**. The authors of /BMU 2004/ state that more than 95 % of the environmental impacts are caused in the construction phase of the wind turbines. This is a larger share than the one determined in /Chataignere; Le Boulch 2003/.

5.3   Fuel cell (FC) systems

5.3.1   Technology

/Forschungszentrum Jülich 2003/ describes the basics of fuel cells:

Fuel cells are electrochemical devices converting chemical energy directly into electrical energy. The *energetic conversion rate* η in a FC is given by the ratio of the produced electrical energy E plus the produced heat Q over the *enthalpy change* ΔH:

$$\eta = \frac{E+Q}{\Delta H} \tag{5-10}$$

In a normal thermal combustion, the total enthalpy is converted into heat. In contrast, in a FC, only the *free reaction enthalpy* ΔG_T is converted. The free reaction enthalpy results from the enthalpy change minus the product of *temperature* T and *reaction entropy* ΔS by the relation:

$$\Delta G_T = \Delta H - T \cdot \Delta S \tag{5-11}$$

The free reaction enthalpy ΔG_T which depends on the temperature is converted into energy resulting in a *maximum theoretical efficiency* η_{max} of:

$$\eta_{max} = \frac{\Delta G_T}{\Delta H} = \frac{\Delta H - T \cdot \Delta S}{\Delta H} = 1 - \frac{T \cdot \Delta S}{\Delta H} \tag{5-12}$$

This relation shows that the efficiency of a FC decreases with increasing temperature in contrast to a normal thermal combustion where the maximum efficiency, so-called *Carnot efficiency*, η_{carnot} increases with increasing temperature (based on a certain lower temperature T_0) following the relation:

$$\eta_{carnot} = 1 - \frac{T_0}{T} \tag{5-13}$$

In real conditions, this maximum efficiency is not achieved due to several losses.

A FC consists of three basic elements: the anode (fuel electrode), the cathode (oxygen electrode) and the interconnecting ion-conducting electrolyte. The anode and the cathode are electrically connected with a consumer load. Electrons flow over this load from the anode to the cathode whereas the ions move through the electrolyte. Thus, a closed circuit for the current is achieved. In detail, these electrochemical processes vary by their operation temperature, the used oxidant and fuel gas, and the ion flows, depending on the type of FC. Different types of FCs are summarized in **Figure 5-42**.
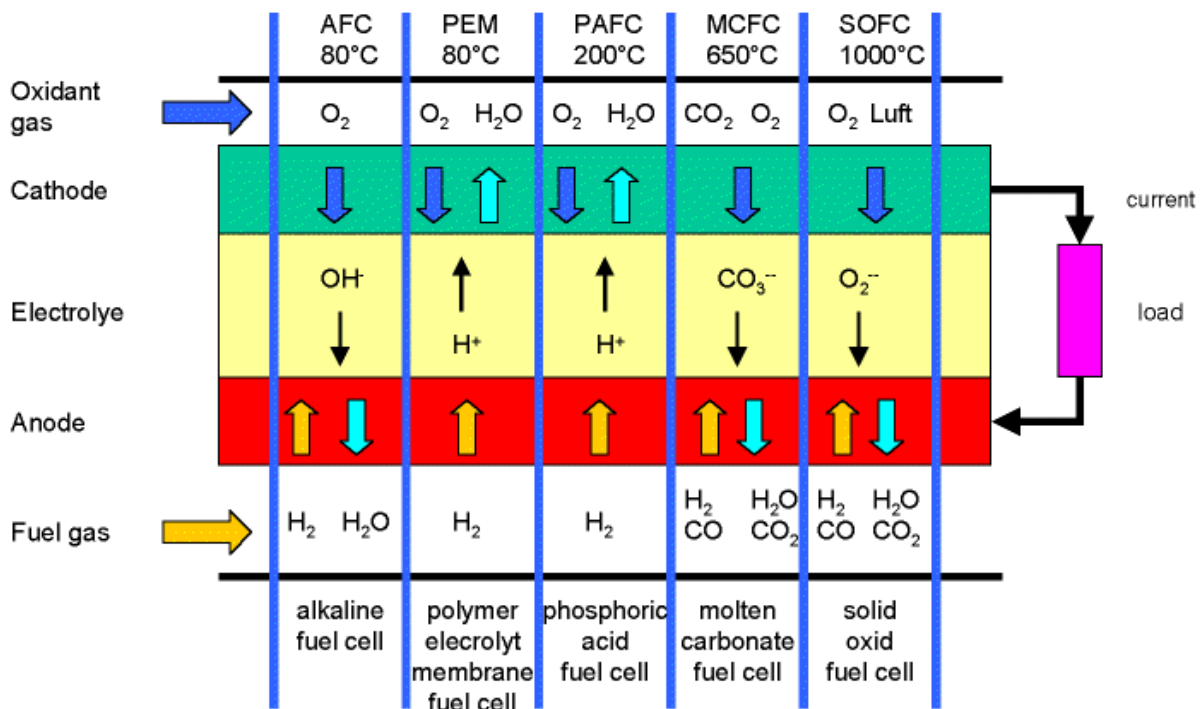
Figure 5-42:   Types of fuel cells /Forschungszentrum Jülich 2003/

Table 5-13:   Advantages and disadvantages of the different FCs /Krewitt et al. 2004/

FC	Advantages	Disadvantages
PEFC	- high power density - simple cell structure - fast starting behaviour - high dynamic operation possible - long lifetime - market potential for mobile applications	- only pure fuel gas - heat and water management necessary - high costs
PAFC	- lifetime of 40,000 hours demonstrated - availability > 90 % demonstrated - operation at ambient pressure - highly developed	- a maximum electrical efficiency of 40 % - slow starting behaviour (1.5-3 hours) - low development potential - high costs
SOFC	- simple system structure - long lifetime - high efficiency - process heat usable - no electrolyte management	- high operation temperature - corrosion of the components - slow starting and stopping behaviour - high costs

FCs can be differentiated into stationary, portable and mobile systems. In the study at hand, only stationary systems are considered. The PAFC, MCFC, SOFC and PEFC are for stationary applications. Their name refers to their specific electrolyte. /Viebahn; Krewitt 2003/ analyse the PAFC, PEFC and SOFC. The *Phosphoric Acid Fuel Cell* (PAFC) is the only commercial FC and already used in many applications at present. A high power density and low operating temperatures are characteristics of the *Polymer Electrolyte Fuel Cell* (PEFC), which is therefore considered to have various application possibilities. The *Solid Oxide Fuel Cell* (SOFC) has the highest electrical efficiencies of all FCs. High operating temperatures of 800-1,000 °C make the SOFC appropriate for stationary applications such as combined heat and power plants.

Table 5-13 lists advantages and disadvantages of the different FCs and **Table 5-14** gives an overview of the analysed systems.

Table 5-14:   Parameters of different FCs according to /Krewitt et al. 2004/, /VIK 1999/ and /Ledjeff-Hey et al. 2001/

Parameters	PEFC	PAFC	SOFC
Electrolyte	proton exchange membrane	phosphoric acid in carbide matrix	solid ceramic membrane (e.g. yttrium stabilized zirconia)
Electrodes	platinum-impregnated porous carbon	porous graphite coated with platinum	porous, conducting metal-ceramics
Fuel	H_2 (or others with reformer)	H_2 (or others with reformer)	H_2, natural gas, biogas, coal gas
Oxidant	O_2, air	O_2, air	O_2, air
Anode reaction	$H_2 \rightarrow 2\,H^+ + 2\,e^-$		$H_2 + O^{2-} \rightarrow H_2O + 2\,e^-$
Cathode reaction	$2\,H^+ + 0.5\,O_2 + 2\,e^- \rightarrow H_2O$		$0.5\,O_2 + 2\,e^- \rightarrow O^{2-}$
Electrical efficiency (natural gas, CHP)	small: 28-32 % large: 40 %	37 %	small: 28 % large: 47 % hybrid: 58 %
Total efficiency	80-90 %	80-90 %	80-90 %
Operating temperature	60–80 °C	200 °C	800-1,000 °C
Development status (2003)	prototype	limited-lot production	demonstration

Solid Oxide Fuel Cell (SOFC):

In a SOFC, no external fuel reforming of natural gas into H_2 and CO is necessary. It is performed internally with the catalytic converter at the anode after the sulphur is removed from the fuel by a desulphuriser. The electrolyte is a solid ceramic membrane which is conductive for oxide ions at temperatures above 750°C. Air is introduced into the cell. The catalytic effect of the cathode and the electrolyte ionises the oxygen in the air at high temperatures (800–1,000°C). These O_2 ions move from the cathode across the electrolyte to the anode. The H_2 and CO from the fuel react with the O_2 ions so that H_2 is oxidised to H_2O. CO is oxidised to CO_2. Electrons are released during this process and flow to the cathode (see **Figure 5-42**). Individual cells are composed in an array to get a higher power supply.

A further development is the SOFC/Gas Turbine Hybrid System with a higher electrical efficiency due to a combined cycle using the same air flow. The air is pressurised by the turbine's compressor and heated in a recuperator. Then the hot air enters the FC module in order to heat it to operating temperatures. The resulting exhaust gas drives the gas turbine.

Phosphoric Acid Fuel Cell (PAFC):

In a PAFC the electrodes are made of a finely dispersed platinum catalyst on carbon paper. A silicon carbide matrix holds the *phosphoric acid* (H_3PO_4) as electrolyte by capillary forces. The operation temperature has to be about 200°C because the by-product water has to be removed as steam. At lower temperatures, the water will be dissolved in the electrolyte and not be removed as steam. However, at higher temperatures, the phosphoric acid starts to decompose.

The H_2 which may be generated by a reformer or by electrolysis is converted into protons by a catalytic reaction. These protons flow through the electrolyte and react with oxygen to water while the released electrons flow over the load to the cathode.

Polymer Electrolyte Fuel Cell (PEFC):

A PEFC (or PEM = Proton Exchange Membrane) consist of two platinum-impregnated porous electrodes. Between these electrodes, there is a proton conducting membrane. This type of cell can be operated on either hydrogen or liquid methanol (interesting for mobile applications). For efficient performance the membrane has to be moistened with water all the time. Therefore, water management is very important. Because of operating temperatures of 60-80 °C this type of FC is not only interesting for stationary use but also for portable use, e.g. replacing batteries.

5.3.2   Market development

/Krewitt et al. 2004/ give an overview of actual stationary FC systems. They distinguish a lower, middle and higher range of performance.

In the lower range of performance with capacities below 5 kW there are mainly PEFCs which are dynamically operable. Also some SOFCs are available. They are considered for private households. The most advanced systems are tested in demonstration systems.

A higher market development is achieved in the middle range of performance which consists of systems with more than 5 kW but less than 1 MW. Since 1991 the manufacturer ONSI/UTC has delivered approximately 250 PAFC systems with 200 kW. /Krewitt et al. 2004/ note that UTC wants to phase out this FC due to little cost reduction potentials. UTC favours the PEFC. Beside those two, other types of FCs for CHP in the middle range of performance are the MCFC and SOFC as well as the SOFC together with a gas turbine. Except for the commercial marketed 200 kW PAFC system the other FC systems are still in the demonstration phase.

In the higher performance range of more than 1 MW, demonstration FC systems use PAFC, MCFC or SOFC technology. Nevertheless, before this high capacity FC will be developed, the technological problems of the systems with lower capacity should be solved.

5.3.3   LCA results in ECLIPSE

/Viebahn; Krewitt 2003/ analyze the following FC systems of the middle range of performance:

For SOFCs, a 250 kW SOFC and a hybrid 300 kW SOFC are studied. The 250 kW SOFC is fired by natural gas, hydrogen and biogas. The 300 kW SOFC Hybrid consists of a 250 kW SOFC and a 40 kW micro gas turbine fired by natural gas. It is an actual technology of Siemens-Westinghouse.

The ONSI 25 C 200 kW PAFC is analysed as a PAFC system. It is fired by natural gas.

For PEFCs, the ALSTOM-Ballard P2B 200 kW is studied. It is fired by natural gas. /Pehnt 2002/ is the source of a life cycle assessment of a 212 kW$_{el}$ pilot plant from Ballard Generation Systems.

Table 5-15:   Efficiencies, functional units and allocation factors for the analysed FC systems /Viebahn; Krewitt 2003/

Type of fuel cell	Fuel	η_{el}	η_{th}	Functional unit	all$_{el}$	all$_{th}$
250 kW SOFC	natural gas	47 %	33 %	1 kWh$_{el}$ + 0.7 kWh$_{th}$	93 %	7 %
	hydrogen	42 %	38 %	1 kWh$_{el}$ + 0.9 kWh$_{th}$	92 %	8 %
	biogas	47 %	33 %	1 kWh$_{el}$ + 0.7 kWh$_{th}$	93 %	7 %
300 kW SOFC Hybrid	natural gas	58 %	22 %	1 kWh$_{el}$ + 0.38 kWh$_{th}$	96 %	4 %
200 kW PAFC	natural gas	37 %	50 %	1 kWh$_{el}$ + 1.35 kWh$_{th}$	88 %	12 %
200 kW PEFC	natural gas	40 %	40 %	1 kWh$_{el}$ + 1 kWh$_{th}$	91 %	9 %

Besides the generated power, FCs also produce a certain amount of heat. The ratio of heat and electricity depends on the configuration, the efficiency and the fuel of the FC system. For each combination, a unique functional unit is defined determining the amount of heat which is produced additionally while generating 1 kWh of electricity. Allocation between electricity and heat is performed on the basis of exergy following the ECLIPSE methodological guidelines. /Viebahn; Krewitt 2003/ assume the outgoing temperature T_{in} = 65°C, the returning temperature T_{out} = 40°C and the ambient temperature T_0 = 20°C, in accordance with /Setterwall et al. 2004/. Based on literature data and data from pilot plants, the efficiencies of SOFC and PEFC are adjusted to a projected situation in 2010. **Table 5-15** gives an overview of the studied systems with the considered efficiencies and the resulting allocation factors.

The technical lifetime of the stacks is assumed to be 40,000 hours and that of the periphery, so-called *balance of plant* (BoP), 100,000 hours resulting in 2.5 units of stack for the lifetime of one unit of BoP.

Life cycle of FC systems:

The life cycle of a FC system consists of the six main phases fuel supply, manufacturing of the stack, manufacturing of the BoP, manufacturing of the gas turbine (in the case of a hybrid FC), operation and end of life. The life cycle phases are illustrated in **Figure 5-43**.
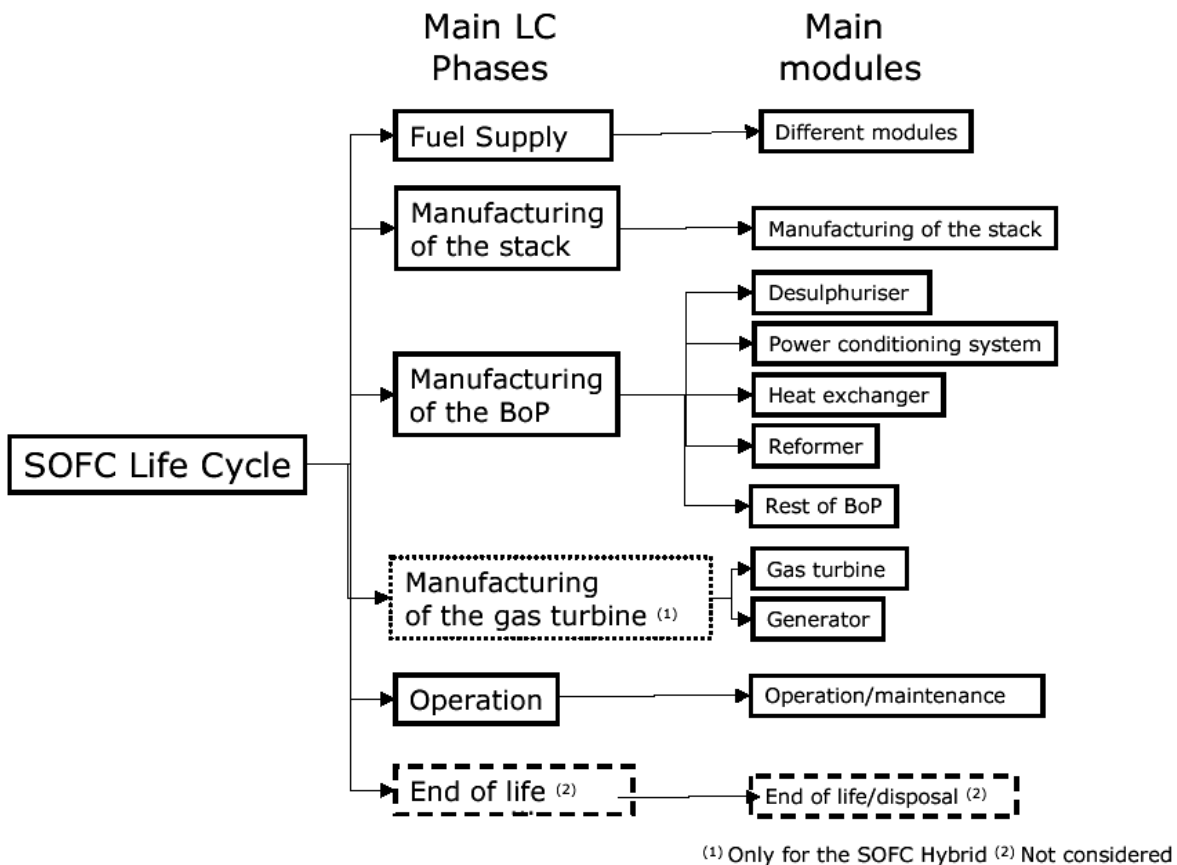
Figure 5-43:   Life cycle of fuel cells /Viebahn; Krewitt 2003/

Natural gas supply:

The natural gas supply is based on the assumptions of the natural gas upstream processes which are stipulated in ECLIPSE.

Hydrogen supply:

The requirements of materials and energy for the production of hydrogen by advanced alkaline electrolysis are taken from /Pehnt 2002/ who determines electricity demand of 1.43 MJ to generate 1 MJ of hydrogen corresponding to an efficiency of 70 %. /Viebahn; Krewitt 2003/ combine the electrolysis with electricity generated by a 1.5 MW onshore wind turbine according to /Marheineke 2000/. However, /Marheineke 2000/ estimates emissions of wind turbines which are much higher than those in /Chataignere; Le Boulch 2003/. Thus, the LCI of the hydrogen supply tends to be lower if the data for the ECLIPSE study are used.

Biogas supply:

The requirements of materials and energy for the production of biogas from wood chips are taken from /Pehnt 2002/.

Manufacturing of the fuel cell:

A FC system can be distinguished between the FC stack and the BoP. The main components of the BoP are the reformer and desulphuriser unless hydrogen is used as fuel, the power conditioner converting DC into AC, and the water and heat management units. Additional components of the BoP are compressors, expanders, pumps, controls, insulation, the safety system and others.

During the manufacturing of the 250 kW SOFC, about two thirds of CO_2 are contributed to the stack and the other third to the BoP. Nearly 90 % of the CO_2 emissions can be contributed to four processes. The cathode powder preparation for the stack with its demand for $LaMnO_3$ has a share of 41.85 %, the pressure vessel of the BoP with its high demand of steel has a share of 22.30 %, the deposit interconnect for the stack with its electricity demand has a share of 13.06 % and the electrolyte for the stack with its demand for *zirconium tetrachloride* ($ZrCl_4$) and *yttrium chloride* (YCl_3) has a share of 10.69 %. The contribution of the stack and the BoP to the analysed emissions is illustrated in **Figure 5-44**.

In the case of the PAFC, the processes manufa*cturing of graphite for the stack and electrodes* and *manufacturing of steel for the frame of the FC* are responsible for the main part of the CO_2 emissions. The contribution of the stack and the BoP to the analysed emissions is illustrated in **Figure 5-45**.

/Viebahn; Krewitt 2003/ used confidential data from Ballard Generation Systems in the case of the PEFC which are not allowed for publication. Therefore, no analysis of these data is shown.
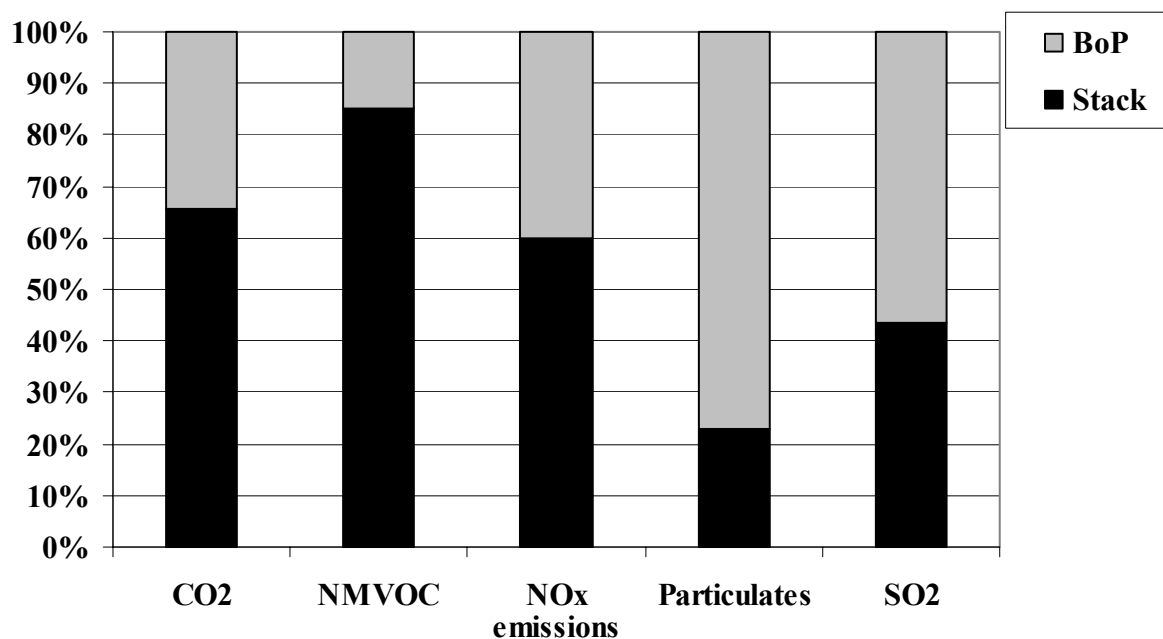
Figure 5-44:   Contribution of stack and BoP to the emissions caused by their manufacturing in case of a 250 kW SOFC (in kg/kWh$_{el}$)
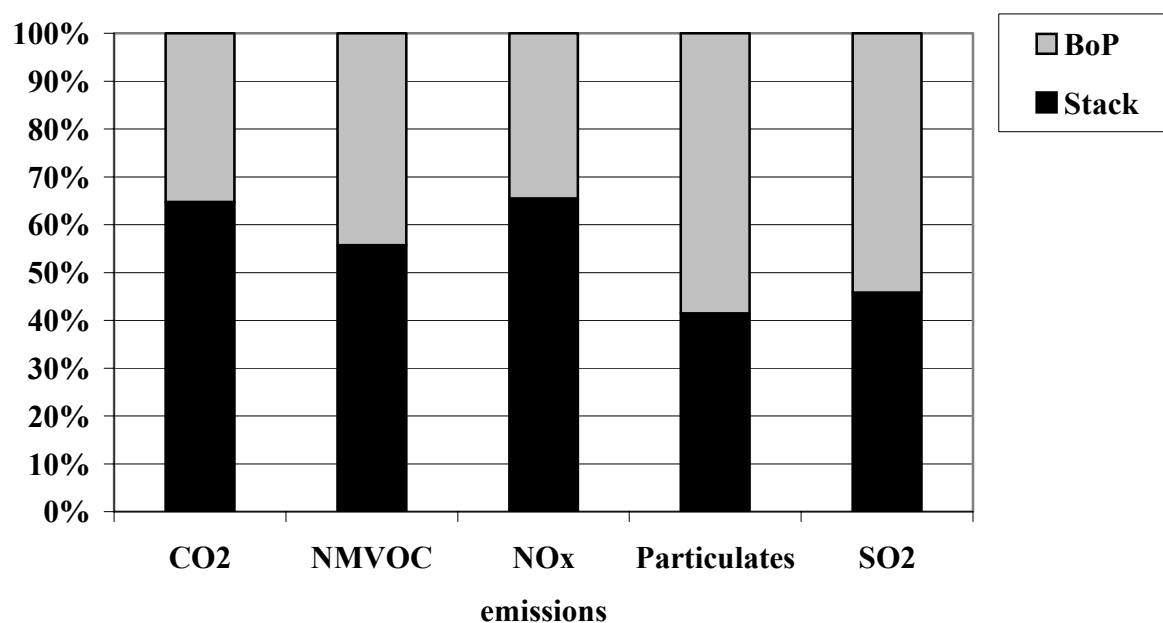
Figure 5-45:   Contribution of stack and BoP to the emissions caused by their manufacturing in case of a 250 kW PAFC (in kg/kWh$_{el}$)

/Viebahn; Krewitt 2003/ state that the data quality regarding the production of the fuel cells is not very good because literature data are partly incomplete or out of date with the only exception of PEFC with original but confidential data from the industry. The direct emissions of the SOFC are given by the developing company. This restriction seems not too critical as the emissions caused by the FC production are very small compared to those by

fuel supply (see below). Thus, improvements of stack and BoP do not result in large improvements of the LCI. With the exception of PAFC, the efficiencies are adopted to the year 2010. /Viebahn; Krewitt 2003/ assume that the FCs will then be produced commercially.

Manufacturing of the gas turbine:
The requirements of materials are taken from a study about a 10 MW gas turbine from the company MAN/GHH. Data for energy requirements is not given. The MW-specific data are scaled down to get the material and energy flows for the 40 kW gas turbine. This life cycle phase is only considered in the case of the hybrid FC system.

Operation of the fuel cell:
The emission factors of the natural gas-fired SOFC are taken from a personal notice of Siemens. For CO_2, the emission factor is adapted to the carbon content of the natural gas mix which is used for the ECLIPSE studies. Hydrogen fired SOFC are assumed to have no emissions. For biogas, the emission factor of CO_2 is assumed to be zero because the fired biomass has removed the now emitted CO_2 from the atmosphere during its growth time. /Viebahn; Krewitt 2003/ make the assumption that no CH_4, SO_2 and particulates are emitted during the operation fired by biogas. During the operation, CO_2 is only emitted by natural gas and NMVOC and NO_x by natural gas and by biogas.

The quality of the natural gas used in ECLIPSE represents the situation from the beginning of the nineties.

Operation of the gas turbine:
The exhaust gas with the emissions from the FC is powering the gas turbine without further emissions. The electrical efficiency is derived from the company Solar Turbines Corp. with a maximum efficiency of 41 % for turbines in the megawatt class. Aging is included with losses of 2 % following /Pehnt 2002/ so that the mean electrical efficiency is assumed to be 39 % and the mean thermal efficiency 35 % for steam and 45 % for high temperature water. 100,000 hours are taken into account for the lifetime of the gas turbine.

End of life:
The end of life of the plant is not considered because of the lack of data but recycling rates for the most important materials (steel, aluminium, copper, platinum, nickel) are included with input flows as a mixture of primary and secondary materials.

Examples:

The emissions of the examples described in the following paragraphs are listed in **Table 5-16** and compared in **Figure 5-55**.

SOFC 250 CHP (natural gas-fired):

The life cycle phase natural gas supply dominates the emissions of SO_2, particulates, NO_x and NMVOC with 72 % to 99.6 % of the total emissions from the SOFC 250 kW fired with natural gas. The share of natural gas supply of the CO_2 emissions dominated by the operation phase is only 12 % (see **Figure 5-46**).

Without the dominating natural gas supply, the shares are distributed as shown in **Figure 5-47**. 98.5 % of the CO_2, 73 % of the NMVOC and 34 % of the NO_x emissions are caused in the operation phase. The other emissions result from the production phase only. CO_2, NMVOC, NO_x and CH_4 emissions are mainly caused by the production of the stack and SO_2 as well as particulates are mainly caused by the production of the BoP.

300 kW SOFC Hybrid (natural gas-fired):

The emissions resulting from the production of the BoP decrease slightly, because a smaller heat exchanger is needed as the exhaust gas from the FC is powering the gas turbine without further emissions during the operation phase. Additional emissions from the production of the turbine are negligible compared to the total emissions. The emissions per kWh_{el} of this type of SOFC are about 12-16 % lower than those without a gas turbine because the total electrical efficiency is higher (58 % instead of 47 %) and, therefore, the amount of generated electrical energy is higher (29 GWh_{el} instead of 25 GWh_{el} over the total lifetime). **Figure 5-48** illustrates the distribution of the contribution to the emissions between the life cycles.

250 kW SOFC (hydrogen fired):

The natural gas supply is replaced by hydrogen supply. Since no cleaning is required anymore, the desulphuriser and the reformer are removed with a very small effect on the emissions of the fuel cell production. The emissions during the operation are set to zero. No heat is needed to run the reformer resulting in a higher thermal efficiency. The hydrogen must be injected electrically resulting in a decreased electrical efficiency. **Figure 5-49** displays the contribution of the life cycle phases to the emissions.

The emissions per kWh_{el} of NMVOC, CO_2, NO_x and SO_2 are reduced by 1.5-84 % compared with the natural gas-fired SOFC (see **Figure 5-55** and **Figure 5-56**). Only particulates emissions increase to 530 % relative to the 250 kW SOFC fired with natural gas.

/Viebahn; Krewitt 2003/ note that 88 % of the still high emissions of SO_2 and 99 % of the particulates emissions are caused by German electricity mix used to model the wind turbine in /Marheineke 2002/. So that the life cycle phase hydrogen supply still dominates the emissions of SO_2, NO_x, CO_2, and particulates with shares from 82 % to 95 %. Only NMVOC is dominated by the stack production.
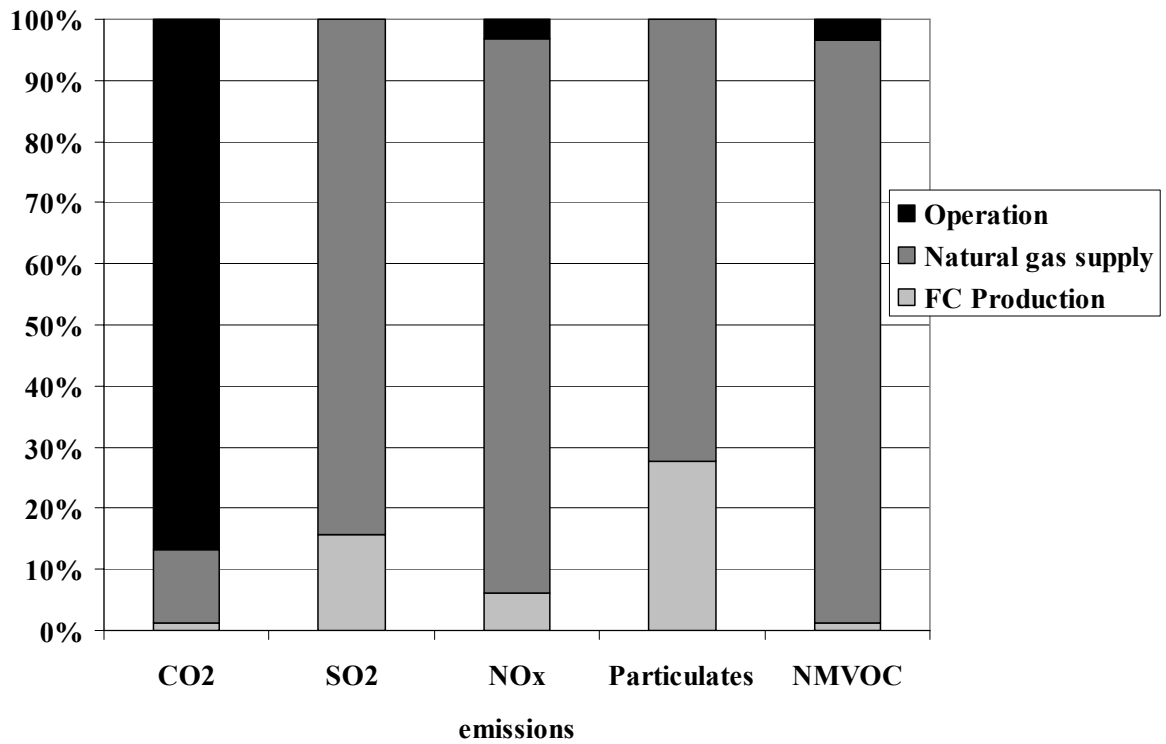
Figure 5-46: Contribution of different life cycle phases to the emissions of a natural gas-fired SOFC 250 kW (in kg/kWh$_{el}$)
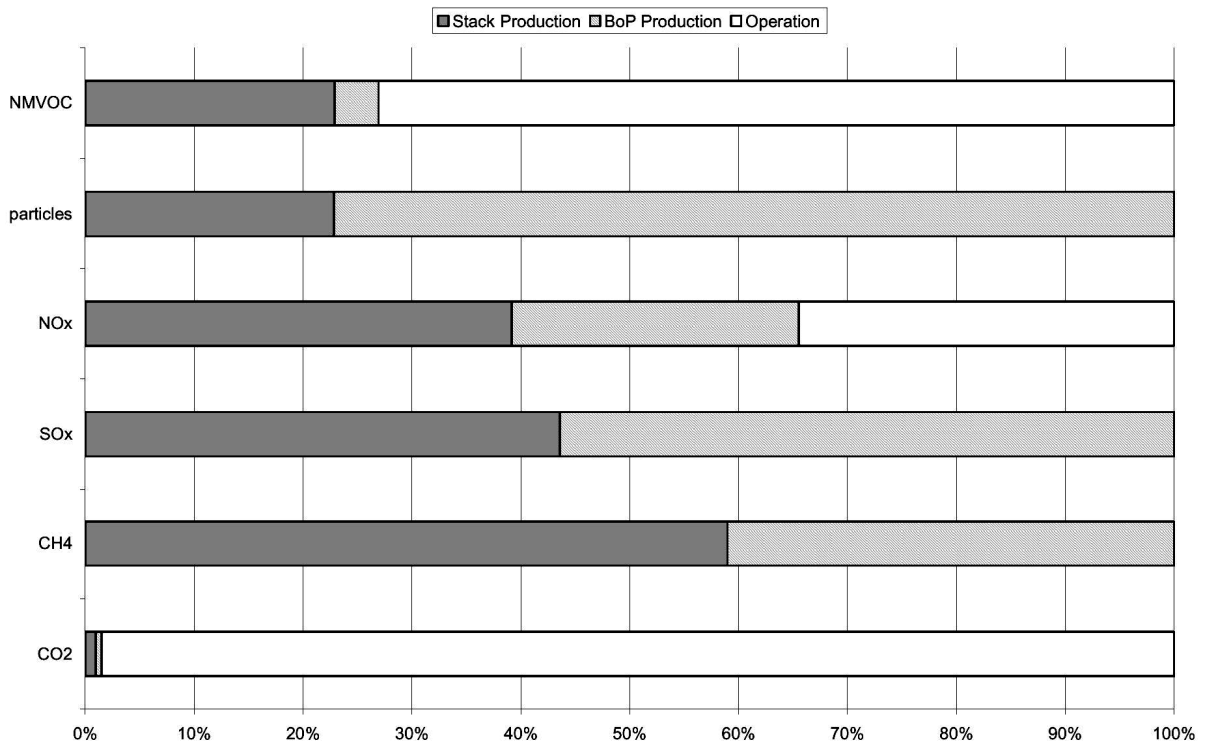
Figure 5-47: Contribution of different life cycle phases to the emissions (in kg/kWh$_{el}$) of a SOFC 250 kW (without natural gas supply) /Viebahn; Krewitt 2003/
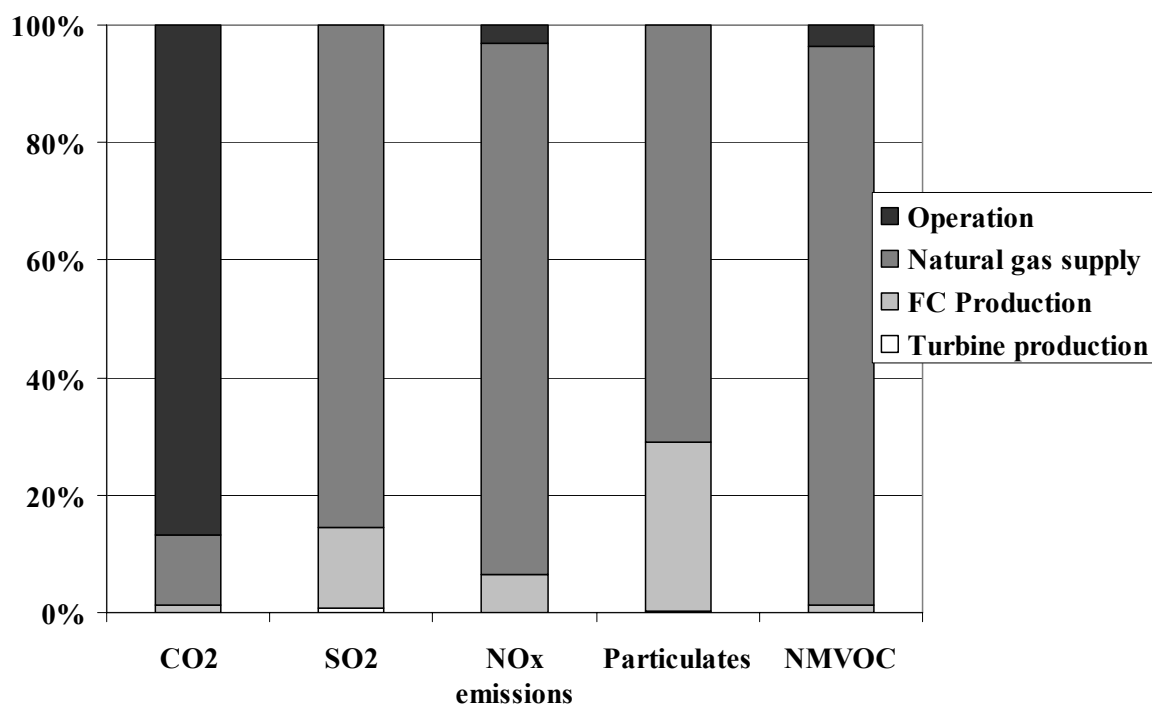
Figure 5-48:   Contribution of different life cycle phases to the emissions (in kg/kWh$_{el}$) of a SOFC 300 kW (natural gas)
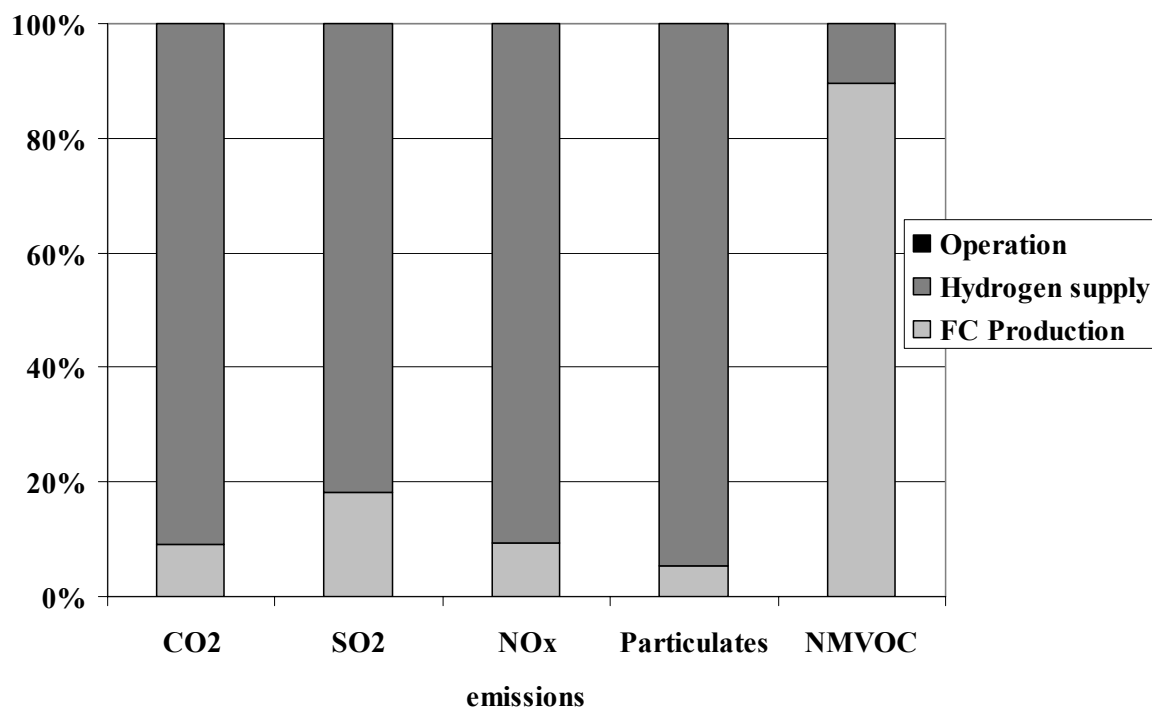
Figure 5-49:   Contribution of different life cycle phases to the emissions (in kg/kWh$_{el}$) of a SOFC 250 kW (hydrogen)

250 kW SOFC (biogas-fired):
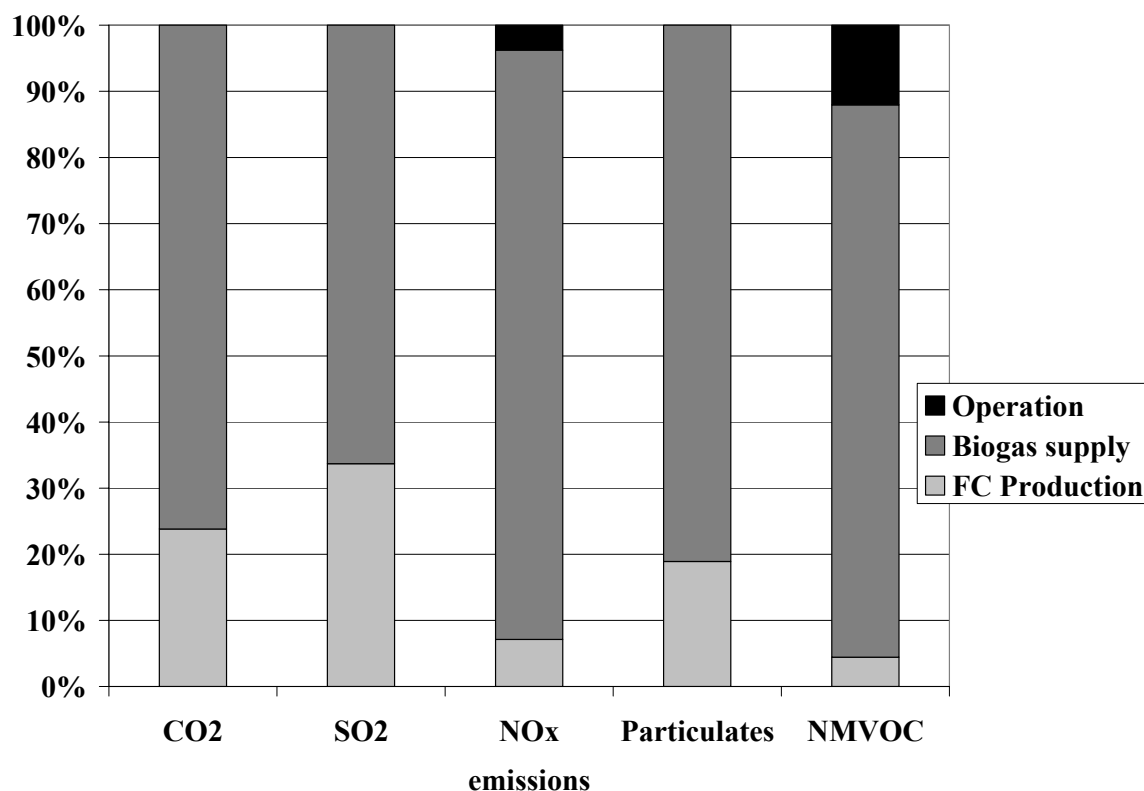
Figure 5-50: Contribution of different life cycle phases to the emissions (in kg/kWh$_{el}$) of a SOFC 250 kW (biogas)

The natural gas supply is replaced by biogas supply. During the operation, the emissions of CO_2 are set to zero. No additional units for the cleaning of the biogas are modelled, leaving the efficiencies at the same values as for the natural gas-fired SOFC.

Compared with the natural gas-fired SOFC, the fuel supply's share of particulates increased to 165 %, whereas its shares of NMVOC (-75 %), CH_4 (-99 %), SO_2 (-75 %), NO_x (-15 %) and CO_2 (-65 %) decreased significantly as shown in **Figure 5-55** and **Figure 5-56**. Thus, the share of emissions caused by FC production increases significantly but the biogas supply still dominates the emissions. **Figure 5-50** displays the contribution of the life cycle phases to the emissions.

200 kW PAFC (natural gas-fired):

In the case of a PAFC, the natural gas supply is dominating the emissions of SO_2, particulates, NO_x, NMVOC and CH_4 with 64 % to 99.5 % (see **Figure 5-51**), but not the CO_2 emissions with a share of 12 %. The latter are dominated by the operation phase. /Viebahn; Krewitt 2003/ state as the reason for the small operation's share of NMVOC that they did only find VOC emissions in literature.
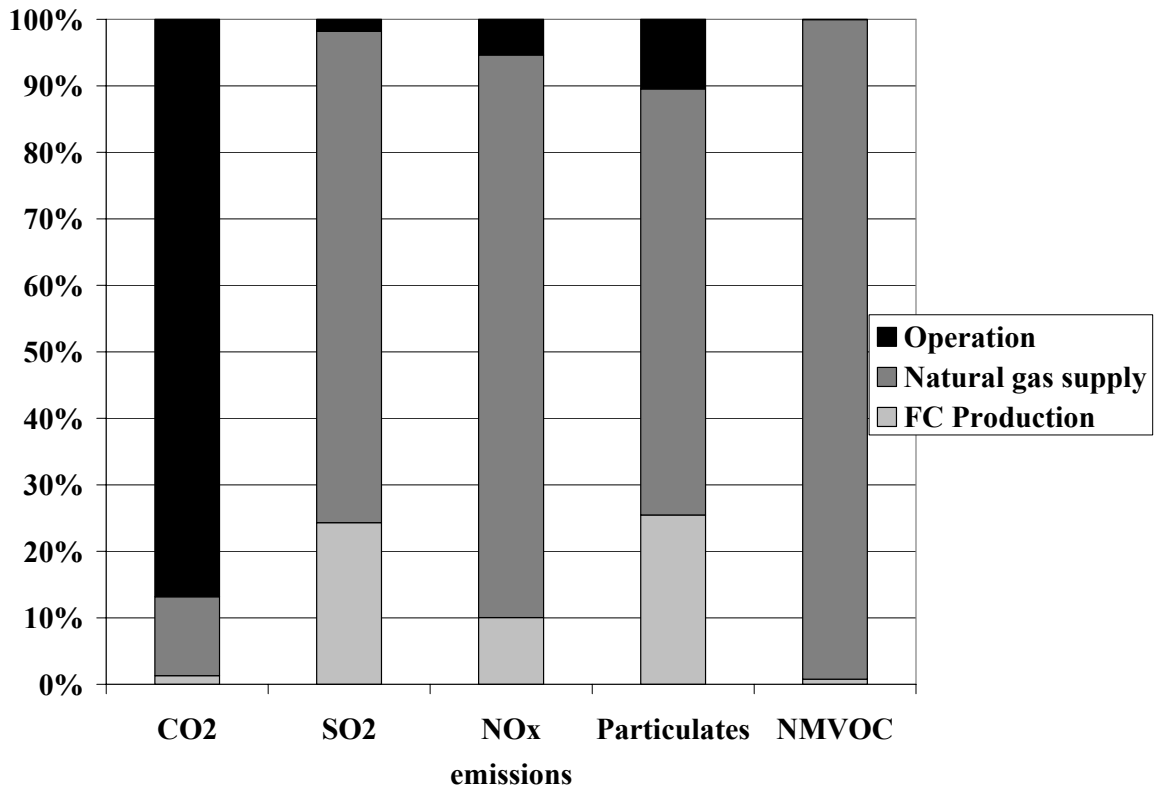
Figure 5-51:   Contribution of different life cycle phases to the emissions (in kg/kWh$_{el}$) of a PAFC
200 kW (natural gas)
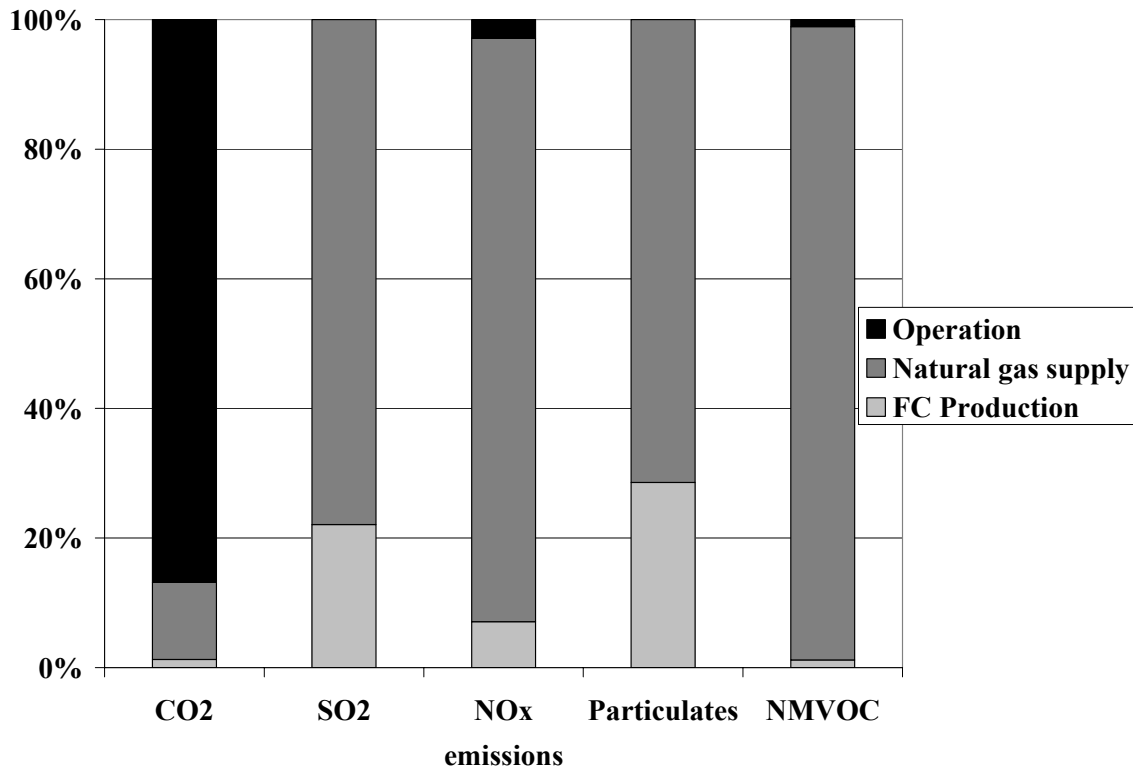
Figure 5-52:   Contribution of different life cycle phases to the emissions (in kg/kWh$_{el}$) of a PEFC
200 kW (natural gas)

200 kW PEFC (natural gas-fired):

The natural gas supply is dominating the emissions of SO_2, particulates, NO_x, NMVOC and CH_4 with 71 % to 97.8 %, but not the CO_2 emissions with a share of 12 %. CO_2 emissions are mainly caused in the operation phase due to the natural gas combustion. These contributions are illustrated in **Figure 5-52**.

Sensitivity analysis:

/Viebahn; Krewitt 2003/ conduct several sensitivity analyses with the following results summarized:

An increase of the lifetime of the stack from 40,000 to 80,000 hours has only little effect on the emissions per kWh_{el} because the life cycle emissions are mainly caused by operation and fuel supply which are both variable impacts occurring during the operation. Only fixed impacts may be distributed over a longer lifetime but they are relatively small.

In another sensitivity analysis, /Viebahn; Krewitt 2003/ illustrate that a different natural gas mix (not the ECLIPSE one) may result in significant reductions regarding CH_4, SO_2 and NMVOC. Therefore, it is necessary to have data with the same natural gas mix for the comparison of different technologies. Since a change of the natural gas mix alters the results significantly, the natural gas supply has to be considered very carefully.

Fuel supply:

The fuel supply is the dominating life cycle phase in all analysed FC systems. Therefore, a more detailed analysis is necessary. The change in emissions due to different fuel supplies and FC systems with 250 kW SOFC natural gas as the reference case is shown in **Figure 5-53** and **Figure 5-54**. **Figure 5-53** includes particulates emissions which are degrading the scale. Therefore, **Figure 5-54** shows the same picture but without particulates emissions so that the scale for comparison is improved.

All emissions of the four FC systems which are fired with natural gas are at a comparable level. In the case of hydrogen supply, CO_2 emissions are 10 % and particulates emissions even 600 % higher, but SO_2 emissions are 20 % and NO_x emissions 35 % lower than those caused by natural gas supply. /Viebahn; Krewitt 2003/ state that the reason is the CO_2-, SO_2- and particulates-intensive German electricity mix used to model the onshore wind turbine as well as the SO_2-intensive production of nickel used for the electrolyser. The emissions of NMVOC and NO_x are the lowest in the case of hydrogen supply. Biogas supply has the lowest values of all fuel supplies in the case of SO_2 and CO_2 so that this results in the lowest values for the total life cycle. Natural gas supply tends to have higher emissions than biogas or hydrogen supply. However, in the case of particulates, natural gas supply has lower emissions than biogas or hydrogen supply.
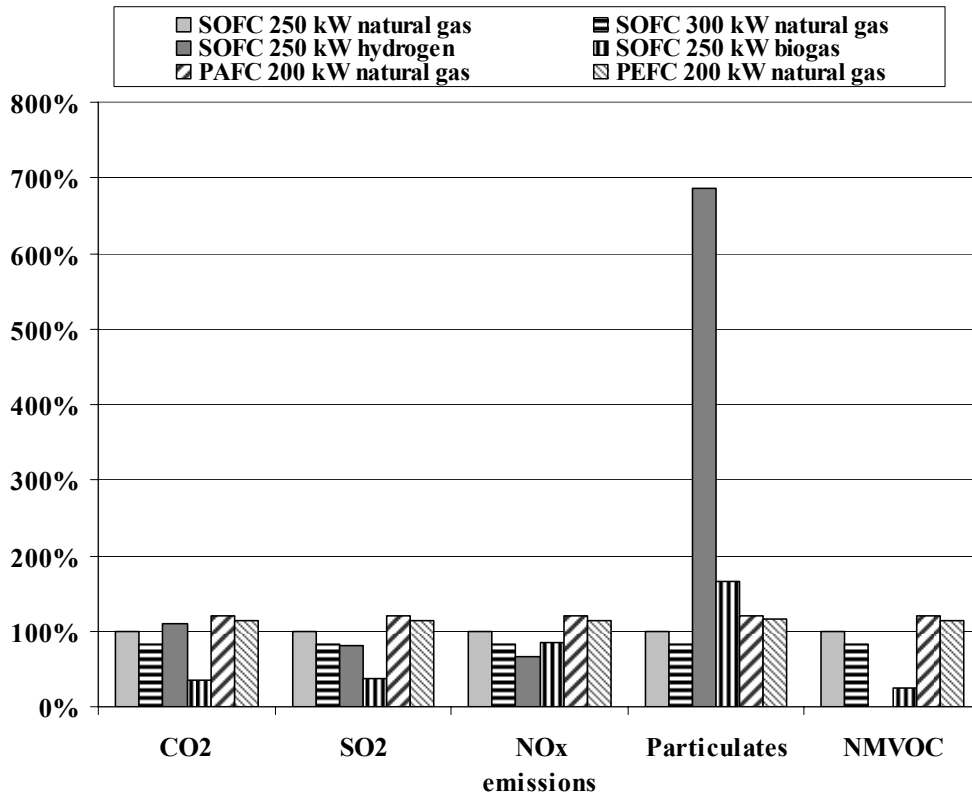
Figure 5-53: Comparison of the fuel supply emissions (in kg/kWh$_{el}$) from different FC systems (with particulates) in relation to the natural gas-fired 250 kW SOFC
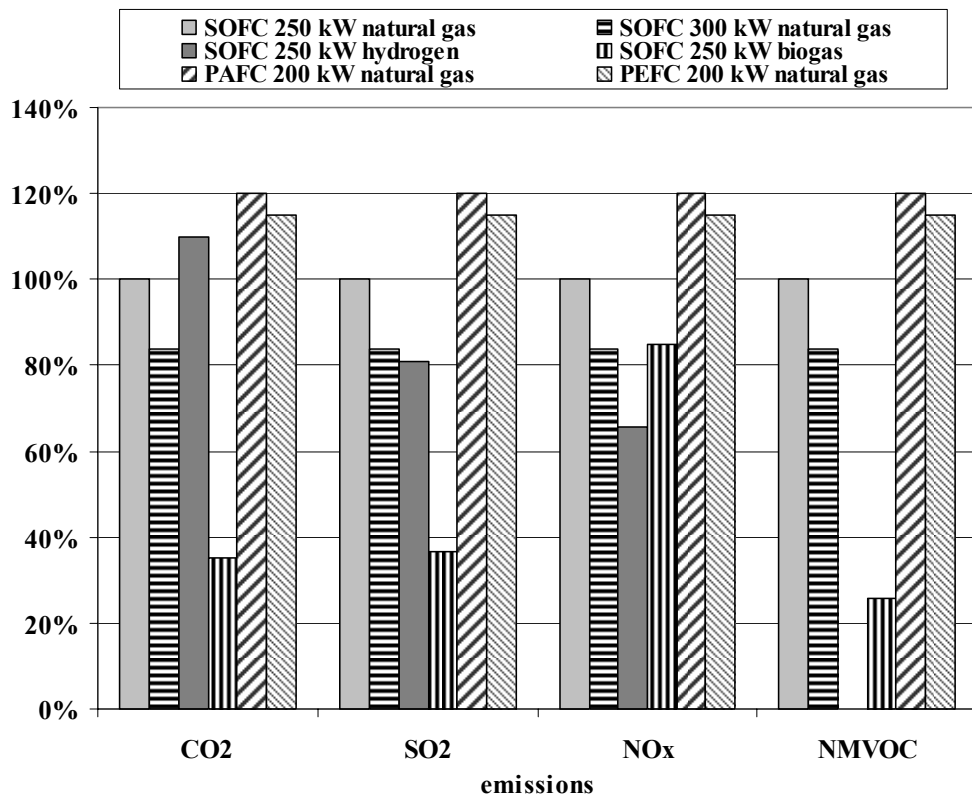
Figure 5-54: Comparison of the fuel supply emissions (in kg/kWh$_{el}$) from different FC systems (without particulates) in relation to the natural gas-fired 250 kW SOFC

5.3.4   Emissions of fuel cell systems

The life cycle emissions allocated to the electricity production of the analysed FC systems are given in **Table 5-16** and compared in **Figure 5-55** and **Figure 5-56**.

Compared to the natural gas-fired 250 kW SOFC, the emissions of the natural gas-fired PAFC and PEFC are ca. 10-40 % higher and the emissions of the hybrid SOFC are ca. 20 % lower. A higher variation is achieved with different fuels. The CO_2 emissions are significantly reduced by ca. 90 % in case of biogas or hydrogen. With the exception of the hybrid SOFC which is sometimes in the same range, the life cycle emissions of the biogas and hydrogen fired FCs are by far lower than those of the natural gas-fired FCs. The outlier of particulates emissions from the hydrogen fired SOFC originates from the hydrogen supply which is discussed above. This outlier makes it difficult to compare the other emissions. Therefore, **Figure 5-56** shows the same comparison but without the particulates emissions.
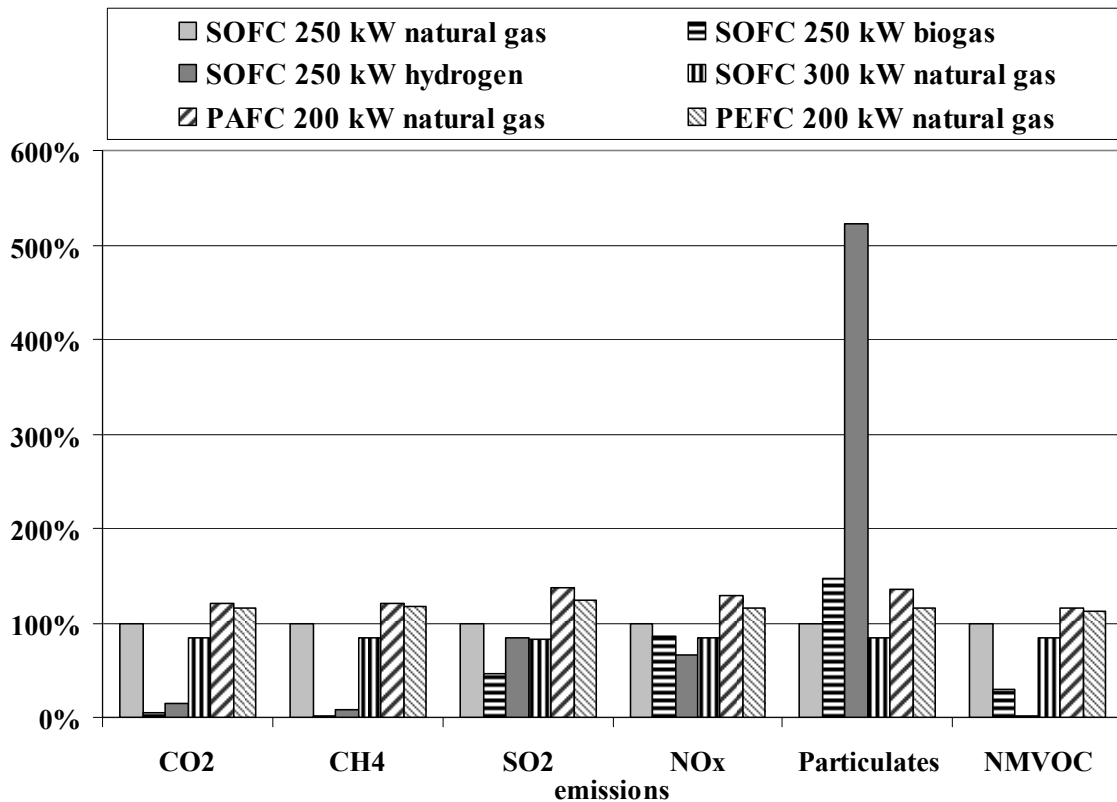
Figure 5-55:   Comparison of the emissions (in kg/kWh$_{el}$) of the FC technologies in relation to the natural gas-fired 250 kW SOFC
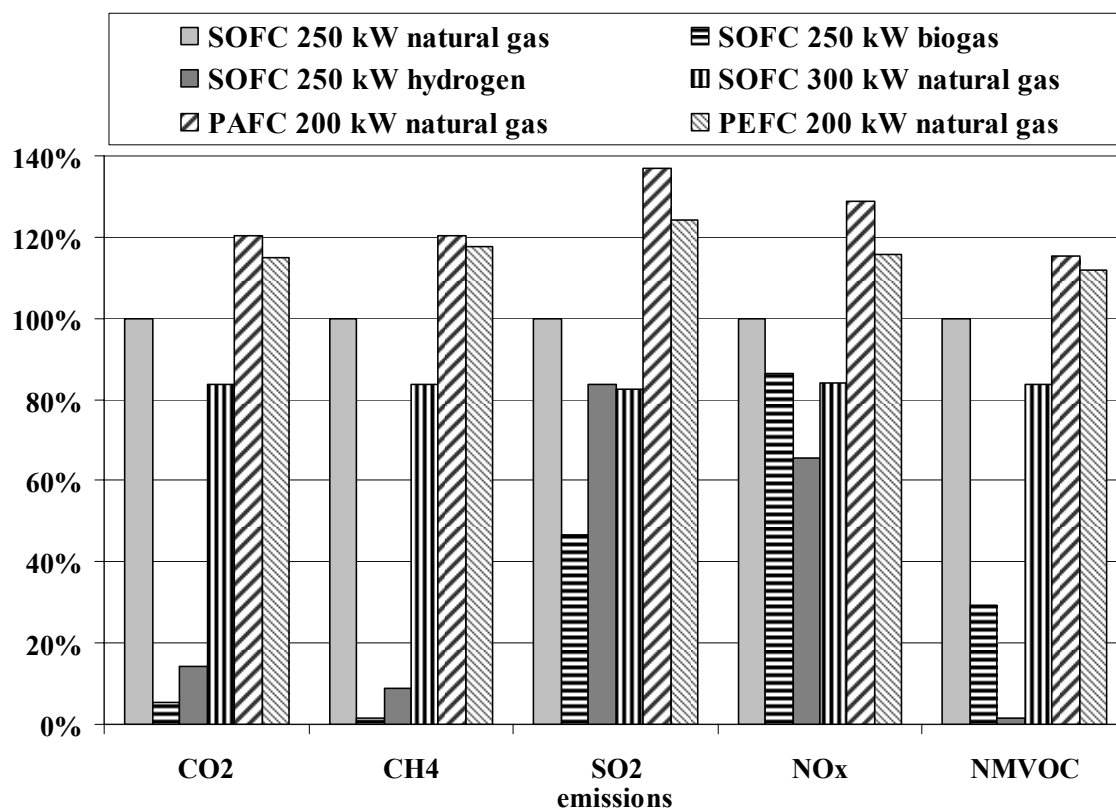
Figure 5-56:   Comparison of the life cycle emissions (in kg/kWh$_{el}$) from different FC systems (without particulates) in relation to the natural gas-fired 250 kW SOFC

Table 5-16:   Emissions of different FC systems (in kg/kWh$_{el}$)

Emissions	PAFC 200 kW natural gas	PEFC 200 kW natural gas	SOFC 300 kW natural gas	SOFC 250 kW natural gas	SOFC 250 kW biogas	SOFC 250 kW hydrogen
CO_2	5.53E-01	5.29E-01	3.85E-01	4.60E-01	2.51E-02	6.60E-02
CH_4	3.09E-03	3.02E-03	2.15E-03	2.57E-03	3.48E-05	2.33E-04
SO_2	3.13E-04	2.84E-04	1.88E-04	2.28E-04	1.07E-04	1.91E-04
NO_x	2.83E-04	2.55E-04	1.85E-04	2.20E-04	1.90E-04	1.44E-04
Particulates	4.96E-05	4.26E-05	3.11E-05	3.66E-05	5.37E-05	1.91E-04
NMVOC	2.33E-04	2.26E-04	1.69E-04	2.02E-04	5.91E-05	2.80E-06

Similar results are given for the distribution of the different life cycle phases to the life cy-cle emissions of the FC systems which are analysed in /Viebahn; Krewitt 2003/ as well as /BMWA 2004/. Both studies are performed by the *Deutsches Zentrum für Luft- und Raum-fahrt* (DLR). Therefore, the analysed systems are assumed to be similar. The difference be-

tween the studies, which is shown in **Figure 5-57** and **Figure 5-58**, is caused by the assumptions which are explained at the introduction of chapter 5.

The SO_2 emissions of the PAFC studied in /BMWA 2004/ are very different to those of the other FCs (cf. **Figure 5-58**). This deviation may be caused by the use of 90 % secondary materials for platinum and recycling rates for other materials in /Viebahn; Krewitt 2003/ whereas /BMWA 2004/ does not consider recycling activities to that extent.
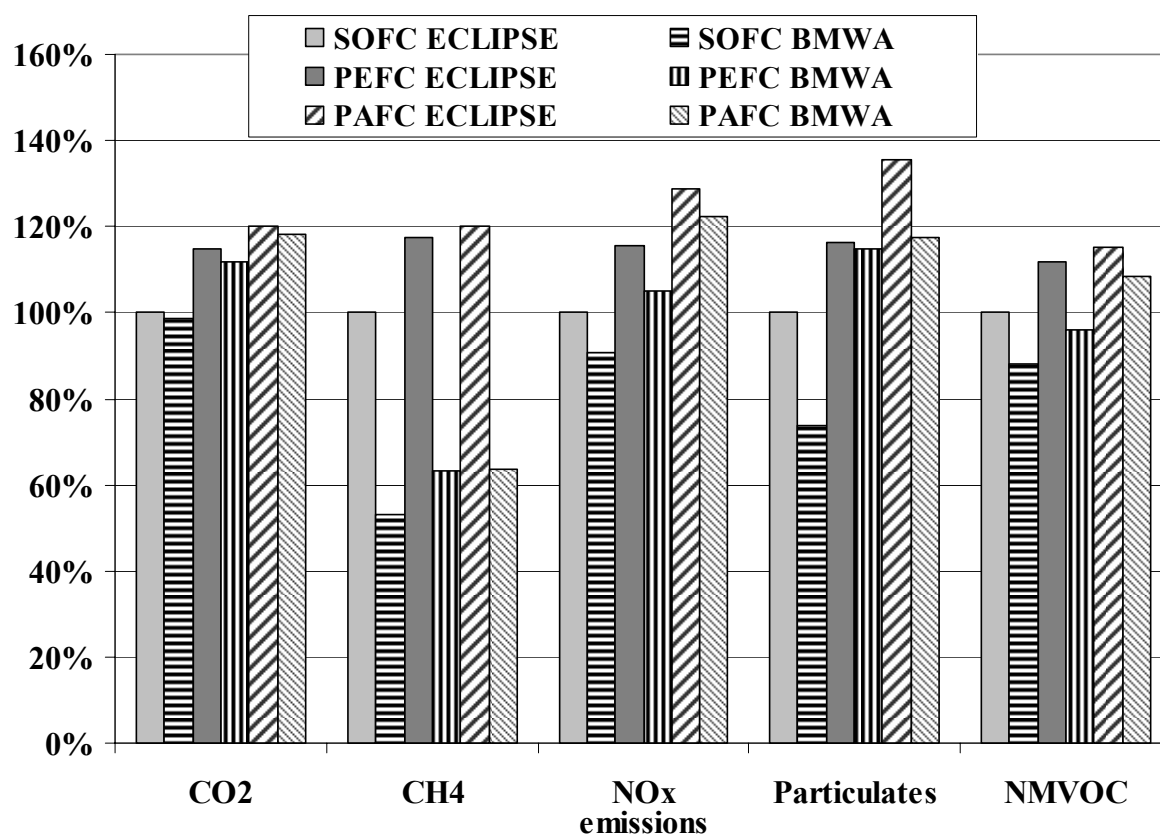
Figure 5-57: Comparison of the life cycle emissions (in kg/kWh_{el}) from different 200/250 kW_{el} FC systems between /Viebahn; Krewitt 2003/ (ECLIPSE) and /BMWA 2004/ (BMWA) (without SO_2)
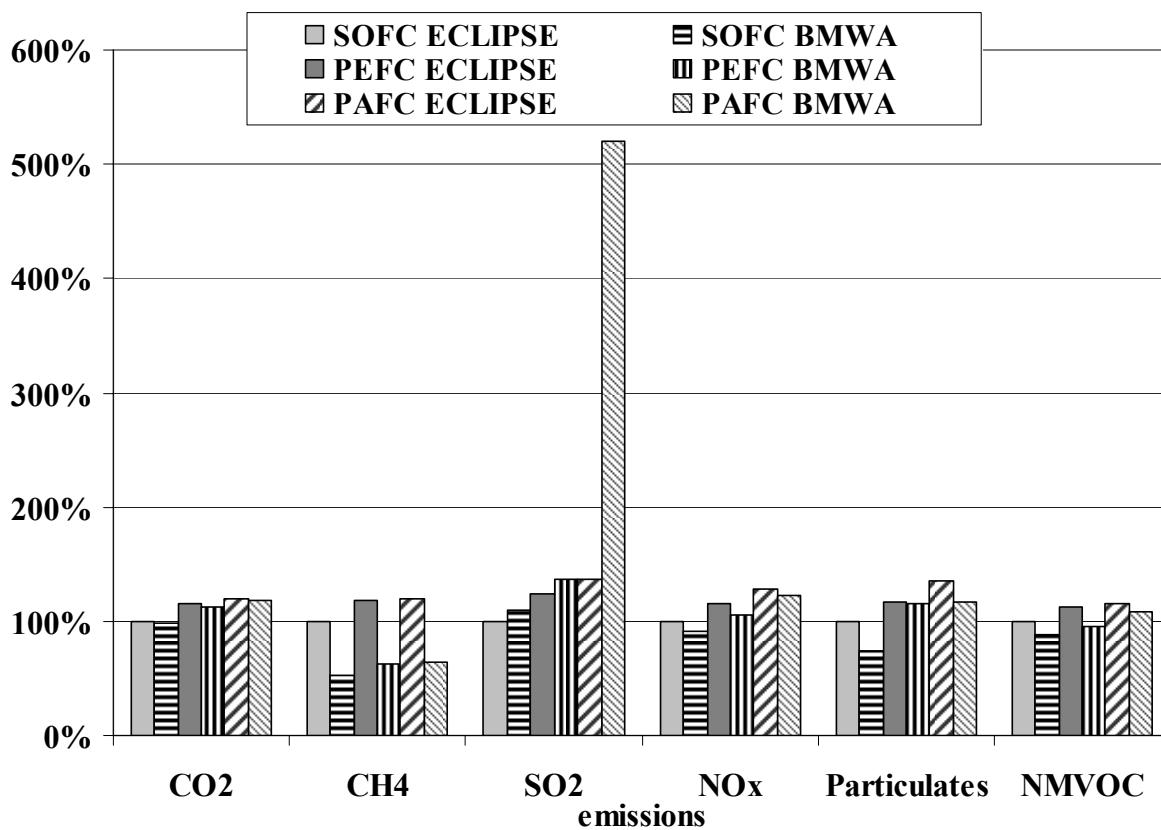
Figure 5-58: Comparison of the life cycle emissions (in kg/kWh$_{el}$) from different 200/250 kW$_{el}$ FC systems between /Viebahn; Krewitt 2003/ (ECLIPSE) and /BMWA 2004/ (BMWA) (with SO$_2$)

5.4   Bio-fuelled CHP systems

5.4.1   Technology

In a combined heat and power plant (CHP) electricity as well as heat are produced. The amount of produced electricity is less than in a power plant optimised to generate only electricity, but the condense water temperature can be used for heating so that total efficiency can be up to 90 % based on the lower heating value of the fuel. Combustion with steam power and gasification are two general ways to make use of the biofuel's energy.

Combustion with steam cycle:

The steam power technology is the only technology for large-scale electricity generation from biofuel which is commercially available. It can be distinguished between *fire grate* (FG), *circulating fluidised bed* (CFB) and *pressurized fluidised bed combustion* (PFBC), whereas, fire grate is the most common combustion technology for biofuels.

In combustion with steam cycle, water is heated under pressure to steam in a boiler. Therefore, FG, CFB or PFBC technology can be used. The hot steam is led into a steam turbine which drives a generator. Electricity from the generator is converted into higher voltage in order to be fed into the power grid. The remaining steam from the turbine enters a condenser, which is cooled by the local heating system. PFBC systems have a gas cycle in which the flue gas is used in a gas turbine. This procedure increases the electricity yield. /Setterwall et al. 2003/ state that the electricity efficiency of conventional steam power technology in CHP application (> 20 MW_{el}) is at most 30 % and with PFBC technology about 35 %.

In case of fire grate, the fuel is combusted on a grid. An advantage of this technology is that several fuels with different moisture content can be combusted in the same boiler. The combustion air is delivered through spray nozzles at the bottom of the bed. In a suspension of bed material the combustion of the fuel is performed. This bed material consists of sand, dolomite, lime and ash. Low temperatures result in low emissions of NO_x. Lime or dolomite are parts of the bed material and reduce SO_2.

Combustion with gasification:

Gasification implies that the different kinds of solid hydrocarbons in the fuel are converted to gases such as CO, CO_2, H_2 and water steam at high temperatures. The energy rich gases, i.e. CO and H_2, can be used at high pressure in a gas turbine or at atmospheric pressure in an internal combustion engine.

In pressurized gasification, the fuel gas has to be cleaned before it gets into the gas turbine. The flue gases from the gas turbine are used in a steam turbine process to generate additional electricity. Additionally, a fuel drying process might be necessary because crude biofuel has high moisture contents. Since the dryer needs a lot of heat, a combination with dis-

trict heating is useful in order to use remaining heat. The maximum electric system efficiency in CHP application with more than 20 MW_{el} at high pressure is about 40 % with biofuel (50 % moisture content).

In the gasification process at atmospheric pressure, the fuel gas from the atmospheric gasifier is cooled, cleaned and compressed and then fed to the gas turbine. In CHP application with more than 20 MW_{el} at atmospheric pressure, the maximum electric system efficiency is about 30 %.

Flue gas emissions:

Bio fuel has low sulphur content and the alkaline ash tends to bind sulphur during combustion so that the specific emission is less than 20 mg sulphur per MJ bio fuel. Emissions of NO_x depend on technology, process design and fuel characteristics. Combustion with fire grate has the highest specific emissions with 90-250 mg NO_2 / MJ fuel. Less NO_x is produced with CFB in the range of 60 to 150 mg NO_2 / MJ fuel. For gasifiers with internal combustion engines less than 100 mg NO_2 / MJ fuel can be achieved. Also low emissions are possible for PFBC. Carbon monoxide and hydrocarbon emissions can be reduced with improved combustion which is in general easier to achieve in larger plants. Specific emissions of CO_2 are 100-115 g biogenic CO_2 / MJ biofuel.

Flue gas condensing:

If a fuel has high moisture content a lot of steam is in the flue gases whose heat of vaporization can be regained and used for heating purposes. This may lead to a total efficiency for a plant with flue gas condensing, based on the lower heating value of the fuel, of up to 110 % because the lower heating value does not account for the heat of vaporization.

Application of the CHP technology:

The CHP technology is used when there is a tolerably constant and stable need for heat or steam. For heating purposes a minimum temperature of 50 °C and for process purposes 100 °C are required. The demand for heat determines the operation of CHP plants in Northern Europe so that during the warmer part of the year the plants are operated at partial load with lower efficiency. A minimum steam production is required in order to enable the generation of electricity.

Biomass:

Biomass is "*the biodegradable fraction of products, waste and residues from agriculture (including vegetal and animal substances), forestry and related industries, as well as the biodegradable fraction of industrial and municipal waste*" /European Parliament 2003/. Theoretically, biomass can be grown in a *closed loop* so that no net CO_2 contribution to the atmos-

phere arises as the same amount released during combustion is absorbed through photosynthesis. This advantage benefits bio-fuelled CHP compared to natural gas-fired CHP.

The CO_2 emissions caused in the combustion of biomass are called *biogenic CO_2* because it is CO_2 which has been absorbed in the growth of the biomass. In contrast, CO_2 emissions caused in the combustion of fuels which are not biomass, e.g. coal, lignite and natural gas, are called *fossil CO_2*. In the following paragraphs, CO_2 emissions are assumed to be fossil CO_2 emissions. Biogenic CO_2 is not comprised.

5.4.2   Market development

The amount of electricity produced with solid biomass in CHP plants in the ECLIPSE region in the year 2001 is 15,931 GWh. This is 0.56 % of the total electricity generation of 2,840,734 GWh /IEA 2003/. The amount of energy generation from solid biomass in CHP plants in the ECLIPSE region has been increasing by 100 % from 1991 to 2001 (see **Figure 5-59**). In the year 2001 the main contribution comes from Finland, Sweden, Spain, Austria, France and Portugal.
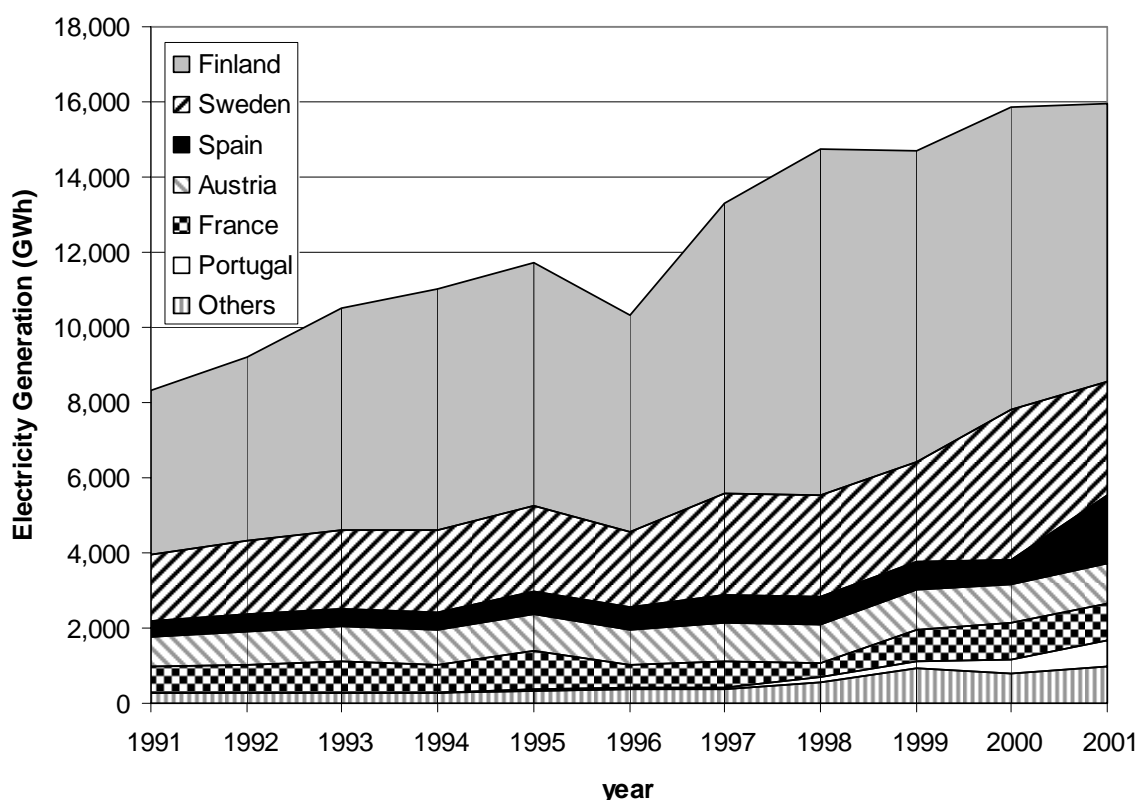
Figure 5-59:   Electricity generation (in GWh) from solid biomass in the ECLIPSE region in the years 1991-2001 /IEA 2003/

The amount of heat produced with solid biomass in the EU-15 region in the year 2001 is 129,892 TJ. This is 11.92 % of the total heat generation of 1,089,519 TJ /IEA 2003/. The

amount of heat generation from solid biomass in the ECLIPSE region has been increasing by the factor four from 1991 to 2001 (see **Figure 5-60**). In the year 2001 the main contribution comes from Sweden, Finland and Denmark.

/Setterwall et al. 2003/ describe the state of the art as follows. The steam power technology is dominating in industries. Using this technology, investment costs are a little larger than for a coal-fuelled plant because of the more complicated fuel feeding system but the ash volume is lower. Gasification at atmospheric pressure with CFB gasifiers is used at some pulp industries. For pressurized gasification there are no commercial plants. It would reach the highest electricity yields but the investment costs are too high due to the need for high pressure so that only at large scale production costs may become economic. The price for wood chips is more than twice the price of coal but as a renewable energy source it may save, e.g. CO_2 taxes and certificates.

The technical biomass potentials in the EU-15 are described in **Table 5-17**. In the year 2001 the energy generation with solid biomass in the EU-15 was ca. 200 PJ. Compared to the technical potentials of more than 5,000 PJ there is a high development potential for biomass in the European Union.

Table 5-17:   Technical biomass potentials in the EU in PJ/a /Kaltschmitt et al. 2003/

Country	Technical biomass potential (PJ/a)
Belgium and Luxemburg	73
Denmark	110
Germany	887
Finland	615
France	1,252
Greece	80
Ireland	51
Italy	387
Netherlands	39
Austria	191
Portugal	127
Sweden	700
Spain	427
Great Britain	284
EU-15	5,224
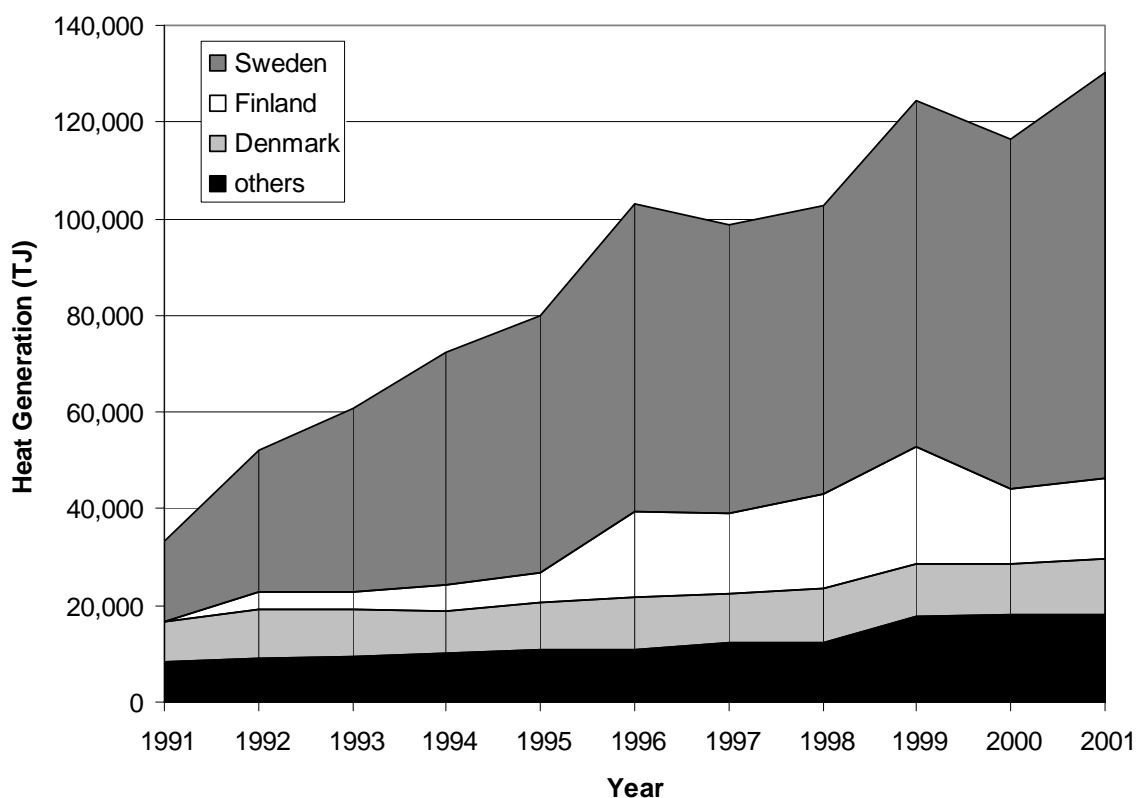
Figure 5-60: Heat generation (in TJ) from solid biomass in the ECLIPSE region in the years 1991-2001 /IEA 2003/

5.4.3 LCA results in ECLIPSE

/Setterwall et al. 2003/ study examples for steam power and gasification technology.

Fire grate and CFB are chosen as the two most common boiler technologies for bio-fuelled CHPs with steam power technology. Two common types of biofuel are analysed: crude wood chips from coniferous forest residues (moisture: 50 %) and dried wood chips (moisture: 10-15 %) dried in an integrated process. Plants combusting moist fuel use flue gas condensation in order to increase the heat yield. Data are derived from three existing plants in Sweden.

There are only some pilot plants for gasification in Sweden, Finland and England. A pressurized gasification system is chosen by /Setterwall et al. 2003/. Data is based on calculations and full-scale component tests, acidification rig tests, turbine tests with artificially composed gas performed during the projection of a plant situated in Sweden, and guarantee data from sub-system suppliers. The data are based on the project planning documents and are, thus, a little less reliable than the data of the other three systems.

Further assumptions are the following:
-   All studied systems produce electricity at 10 kV to the grid.
-   Fuel preparation and district heating systems are typical for Swedish conditions.

- The technical lifetime of the bio-fuelled systems is 40 years.
- For the allocation of the life cycle emissions between electricity and heat, the method based on exergy is chosen following the methodological guidelines of ECLIPSE. The mean temperature in the district heating system is assumed to be 90°C and the ambient temperature is assumed to be 5 °C according to an average year in Sweden.
- The biofuel consists of crude chipped forest residues.

Life Cycle of bio-fuelled CHP systems:
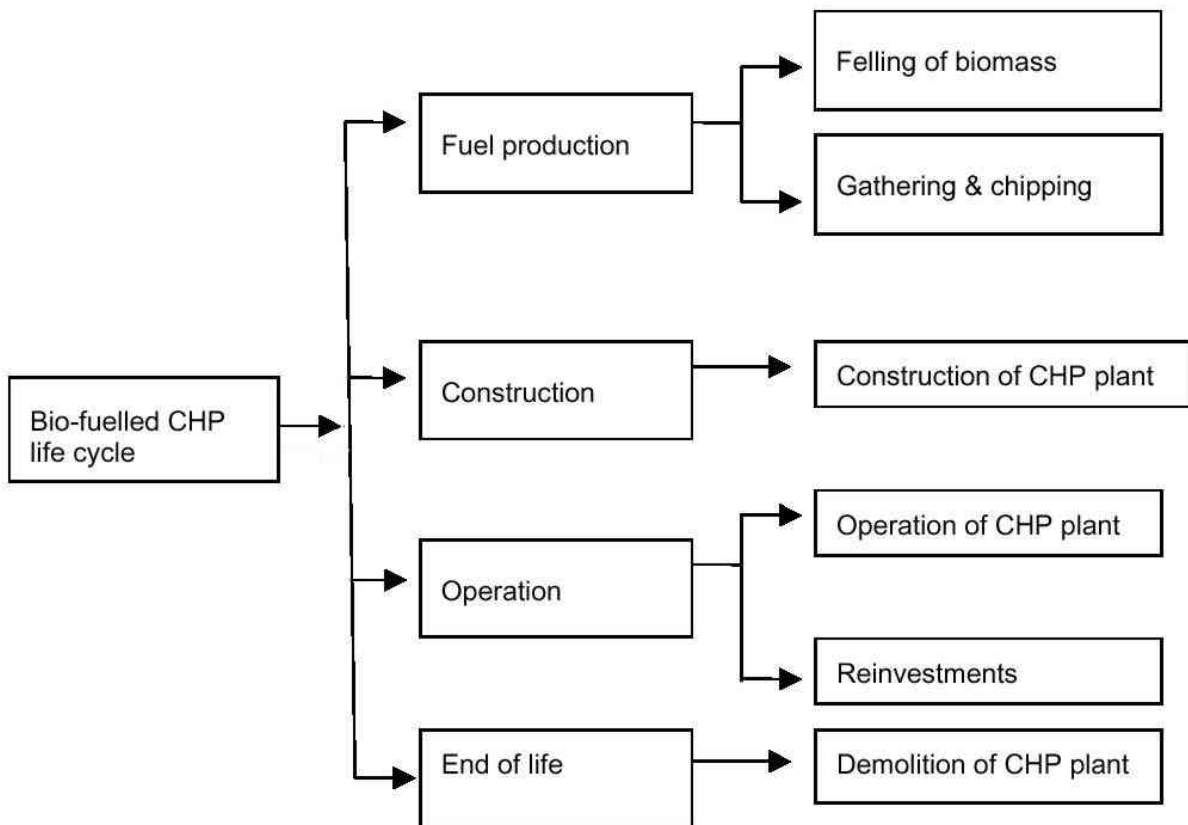
Figure 5-61:   Life cycle of bio-fuelled CHP systems /Setterwall et al. 2003/

The life cycle of a bio-fuelled CHP system consists of the four main phases fuel production, construction, operation and end of life. In the phase of fuel production, the felling, gathering and chipping of wood as well as the transport to the CHP plant are included. The construction of the CHP plant refers to all construction materials and their upstream processes and transports. During the operation phase the use of fuel and chemicals as well as emissions and wastes of the plant including all transport processes are considered. Eventually, the end of life phase describes the demolition of the CHP plant.

Not included into the considered life cycle are forestry activities (e.g. plant nursing, fertilizing, thinning, etc.), manufacturing of plant components (e.g. turbines, generators etc),

ground work, electricity used during the construction of the plants, and the power grid behind the plant transformer.

The four life cycle phases are described in the following paragraphs.

Fuel production:

The life cycle unit felling of biomass within the life cycle phase fuel production covers the diesel consumption and emissions from forest machines during the felling of the trees. /Setterwall et al. 2003/ allocate the impacts of this process with the respective economic value of the products. The allocation for the forest residues, which have an economic value of 7 % of the total economic value of all products, is 7 % of the total impacts. The life cycle unit gathering and chipping of the forest residues in a mobile chipping machine covers diesel consumption and emissions as well as a 50 km transport of the crude wood chips by heavy lorry with trailer to the plant. In the following descriptions, the fuel production phase is sometimes split into *biofuel transport* and *crude fuel production*. The data for fuel consumption for wood felling are from a large forest company and those for gathering and chipping are from an extensive project cited in Vattenfall's life cycle assessments for electricity generation. Used machines are supposed to be quite representative for forest machines used today.

Construction:

The bio-fuelled CHP systems analysed by /Setterwall et al. 2003/ consist of identical and specific components. Identical components are the building, the transformer, the generator, the steam turbine connecting the generator and cooled by the district heating system, and a cyclone separator which filters the dust. The system specific components are displayed in **Table 5-18**.

With the exception of Gas+dry, data for the construction are from Vattenfall's LCA for electricity generation from 1996. For the two systems FG+FGC and FG+dry, data of another bio-fuelled CHP plant are taken and scaled according to their respective input capacity.

Operation:

CO_2 emissions during the combustion of the biofuel are considered as biogenic and therefore not shown in the following. The life cycle unit reinvestments comprises the assumption that 1 % of the machines in the plant (except for buildings and foundations) should be renewed every year. With a life time of 40 years, 40 % of the machines are exchanged. Data for the operation of the systems CFB+FGC, FG+FGC and FG+dry are from the plants environmental report to the authorities in the year 1996 and thus reflect the actual operation in an existing plant with good quality. The CFB+FGC system is completed with operating statistics. However, in the case of the FG-FGC system, the ratio between electricity and heat production is altered from 0.085 to 0.39. For urea production only the stoichiometric need for raw materials

ammonia and natural gas is considered. The energy demand during the formation process of urea is considered to be low according to a manufacturer.

End of life:

The unit process end of life covers the emissions from the demolition of the machines and waste. The data of construction, reinvestments and demolition are not very detailed but this may be acceptable because these life cycle phases contribute only a small part to the environmental impact.

Table 5-18:   System specific components of the bio-fuelled CHP systems /Setterwall et al. 2003/

CHP plant with CFB, steam power technology and moist fuel	CHP plant with fire grate, steam power technology and moist fuel	CHP plant with fire grate, steam power technology and dried fuel	CHP plant with pressurized gasification, combined cycle and dried fuel
Fuel-feeding system			Pressurized fuel-feeding system
Flue gas condensing (cooled by the district heating system)			
		Steam dryer for drying of fuel (cooled by the district heating system)	Pressurized steam dryer for drying of fuel (cooled by the district heating system)
Steam boiler, CFB	Steam boiler, fire grate		Pressurized gasifier
			Gas cleaning system
			Gas turbine connected to the generator
			Flue gas boiler (cooled by the district heating system)
Electric filter for dust reduction	Electric filter for dust reduction, Selective Non-Catalytic Reduction (SNCR) for NO$_x$-reduction		Electric filter for dust reduction

Examples:

Table 5-19 gives an overview of the technical parameters of the studied systems. They are described in more detail in the paragraphs below.

Table 5-19:   Technical parameters of the examples of bio-fuelled CHP systems from /Setterwall et al. 2003/

Parameter	CFB+FGC	FG+FGC	FG+dry	Gas+dry
Electric capacity	9,000 kW	9,300 kW[33]	25,000 kW + 20,000 kW	59,000 kW
Thermal capacity (Boiler + FGC)	27,000 kW + 6,000 kW	78,000 kW + 13,000 kW	80,000 kW + 80,000 kW	60,000 kW
Heat production (MWh$_{th}$/a)	101,812	231,892	396,800	264,000
Internally used electricity (MWh$_{el}$/a)	2,200	5,000	4,950	15,000
Electricity production to grid (MWh$_{el}$/a)	30,101	90,709	97,450	260,000
Total fuel consumption[34] (MWh/a)	137,872	319,031	575,500	620,000
Thermal efficiency	73.8 %	72.7 %	68.9 %	42.6 %
Electrical efficiency (net)	21.8 %	28.4 %	16.9 %	41.9 %
Efficiency (gross)	97.3 %	102.7 %	86.7 %	86.9 %
Efficiency (net)	95.7 %	101.1 %	85.9 %	84.5 %
Emission control	Electric filter	Electric filter + SNCR	Electric filter + SNCR	Electric filter
Technology level	available	available	available	coming
Allocation factor for electricity[35]	57 %	64 %	55 %	81 %
Allocation factor for heat	43 %	36 %	45 %	19 %

---

[33] Total electric capacity is 103 MW from different types of boilers with a common steam pipe. Approximately 9 % of the electric capacity is allocated to the studied fire grate boiler.

[34] The total fuel consumption is given with the lower heating value.

[35] Re-calculating leads to an allocation factor for electricity that is 0.2-3.8 percentage points lower than given by /Setterwall et al. 2003/. This variation is not adjusted in the following.

CFB boiler with steam power technology, crude biofuel and flue gas condensation (CFB+FGC):
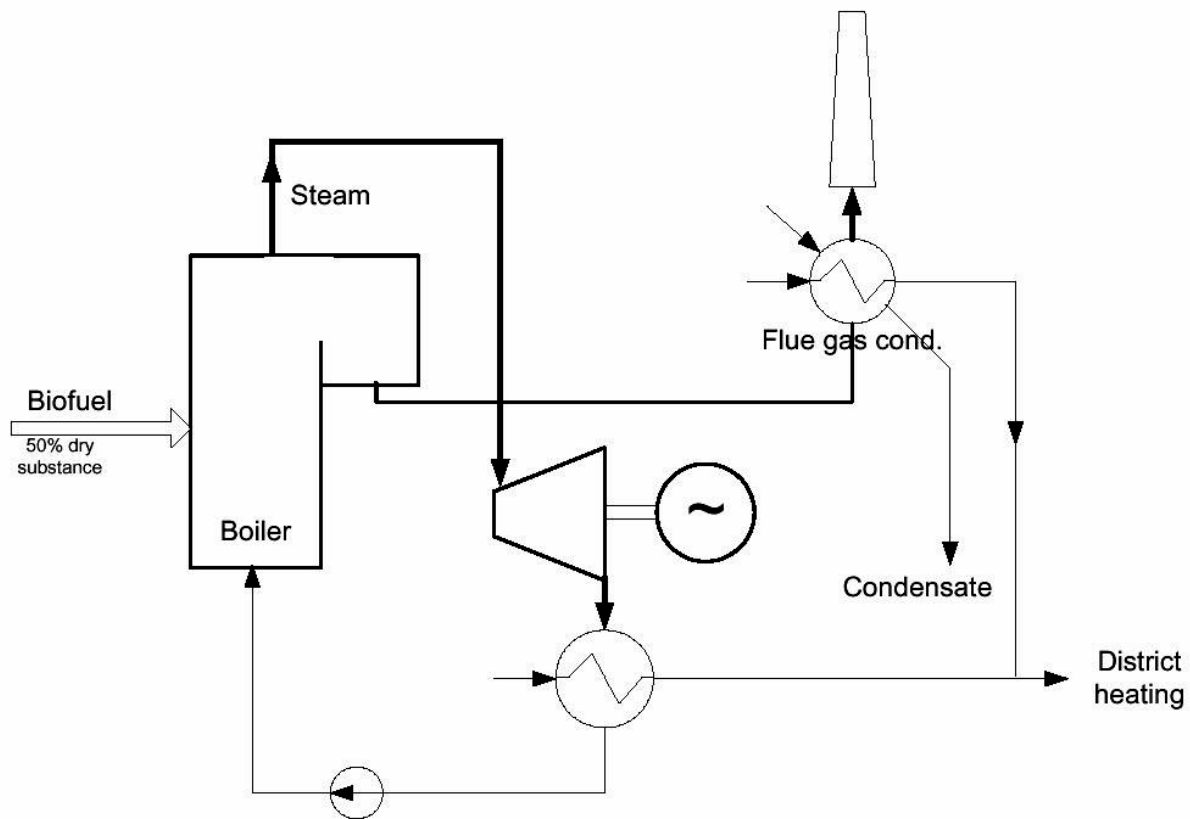
Figure 5-62:   Flow chart of CFB+FGC /Setterwall et al. 2003/

Figure 5-62 shows the flow chart of the CFB+FGC bio-fuelled CHP system. The biofuel only emits biogenic CO_2 which is not accounted for. Thus, the small amount of CO_2 during the operation is not from the biofuel but fossil CO_2 from incineration of operational waste and from chemical and raw material production and transport. However, NO_x, SO_2 and particulates are mainly emitted in the operation phase (see **Figure 5-63**). Biofuel from coniferous wood has only little sulphur content. Additionally, the alkaline ash in the fluidised bed material bonds some of the sulphur. Fuel production is dominating the CO_2 and NMVOC emissions. 14-23 % of NO_x, SO_2 and particulates originate from diesel combustion in the fuel production phase. The construction phase contributes about 10 % to the CO_2 and SO_2 emissions. For the other emissions, the construction phase is of little importance. The other life cycle phases, i.e. construction, reinvestment, demolition and biofuel transport, have only minor contribution.

A sensitivity analysis with the alternative production allocation method results in a lower allocation factor for electricity of 44 %. In this calculation, the efficiency of the alternative heating plant is assumed to be 110 % and the efficiency of the alternative electricity generation plant is assumed to be 42 %. Thus, the emissions per kWh electricity are 23 % lower compared with the exergy allocation method.
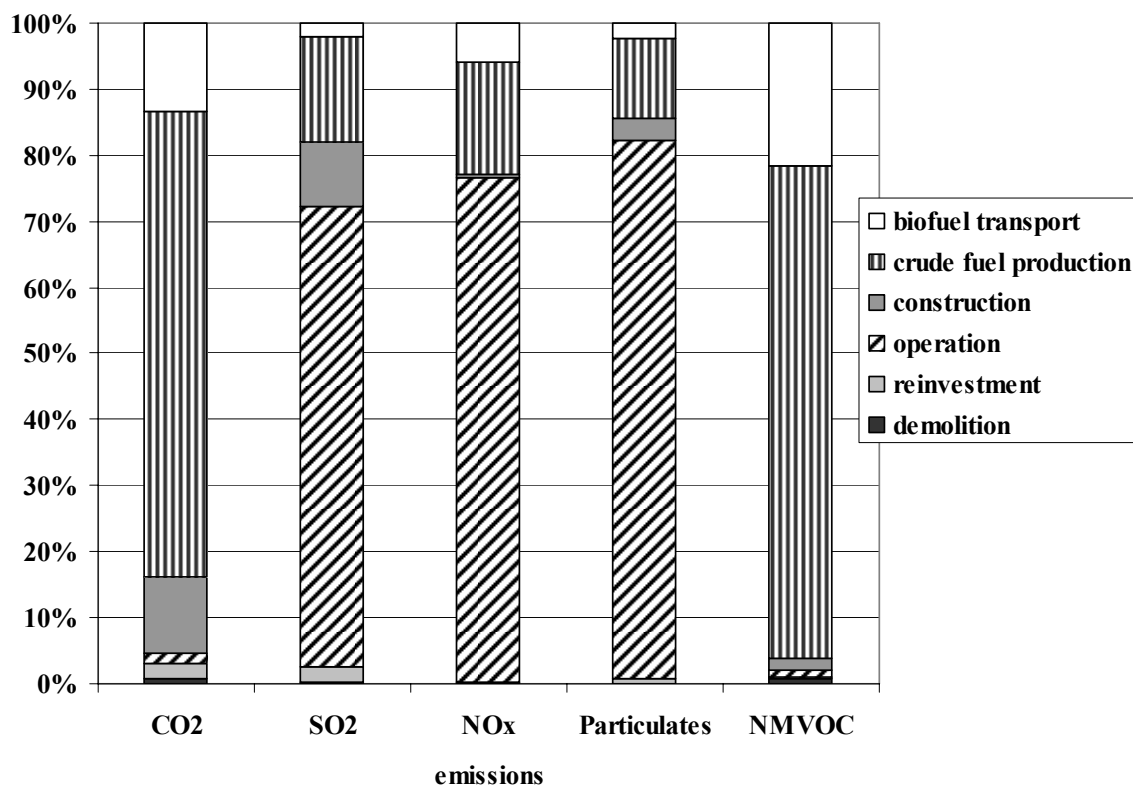
Figure 5-63:   Contribution of the life cycle phases to the emissions of CFB-FGC (in kg/kWh$_{el}$)

Fire grate with steam cycle, crude biofuel and flue gas condensation (FG+FGC):
Compared to CFB-FGC, the FG-FGC bio-fuelled CHP system has a fire grate steam boiler instead of a CFB steam boiler and the flue gases are cleaned with an additional *Selective Non-Catalytic Reaction* (SNCR). For the SNCR, urea is added during combustion in order to reduce NO$_x$ emissions. The removal efficiency is approximately 50 %. However, during the production of urea NO$_x$ is emitted. Thus, the net reduction over the whole life cycle is about 35 %. Flue gases are recycled to the boiler in order to reduce furnace temperature and excess oxygen, which leads to less formation of NO$_x$. With NH$_3$ NO$_x$ is reduced to nitrogen (N$_2$) and water (H$_2$O). Excess ammonia (NH$_3$) in the flue gases is partly caught during flue gas condensation and ends up in the condensate. Fossil CO$_2$ emitted during the operation phase originates with more than 90 % from the production of urea and the remaining share from the incineration of operational waste, chemical and raw material production and transport. NO$_x$, SO$_2$ and particulates are mainly (70-80 %) emitted in the operation phase and urea production contributes 8-17 % of the total life cycle emissions. Regarding NMVOC, urea production is responsible for 43 % of the total life cycle emissions. Those contributions of the life cycle phases can be seen in **Figure 5-64**.

Fuel production contributes a similar amount of CO$_2$ and NMVOC as the operation phase. With respect to NO$_x$, SO$_2$ and particulates 12-28 % of the total life cycle emissions originate from diesel combustion in the fuel production.

The high overall efficiency is achieved with a fire grate especially designed for biofuel, flue gas recycling to the boiler, flue gas condensation regaining the heat of vaporization and a minimization of partial load operation. These improvements increase the overall efficiency from about 80 % to more than 100 %. Thus, specific LCI results decrease by 20 %.

The NO_x reduction activities in the FG+FGC plant are illustrated in **Figure 5-69** with about 35 % lower NO_x emissions than the CFB-FGC plant without SNCR. However, the production of the urea contributes 36 % of fossil CO_2, 43 % of NMVOC, 8 % of NO_x, 14 % of particulates and 17 % of SO_2 to the total life cycle emissions. This results in a move of the emissions from the site of the bio-fuelled CHP plant to the site of the urea production facility. Altogether, CO_2, SO_2 and NMVOC emissions increase by more than 40 % compared to the CFB-FGC. In further calculations of external costs, it can be estimated which configuration causes the lowest damage costs.
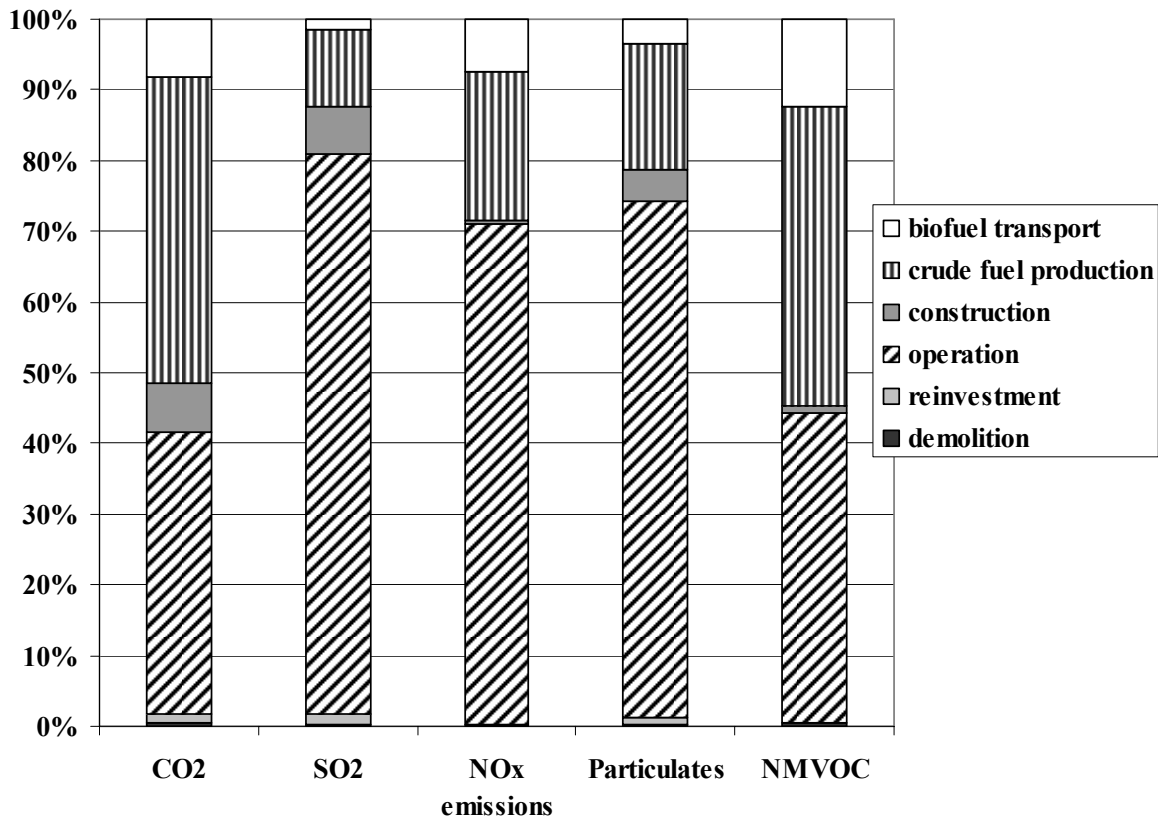
Figure 5-64:   Contribution of the life cycle phases to the emissions of FG+FGC (in kg/kWh$_{el}$)

Fire grate with steam cycle and integrated steam dryer for biofuel drying (FG+dry):
Figure 5-65 shows the flow chart of the FG+dry CHP system. It displays the additional steam dryer which reduces the moisture content from 50 % to 15 %. The FG+dry system uses SNCR and flue gas recycling to reduce NO_x but it has no FGC to take care of the ammonia slip in the flue gases. Therefore, a limit value for ammonia of 5 ppm with the according dosage of urea has to be ensured.
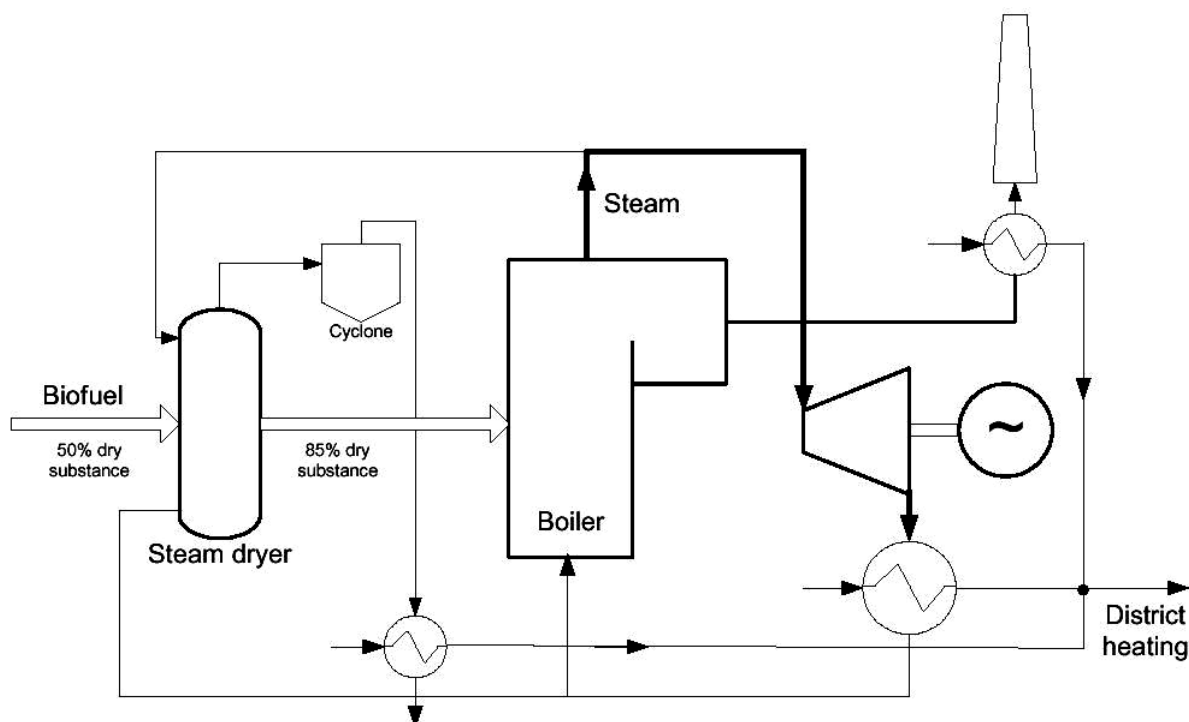
Figure 5-65:   Flow chart of FG+dry /Setterwall et al. 2003/

Figure 5-66 illustrates the contribution of the different life cycle phases to the life cycle emissions of the FG+dry bio-fuelled CHP system.

The fossil CO_2 emissions during the operation phase arise with 64 % by the production of urea, with 24 % by the incineration of operational waste and with 12 % by chemical and raw material production as well as transports. The main part of NO_x, SO_2 and particulates are emitted in the operation phase. Biofuel from coniferous wood contains little sulphur resulting in a relatively small direct emission from fire grate operation.

The fuel production is responsible for the main part of the life cycle's fossil CO_2 emissions. Additionally, 20 % of NO_x, 14 % of SO_2 and 33 % of particulates are emitted due to diesel combustion in the fuel production phase. 88 % of NMVOC arise in the fuel production phase and 7 % in the urea production.

In the construction phase, 18 % of the CO_2 as well as 14 % of SO_2 and particulates are emitted. The construction phase is more important than in case of CFB+FGC and FG+FGC systems because of the additional drying system.

The analysed FG+dry plant has a high overall efficiency because of a fire grate especially designed for biofuel, flue gas recycling to the boiler, an integrated steam dryer for biofuel drying with recovery of excess heat, an economizer connected to the district heating system (flue gas is cooled from 250 to 90 °C) and a minimization of partial load operation.

NO_x reduction in this plant is restricted by the limited value of ammonia slip. Therefore, the urea dosage is relatively low resulting in higher NO_x emissions during the operation but lower emissions due to urea production compared to FG+FGC. Thus, the contribution of the urea production to NO_x as well as to other emissions is quite small.
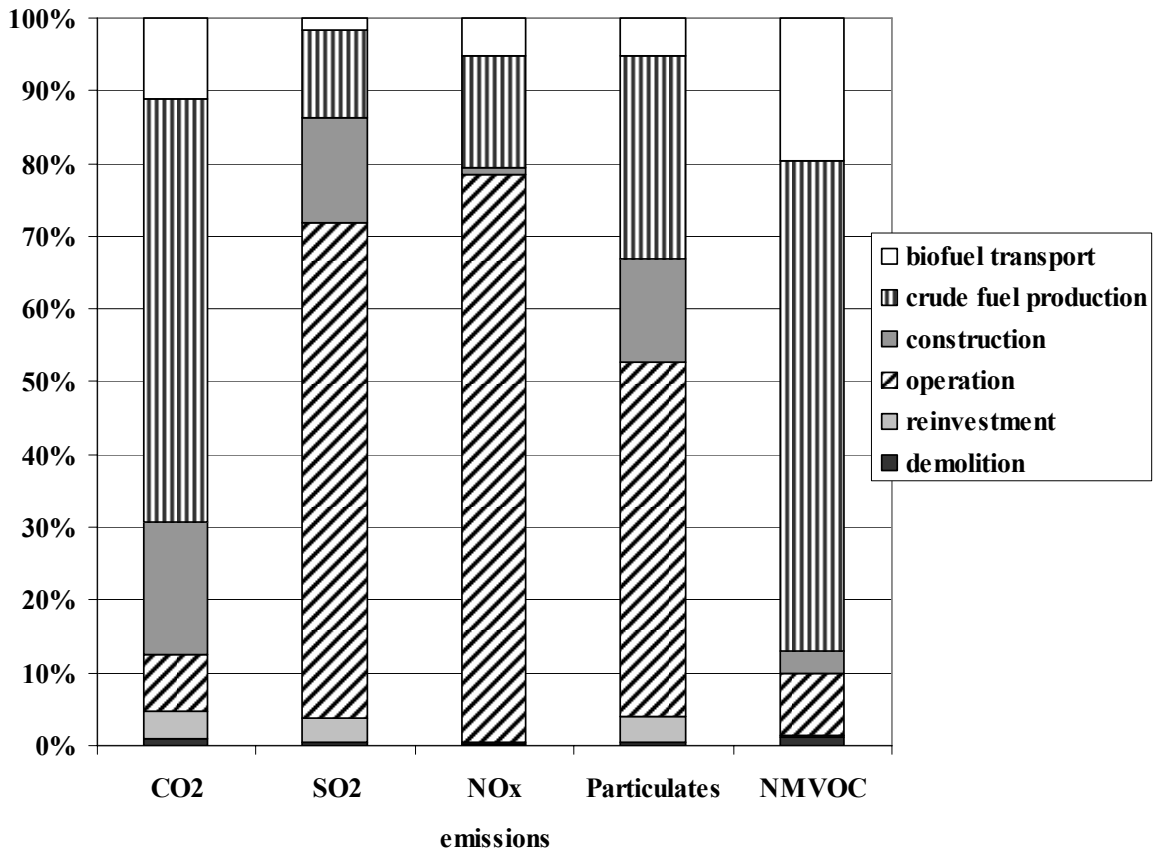
Figure 5-66:   Contribution of the life cycle phases to the emissions of FG+dry

Pressurized gasification, combined cycle and integrated steam dryer for biofuel drying (Gas+dry):

Figure 5-67 shows the flow chart of the Gas+dry bio-fuelled CHP system. The system has an integrated steam dryer for drying of crude wood chips from 50 % to about 15 % moisture content. Excess heat from the steam dryer is regained as district heat. Additionally, the gasifier generates the gas to run the gas turbine. The advantage of this system is the high proportion of electric capacity compared to the other systems studied. It is as high as the heat capacity so that the focus is more on electricity generation than on heat generation.

   Figure 5-68 illustrates the contribution of the life cycle phases to the emissions of the total life cycle emissions. The fuel production and transport cause 88 % of the life cycle's fossil CO_2 emissions, 97 % of NMVOC emissions, 9 % of NO_x emissions, 14 % of particulates emissions and 18 % of SO_2 emissions. SO_2, NO_x and particulates are mainly emitted in the operation phase. The construction phase contributes about 8 % to the life cycle's fossil CO_2 and SO_2 emissions.
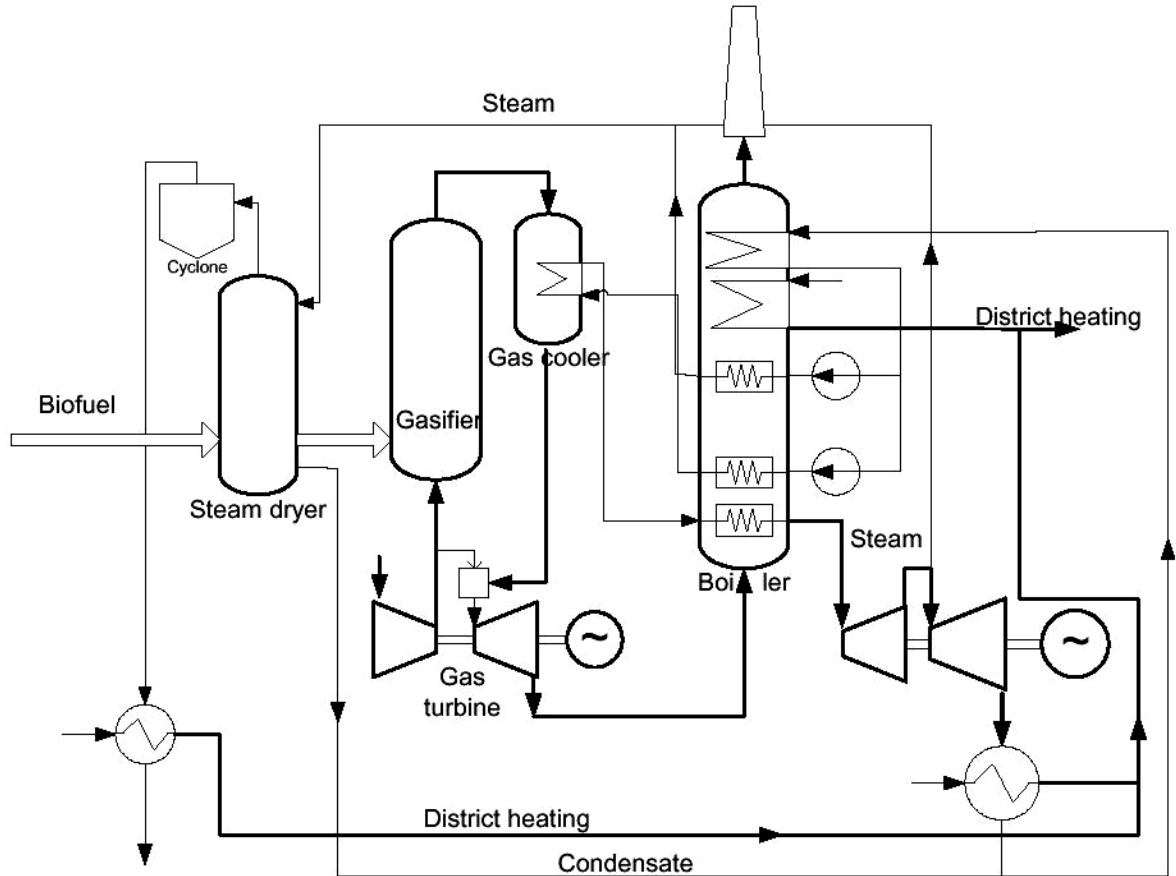
Figure 5-67:   Flow chart of Gas+dry /Setterwall et al. 2003/
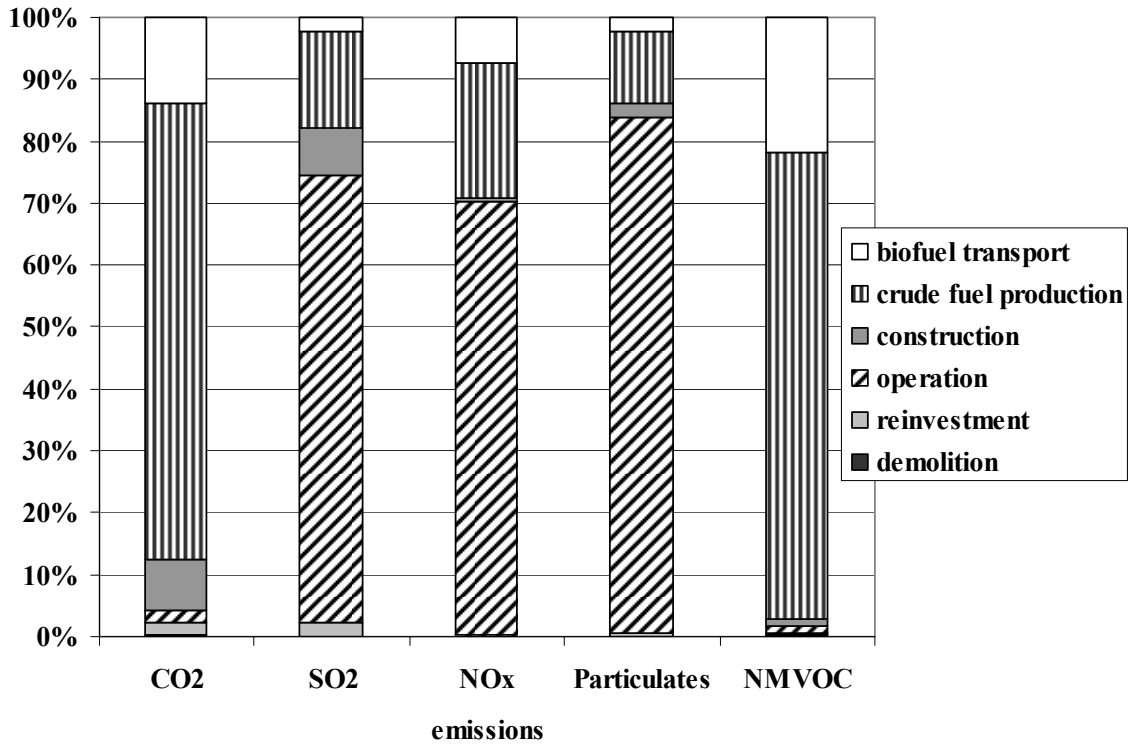
Figure 5-68:   Contribution of the life cycle phases to the emissions of Gas-dry (in kg/kWh$_{el}$)

5.4.4 Emissions of bio-fuelled systems

In general, the contribution of the life cycle phases to environmental impacts is similar in all four technologies. Fuel production and transport dominates the fossil CO_2 and NMVOC emissions. Operation dominates the emissions of biogenic CO_2, NO_x, particulates and SO_2. Emissions of biogenic CO_2, SO_2, NO_x and particulates can only be influenced significantly through efficiency change, since they are determined by the chemical constitution of the input fuel. The life cycle emissions of the four analysed bio-fuelled CHP systems are listed in **Table 5-20**. A comparison of the four analysed bio-fuelled CHP systems is performed in **Figure 5-69** referring to the CFB+FGC system.

The high dosage of urea for NO_x reduction in FG+FGC leads to higher life cycle emissions of CO_2, SO_2 and NMVOC. However, the resulting NO_x emissions are only slightly lower than for the FG+dry system using less urea. In case of the FG+dry system, all other emissions are significantly lower than those from the CFB+FGC and FG+FGC systems.

The NO_x emissions of FG+dry are higher than those of CFB+FGC despite the activities for NO_x reduction due to the additional dryer process and a different ratio of electricity generation and heat production of the respective bio-fuelled CHP systems.

Altogether, the CFB+FGC technology has lower CO_2, CH_4, SO_2 and NMVOC emissions than the FG+FGC and FG+dry technology as well as lower NO_x emissions than the FG+dry technology. Only particulates emissions of the FG+FGC and FG+dry technology and the NO_x emissions of the FG+FGC technology are lower. However, it should be noted that the quality of particulates emissions is not very good as there is no distinction of different sizes. The future Gas+dry technology has the lowest emissions per kWh_{el} with the exception of particulates emissions with their low data quality.

Table 5-20:   Emissions in kg/kWh_{el} of different bio-fuelled systems

Emissions	CFB+FGC	FG+FGC	FG+dry	Gas+dry
CO_2	2.44E-02	3.43E-02	2.81E-02	1.63E-02
CH_4	2.63E-05	5.73E-05	3.06E-05	1.83E-05
SO_2	1.11E-04	1.39E-04	1.39E-04	7.71E-05
NO_x	9.02E-04	6.28E-04	9.59E-04	4.96E-04
Particulates	5.78E-05	3.40E-05	2.40E-05	4.19E-05
NMVOC	6.36E-05	9.66E-05	6.69E-05	4.39E-05
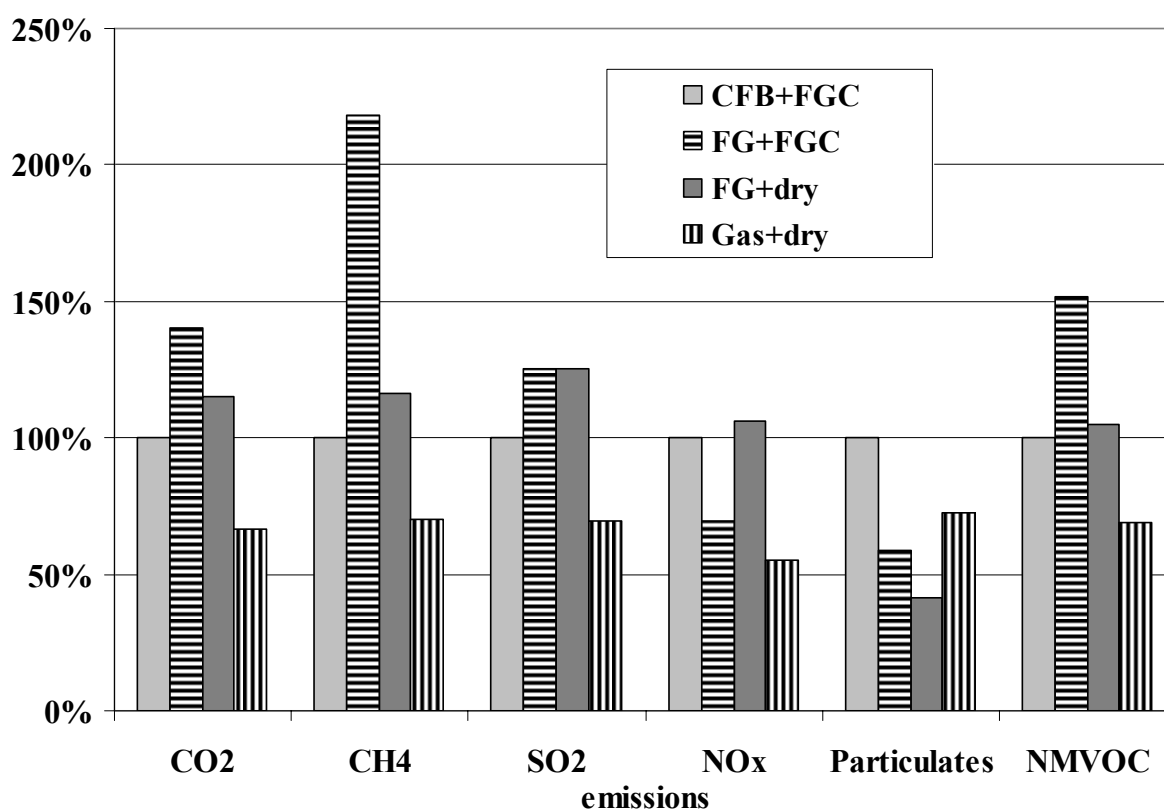
Figure 5-69: Comparison of the emissions of different bio-fuelled systems related to CFB+FGC (in kg/kWh$_{el}$)

Comparison with /BMWA 2004/:

/BMWA 2004/ analyses three bio-fuelled CHP systems:
- CHP system with an extraction condensing steam turbine (steam turbine)
- CHP system with an Organic Rankine Cycle (ORC CHP)
- Circulating fluidised bed gasification at atmospheric pressure with two downstream gas engines (Gas+Engines)

The technical data are given in **Table 5-19**. All three systems are fired with wood and the ambient temperature of the CHP systems is assumed to be 10 °C. The life time of the systems is assumed to be 50 years for the buildings, 20 years for the machines and 15 years for the ORC and the gasifier. Emissions of fossil-fired backup systems are not allocated to the bio-fuelled CHP systems.

CHP system with an extraction condensing steam turbine (steam turbine):

Heat is extracted at temperatures of 210 °C with a pressure of 13 bar as process steam as well as with a pressure of 3.5 bar at 130 °C, 85 °C and 45 °C. The heat at 130 °C runs absorption refrigerating plants and the lower temperature heat is fed in a local district heating system. If

the heat is not consumed totally the air-cooled condenser (LUKO) can be used. For backup considerations, two oil or natural gas-fired boilers are available. Altogether, 95 % of the generated energy comes from wood.

The emissions from the construction of this bio-fuelled CHP plant do not contribute more than 10 % to the total life cycle emissions. In contrast, emissions from operation contribute more than 90 % to all considered emissions. The end of life of the system does not have significant emissions. **Table 5-22** lists the total emissions of this bio-fuelled CHP plant.

CHP system with an Organic Rankine Cycle (ORC CHP):
The ORC CHP plant is used for base load heat supply in an existing local district heating system. Formerly used natural gas-fired boilers are available to backup the supply.

A thermo oil boiler on a fire grate supplies the ORC module with an electrical capacity of 1 MW. Heat which is extracted from the ORC and heat which is extracted from the flue gas and the thermo oil by economizers is supplied to the local district heating system. An air cooled recooling can be used in the ORC module in order to operate the ORC in condensation operation.

Similar to the distribution of the steam turbine system, the emissions from the construction of the ORC CHP plant does not contribute more than 15 % to the total life cycle emissions. In contrast emissions from operation are with more than 85 % responsible for the main part of all considered emissions. The end of life of the system does not have significant emissions. **Table 5-22** lists the total emissions of this bio-fuelled CHP plant.

Circulating fluidised bed gasification at atmospheric pressure with two downstream gas engines (Gas+Engines):
First of all, the bio-fuel is dried from a moisture content of 45 % to 20 % with internal waste heat. Thus, the total utilisation factor is increased. At atmospheric pressure, the gasification of the bio fuel is performed in an air based circulating fluidised bed. The generated gas is filtered and cooled and finally combusted in two gas engines.

Similar to the distribution of the ORC CHP system, the emissions from the construction of the Gas+Engines CHP plant does not contribute more than 15 % to the total life cycle emissions. In contrast, emissions from operation contribute more than 85 % of all considered emissions. The end of life of the system does not have significant emissions. **Table 5-22** lists the total emissions of this bio-fuelled CHP plant.

The comparison between the results of /BMWA 2004/ and /Setterwall et al. 2003/ is illustrated in **Figure 5-70**. This figure displays that the CO_2 emissions calculated in /BMWA 2004/ are by a factor of 1.5-2.8 higher than those calculated in /Setterwall et al. 2003/. The Gas+Engines CHP system of /BMWA 2004/ has approximately 20 % higher emissions (with the exception of CO_2) compared to the CFB+FGC CHP system of /Setterwall et al. 2003/ which is quite similar. However, the CH_4 and SO_2 emissions from the steam turbine and ORC

CHP system of /BMWA 2004/ are higher than those from the CFB+FGC system by a factor of ca. 2.5 and 4.7, respectively,. These large variations can not be explained in this context but may be analysed in further research.

Table 5-21: Technical parameters of the examples of bio-fuelled CHP systems from /BMWA 2004/

Parameter	Steam turbine	ORC CHP	Gas+Engines
Electric capacity (gross)	6.1 MW	1.0 MW	2 * 1.2 MW
Thermal capacity	max. 22 MW	6.26 MW	max. 4.4 MW
Heat production	102,573 MWh/a	30,590 MWh/a	8,278 MWh/a
Electricity production to grid	36,000 MWh/a	4,048 MWh/a	15,966 MWh/a
Total fuel consumption	204,737 MWh/a	43,452 MWh/a	62,240 MWh/a
Thermal efficiency	50.1 %	70.4 %	13.3 %
Electrical efficiency (net)	19.5 %	10.6 %	28.9 %
Efficiency (net)	69.7 %	81.0 %	42.2 %
Allocation factor for electricity	55.7 %	40.6 %	90.8 %
Operation optimization	Energy optimized	Heat optimized	Power optimized
Heat backup	Oil or natural gas-fired boiler	Natural gas-fired boiler	-
Full load hours (electricity)	6,560 h/a	4,600 h/a	7,500 h/a
Full load hours (heat)	4660 h/a	4,890 h/a	2,620 h/a

Table 5-22: Emissions in kg/kWh$_{el}$ of different bio-fuelled systems /BMWA/

Emissions	Steam turbine	ORC CHP	Gas+Engines
CO_2	6.15E-02	6.92E-02	9.37E-02
CH_4	1.29E-04	1.44E-04	2.57E-04
SO_2	3.93E-04	6.37E-04	1.33E-04
NO_x	7.15E-04	1.42E-03	1.11E-03
Particulates	9.62E-05	2.04E-04	6.87E-05
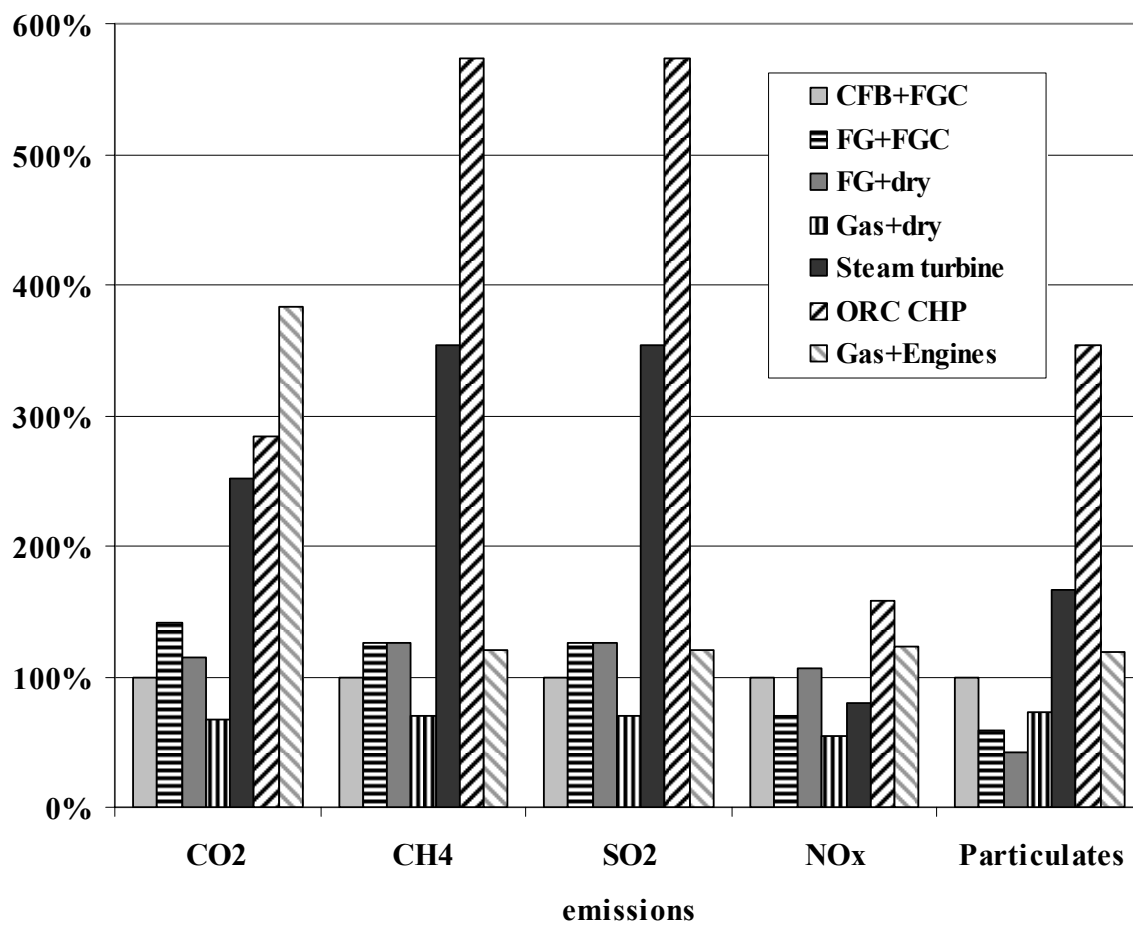
Figure 5-70: Comparison of the /BMWA 2004/ and the results of /Setterwall et al. 2003/ (in kg/kWh$_{el}$)

5.5 Biomass systems

In contrast to chapter 5.4 this chapter describes the use of biomass for electricity production without the additional use of the heat. This technology leads to higher electrical efficiency but a lower total efficiency. Actually, it is difficult to find an appropriate heat demand. Therefore, the pure electricity generation seems necessary and is described in an own chapter. The third possibility for the use of biomass is the pure generation of heat without electricity generation. This technology is not analysed in the study at hand because the focus is on the electricity generation.

5.5.1 Technology

The technology of biomass combustion analysed in /Cuperus 2003/ and this study are:
- *Direct co-combustion* (CC)
- *Circulating fluidised bed combustion* (CFBC)
- *Circulating fluidised bed gasification* (CFBG)
- *Circulating fluidised bed gasification combined with co-combustion* (CFBG+CC)

They are described in more detail in the following paragraphs.

Direct co-combustion (CC):
Direct co-combustion of biomass in a coal-fired power plant is a common technology. The biomass has to be pre-treated by pulverising, pelletising, mixing or drying. Then, the pre-treated biomass is mixed with the coal or transported directly to the burners. The resulting flue gas from the combustion of the fuel mix is cleaned, e.g. with electrostatic filter in order to remove the fly-ash and flue gas desulphurisation (FGD) in order to remove SO_2.

Circulating fluidised bed combustion (CFBC):
The CFBC plant is fired with 100 % biomass. Fluidised beds suspend solid fuels on upward-blowing jets of air during the combustion process. This combustion process results in a turbulent mixing of gas and solids providing more effective chemical reactions and heat transfer. Additionally, the mixing action of the fluidized bed enables the flue gases to get near to sulphur-absorbing chemicals, e.g. limestone,

Circulating fluidised bed gasification (CFBG):
The studied CFBG plant is fired with 100 % biomass. During the process of gasification at a temperature of 850 °C, the biomass is converted to a fuel gas containing carbon monoxide and hydrogen. The fuel gas is cleaned by means of limestone, a dust filter and a scrubber. In the scrubber NH_3, HCl and the larger part of the heavy metals are removed. The cleaned fuel gas is used to generate electricity in a gas and steam turbine.

Circulating fluidised bed gasification combined with co-combustion (CFBG+CC):
In this technology 100 % biomass is turned into a fuel gas by means of gasification in a conventional circulating fluidised bed at a temperature of 850 °C. Afterwards, it is co-combusted in a coal-fired power plant. Before co-combustion, the fuel gas is led through a cyclone, a heat exchanger and a ceramic filter. During the cooling, steam is produced in the heat exchanger and integrated in the existing steam system of the coal-fired power plant. The flue gas is cleaned in the existing flue gas cleaning system with an electrostatic filter and a desulphurisation unit.

The four technologies are described in more detail in chapter 5.5.3.

5.5.2   Market developments
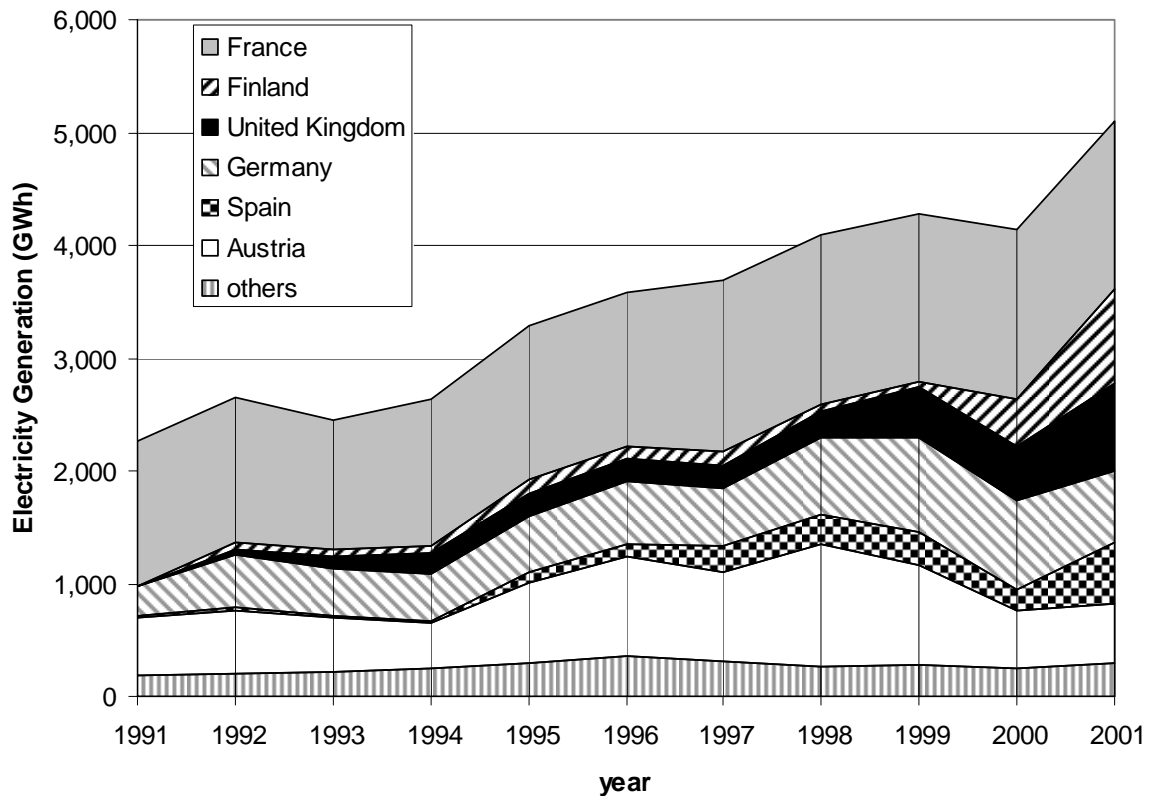
Figure 5-71:   Electricity generation without usage of heat (in GWh) from solid biomass in the ECLIPSE region in the years 1991-2001 /IEA 2003/

The amount of electricity produced with solid biomass in power plants without usage of heat in the ECLIPSE region in the year 2001 is 5,107 GWh. This is 0.18 % of the total electricity generation of 2,840,734 GWh /IEA 2003/. The amount of electricity generation from solid biomass in power plants without usage of heat in the ECLIPSE region has been increasing by 150 % from 1991 to 2001 (see **Figure 5-71**). In the year 2001, the main contribution comes from France, Finland, United Kingdom, Germany, Spain and Austria.

5.5.3 LCA results in ECLIPSE

/Cuperus 2003/ analyses direct co-combustion (CC), circulating fluidised bed combustion (CFBC), circulating fluidised bed gasification (CFBG) and gasification followed by co-combustion (CFBG+CC) as technologies to convert biomass into electricity. Demolition wood, cuttings and prunings, meat and bone meal, sewage sludge and poultry litter are the analysed types of biomass used for combustion in the technologies.

The studied plants are primarily situated in the Netherlands/Western Europe and the fuel preparation and transportation are typical for Dutch and Western European conditions.

Table 5-23 lists the technical parameters of the plants studied in /Cuperus 2003/.

Table 5-23:   Technical parameters of the examples of biomass systems from /Cuperus 2003/[36]

Parameter	Coal-fired power plant	CFBC	CFBG
Net power	600 MW_{el}	30 MW_{el}	30 MW_{el}
Net electrical efficiency	40.5 %	29.0 %	37.0 %
Full load hours	6,000 h	6,000 h	6,000 h
Net production per year	3,600 GWh	180 GWh	180 GWh
SO₂ removal efficiency	90 %	99 %	-
NOₓ removal efficiency	yes	99 %	99 %
Dust removal efficiency	99.957 %	80 %	99.99 %
Life time	40 years	40 years	40 years

Life cycle of biomass systems:

The life cycle of biomass systems consists of the four main life cycle phases production of fuels, construction of the plant, operation of the plant and the end of life with its demolition of the plant (see **Figure 5-72**). They are described in the following paragraphs in more detail.

Coal:

For coal (mining and transport), /Cuperus 2003/ uses data from /Frischknecht et al. 1996/ for transported imported coal which comprises the average of all transports of imported coal to Europe coming from various production countries including coal mining, preparation, coal processing, coal storage, transportation in the export countries by truck or railway and transportation to Europe by ship.

---

[36] It was not possible to derive all figures from the /Cuperus 2003/. Therefore not all cells of the table could be completed.

Biomass:

Several kinds of biomass are studied in /Cuperus 2003/. The data are from /KEMA 1999/. This study only focuses on cuttings and prunings. The cuttings and prunings are gathered, collected and transported by means of a medium lorry over a distance of 150 km to the biomass plant.
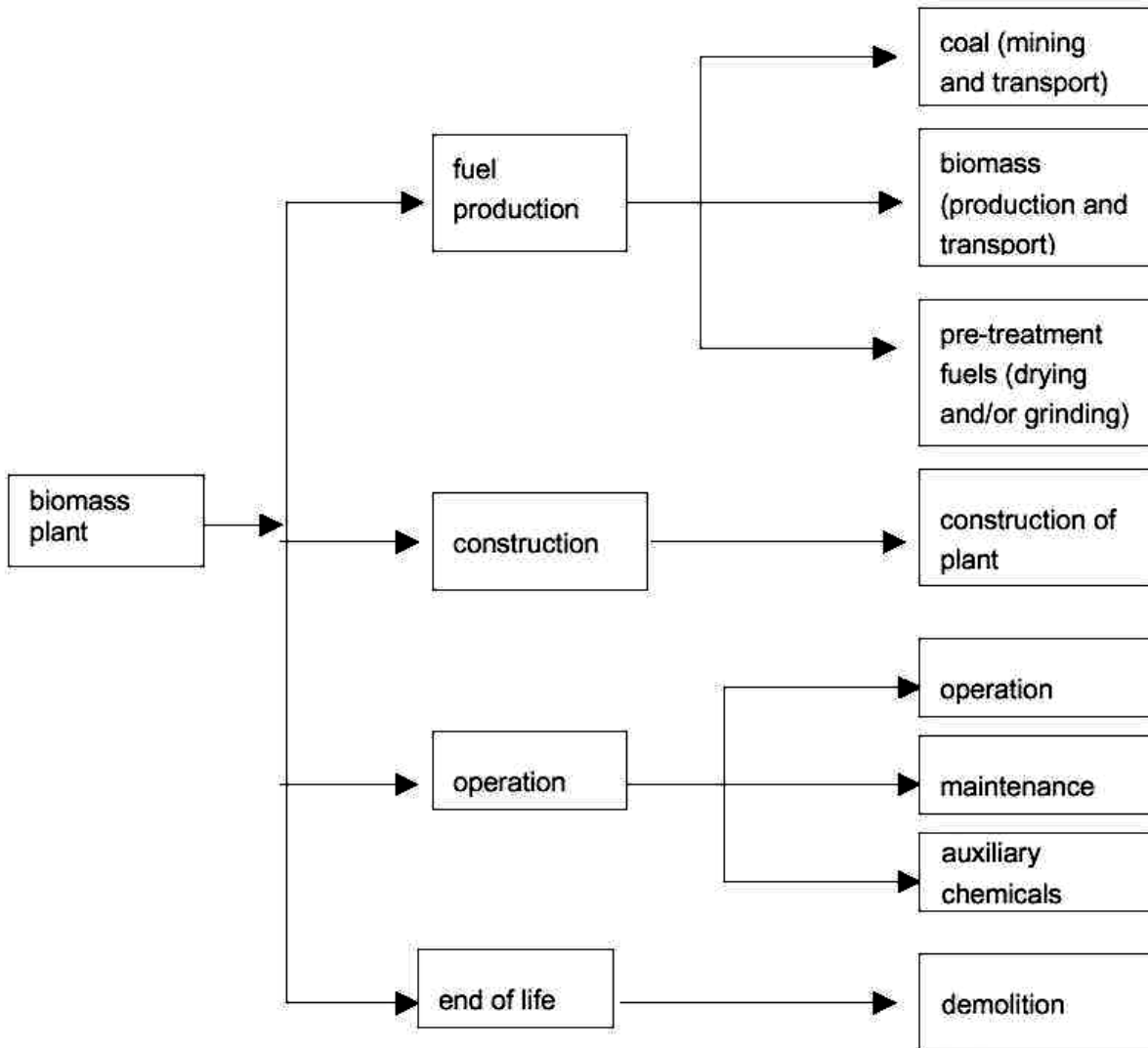
Figure 5-72:   Life Cycle of biomass systems /Cuperus 2003/

Pre-treatment of fuels:

The pre-treatment of the fuels concerns coal as well as biomass. Coal is grinded in the coal grinder within the coal-fired power plant. Cuttings and prunings with a water content of 41 % are dried to 10 % by means of the fuel natural gas. In a further pre-treatment process the cuttings and prunings are grinded.

Construction of the biomass plant:

The construction of the biomass plant includes the manufacturing of materials and metals as well as the use of electricity with all the respective upstream processes. The data are from /FfE 1996/ which analyses a 600 MW coal-fired power plant. For the de-centralised 30 MW plants the data from /FfE 1996/ are scaled down with a factor of 20. Data for machines digging in ground as well as the electricity consumption during the building phase are not considered. The life span of the biomass plant is assumed to be 40 years.

Operation:

In the life cycle phase operation, the environmental effects which occur during the production of electricity are considered. The assessed emissions are calculated by means of the KEMA TRACE MODEL, which is a computer model built by KEMA. It is based on more than 20 years of measurements at Dutch power plants /Cuperus 2003/.

Maintenance:

In the unit process maintenance, the replaced materials from the worn out components are taken into account as well as their necessary transportation. Data for the 600 MW coal-fired power plant originate from /FfE 1996/. These data are also used for the decentralised plants scaled down by 20.

Auxiliary chemicals:

For the production of electricity, several chemicals are necessary. Limestone is used for the FGD. Bed material SiO_2 is used in the CFB technologies. For FGD in CFB combustion ammonia and for FGD in CFB gasification N_2 and NaOH are taken into account.

End of life – demolition of the biomass plant:

The power plant will be demolished after its lifetime of 40 years. Data for the 600 MW coal-fired power plant originates from /FfE 1996/. These data are also used for the decentralised plants scaled down by 20.

Examples:

In /Cuperus 2003/ there are some inconsistencies between the emission data in the total result list, the common minimum list and the report. The study at hand derives the emission data from the total result list. The displayed CO_2 is always fossil CO_2. Biogenic CO_2 is not displayed as it is assumed to be neutral in its cycle of absorption in the biomass growth process and emission in the combustion process. SO_2 is derived from the total result list as the sum of SO_2, SO_x and SO_x (as SO_2). NO_x is calculated as the sum of NO_2, NO_x and NO_x (as NO_2) as listed in the total result list. Particulates are derived from the total result list as the sum of

dust, dust (coarse) process, dust (PM10) mobile, dust (PM10) stationary, dust (SPM) and particulates.

Selected examples from /Cuperus 2003/ are described in the following paragraphs.

Co-combustion of 10 % cuttings and prunings in a coal-fired power plant (CC):

The 10 % are based on dry mass, corresponding to 14.3 % based on wet mass or 10.5 % based on energy. **Figure 5-73** shows the contribution of the different life cycle phases to the emissions. Almost all of the emissions of CH_4, particulates and NMVOC are caused by the mining and transportation of the coal. Also a large part of the emissions of NO_x and SO_x are caused by this life cycle phase, whereas the other part is nearly completely caused by the operation phase that is responsible for more than 90 % of the CO_2 emissions.

With co-combustion of 20 % instead of 10 %, the distribution does not change significantly. However, the absolute emissions per kWh_{el} change as displayed in **Figure 5-74**. All emissions decrease by 5-12 %.
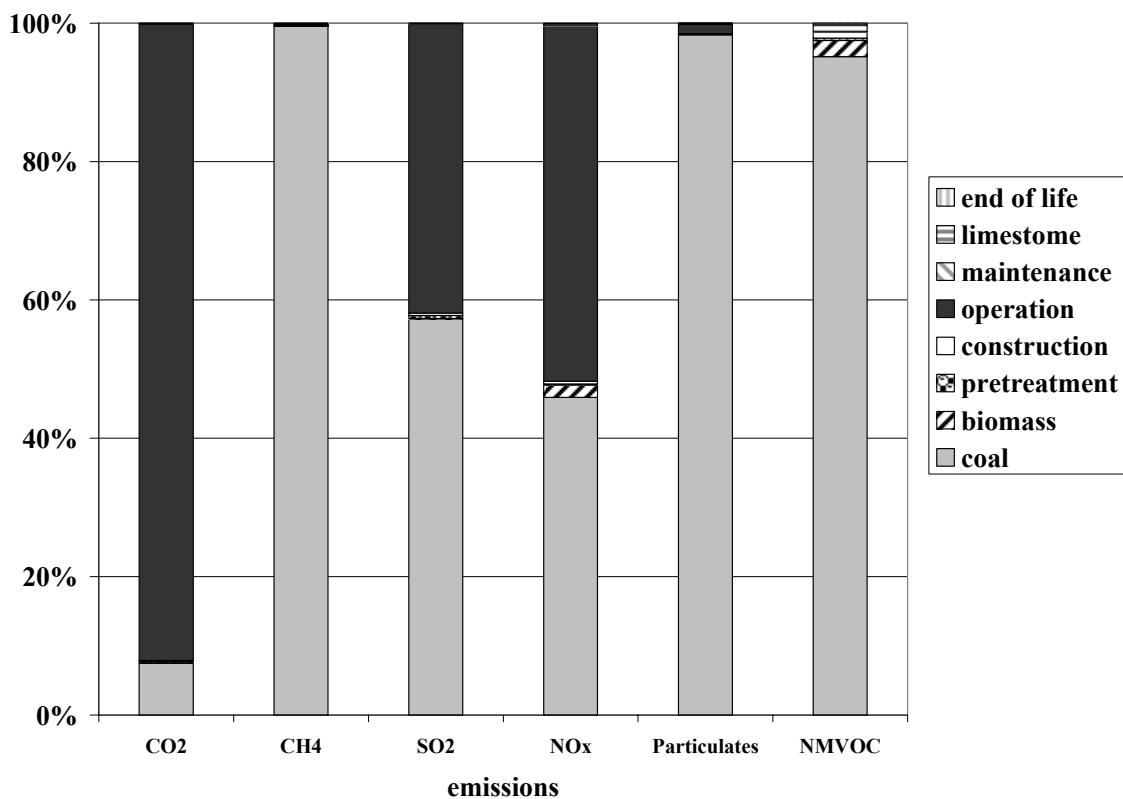
Figure 5-73:   Contribution of the life cycle phases to the emissions with co-combustion of 10 % cuttings and prunings in a coal-fired power plant (in kg/kWh_{el})
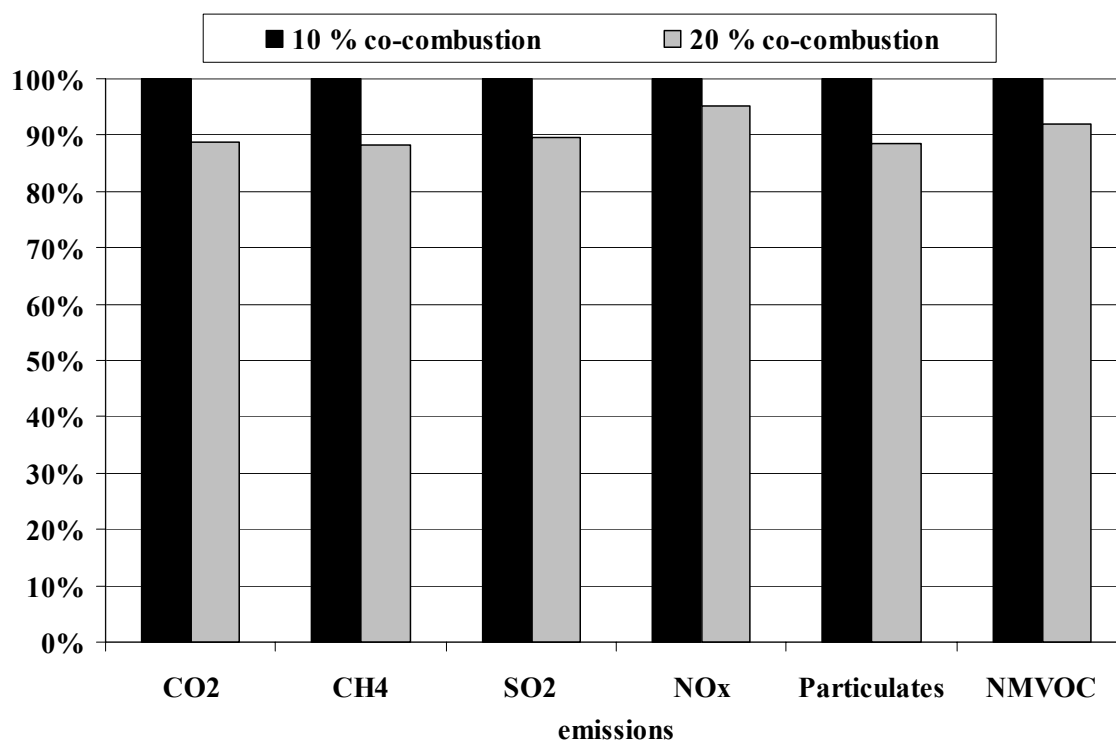
Figure 5-74:   Change in emissions due to 20 % instead of 10 % co-combustion of cuttings and prunings (in kg/kWh$_{el}$)

Circulating fluidised bed combustion (CFBC) of cuttings and prunings:

Figure 5-75 shows the contribution of the life cycle phases to the emissions of a CFBC plant. The production of biomass is the dominating process in the case of NMVOC emissions. In the case of CO_2 and CH_4, the production of biomass and the pre-treatment of the biomass are responsible for one half of the emissions each. During the operation phase, about 70-80 % of the SO_2, NO_x and particulates emissions are emitted.

/Cuperus 2003/ perform a sensitivity analysis showing the change of emissions due to the use of ammonia for FGD instead of limestone addition. The changed distribution is displayed in **Figure 5-76** and the relative change is illustrated in **Figure 5-77**. The NO_x and NMVOC emissions are very similar in absolute terms and in terms of distribution. Emission reductions are achieved for SO_2 and particulates emissions which are reduced by ca.60 %. This reduction is mainly achieved in the operation phase. The use of chemicals for FGD contributes much more to the life cycle emissions than the addition of limestone. This leads to more CO_2 (ca. +20 %) and CH_4 (ca. +60 %) emissions. In the case of SO_2 and particulates, the additional emissions due to the use of chemicals for FGD emissions are compensated by the reduction of the emissions due to FGD.
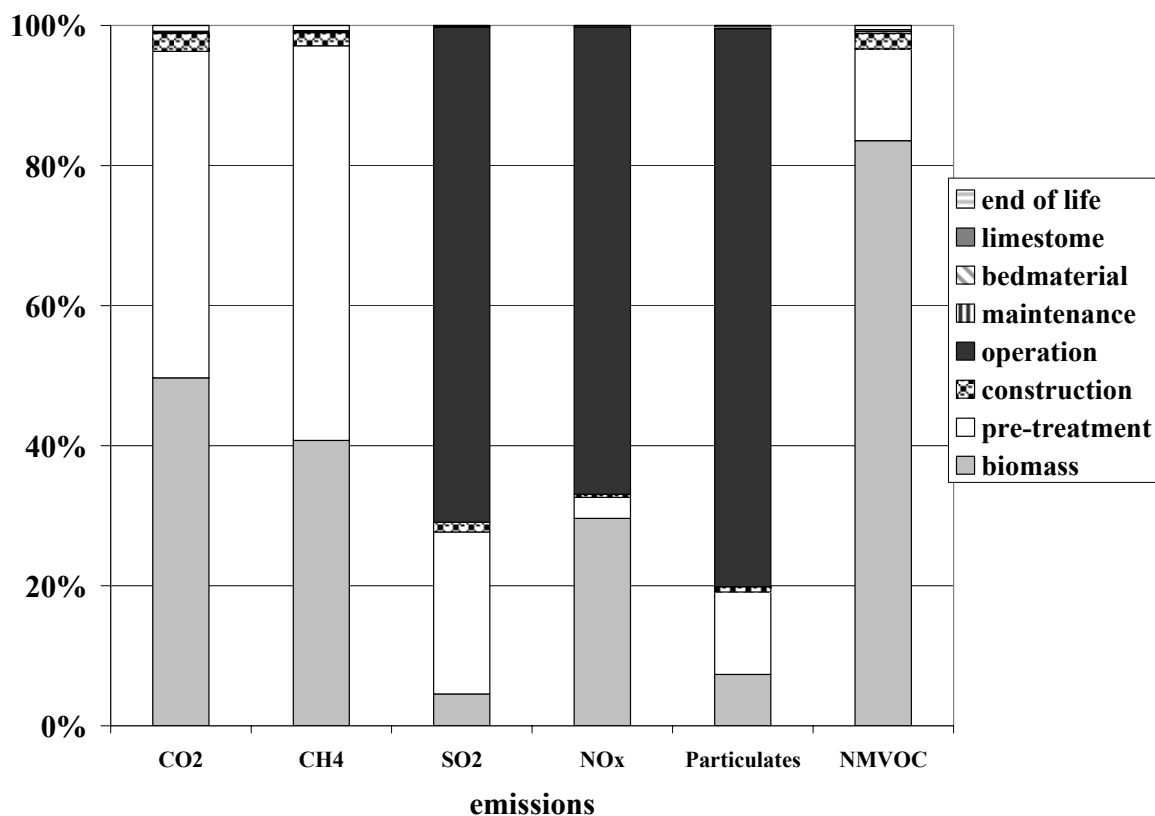
Figure 5-75: Contribution of the life cycle phases to the emissions (in kg/kWh$_{el}$) with CFBC of cuttings and prunings (no FGD but addition of limestone)
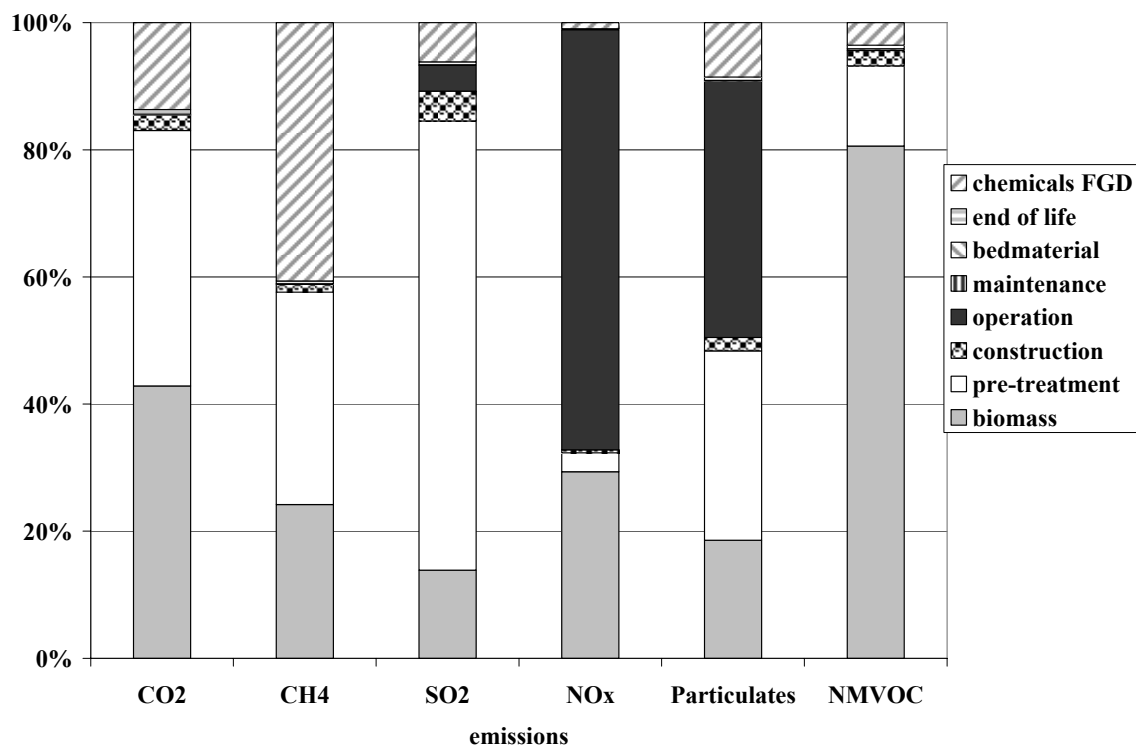
Figure 5-76: Contribution of the life cycle phases to the emissions (in kg/kWh$_{el}$) with CFBC of cuttings and prunings (with FGD but no addition of limestone)
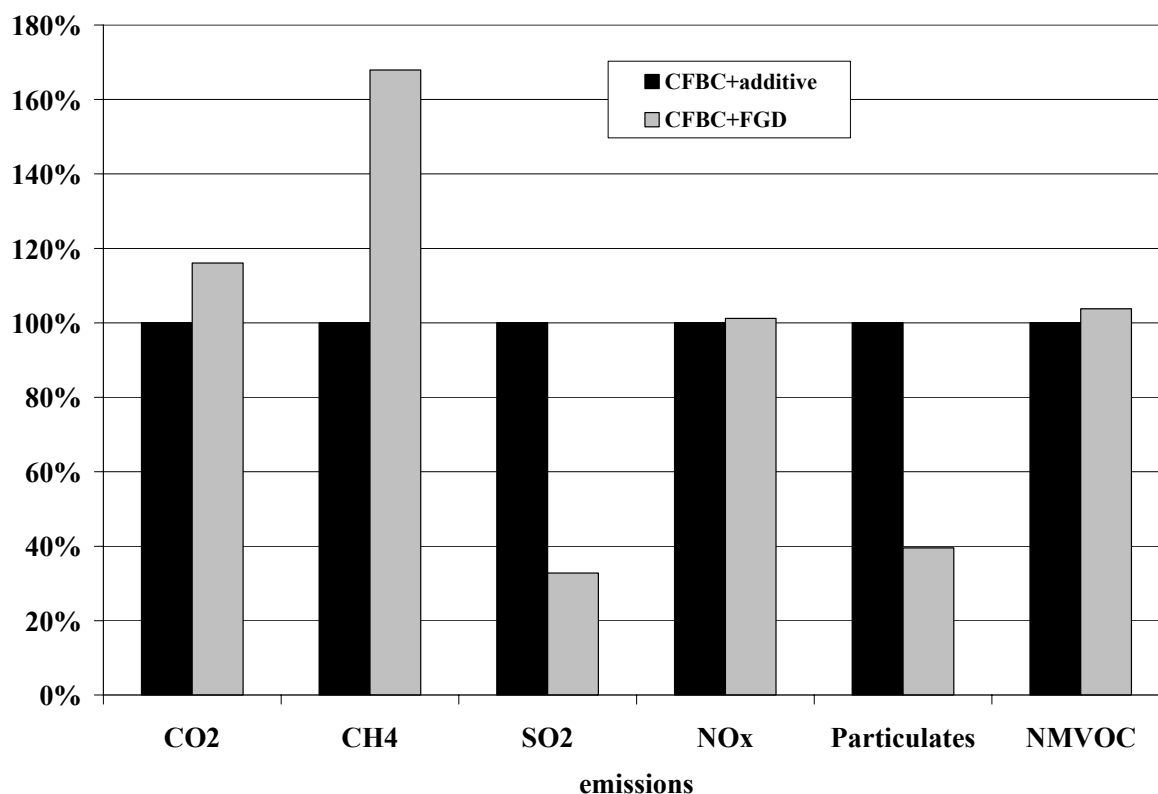
Figure 5-77:   Comparison between CFBC+additive and CFBC+ FGD in relation to CFBC+additive (in kg/kWh$_{el}$)

Circulating fluidised bed gasification (CFBG) of cuttings and prunings:

The contribution of the life cycle phases is illustrated in **Figure 5-78**. More than 80 % of the emissions of NO$_x$ and NMVOC are caused by the production of the biomass. This life cycle phase also contributes 33-47 % to the CO$_2$, CH$_4$ and particulates emissions whose remaining part is mainly caused by the pre-treatment of the biomass. Biogenic CO$_2$, which is not displayed in **Figure 5-78**, and nearly half of the SO$_2$ emissions are caused by the operation of the CFBG plant.

Circulating fluidised bed gasification followed by co-combustion (CFBG+CC) of cuttings and prunings:

Figure 5-79 shows the contribution of the different life cycle phases to the emissions of CFBG+CC of cuttings and prunings (cf chapter 5.5.1). The operation phase dominates the fossil and biogenic CO$_2$ emissions with more than 90 %. SO$_2$ and NO$_x$ are mainly emitted by the operation and the coal production phase (ca. 50 % each). The coal supply is responsible for nearly all the CH$_4$, particulates and NMVOC emissions.
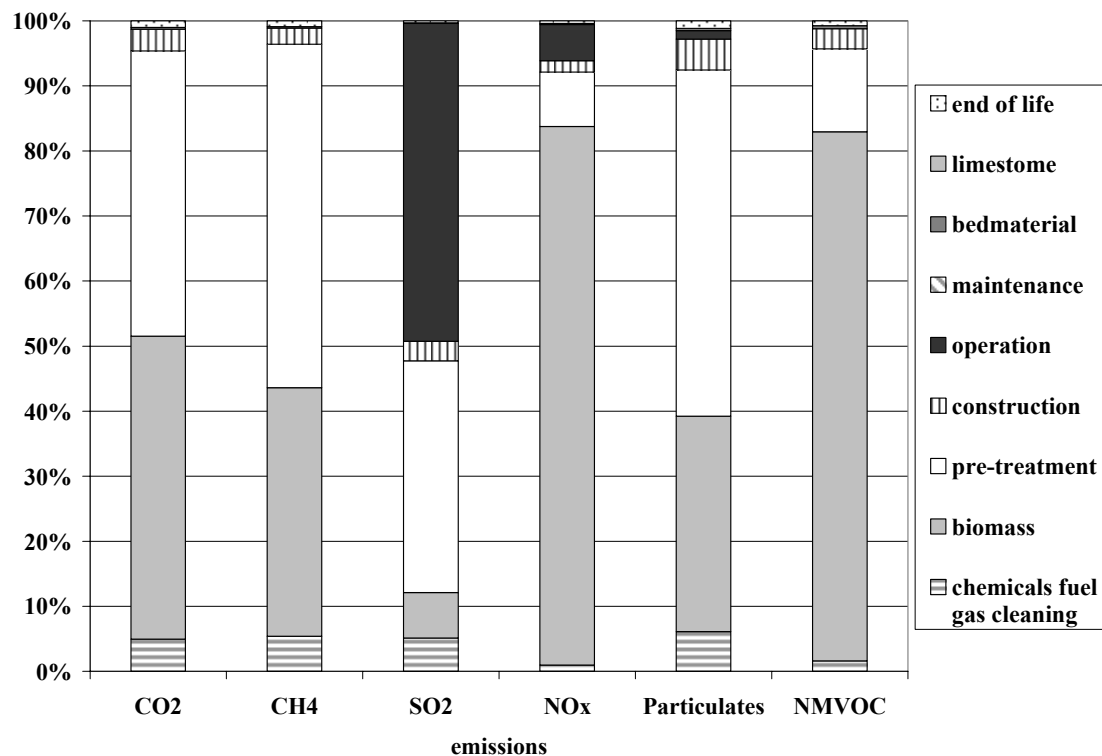
Figure 5-78:   Contribution of the life cycle phases to the emissions with CFBG of cuttings and prunings (in kg/kWh$_{el}$)
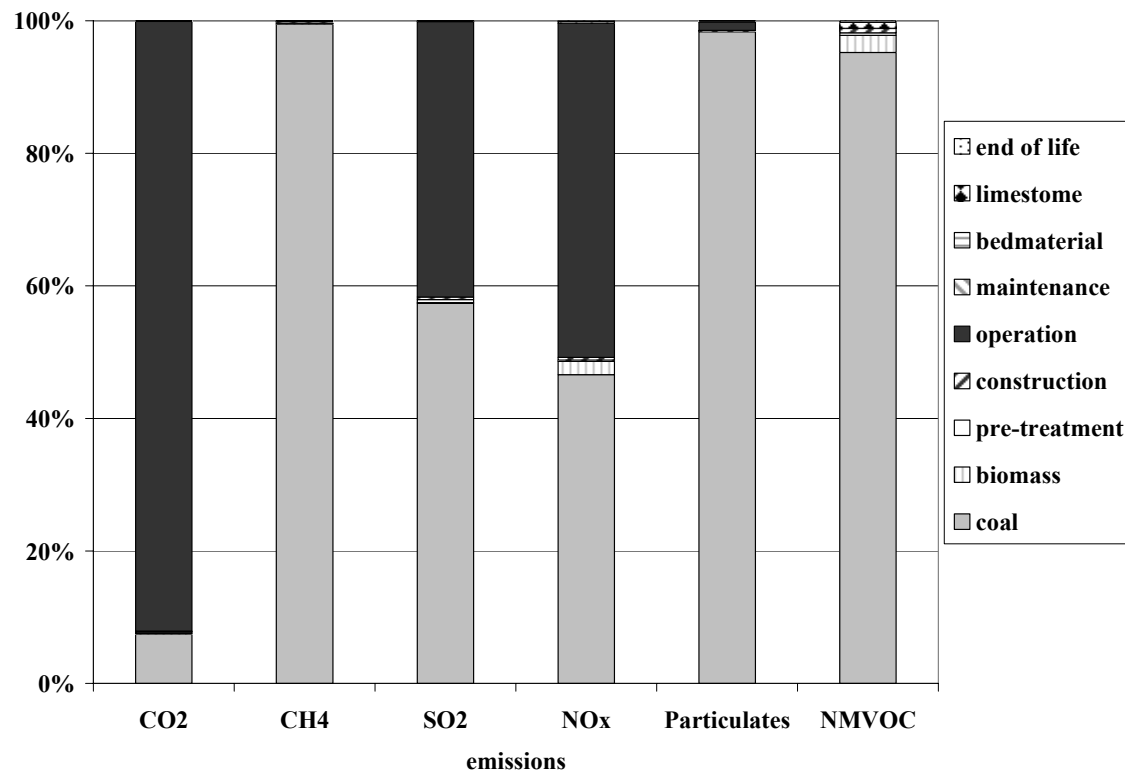
Figure 5-79:   Contribution of the life cycle phases to the emissions with CFBG followed by co-combustion of cuttings and prunings (in kg/kWh$_{el}$)

5.5.4 Emissions of biomass systems

For construction, maintenance and end of life of the CFBC and CFBG technologies, data from a coal-fired power plant are scaled down which results in low data quality. However, this is not very important as these life cycle phases have only minor environmental impacts compared with other ones (cf. figures above).

The emissions of the analysed biomass systems are given in **Table 5-24**. **Figure 5-80** compares the three studied technologies without co-combustion. In contrast to the comparison of the co-combustion technologies in **Figure 5-81**, the technologies in **Figure 5-80** do have significantly different emissions per kWh_{el}. Emissions of fossil CO_2, CH_4, SO_2, particulates and NMVOC are several fold higher in case of co-combustion compared to the technologies without co-combustion because of the mining and transport of coal. This is illustrated in **Figure 5-82**.
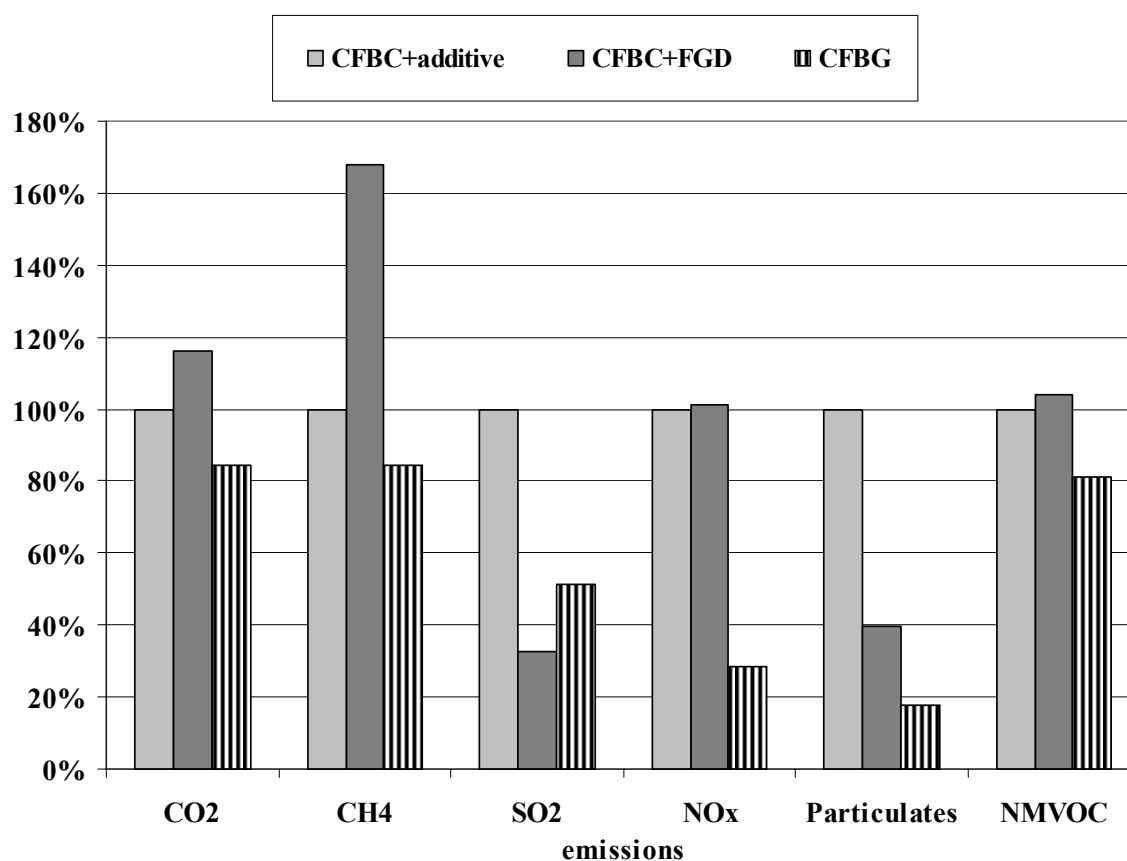
Figure 5-80:   Comparison of the emissions of CFBC+additive, CFBC+FGD and CFBG (in kg/kWh_{el})

Table 5-24:   Emissions in kg/kWh$_{el}$ of different biomass systems

Emissions	CFBC +additive	CFBC +FGD	CFBG	CFBG +Co-combustion	10 % Co-combustion	20 % Co-combustion
CO$_2$	3.92E-02	4.55E-02	3.30E-02	8.70E-01	8.13E-01	7.22E-01
CH$_4$	6.67E-05	1.12E-04	5.62E-05	1.54E-03	1.44E-03	1.27E-03
SO$_2$	3.76E-04	1.23E-04	1.93E-04	1.47E-03	1.38E-03	1.23E-03
NO$_x$	1.06E-03	1.07E-03	3.00E-04	1.26E-03	1.19E-03	1.13E-03
Particulates	1.11E-04	4.39E-05	1.94E-05	1.22E-03	1.15E-03	1.02E-03
NMVOC	6.12E-05	6.35E-05	4.97E-05	1.58E-04	1.48E-04	1.36E-04
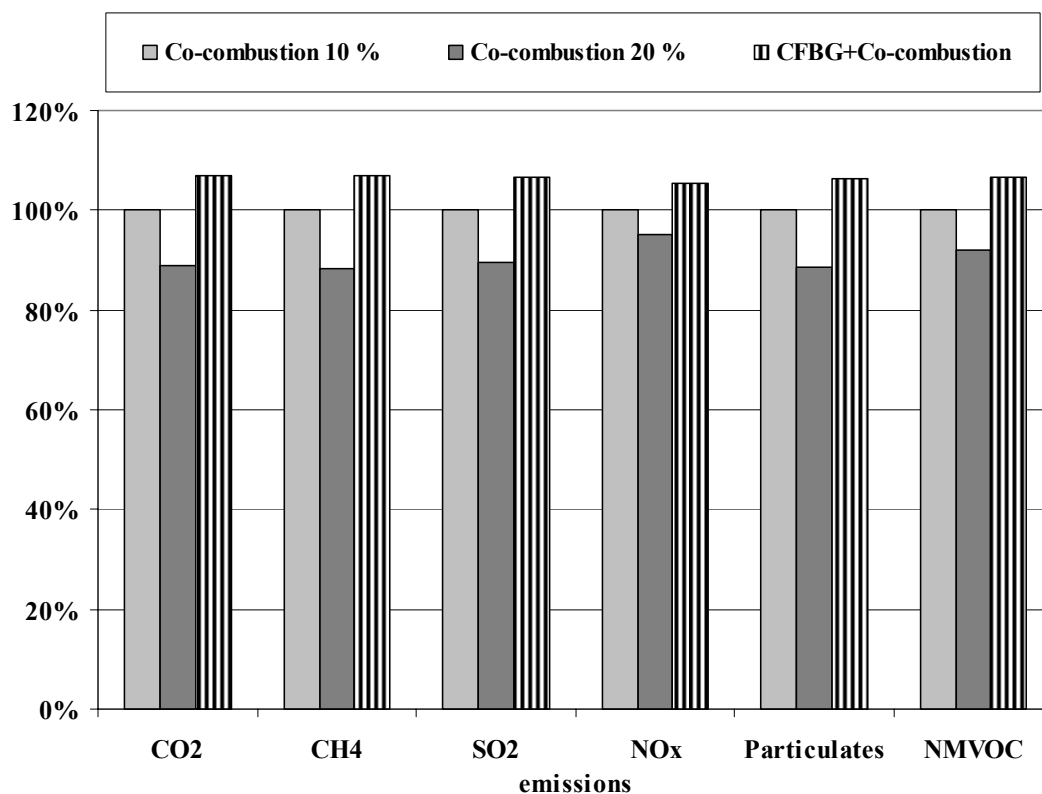
Figure 5-81:   Comparison of the emissions of different Co-combustion biomass systems (in kg/kWh$_{el}$)
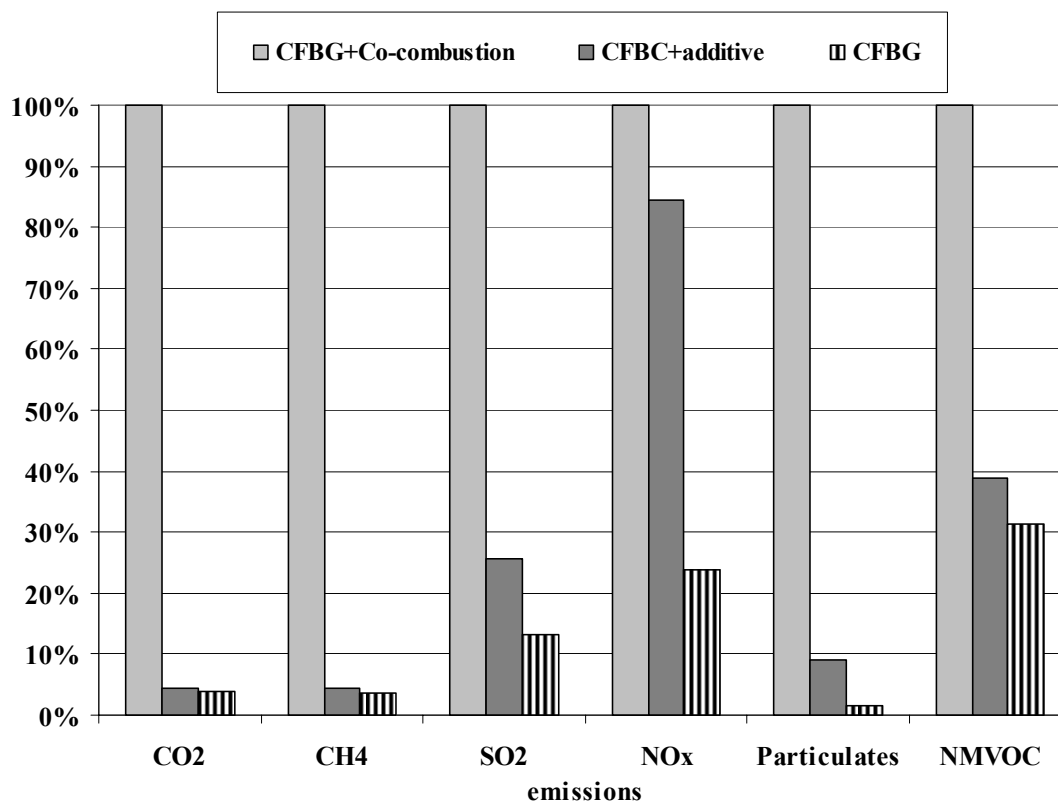
Figure 5-82:   Comparison of the emissions of CFBG+Co-combustion, CFBC+additive and CFBG
(in kg/kWh$_{el}$)

In the comparison of the studied biomass systems, the CFBG system has the lowest of all emissions with the exception of SO_2. NO_x-emissions from CFBG plants are comparably low due to fuel gas cleaning (see **Figure 5-80** and **Figure 5-82**).

In contrast, the CFBC+additive and the CFBC+FGD system can not be brought into an ranking of environmental impact as described above. This is easier in the case of the analysed co-combustion technologies. The co-combustion of 20 % instead of 10 % reduces all emissions as described above whereas the CFBG together with co-combustion has more emissions compared to all other considered systems.

These results can be compared with the topical study /BMU 2004/. The comparison is illustrated in **Figure 5-83**. It shows that except for NO_x all emissions calculated for the steam turbine biomass power plants in /BMU 2004/ are below the figures of the circulating fluidised bed combustion with limestone as additive. In direct comparison of the both technologies in /BMU 2004/, the steam turbine fired with forest wood tends to cause less emissions than the steam turbine fired with short rotation forestry wood because the production and the use of fertilizers for accelerated growth cause additional environmental impacts compared to waste wood. The considered configuration of the technology studied in /BMU 2004/ is a steam turbine power plant with a power of 5 MW$_{el}$ using a circulating fluidised bed combustion at atmospheric pressure with an electrical utilization factor of 29 %. This power plant also has

emissions reductions facilities which are a selective non catalytic reduction in order to reduce nitrogen oxides emissions as well as a cyclone in order to reduce particulates emissions.
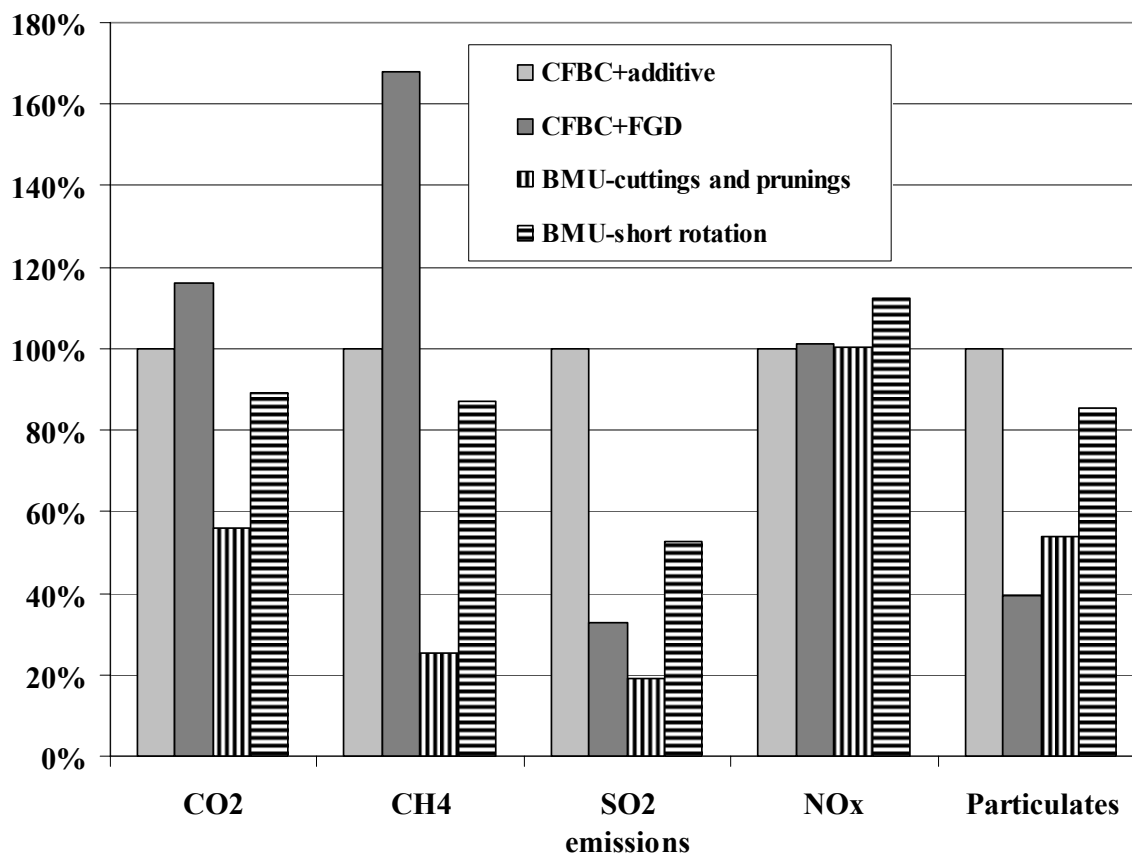
Figure 5-83:   Comparison of the emissions (in kg/kWh$_{el}$) of biomass system from /BMU 2004/ and /Cuperus 2003/

5.6   Water power plants

It should be noted that the LCI data for the river power plant from /BMU 2004/ as well as the reservoir power station from /Frischknecht et al. 1996/ are not consistent with the LCI data from ECLIPSE. However, they are described to give also an overview of renewable technologies which are not analysed in the ECLIPSE studies.

5.6.1   Technology

River power plants convert the energy in the water flow of rivers into electricity. The usable energy stored in the water flow is potential energy (height difference), kinetic energy (velocity difference) and energy in the water of higher pressure (pressure difference). Between the headwater and the run-off water, the energy difference can be used with a water turbine for electricity generation. The usable energy difference ΔE between the head water (indexed with 1) and the run-off water (indexed with 2) is given as the sum of the potential energy difference, the kinetic energy difference and the pressure energy difference. Therefore, the equation uses the *mass of the water flow* m, the *acceleration of gravity* g_{earth}, the *height* h, the *pressure of the water flow* p, the *volume of the water flow* V and the *velocity of the water flow* v:

$$\Delta E = m \cdot g_{earth} \cdot (h_1 - h_2) + V \cdot (p_1 - p_2) + \frac{1}{2} \cdot m \cdot (v_1^2 - v_2^2) \qquad (5\text{-}14)$$

It can be distinguished between river power plants and reservoir power stations. While the energy used in river power plants is mainly kinetic energy, the energy used in reservoir power stations is mainly potential and pressure energy.

The turbines have electrical efficiencies of 80-90 % at full load. Most turbines also have good part load behaviour.

5.6.2   Market development

River power plants are a renewable energy source, which has been developed over decades. Thus, it has not the growth rates as other renewable energy sources because a large part of the potentials are already used. However, refurbishment and upgrading of existing systems becomes very interesting. The market development in the ECLIPSE region is shown in **Figure 5-84** and **Figure 5-85**.
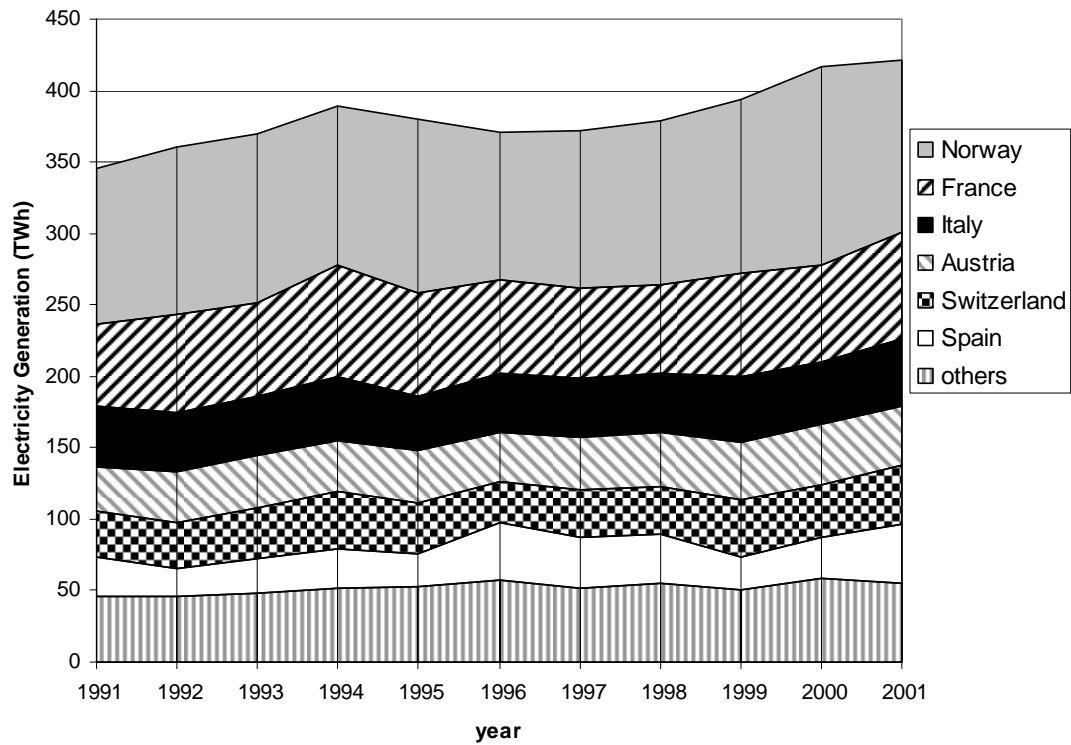
Figure 5-84:   Market development (in TWh) of river power plants in the ECLIPSE region /IEA
2003/
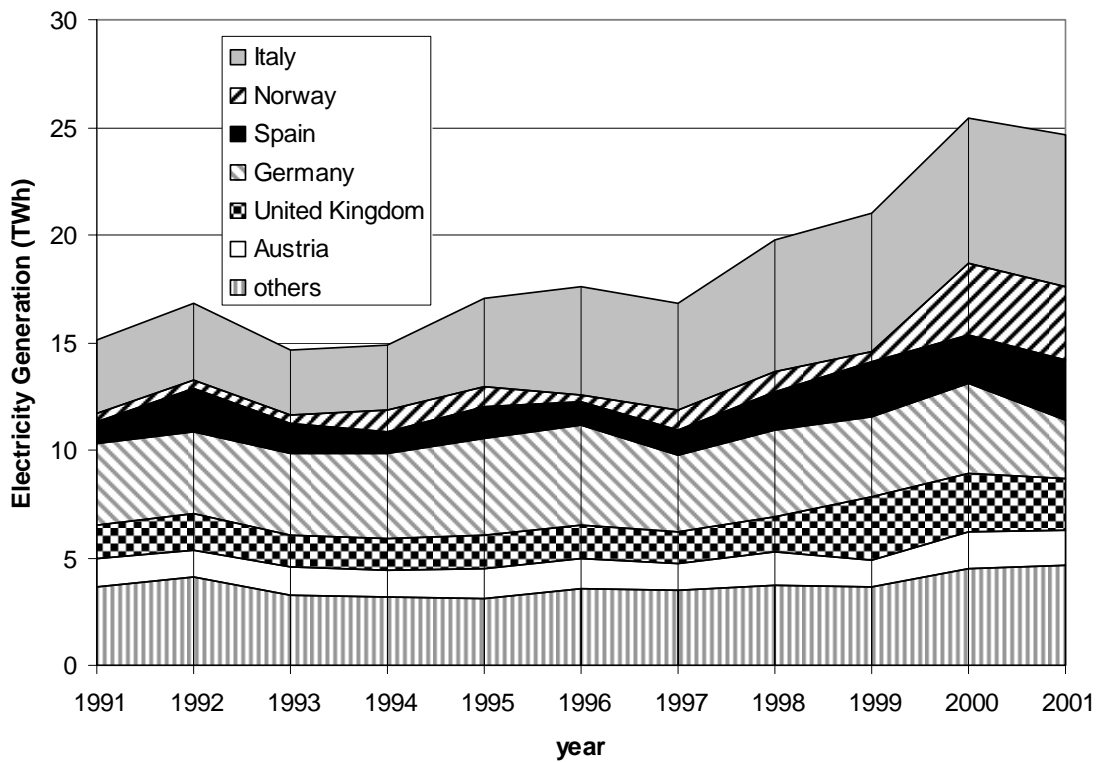
Figure 5-85:   Market development (in TWh) of pumped storage power plants in the ECLIPSE re-
gion /IEA 2003/

/Horlacher 2003/ estimates the global water power potentials. For Europe, the author states a theoretical potential of 3,220 TWh/a, a technical potential of 1,035 TWh/a and an economic potential of 791 TWh/a. The region of focus produces 593 TWh in 2001. Thus it uses ca.75 % of the economic potential.

5.6.3   LCA results

/BMU 2004/ refers to /Hartmann 2001/. The main part of the emissions is caused by the concrete and steel consumption for the construction of the buildings whereas the minor part is caused by the machine materials and the operating phase. In contrast to new developed technologies, e.g. PV, the data quality is quite good as there is much and long term experience with water power plants.

5.6.4   Emissions of water power plants

The emissions of the analysed river power plants with 3.1 MW and 0.3 MW as well as those of the analysed reservoir power plant are listed in **Table 5-25**

Table 5-25:   Emissions in kg/kWh_{el} of the river power plants /BMU 2004/ and the reservoir power station /Frischknecht et al. 1996/

Emissions	River-3.1	River-0.3	Reservoir
CO_2	1.00E-02	1.30E-02	4.03E-03
CH_4	2.10E-05	2.90E-05	9.40E-06
SO_2	1.70E-05	2.80E-05	1.17E-05
NO_x	3.60E-05	4.90E-05	1.08E-05
Particulates	2.60E-05	3.10E-05	-
NMVOC	-	-	3.11E-06

5.7   Solar thermal power plants

It should be noted that the LCI data for this system from /BMU 2004/ are not consistent with the LCI data from ECLIPSE. However, they are described to give also an overview of renewable technologies which are not analysed in the ECLIPSE studies.

5.7.1   Technology

Different technologies of solar thermal power plants can be distinguished. On the one hand, there are concentrating systems and, on the other hand, there are solar chimney power plants. The first mentioned concentrate the direct solar radiation on an absorber while the second mentioned heat the air which flows due to the chimney effect through a chimney and drives thus a turbine. Concentrating systems are of different kind. One technology uses a central receiver on a tower which is irradiated with reflected sunlight from a heliostat field. Another technology is a parabolic dish which concentrates the sunlight on a focal point. There the heat can be used, e.g. with a Stirling engine. The technology which is analysed in the study at hand is the parabolic trough solar collector using a linear concentrating system. All concentrating technologies use the direct radiation of the sun and enforce the energy flow by concentration. This is necessary to reach higher temperatures so that the energy can be used with a higher efficiency which is determined by the Carnot efficiency (cf. chapter 5.3.1).

5.7.2   Market development

In contrast to the other solar thermal technologies described above, the parabolic-trough solar collectors are leaving the demonstration state and become commercially available. Nevertheless, a market development for Europe is still not available.

5.7.3   LCA results

/BMU 2004/ analyse a SEGS facility with LC-3 collectors. This power plant has a solar capacity of 80 MW. It is assumed to be without an additional fossil combustion and without a storage unit. The life time of this plant is defined as 30 years. Data for materials and services are derived from studies which use manufacturer data. They are updated with new technologies for mirror cleaning. The plant site is located in Southeast Morocco with a solar radiation of 2,654 $kWhm^{-2}a^{-1}$ resulting in 2,340 full load hours per year. Most of the components are imported from Germany by ship.

In case of thermal power plants, the site dependency is similar to that of photovoltaic systems. However, the concentrating systems of thermal power plants do need direct radiation

and can not use the indirect radiation which contributes a significant share of the energy input to the PV systems. Thus, thermal solar power plants should be located in Europe as southern as possible because the contribution of indirect radiation to the total radiation decreases and the contribution of direct radiation increases. One of the most promising countries in Europe is Spain which also has a large solar demonstration project at the Plataforma Solar de Almería[37].

The main part of the emissions (62-95 %) is caused in the construction phase due to the material demand dominated by steel production. Operation and end of life contribute the other part which is not negligible. In the operation phase 90 % of the emissions are caused by the vehicle which cleans the mirrors. The NO_x emissions of this vehicle are significant and contribute ca. 20 % to the total life cycle NO_x emissions.

5.7.4 Emissions of solar thermal power plants

The emissions of the parabolic-trough power plant are listed in **Table 5-26**.

Table 5-26:   Emissions in kg/kWh_{el} of the parabolic-trough solar collector facility

Emissions	Parabolic-trough
CO_2	1.34E-02
CH_4	3.52E-05
SO_2	4.67E-05
NO_x	7.29E-05
Particulates	4.01E-05

---

[37] http://www.psa.es

5.8   Geothermal power plants

It should be noted that the LCI data for this system from /BMU 2004/ are not consistent with the LCI data from ECLIPSE. However, they are described to give also an overview of renewable technologies which are not analysed in the ECLIPSE studies.

5.8.1   Technology

Geothermal energy arises from the decay of radioactive elements and the ancient heat remaining in the earth's core. These energy sources result in a heat flow from the lower levels of the earth's crust to the earth's surface of 0.065 W/m². This heat flow is caused by a temperature gradient of 30 K/km on the average. However, this temperature gradient can be much higher at certain sites, e.g. Iceland with lots of geothermal anomalies.
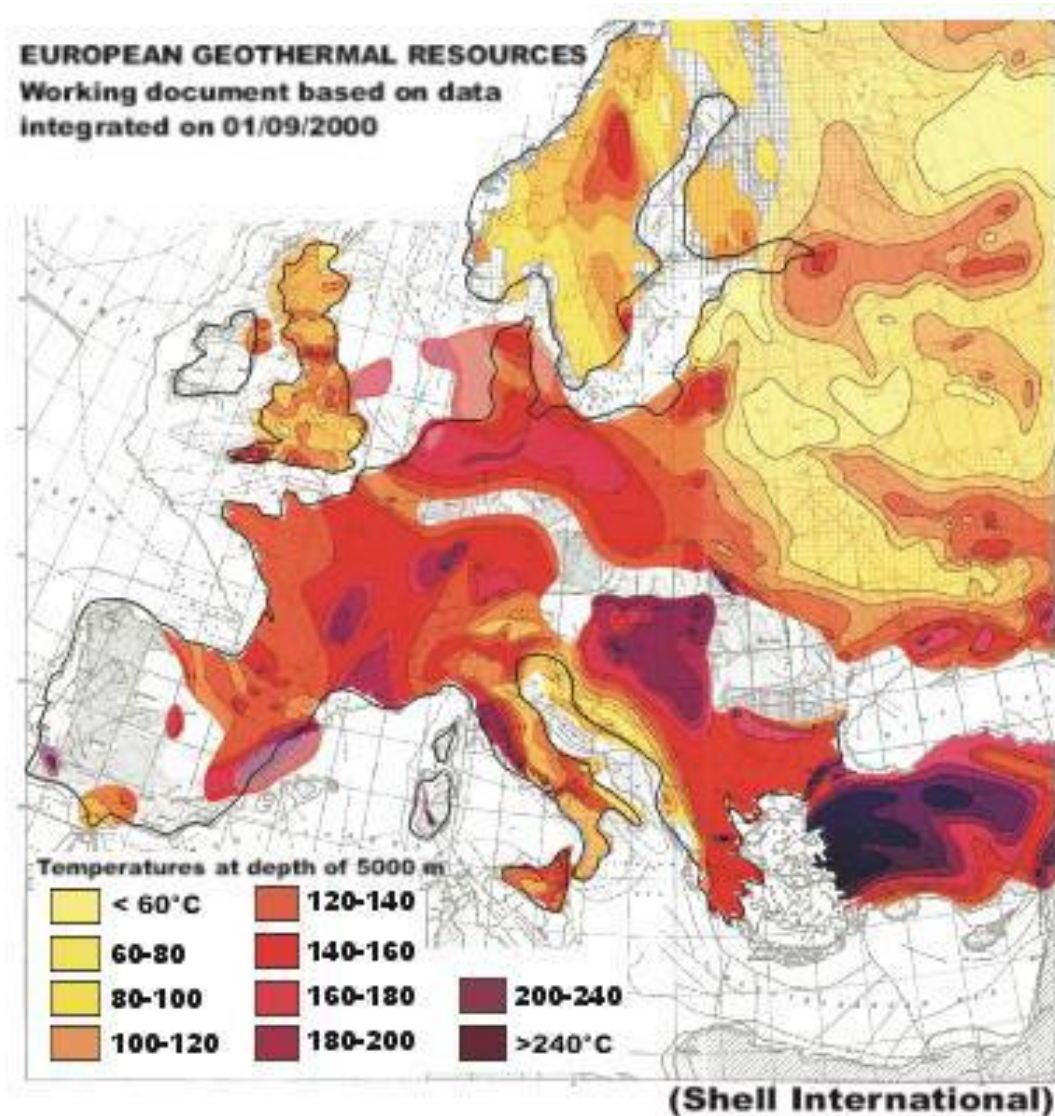
Figure 5-86:   European geothermal resources (in °C at depth of 5000 m) /E.E.I.G. 2004/

Figure 5-86 shows the temperatures in Europe at a depth of 5 km. /E.E.I.G. 2004/ estimate that 1 km³ rock which is cooled 20 °C delivers 15,000 GWh thermal energy or a power of 10 MW$_{el}$ base load for 20 years if the temperature of the rock is more than 200 °C. It is derived from a Shell study that the available resource of 125,000 km² in Western Europe with more than 200 °C at an approximate depth of 5 km may deliver ca. 900 TWh$_{el}$ per year if 10 % of the area with a thickness of 1 km is used. This is approximately a third of the electricity production of the European Union in 2001.

In depths of ca. 5 km with temperatures of the rocks of 200 °C, the geothermal energy can be used. By drilling in these depths and fracturing the rocks it is possible to heat water which is injected with the injection well into the fractions and extracted with production wells at some distance. The natural fracture system is used as a heat exchanger but as the permeability is not good enough it is enlarged through massive stimulation which widens the fractions. The described technology is called *Hot Dry Rock* (HDR) and is widely applicable and not reliant on anomalies.

5.8.2   Market development
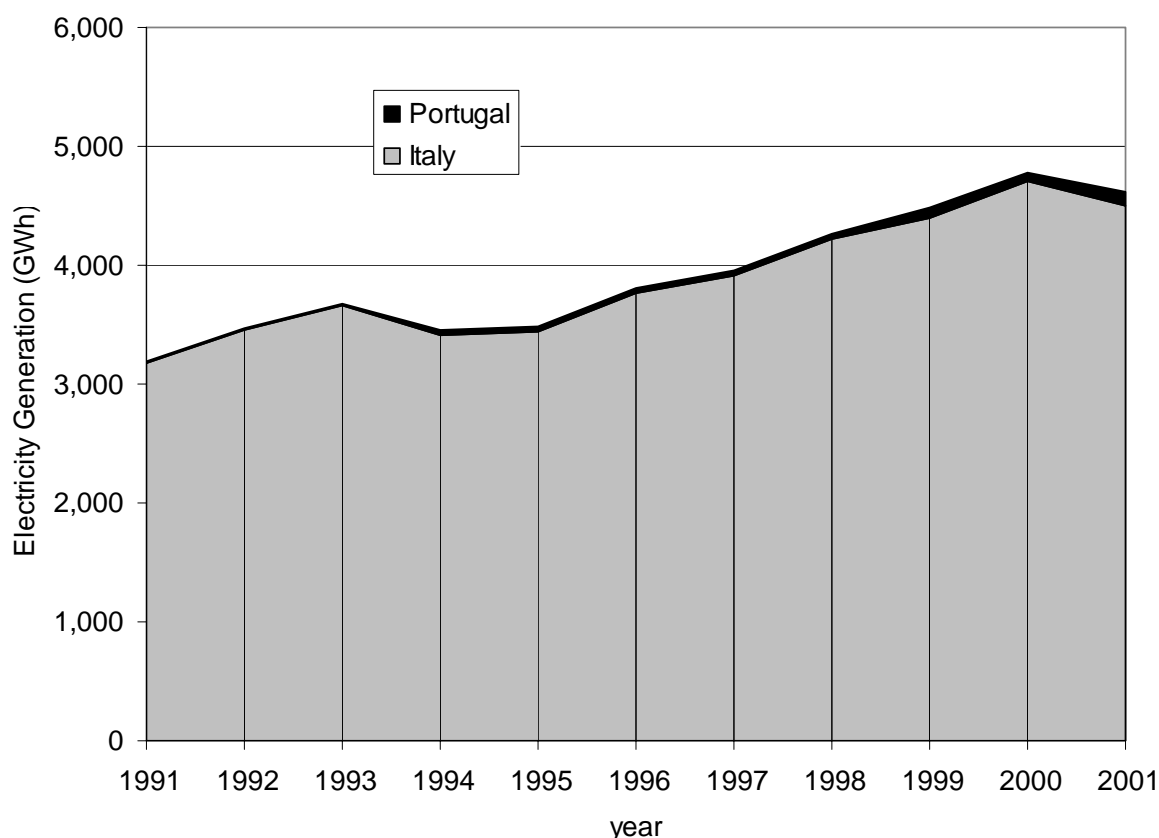
Figure 5-87:   Geothermal electricity generation (in GWh) in Europe /IEA 2003/

Geothermal electricity production of 4,612 GWh (2001) has a share of 0.16 % of the total electricity production of 2,840,734 GWh in the ECLIPSE region (2001). Only two countries

in the ECLIPSE region contribute to this small share as can be seen in **Figure 5-87**, Portugal and Italy of which Italy has the main part with 98 %.

5.8.3   LCA results

Data for the HDR system are derived from studies of the years 2002 and 2003. Relatively optimistic conditions are assumed because the HDR system delivers water with a temperature of 150 °C from a depth of 2,700 m with a rate of 100 m³ per hour. This hot water is used in an ORC process with an electrical capacity of 850 kW and an electrical efficiency of 11 %. The HDR system runs 7,500 full load hours per year. Besides the power product, the analysed system also supplies heat to a local district heating system with a temperature of 70 °C and 1,900 full load hours per year.

The life cycle emissions are nearly totally caused in the construction phase in which the underground installations are responsible for 80 % of the CO_2 emissions and 90 % of the SO_2 and NO_x emissions because of the high energy demand of the drilling process which causes one third of the life cycle CO_2 emissions and two thirds of the life cycle SO_2 emissions. In contrast the ORC system contributes only 15 % to the impacts. The operation and end of life phase is negligible.

5.8.4   Emissions of geothermal power plants

The emissions of the HDR power plant are listed in **Table 5-27**.

Table 5-27:   Emissions in kg/kWh$_{el}$ of the Hot Dry Rock (HDR) system /BMU 2004/

Emissions	HDR
CO$_2$	3.78E-02
CH$_4$	1.03E-04
SO$_2$	6.16E-05
NO$_x$	1.89E-04
Particulates	3.54E-05

5.9   Fossil power plants

In this chapter, several studies on fossil power plants are analysed. First of all, it should be noted that the emissions of the described fossil power plants are estimated but the applied assumptions are different. Also compared to the studies described in the previous chapters the methodology to estimate the emissions is different. They do not represent the average European fossil power plant but are examples of typical power plants. Therefore, the comparison of these technologies has to be treated with caution. However, on the other hand, it is difficult to generate data for an average European power plant as every individual plant has its own process chains generating different emissions at different sites.

5.9.1   ExternE plants

In the 1990s, the ExternE study was performed. **Table 5-28** gives the technical parameters and **Table 5-29** shows the results of four German power plants analysed in /European Commission 1999c/. The studied technologies are

- a coal-fired power plant burning domestic coal (underground coal mining), equipped with electrostatic dust precipitators, flue gas desulphurisation and DENOX;
- a lignite-fired power plant, open pit mining, equipped with electrostatic dust precipitators, flue gas desulphurisation and DENOX;
- an oil fired power plant with gas turbine;
- and a combined cycle natural gas-fired power plant.

They describe the state of the art in the 1990s and are therefore examples of partly still existing technologies.

Table 5-28:   Technical parameters of reference power plants /European Commission 1999c/

Characteristics	Coal	Lignite	Oil	Gas
Plant type	pulverised coal power plant with FGD, DENOX and dedusting	pulverised lignite power plant with FGD and dedusting	gas-turbine peak load power plant	combined cycle
Generator capacity	652.2 MW	887.9 MW	157.2 MW	790.8 MW
Net efficiency	43.0 %	40.1 %	31.1 %	57.6 %
Full load hours per year	6,500 h	6,500 h	675 h	6,500 h
Projected life time	35 a	35 a	35 a	35 a

Table 5-29: Emissions in kg/kWh$_{el}$ of reference power plants /European Commission 1999c/

Emissions	ExternE-Coal	ExternE-Lignite	ExternE-Oil	ExternE-Gas
CO$_2$	8.15E-01	1.05E+00	9.25E-01	3.63E-01
CH$_4$	3.31E-03	2.59E-05	2.45E-05	1.67E-03
SO$_2$	3.26E-04	4.25E-04	1.61E-03	3.25E-06
NO$_x$	5.60E-04	7.90E-04	9.84E-04	2.77E-04
Particulates	1.76E-04	5.10E-04	6.69E-05	1.79E-05

The contributions of the life cycles to the emissions of the respective power plant are given in **Figure 5-88**, **Figure 5-89**, **Figure 5-90** and **Figure 5-91**. All of them do not display the contribution of the construction and end of life phase of the power plant. However, it is described in /BMWA 2004/ that both life cycle phases do not have a significant contribution and therefore they may be neglected.

Figure 5-88 shows that 60 % of the particulates emissions of the analysed coal-fired power plant are caused during the extraction process of the coal. This process is not relevant for the other emissions but they are caused in the transport process and during the electricity generation phase.
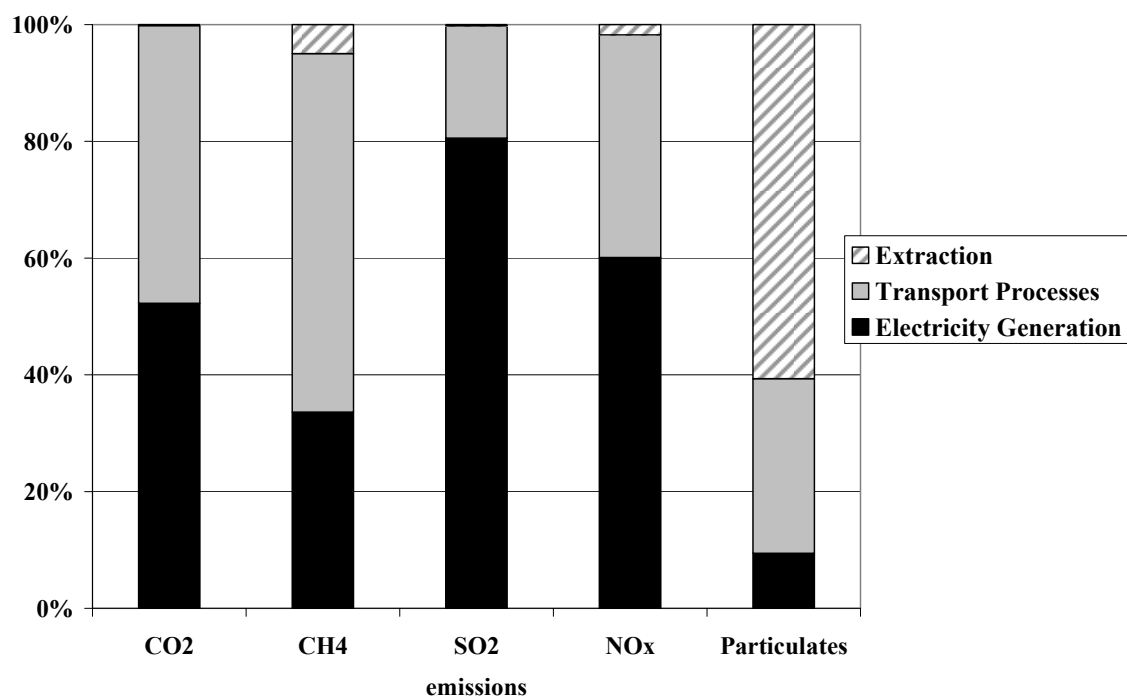
Figure 5-88: Contribution of life cycle phases to the emissions (in kg/kWh$_{el}$) of the coal-fired power plant /European Commission 1999c/
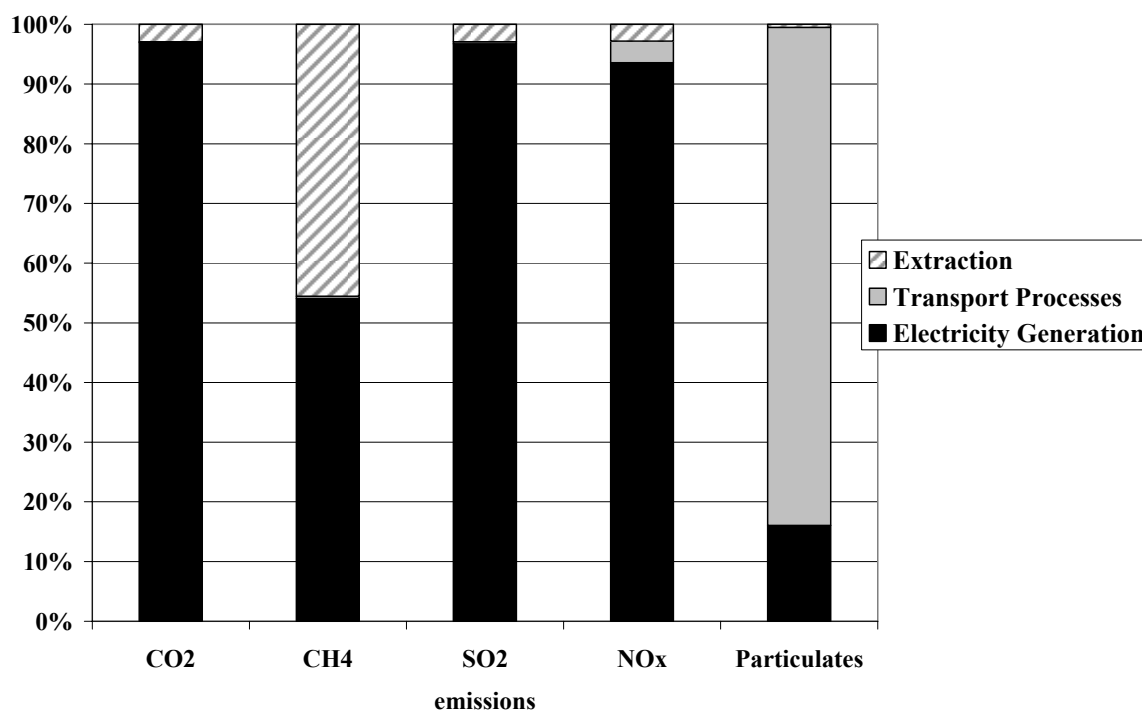
Figure 5-89:   Contribution of life cycle phases to the emissions (in kg/kWh$_{el}$) of the lignite-fired power plant /European Commission 1999c/

Figure 5-89 illustrates that, in contrast to the coal-fired power plant, the lignite-fired power plant does not have significant emissions in the transport process with the exception of 85 % of the total life cycle particulates emissions. This difference results from the short distance between extraction and the combustion site. Lignite-fired power plants are always erected close to the lignite mines because the low energy content of lignite compared to coal makes larger distances economically disadvantageous. The extraction phase is responsible for half of the methane emissions but contributes less than 5 % to the other emissions. All other emissions are caused in the electricity generation phase which contributes more than 90 % to the CO_2, NO_x and SO_2 emissions.

The contribution of the life cycle phases of an oil fired fossil power plant is displayed in **Figure 5-90**. An additional process which is not considered in the other three technologies is the refinery. However, this refinery process does not play an important role. Also the extraction and the transport processes contribute only little, except for 70 % of the particulates emissions. Similar to the lignite-fired power plant the electricity generation process of the oil fired power plant is responsible for the main part of the CO_2 and CH_4 emissions (more than 90 %) as well as the NO_x and SO_2 emissions (more than 75 %).

The fourths technology which is analysed is a gas-fired power plant. The contribution of the different life cycle phases to the emissions is illustrated in **Figure 5-91**. Electricity generation is mainly responsible for the CO_2 and NO_x emissions and the extraction phase is mainly responsible for the CH_4, SO_2 and particulates emissions.
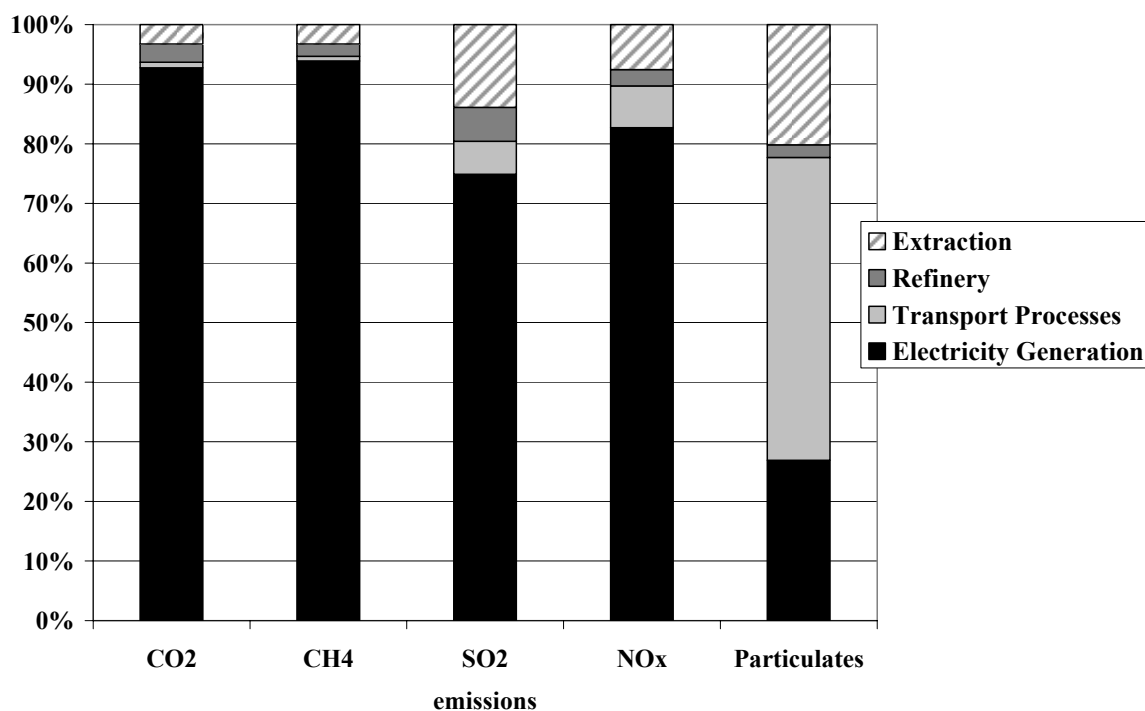
Figure 5-90: Contribution of life cycle phases to the emissions (in kg/kWh$_{el}$) of the oil fired power plant /European Commission 1999c/
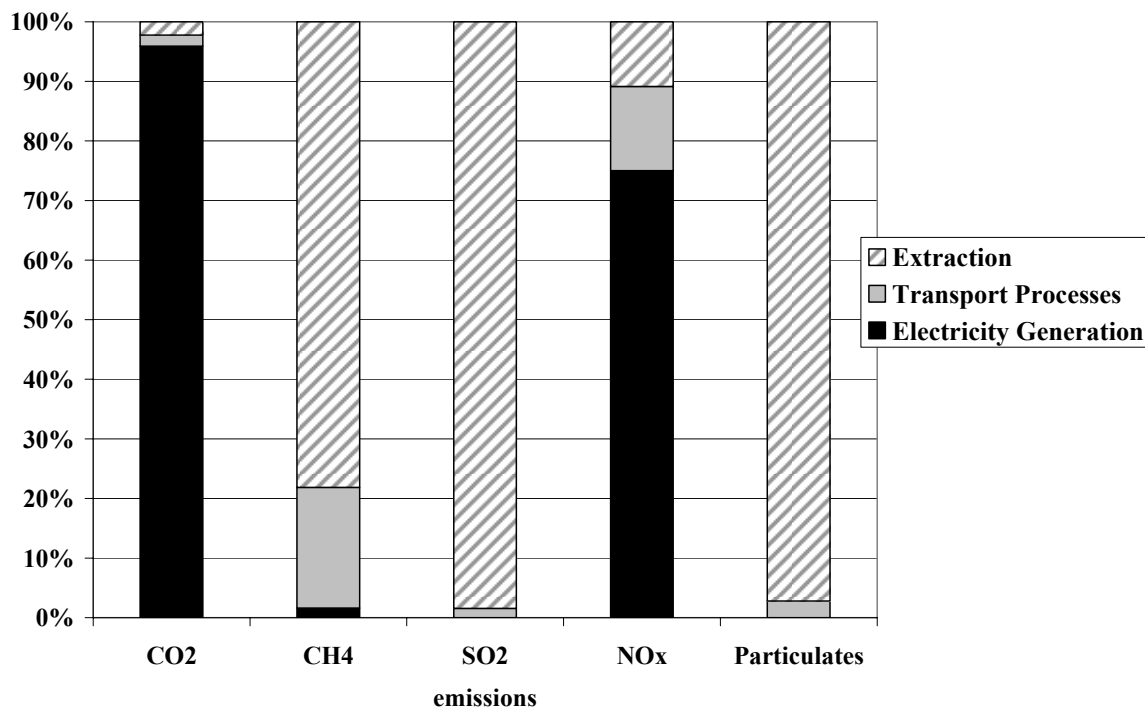
Figure 5-91: Contribution of life cycle phases to the emissions (in kg/kWh$_{el}$) of the gas-fired power plant /European Commission 1999c/

Figure 5-92 gives an overview of the emissions of the four analysed systems. From this figure, it can be derived that the CO_2 emissions of the coal, lignite and the oil fired power plant are quite similar whereas those of the natural gas-fired power plant are only about a half. Also the specific CH_4 and NO_x emissions of the natural gas-fired power plant are about a half of the coal-fired power plant ones. SO_2 and particulates emissions are even far less. The CH_4 emissions of the lignite and the coal-fired power plant are nearly negligible compared to those from the coal-fired one. However, the SO_2 and NO_x emissions are much higher with an outlier of the SO_2 emissions from the oil fired power plant which are nearly four times higher. Also the particulates emissions of the lignite-fired power plant are significantly higher, i.e. the twofold compared to the coal-fired one. Further comparisons with other technologies are performed in the following.
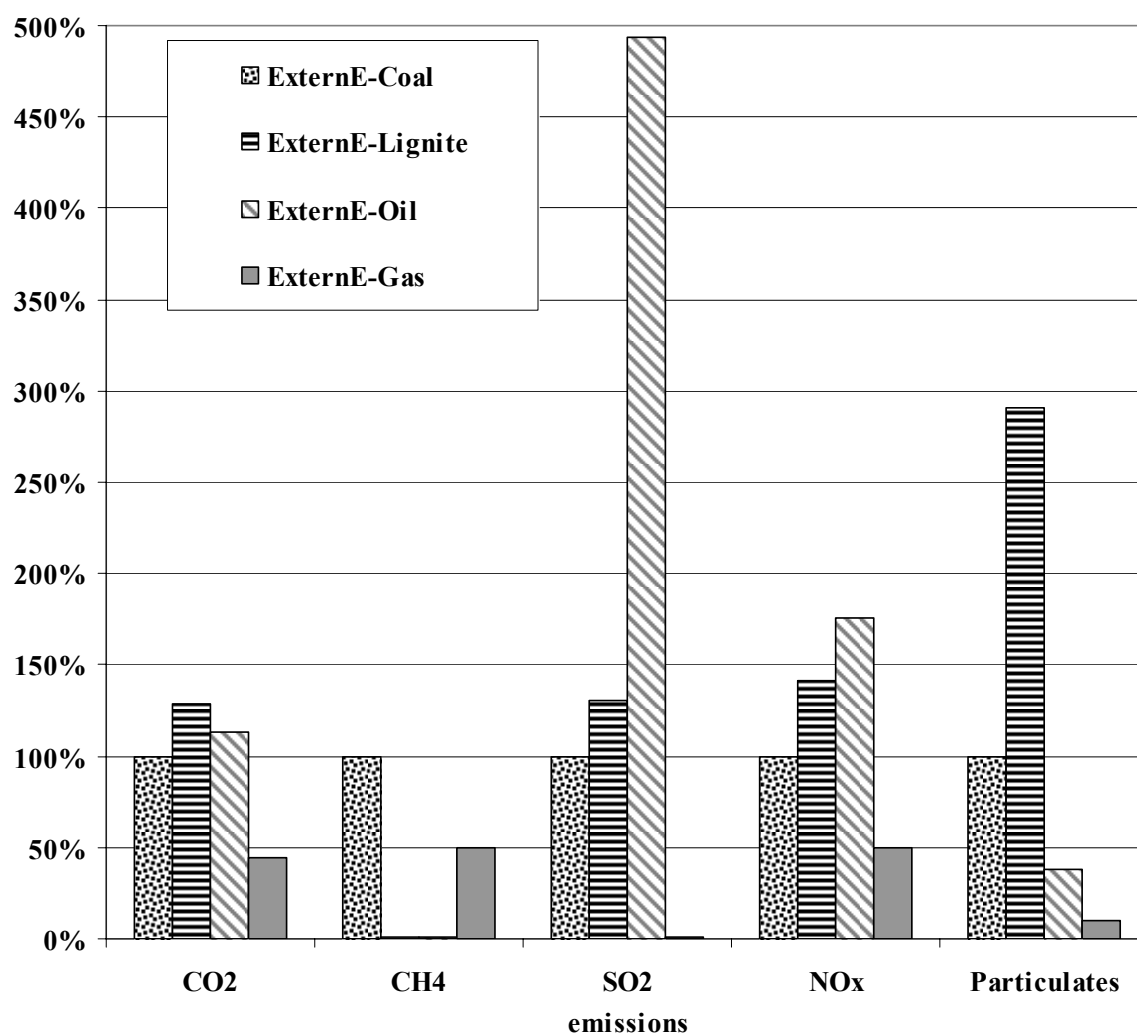
Figure 5-92:   Comparison of the emissions (in kg/kWh$_{el}$) of the fossil power plant in /European Commission 1999c/ relative to the coal-fired power plant

5.9.2   BMWA plants

/BMWA 2004/ studies six different future (year 2010) fossil power plants:

- *Natural gas-fired gas and steam power plant* (NG-GS)
- *Coal-fired steam turbine power plants* (C-ST)
- *Lignite-fired steam turbine power plant with integrated coal dryer* (L-ST)
- *Coal-fired Integrated Gasification Combined Cycle power plants* (C-IGCC)
- *Lignite-fired Integrated Gasification Combined Cycle power plants* (L-IGCC)
- *Coal-fired pressurized circulating fluidised bed (CFB) power plant* (C-CFB)

All six fossil power plants are assumed to have a life time of 35 years and annual 7,500 full load hours. The other technical parameters are given in **Table 5-30**.

Natural gas-fired gas and steam power plant (NG-GS):

Today's gas and steam power plants have electrical efficiencies of ca. 58 %. Besides this high efficiency gas and steam power plants have further advantages. No flue gas reduction is required and thus the specific plant costs are lower than those of other fossil-fired power plants. The environmental impacts are comparably low due to high efficiencies and low fuel specific emissions. In /BMWA 2004/ future configurations are estimated. It is a power plant with two gas turbines and one steam turbine.

The emissions are listed in **Table 5-31**. From all life cycle phases, the operation contributes more than 90 % of the respective emissions. Within the life cycle phase operation, the emissions are mainly caused by direct emissions and the upstream process natural gas supply. The direct emissions contribute ca. 90 % to the CO_2 and ca. 75 % to the NO_x of the operation emissions, whereas the natural gas supply contributes more than 90 % to the CH_4 and SO_2 emissions.

Usually, gas and steam power plants are not used for base load power generation so that their annual full load hours are significantly lower. The specific emissions in the operation phase are relatively independent from the full load hours but the specific emissions due to construction and end of life increase with decreasing full load hours. Since the operation phase contributes by far the most emissions in the life cycle, the specific emissions increase less than 5 % with the reduction to half of the initial 7,500 full load hours.

Coal-fired steam turbine power plants (C-ST):

Present coal-fired power plants have electrical net efficiencies of 42-43 %. In /BMWA 2004/ it is assumed on the basis of actual research activities that it may be improved up to 47 % until 2010.

The contribution of the operation phase to the emissions (listed in **Table 5-31**) is similar to that of the gas and steam power plant. Nearly all emissions are caused in the operation phase. Within the operation phase, the direct emissions and the coal supply are producing nearly all emissions. 90 % of the CO_2 emissions are caused by direct emissions as well as 50 % of the SO_2 and 60 % of the NO_x emissions. The other part of the emissions is mainly caused by coal supply, which is responsible for nearly all of the CH_4 emissions in the operation phase. Coal-fired power plants are usually not used for base load so that the full load hours may be less. However, this will not change the specific emissions significantly because the contribution of construction and end of life of the power plant may be neglected.

Lignite-fired steam turbine power plant with integrated coal dryer (L-ST):

At present, lignite-fired power plants have efficiencies of 45 %. With improved drying processes, e.g. fluidised bed drying with rejected heat, higher efficiencies may be achieved. The projected power plant is assumed to have an efficiency of 50 % in the year 2010.

Similar to the previously described technologies, the operation phase contributes more than 90 % to the life cycle emissions of the power plant. Within the operation phase, more than 90 % of the CO_2, SO_2 and NO_x emissions are direct emissions whereas the CH_4 emissions are caused with about 70 % by direct emissions and about 20 % by lignite supply.

A sensitivity analysis concerning the full load hours shows that the specific emissions do not change significantly as in the cases above.

Coal-fired Integrated Gasification Combined Cycle (IGCC) power plants (C-IGCC):

The highest efficiencies are achieved with gas and steam turbines. However, the fuel is restricted to gas. Solid fuels must be gasified and cleaned in order to be usable for gas turbines. However, the cleaning process can not be performed with the high temperatures of the gas leaving the gasifier. Therefore, it is cooled down and then cleaned from particulates and sulphur components. This is achieved in IGCC power plants by gasification of the coal. The projected efficiency for the year 2010 is 51.5 %. Beside the gasification of coal, also other fuels may be gasified, e.g. lignite and biomass.

Again, the distribution of the life cycle emissions is by more than 90 % caused in the operation phase. Within the operation phase the emissions are by more than 90 % caused by coal supply and direct emissions. The direct emissions contribute 90 % to the CO_2 emissions but only 30 % to the SO_2 emissions. The main part of CH_4 emissions is caused by coal supply which also contributes more than 60 % to the SO_2 and NO_x emissions.

The sensitivity analysis concerning the full load hours shows that the specific emissions do not change significantly.

Lignite-fired Integrated Gasification Combined Cycle (IGCC) power plants (L-IGCC):

The C-IGCC technology is also usable for lignite. Again, more than 90 % of the life cycle emissions are caused in the operation phase and within the operation phase more than 90 % are caused by lignite supply and direct emissions. However, within the operation phase the contributions differ from the C-IGCC technology. Direct emissions contribute more than 90 % to the CO_2, SO_2 and NO_x emissions as well as 65 % to the CH_4 emissions. The remaining part is mainly emitted in the lignite supply phase.

This technology also has no significant changes of specific emissions if the full load hours are reduced by 50 % or even more.

Coal-fired pressurized circulating fluidised bed (CFB) power plant (C-CFB):

This technology also uses a combination of gas and steam turbines. First of all, the fuel is combusted in a pressurized CFB. Besides coal, also other fuels may be combusted. The hot flue gas is cleaned from particulates and than relaxed in a gas turbine. Afterwards the flue gas flows through a heat recovery boiler which generates water steam for the steam turbine. In order to reduce the sulphur content and thus SO_2 emissions, the coal dust gets the additive limestone. Relatively low temperatures reduce the NO_x emissions. The projected efficiency for the year 2010 is assumed to be 48 %.

The distribution of the life cycle emissions are by more than 90 % caused in the operation phase. Within the operation phase, the emissions are by more than 90 % caused by coal supply and direct emissions. The direct emissions contribute 90 % to the CO_2 emissions but only 50 % to the SO_2 and 60 % to the NO_x emissions. Nearly all CH_4 emissions are caused by coal supply which also contributes nearly the rest to the other emissions.

This technology also has no significant changes of the considered specific emissions if the full load hours are reduced by 50 % or even more.

Table 5-30:   Technical parameters of fossil power plants in /BMWA 2004/

Parameter	NG-GS	C-ST	L-ST	C-IGCC	L-IGCC	C-CFB
Electrical net capacity (MW$_{el}$)	816.8	600	1,050	451	451	450
Net efficiency	60 %	47 %	50 %	51.5 %	51.5 %	46 %

Table 5-31: Emissions in kg/kWh$_{el}$ of fossil power plants in /BMWA 2004/

Emissions	NG-GS	C-ST	L-ST	C-IGCC	L-IGCC	C-CFB
CO$_2$	3.77E-01	7.92E-01	8.30E-01	7.23E-01	8.07E-01	8.07E-01
CH$_4$	4.98E-04	1.85E-03	1.59E-04	1.69E-03	6.20E-05	1.88E-03
SO$_2$	1.00E-04	1.05E-03	6.29E-04	6.69E-04	6.22E-04	1.07E-03
NO$_x$	3.91E-04	9.10E-04	6.26E-04	5.01E-04	4.29E-04	9.11E-04
Particulates	1.40E-05	3.37E-04	4.18E-04	3.07E-04	4.04E-04	3.44E-04
NMVOC	8.40E-05	1.34E-04	3.70E-05	1.15E-04	3.50E-05	1.27E-04
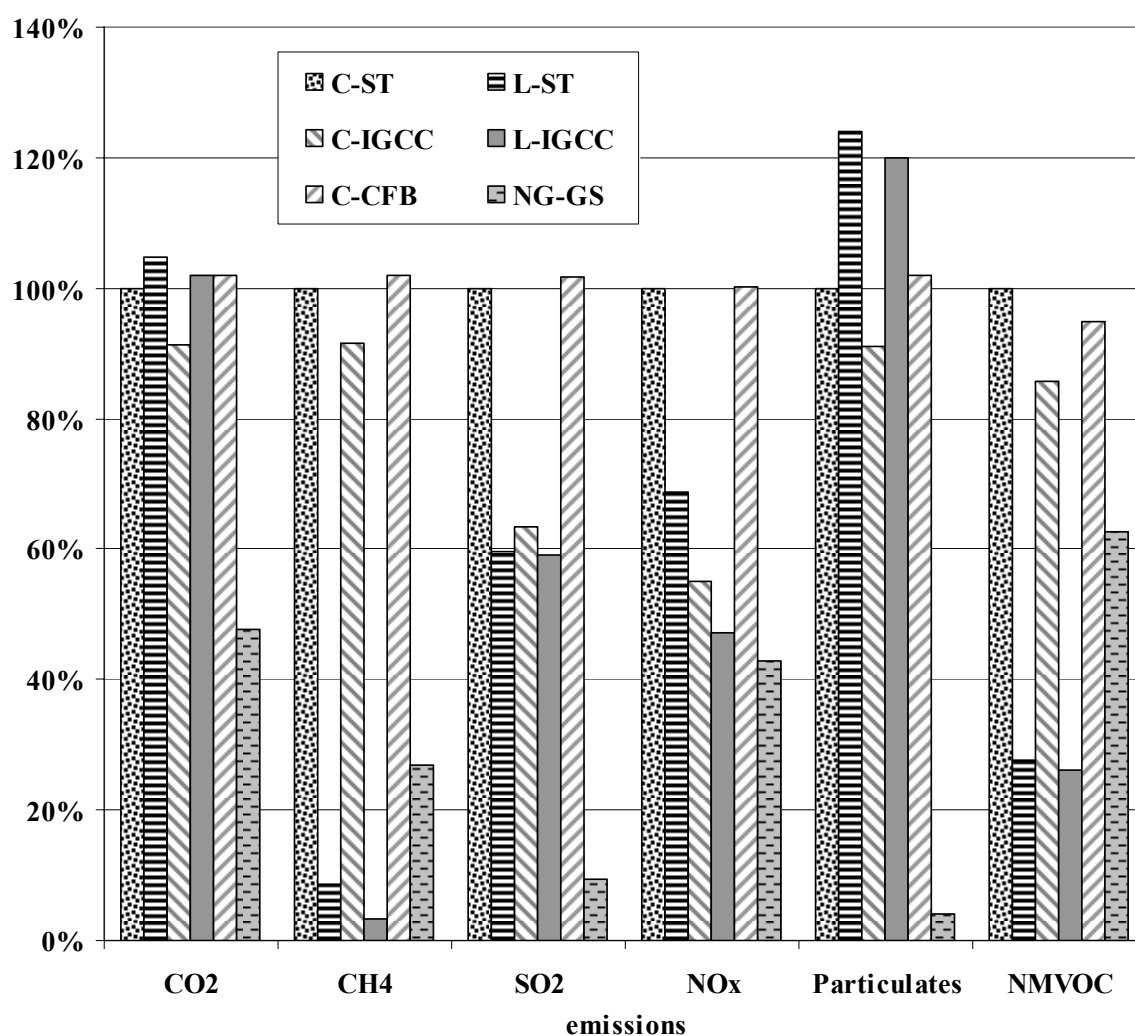
Figure 5-93: Comparison of the emissions (in kg/kWh$_{el}$) of the fossil power plants studied in /BMWA 2004/ in relation to the coal-fired power plant with steam turbine

The comparison of the studied fossil power plants in /BMWA 2004/ is illustrated in **Figure 5-93**. It shows that the CO$_2$ and particulates emissions of the coal and lignite-fired

power plants are quite similar. The exception is the natural gas-fired gas and steam turbine which causes only about 50 % of the CO_2 and 5 % of the particulates emissions compared to the other ones. A significant variation is estimated for the CH_4 and NMVOC emissions which are quite similar for all three coal-fired power plants. However, the lignite-fired power plants have significantly lower emissions of this type and the NG-GS system has emissions in between. The SO_2 and NO_x emissions are similar from the C-ST and the C-CFB system but about 40 % lower in case of the L-ST, C-IGCC and L-IGCC systems. For both emissions, the natural gas-fired power plant has the lowest emissions.

5.9.3   FfE plants

In /FfE 1999/, the *Forschungsstelle für Energiewirtschaft e.V.* (FfE) analyses the emissions occurring in the life cycle of a coal, lignite, natural gas and nuclear power plant. Some technical parameters of the studied power plants are listed in **Table 5-32** and the emissions in **Table 5-33**. All four power plants have a technological state of the mid 1990s in Germany.

Table 5-32:   Technical parameters of fossil power plants in /FfE 1999/

Parameter	FfE-Coal	FfE-Lignite	FfE-Gas	FfE-Nuclear
Electrical net capacity (MW$_{el}$)	509	929	348	1,330
Net efficiency	43 %	43 %	58 %	34 %
Full load hours	5,000 h/a	7,500 h/a	7,000 h/a	7,700 h/a
Life time	40 a	40 a	30 a	40 a

Table 5-33:   Emissions in kg/kWh$_{el}$ of fossil power plants in /FfE 1999/

Emissions	FfE-Coal	FfE-Lignite	FfE-Gas	FfE-Nuclear
CO_2	9.42E-01	1.19E+00	5.17E-01	1.08E-02
CH_4	4.93E-03	5.30E-05	1.49E-03	3.60E-05
SO_2	6.95E-04	4.78E-04	5.20E-05	1.40E-05
NO_x	5.47E-04	7.48E-04	9.01E-04	1.62E-05
Particulates	3.20E-05	9.00E-05	5.70E-05	1.00E-06
NMVOC	3.90E-05	2.10E-05	7.70E-05	1.30E-06

The coal-fired power plant has dust, NO_x and SO_2 removal whereas the lignite-fired power plant has only dust and SO_2 removal. While the former one operates at mid load with 5,000 full load hours per year which are not all operated at full load, the latter one operates at base

load with 7,500 full load hours per year. The life time of both power plants is assumed to be 40 years. In contrast, the natural gas-fired power plant is estimated to have a life time of 30 years. It is a gas and steam turbine power plant with a net efficiency of 58 %. The analysed nuclear power plant is a pressurised water reactor with an electrical net capacity of 1,330 MW.
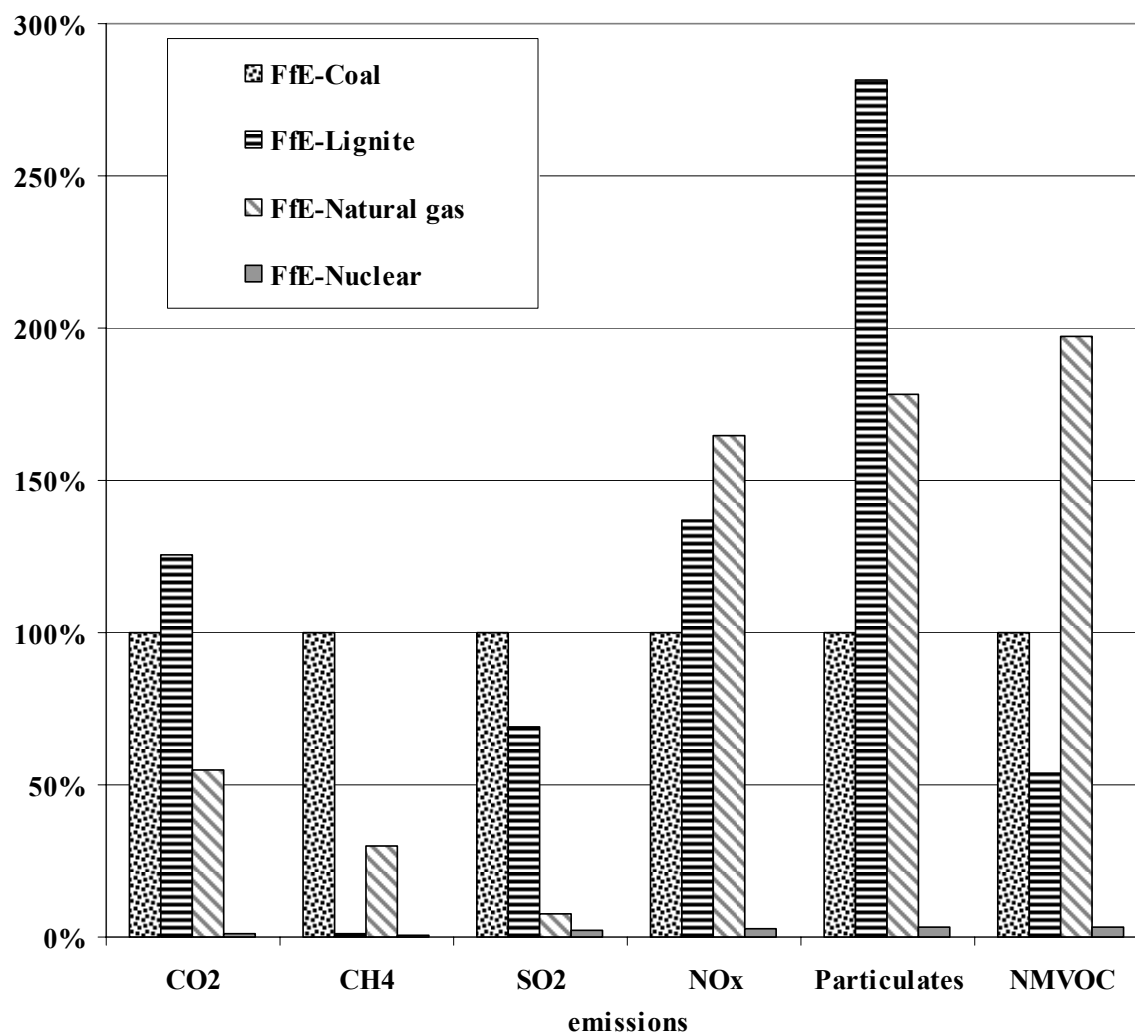
Figure 5-94: Comparison of the emissions (in kg/kWh$_{el}$) from the analysed fossil power plants with relation to the coal-fired power plant /FfE 1999/

5.9.4   Gas-fired CHP plants

/Briem 2003/ analysed gas-fired CHP plants in the ECLIPSE study. Since they only use natural gas, they are described in the chapter of fossil power plants. For small scale applications in the range of some hundred kW up to a few MW, technologies are required which provide acceptable high efficiencies even at low capacities and low investment costs. Today, especially internal combustion engines match these requirements. /Briem 2003/ describes the thermodynamic cycle of four phases which is used by internal combustion engines. Firstly, a

compressed mixture of air and fuel is burned in a cylinder. Secondly, the produced heat increases the pressure within the cylinder and the flue gas expands by pushing a piston to increase the cylinder's volume. A crankshaft converts this translatoric move of the piston into a rotation. In the next stroke, the rotating crankshaft presses back the piston and the flue gas is released out of the cylinder through an outlet valve. Thirdly, the piston is pulled down and a fresh mixture of air and fuel flows through an inlet valve into the cylinder. In the last stroke, the crankshaft pushes the piston into the top of the cylinder and compresses the gas again so that the cycle is closed. The crankshaft is connected to the drive shaft of a generator which produces electricity. In stationary applications with CHP, the produced heat is recovered from the flue gas, the engine's cooling water and the lubricant oil by heat exchangers. This heat is provided as useful energy for heating purposes. Generally, a large variety of gaseous and liquid fuels can be used in internal combustion engines, e.g. natural gas and biogas. However, /Briem 2003/ only considers internal combustion engines fuelled with natural gas.

In the study at hand, a stand-alone plant which is currently available (Gas-engine present) as well as a future system estimated for 2010 which has a higher efficiency and improved emission reduction (Gas-engine future) are analysed. Both system have a gas-fired peak-load boiler and a storage tank in order to secure heat supply, an outflow temperature of 65 °C, a return flow temperature of 40 °C, an ambient temperature of 0 °C, a technical lifetime of 15 years, and a transformator which transforms the produced electricity at 400 V AC to a voltage level of 20 kV. The system specific technical parameters are given in **Table 5-34**.

Table 5-34:   Technical parameters of selected examples of natural gas-fired CHP systems from /Briem 2003/

Parameter	Gas-engine present	Gas-engine future
Electrical net capacity	2,100 kW	420 kW
Thermal capacity	12,223 kW	2,858 kW
Heat production	16,799 MWh/a	2,774 MWh/a
Electricity production	10,733 MWh/a	2,100 MWh/a
Total fuel consumption	31,881 MWh/a	5,417 MWh/a
Electrical engine efficiency (net)	36 %	43 %
Electrical full load operating hours	5,111 h/a	5,000 h/a
Allocation factor for electricity	76.9 %	79.8 %
Engine type	16 cylinder, Otto-cycle	diesel stroke engine
Emission control	lean burn engine, oxidation catalyst	3-way-catalyst, cooled flue gas recirculation
Technology level	available	2010

The operation phase is the life cycle phase which causes most of the emissions. It is responsible for nearly all greenhouse gas emissions and more than 90 % of the NO_x emissions. SO_2, particulates and NMVOC emissions are with 60-80 % caused in this phase.

Table 5-35: Emissions in kg/kWh$_{el}$ of natural gas-fired CHP systems /Briem 2003/

Emissions	Gas-engine present	Gas-engine future
CO₂	5.37E-01	4.98E-01
CH₄	3.07E-03	2.67E-03
SO₂	3.07E-04	3.78E-04
NOₓ	7.93E-04	3.15E-04
Particulates	3.90E-05	4.70E-05
NMVOC	3.44E-04	5.23E-04
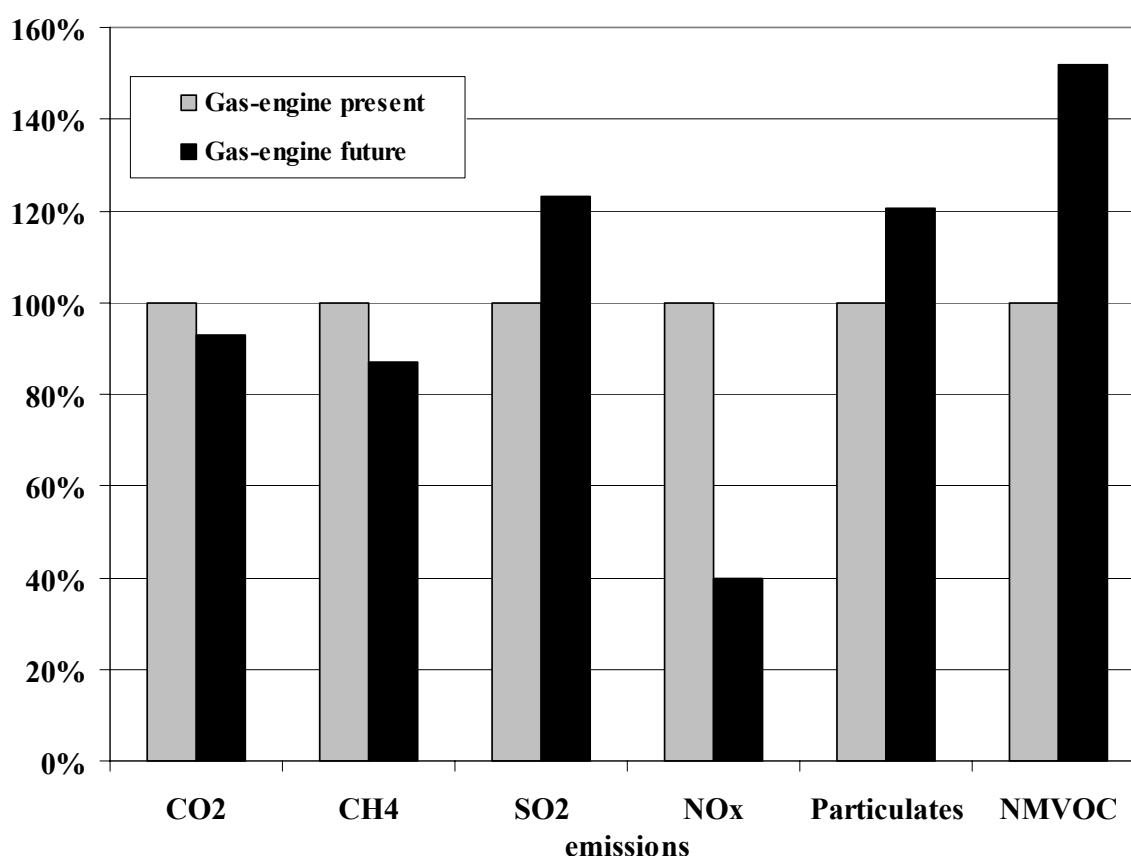
Figure 5-95: Comparison of the emissions (in kg/kWh$_{el}$) from the present and future natural gas-fired CHP plants in relation to the present one

/Briem 2003/ also performs a sensitivity analysis with an alternative allocation method. The allocation based on the alternative production method takes into account technologies which could alternatively be used. However, the alternative production method does not con-

sider the thermo dynamical quality. With this alternative allocation method, the allocation factor for electricity is 60.2 % for the present system and 61.3 % for the future system resulting in 22 % and 23 % lower specific emissions.

The emissions of the two systems are given in **Table 5-35** and compared in **Figure 5-95**. The comparison shows that the future natural gas-fired CHP plant has lower greenhouse gas emissions and 60 % reduced NO_x emissions but higher SO_2, particulates and NMVOC emissions. This shows that the improved efficiency and NO_x reduction with cooled flue gas recirculation has the desired results. Altogether, the comparison shows no clear ranking. The estimation of the external costs in chapter 6 may solve this problem.

5.9.5   Comparison of the different technologies

In the following paragraphs, similar technologies analysed in the described studies are compared directly in order to give an imagination about the variability of technological configurations and assumptions which result in different LCI data.

Comparison of the coal-fired power plants:

The coal-fired power plants analysed in /European Commission 1999c/ (ExternE study) and /FfE 1999/ consider a similar technological state. While CO_2, CH_4 and SO_2 emissions of the FfE-Coal plant are higher, the NO_x and particulates emissions are lower than those of the ExternE-Coal plant (see **Figure 5-96**). In comparison, the future plant technologies which are analysed in /BMWA 2004/ do have lower CH_4 emissions due to the upstream processes described above but they also have slightly lower CO_2 emissions. With the exception of NO_x emissions from the C-IGCC plant, SO_2, NO_x and particulates emissions are even higher compared to the former studies which analyse older plants.
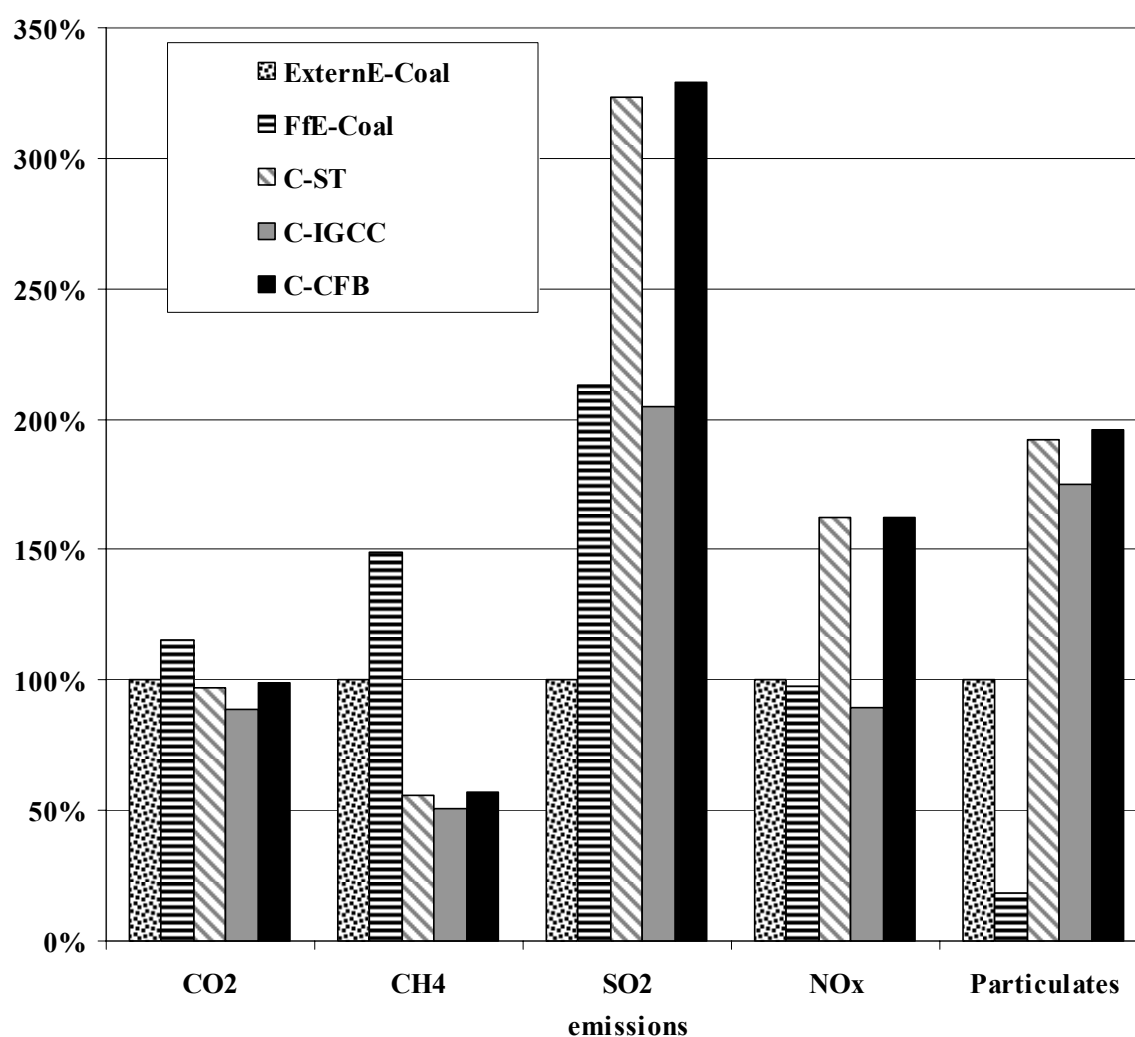
Figure 5-96:   Comparison of the emissions (in kg/kWh$_{el}$) from the coal-fired power plants analysed in /European Commission 1999c/, /BMWA 2004/ and /FfE 1999/ with relation to the ExternE-Coal

Comparison of the lignite-fired power plants:

The lignite-fired power plants analysed in /European Commission 1999c/ (ExternE study) and /FfE 1999/ consider a similar technological state but they differ significantly in the case of CH_4 and particulates emissions (see **Figure 5-97**). On the one hand, the future technologies analysed in /BMWA 2004/ have lower emissions in the case of CO_2, NO_x and particulates emissions compared to the older technologies. On the other hand, CH_4 and SO_2 emissions are higher.
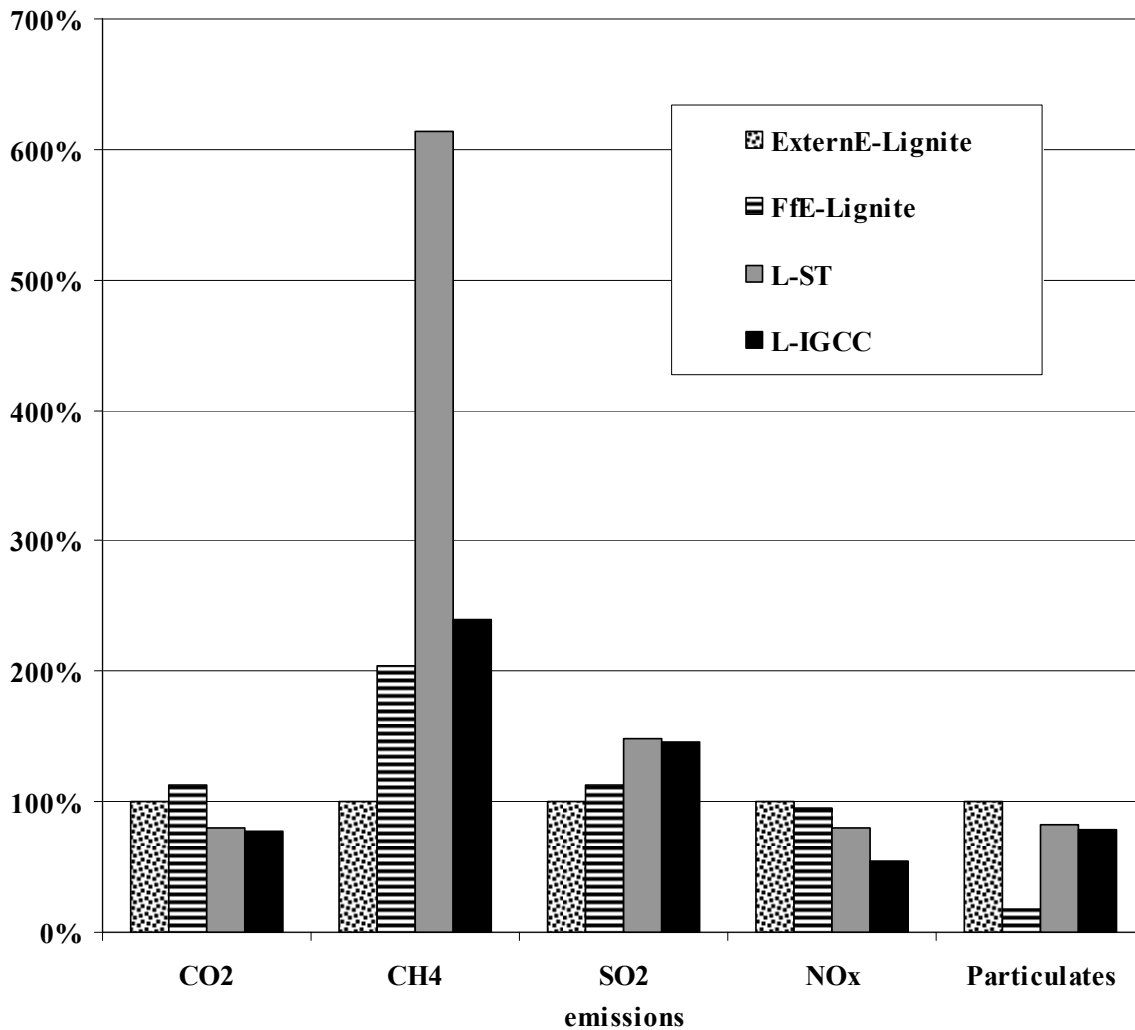
Figure 5-97:   Comparison of the emissions (in kg/kWh$_{el}$) from the lignite-fired power plants analysed in /European Commission 1999c/, /BMWA 2004/ and /FfE 1999/ with relation to the ExternE-Lignite

Comparison of the natural gas-fired power plants:

The natural gas-fired power plants analysed in /European Commission 1999c/ (ExternE study) and /FfE 1999/ consider a similar technological state but they differ significantly in the case of SO_2, NO_x and particulates emissions (see **Figure 5-98** and **Figure 5-99**). On the one hand, the future technology analysed in /BMWA 2004/ (NG-GS) have lower emissions in case of CH_4 and particulates emissions compared to the older technologies. On the other hand, SO_2 emissions are extremely higher.
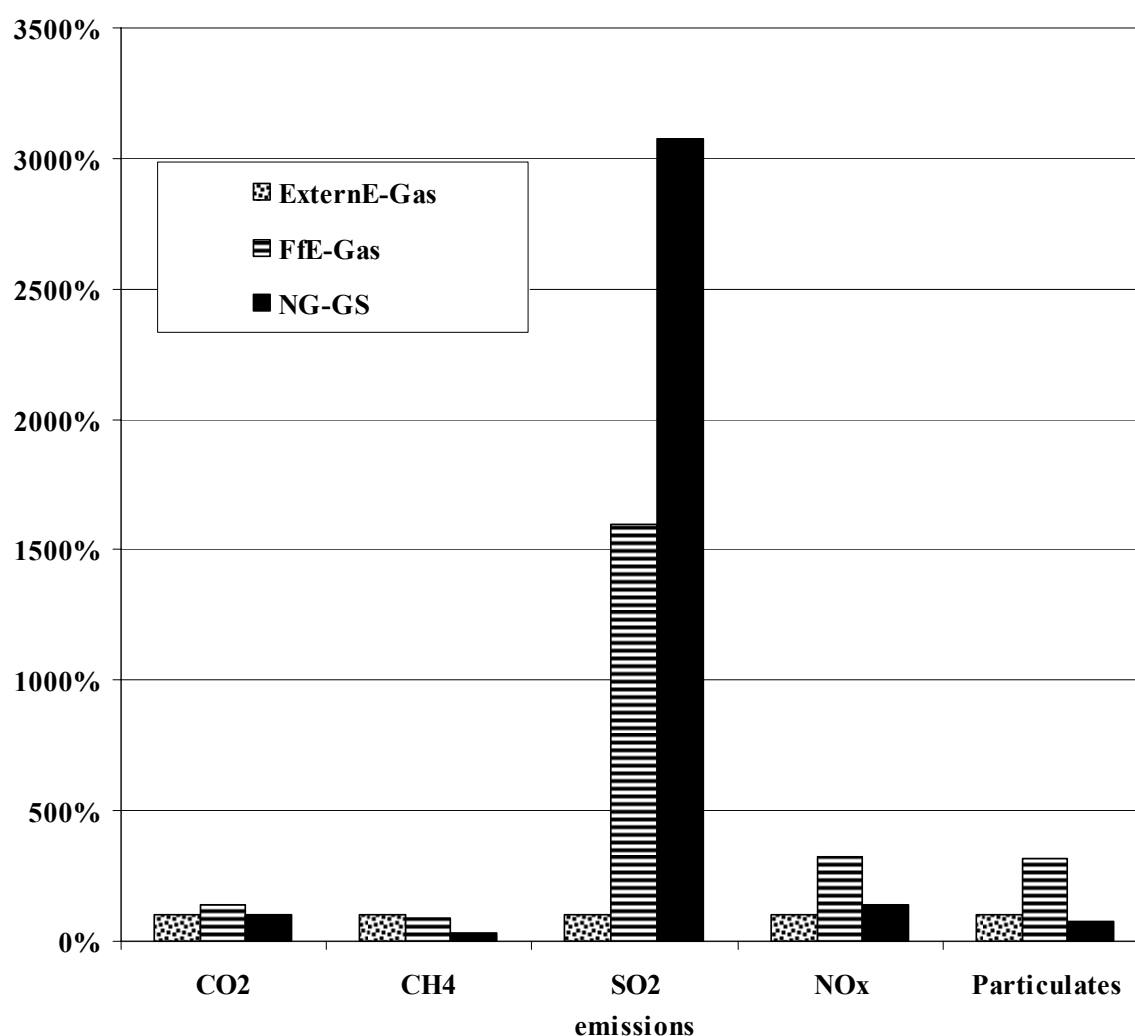
Figure 5-98: Comparison of the emissions (in kg/kWh_{el}) from the natural gas-fired power plants analysed in /European Commission 1999c/, /BMWA 2004/ and /FfE 1999/ (with SO_2) with relation to the ExternE-Gas
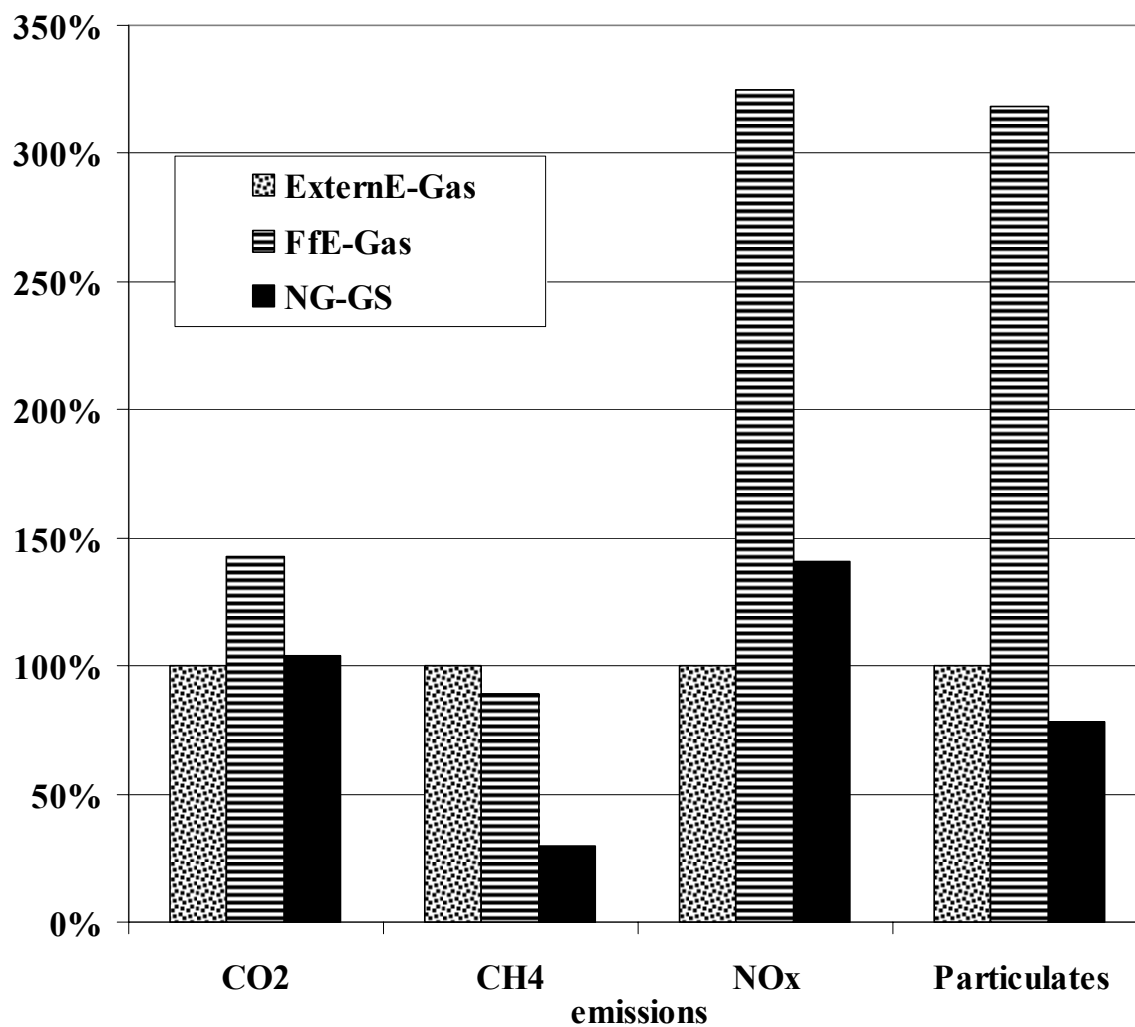
Figure 5-99:   Comparison of the emissions (in kg/kWh$_{el}$) from the natural gas-fired power plants analysed in /European Commission 1999c/, /BMWA 2004/ and /FfE 1999/ (without SO$_2$) with relation to the ExternE-Gas

6   Environmental external costs

The previous chapter describes different technologies and gives a LCI for the emissions of the considered power plants. However, the comparison of the emissions of the technologies does not enable to rank the technologies with regard to the extent of their impact towards environment and human health. Using the damage factors displayed in **Table 3-1** and avoidance costs listed in **Table 4-7** it is possible to compare the technologies with regard to their external costs. **Table 6-1** summarizes the factors of damage and avoidance costs for emissions used for the estimation of the external costs in this chapter.

Table 6-1:   Factors of damage and avoidance costs for emissions ($€_{2003}$/kg)

Emissions	Lower estimate	Damage factor	Upper estimate
CO_2	0.075	0.150	0.225
CH_4	1.725	3.450	5.175
SO_2	0.937	3.750	7.499
NO_x	0.804	3.214	6.429
PM10	20.141	28.774	37.406
NMVOC	1.196	1.196	1.196

Table 6-2:   Links to the corresponding chapter

Abbreviation	For	Chapter
PV	Photovoltaic systems	Chapter 5.1
WT	Wind turbine systems	Chapter 5.2
SOFC, PEFC, PAFC	Fuel cell systems	Chapter 5.3
BF	Bio-fuelled CHP systems	Chapter 5.4
BM	Biomass systems	Chapter 5.5
Water	Water power	Chapter 5.6
ST	Solar thermal power	Chapter 5.7
GT	Geothermal	Chapter 5.8
Fossil	Fossil power plants	Chapter 5.9

The technologies which are compared in the following figures are displayed with abbreviations. **Table 6-2** lists these abbreviations which are in front of each technology and refers to the corresponding chapter where the life cycle analysis of the technology is performed.

Since many technologies are compared, it is not possible to compare them all in the same figure. Therefore, the following figures are divided into two parts. One part shows the non-fossil-fuelled technologies which have less than 4 €-Cent/kWh$_{el}$ external costs with the upper estimate (**Figure 6-1**, **Figure 6-2** and **Figure 6-3**) whereas the other part shows the fossil-fuelled technologies which have higher external costs with the exception of nuclear power plants (**Figure 6-4**, **Figure 6-5** and **Figure 6-6**). It should be noted that the figure of the different parts do also have different scales for the external costs.

Figure 6-1 and **Figure 6-4** show the range of the external costs. The grey bar displays the lower estimate and the sum of the grey and the black bar displays the upper estimate so that the black bar illustrates the range of the external costs. In order to show the contribution of the different emissions to the external costs, **Figure 6-2** and **Figure 6-5** illustrate the contribution of the emissions to the total external costs. The filled parts of the bars display the lower estimate of the external costs caused by the emissions while the striped parts of the bars display the range between the lower and upper estimate. Finally, **Figure 6-3** and **Figure 6-6** illustrate the contribution of the respective emissions to the external costs in percentage values. It should be noted that present and future technologies are mixed and directly compared. This seems possible regarding the uncertainties in these estimations. In the following chapters, future technologies are extracted and analysed in more detail.

Figure 6-1 displays the external costs of renewable energy systems. The lowest external costs are caused by wind turbine systems and water power plants (0.03-0.48 €-Cent/kWh$_{el}$). In contrast, the highest external costs arise from the power generation by bio-fuelled CHP systems (0.77-3.79 €-Cent/kWh$_{el}$) analysed in /BMWA 2004/. However, similar technologies analysed in the ECLIPSE study do have significantly lower external costs (0.26-1.47 €-Cent/kWh$_{el}$). The reason for this difference is not analysed in the study at hand but it is recommended to analyse it in further research. The other CHP technology lies in the same range. While biogas-fired SOFCs cause comparably low external costs (0.33-0.99 €-Cent/kWh$_{el}$) hydrogen fired SOFCs cause comparably high external costs (0.95-2.56 €-Cent/kWh$_{el}$). The external costs of hydrogen fired SOFCs are mainly contributed by old data for wind turbine systems generating electricity for the hydrogen supply. Therefore, an update of these data seems necessary. Similar external costs are caused by biomass systems (0.34-2.30 €-Cent/kWh$_{el}$). Comparably lower external costs arise from the geothermal HDR power plant (0.39-1.20 €-Cent/kWh$_{el}$) and solar thermal parabolic-trough power plant (0.20-0.55 €-Cent/kWh$_{el}$). PV systems show a significant variance between future and present technologies as well as between plant sites in Germany and Spain. While present PV systems in Germany have external costs of 0.67-2.44 €-Cent/kWh$_{el}$ future PV systems in Spain have far lower external costs of 0.05-0.21 €-Cent/kWh$_{el}$ which is even in the range of wind turbine systems and water power plants.

Figure 6-2 and **Figure 6-3** illustrate the contribution of the respective emissions to the external costs. Greenhouse gas emissions contribute by far the main part (39-86 %) of the ex-

ternal costs of renewable energy systems. The largest contribution of greenhouse gases with 64-86 % occurs for PV systems, wind turbine systems and water power plants. NMVOC emissions contribute 0-1 % to the external costs and are thus nearly negligible. Therefore, it is acceptable that no NMVOC emission data are available for the geothermal power plant, the solar thermal parabolic-trough power plant, the river power plants and the bio-fuelled CHP systems analysed in /BMWA 2004/. In contrast, the missing values of particulates emissions in the case of the water reservoir power plant as well as the low quality of particulates emissions in the analysed studies is a more severe problem because particulates emissions have a contribution of 6-28 % to the external cost which can not be neglected. A contribution of the particulates emissions of more than 20 % arises in the case of the parabolic-trough system, the water river plants as well as the biogas and hydrogen fired SOFCs. SO_2 emissions only contribute 3-13 % to the external costs. Therefore, they do not need an as intensive analysis as the NO_x emissions which contribute up to 42 %. NO_x emissions from technologies using biomass have the highest contribution of 16-42 % while the NO_x emissions from the other technologies only have a contribution of 4-12 %.

Figure 6-4 shows the range of the external costs of fossil-fuelled power plants. The outlier is the nuclear power plant with external costs of 0.09-0.29 €-Cent/kWh$_{el}$ which is in the range of water power plants and wind turbine systems. All other displayed technologies have external costs which exceed 3 €-Cent/kWh$_{el}$. Co-combustion of biomass can not be used for direct comparison because the respective coal-fired power plant which is used has to be analysed, too. This comparison is not performed in /Cuperus 2003/. However, it is discussed in chapter 5.5 that co-combustion reduces the emissions and thus the external costs as can be seen in Figure 6-4 which also compares 10 % co-combustion and 20 % co-combustion. The external costs are reduced by 11 % in the case of 20 % co-combustion instead of 10 % co-combustion. Nevertheless, co-combustion technology has external costs of 7.91-26.87 €-Cent/kWh$_{el}$ due to the coal-fired power plant which still combusts coal. The natural gas-fired fuel cells have external costs of 3.37-14.67 €-Cent/kWh$_{el}$ which are much higher than those of the biogas or hydrogen fired ones. Since fuel cells are CHP power plants they should be compared to bio-fuelled CHP systems and the gas engines studied in /Briem 2003/. The comparison leads to the result that natural gas-fired engines have the highest external costs of 4.41-14.60 €-Cent/kWh$_{el}$. They are even higher than those from natural gas-fired power plants which are in the range of 2.99-13.24 €-Cent/kWh$_{el}$. The oil fired power plant has external costs in the range of coal and lignite-fired power plants with a range of 6.45-27.98 €-Cent/kWh$_{el}$. The lower estimate of coal and lignite-fired power plants is from the future IGCC plants.

Figure 6-5 and Figure 6-6 illustrate that 88-97 % of the external costs are caused by the greenhouse gas emissions due to fossil fuels. The contribution of only 76 % is an exception for the co-combustion technologies which also combust biomass.
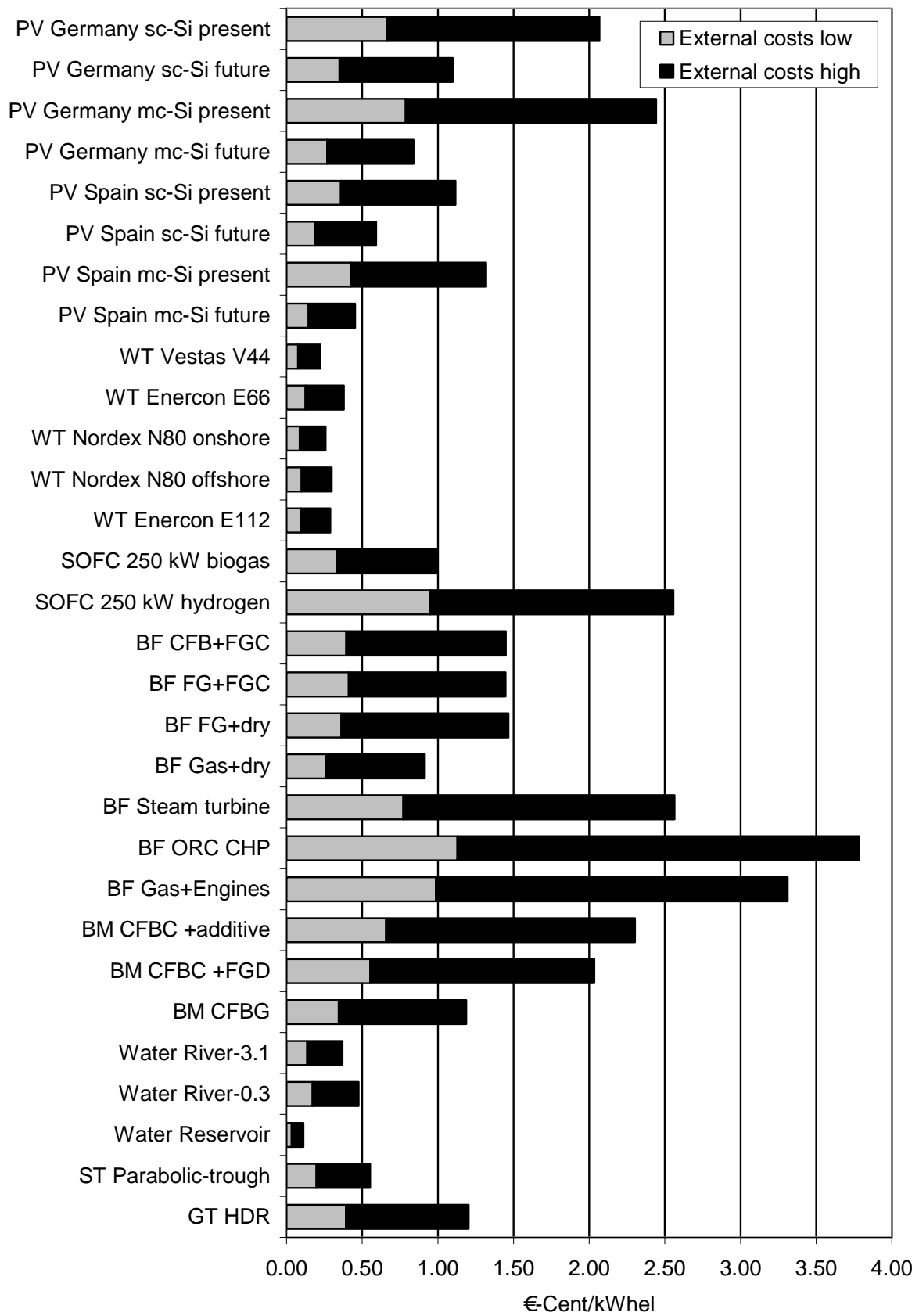
Figure 6-1:   External costs of non-fossil-fuelled power plants (in ϵ_{2003}-Cent/kWh$_{el}$)

Figure 6-2: External costs of non-fossil-fuelled power plants in detail (in €_{2003}-Cent/kWh$_{el}$)
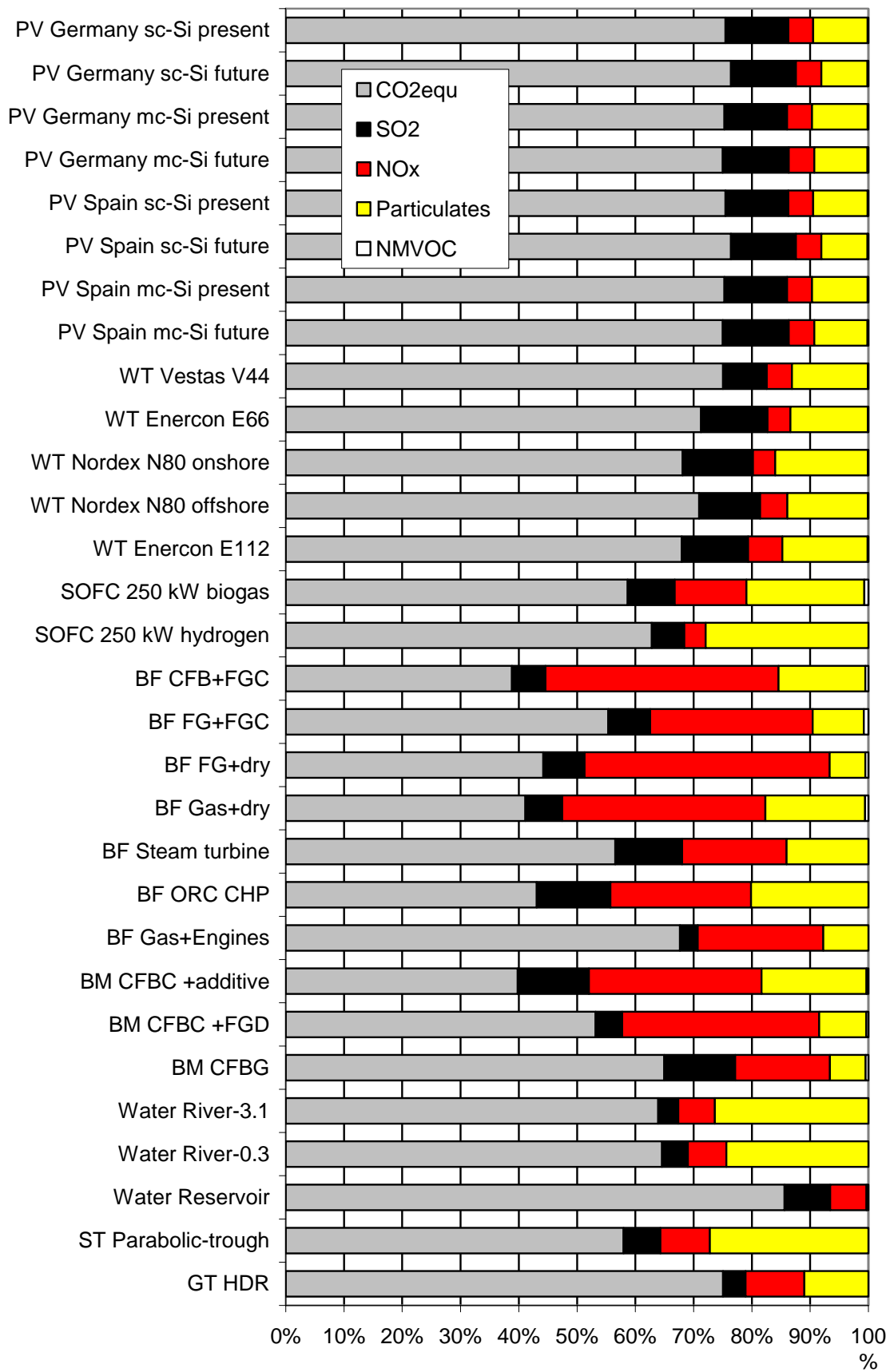
Figure 6-3:   Contribution of the emissions to the external costs of non-fossil-fuelled power plants with the higher estimate (in €$_{2003}$-Cent/kWh$_{el}$)
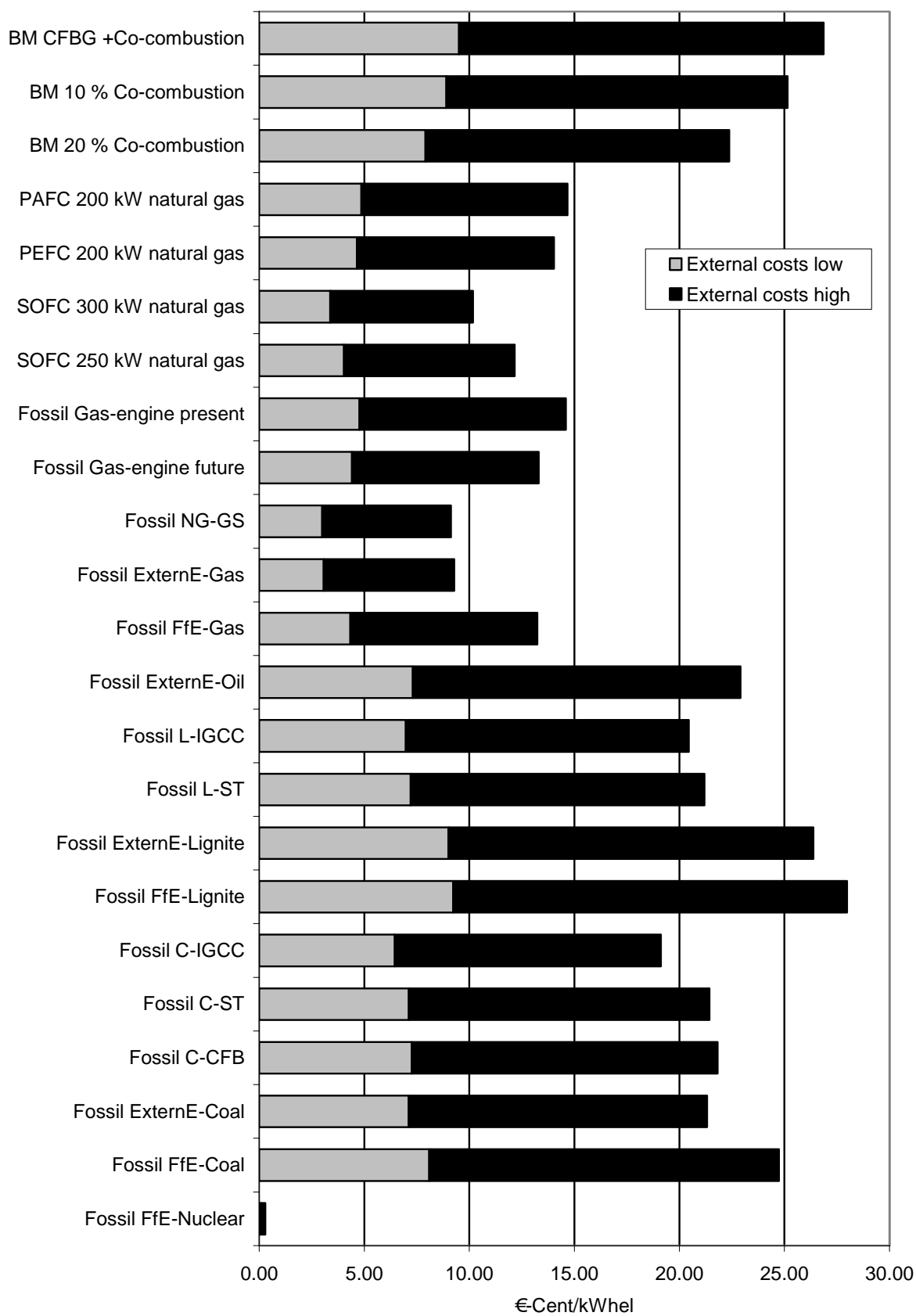
Figure 6-4: External costs of fossil-fuelled power plants (in $€_{2003}$-Cent/kWh$_{el}$)
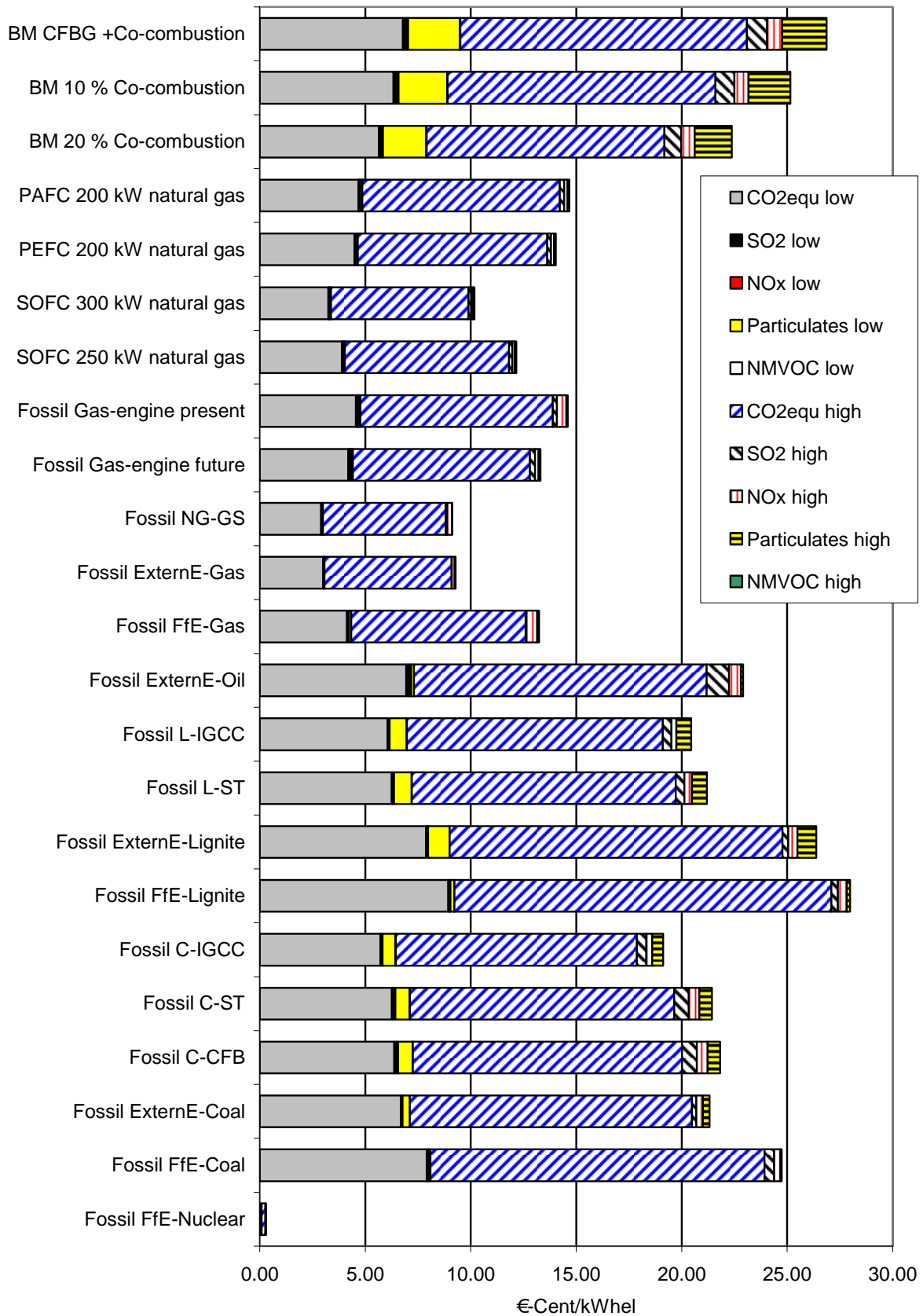
Figure 6-5:   External costs of fossil-fuelled power plants in detail (in €$_{2003}$-Cent/kWh$_{el}$)
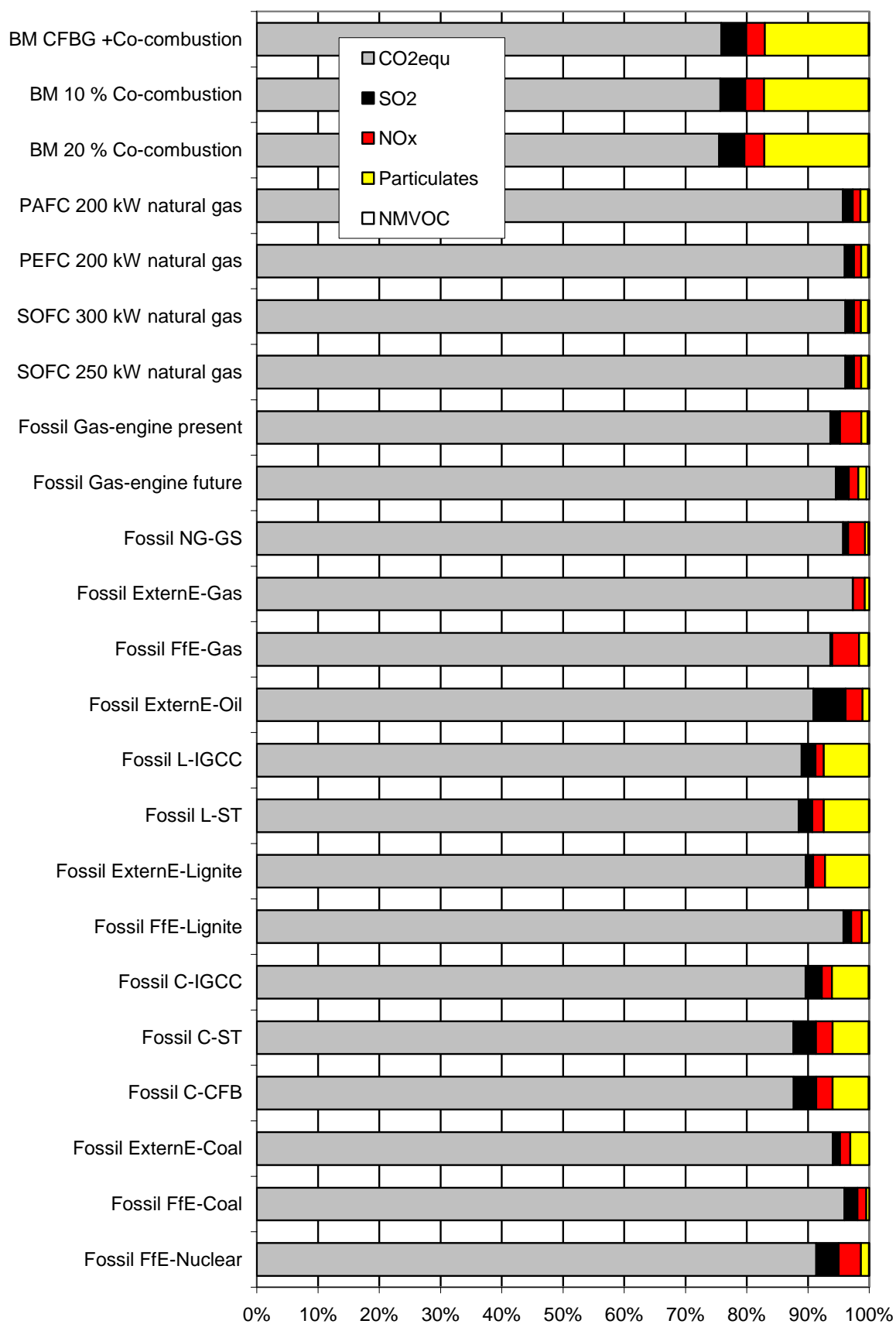
Figure 6-6:   Contribution of the emissions to the external costs of fossil-fuelled power plants with the higher estimate (in $€_{2003}$-Cent/kWh$_{el}$)

The comparison above is not sufficient for decisions because only external costs due to environmental and human health impacts are considered. Therefore, the next chapter analyses the internal costs. A comparison of the internal and the external costs is performed thereafter.

7   Internal costs

This chapter describes the internal costs of power plants which correspond to market prices.

Empirical surveys show that the cost development of new technologies mostly follows a similar behaviour: a doubling in the produced *quantity* Q reduces the *costs per product unit* C approximately by 10-25 %. This cost reduction corresponds to a learning factor L of 0.75-0.9. The reasons for this cost degression are learning effects, which lead to an increasing production speed, economics of scale with larger production capacities, which directly result in lower costs per unit, technological progress, which leads to cheaper process due to innovations, and rationalization with a larger production quantity, which enables optimizations.
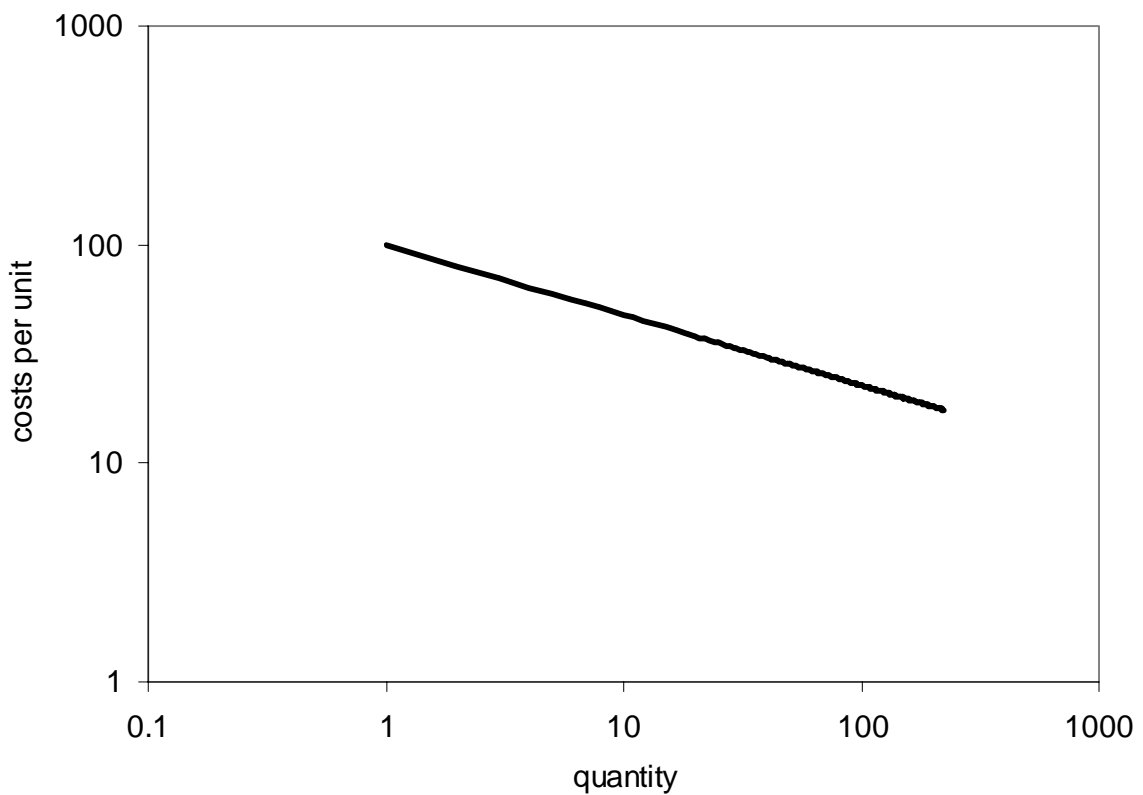
Figure 7-1:   Learning curve

The learning curve, which is displayed qualitatively in **Figure 7-1**, can be expressed with a relation of the *costs per unit* C(t) as a function of *time* t, the *produced quantity* P(t) as a function of the time t, and the *learning factor* L:

$$C(t) = C(t=0) \cdot \left(\frac{P(t)}{P(t=0)} \right)^{\frac{\log L}{\log 2}} \tag{7-1}$$

With this formula it is possible to estimate future cost developments. Therefore, it is necessary to determine the learning factor with previous cost developments as well as to estimate the development of the production capacity.

/BMU 2004/ estimates the cost developments for German conditions. The study at hand concentrates on the development until 2010 as many technologies analysed in chapter 5 are projected to 2010. **Table 7-1** summarizes the internal costs described in more detail in the following paragraphs. It should be noted that these cost estimations are rough, vary from country to country, and are fundamentally dependent on future market growth and technological progress. Additionally, they are dependent on calculation assumptions, e.g. the discount rate, the plant site and the development of fuels.

Photovoltaic systems:

Deriving from /Harmon 2000/, /De Moor et al. 2003/, /UNDP 2000/ and /Swanson 2004/, the learning factor of PV systems is approximately 0.8. This learning factor is also used in /BMU 2004/. For the year 2010, /BMU 2004/ estimates specific power generation costs of PV systems with a capacity of 2-500 kW in Germany in a range of 0.245-0.362 €/kWh$_{el}$. For the year 2020, the specific power generation costs are estimated in the range of 0.151-0.203 €/kWh$_{el}$. The study assumes an annual growth of 20 % which is lower than the annual growth over the previous years so that the cost estimations can be regarded as conservative. In the study at hand, it is assumed that the power generation costs of PV systems in Germany in the year 2010 will be 0.25-0.35 €/kWh$_{el}$

Similar to the dependence of the emissions and external costs, the internal costs have a similar behaviour for more southern plant sites with a higher radiation generating a higher amount of electricity with the same system. It is assumed that the Spanish system has the same internal costs as the German one. With higher radiation, the specific internal costs are reduced by 46 % (cf. **Table 5-5**). Therefore, the specific internal costs of a PV system in Spain in the year 2010 are assumed to be 0.14-0.19 €/kWh$_{el}$. Following the cost reduction in /BMU 2004/ this would correspond to 0.08-0.11 €/kWh$_{el}$ in 2020.

The future cost development of PV systems with high potentials, a high growth rate and a low learning factor can be estimated to lead to significant cost reductions.

Wind turbine systems:

The learning factor for wind turbine systems is given in /UNDP 2000/ and /Neij et al. 2003/ with a value of 0.85. In contrast /BMU 2004/ calculates with 0.94 for onshore turbines and 0.9 for offshore turbines for German conditions which have shown higher learning factors in recent years. The annual market growth, which is described in chapter 5.2.2, has been 35 % in recent years. In contrast /BMU 2004/ assumes 12 % for onshore wind turbines and 28 % for offshore wind turbines so that the estimations may be considered as conservative.

The cost estimations of onshore wind turbines for the year 2010 are 0.053-0.075 €/kWh$_{el}$ for the example of a 1.8 MW wind turbine which operates 2,060-2,930 full load hours per year. This estimation may be used for the Enercon E66 wind turbine with 1.5 MW and 2,500 full load hours per year. For this wind turbine system, the power generation costs are as assumed to be 0.05-0.08 €/kWh$_{el}$ in 2010.

For offshore wind turbines with 4.5 MW, it is estimated that the costs in the year 2010 will be in the range of 0.055-0.063 €/kWh$_{el}$ depending on the distance to the coast. This estimation may be transferred to the Nordex N80 offshore wind turbine. In this study, the same assumption on internal costs is used as for the onshore wind turbine with power generation. However, it should be noted that the costs tend to be lower. Additionally, there are wind potentials in Europe which increase the annual full load hours if they are used. This results in further specific cost reductions.

The future cost development of wind turbine systems with high potentials, a high growth rate and a low learning factor can be estimated to lead to significant cost reductions.

Fuel cell systems:

In the case of fuel cell (FC) systems, no representative previous market developments are available. Additionally, this technology is not analysed in /BMU 2004/. Therefore, future developments are based on the assumptions in /Krewitt et al. 2004/. In the cited study, the specific costs of FC systems are assumed to be 1,440-2000 €/kW$_{el}$ in the year 2010. At this cost level, the electricity costs may be around 0.10 €/kWh$_{el}$ with natural gas costs contributing ca. 0.04 €/kWh$_{el}$ to this estimate. For such a development it is necessary that there will be a growing market in the coming years so that these assumptions should be interpreted as optimistic ones. Therefore, the study at hand takes this estimate as the lower one and assumes an upper estimate of 0.20 €/kWh$_{el}$.

In /BMU 2004/, it is estimated that hydrogen may cost ca. 0.11 €/kWh in 2010 generated with offshore wind turbines. Since it substitutes the natural gas the power generation costs of FC systems fired with hydrogen are estimated to be 0.07 €/kWh$_{el}$ higher than those of the natural gas-fired one.

The future development of the internal costs of FC systems can not be estimated because the technology is not on the market long enough to estimate potentials, growth rates or learning factors. Nevertheless, the possible use of hydrogen generated by renewable energies with low external costs (cf. chapter 6) as well as possible portable, stationary and mobile application seems to enable a fast future development with corresponding cost reductions.

Biomass systems:

In /BMU 2004/ it is estimated that the fuel costs are 0.018 € per kWh of forest residues and that the heat is credited with 0.02 €/kWh. Thus, the power generation costs are 0.15 €/kWh$_{el}$ in the case of a CHP steam turbine system with 5 MW$_{el}$ and 0.12 €/kWh$_{el}$ in the case of a

20 MW$_{el}$ power plant. The cost reduction potential is estimated to be only marginal so that these figures may also be used for the year 2010. It is assumed that the first system corresponds roughly with the FG+FGC analysed in chapter 5.4. Uncertainties of this cost estimation are included by an assumed range of plus and minus 0.03 €/kWh$_{el}$.

Future potentials are high but the components used are developed. Therefore, only small cost reduction may be assumed for this technology.

Water power systems:

Water power systems do not show a relevant market development because the potentials are mainly utilised. The technological development is nearly finished. Thus, the learning factor in /BMU 2004/ is assumed to be one so that their will be no significant cost reductions in the future. Power generation costs for new plants are expected to be 0.091-0.111 €/kWh$_{el}$ in the case of 1-10 MW plants. These estimations may be used for the analysed 3.1 MW river power plant for which this study assumes power generation costs of 0.09-0.11 €/kWh$_{el}$.

Solar thermal power plants:

Learning factors of solar thermal power plants do not have a good data quality as there has been no extensive market development. Rough estimations result in a learning factor of 0.88 in /BMU 2004/ and an annual market growth of 19 %. New SEGS systems with 100 MW capacity (cf. chapter 5.7) are estimated to have power generation costs of 0.09 €/kWh$_{el}$ at a plant site in Southern Spain. The study at hand assumes power generation costs of 0.07-0.11 €/kWh$_{el}$ for the year 2010.

Geothermal power plants:

There are no well known studies on learning curves of geothermal power plants. Therefore, /BMU 2004/ derives the applied learning factor of 0.8 from the oil production industry as both technologies are dominated by drilling activities. Furthermore, it is assumed that the installed capacity of geothermal power plants will grow 6 % annually. Estimations for 2010 are in the range of 0.125-0.155 €/kWh$_{el}$. In this study 0.12-0.16 €/kWh$_{el}$ are assumed.

Fossil power plants:

It is very difficult to get reliable data from fossil power plant manufacturers because they regard them as confidential. Therefore, the costs of fossil power plants can only be estimated. Different assumptions on the discount rate, the development of the fuel costs and plant site generate estimations with large ranges. The *Organisation for Economic Co-operation and Development* (OECD) is performing a survey on electricity generation costs which may be published in 2004/2005. Preliminary results show that the electricity generation costs of coal, lignite, natural gas and nuclear fired power plants may be in the range which is listed in **Table 7-1**.

Table 7-1: Estimations of the power generation costs in the year 2010 of selected examples

Power plant	Estimated Costs 2010 in $€_{2003}$/kWh$_{el}$	
	Lower estimate	**Upper estimate**
PV Germany mc-Si future	0.25	0.35
PV Spain mc-Si future	0.14	0.19
WT Enercon E66	0.05	0.08
WT Nordex N80 offshore	0.05	0.08
SOFC 250 kW natural gas	0.10	0.20
SOFC 250 kW hydrogen	0.17	0.27
BF FG+FGC	0.12	0.18
BM CFBC+additive	0.09	0.15
Water River-3.1	0.09	0.11
ST Parabolic-trough	0.07	0.11
GT HDR	0.12	0.16
Fossil NG-GS (natural gas)	0.04	0.06
Fossil C-IGCC (Coal)	0.03	0.07
Fossil L-IGCC (Lignite)	0.03	0.07
Fossil FfE-Nuclear	0.02	0.06

Figure 7-2 illustrates the comparison of the internal costs of the above selected examples. It can be seen that the fossil-fuelled power plants (with the exception of the natural gas-fired SOFC) have lower internal costs than non-fossil-fuelled power plants in contrast to the situation of external costs in chapter 6.

In order to compare the selected examples with regard to their environmental and economic impacts the external and internal costs are summed up in **Figure 7-3**. The lower estimate of the internal and external costs is illustrated by the filled parts of the bars and the higher estimate by the sum of the filled and the striped parts of the bars. Thus the striped parts of the bars display the range of the cost estimation.

It is difficult to recognize the ranking of the technologies under consideration of external and internal costs due to the different ranges and cost levels. Therefore, **Table 7-2** and **Table 7-3** show the ranking of the technologies with the use of the lower and upper estimate for internal and external costs, respectively. The first row with rank one displays the technology which has the lowest social costs, i.e. internal plus external costs, while the last row with rank fifteen displays the technology with the highest costs.
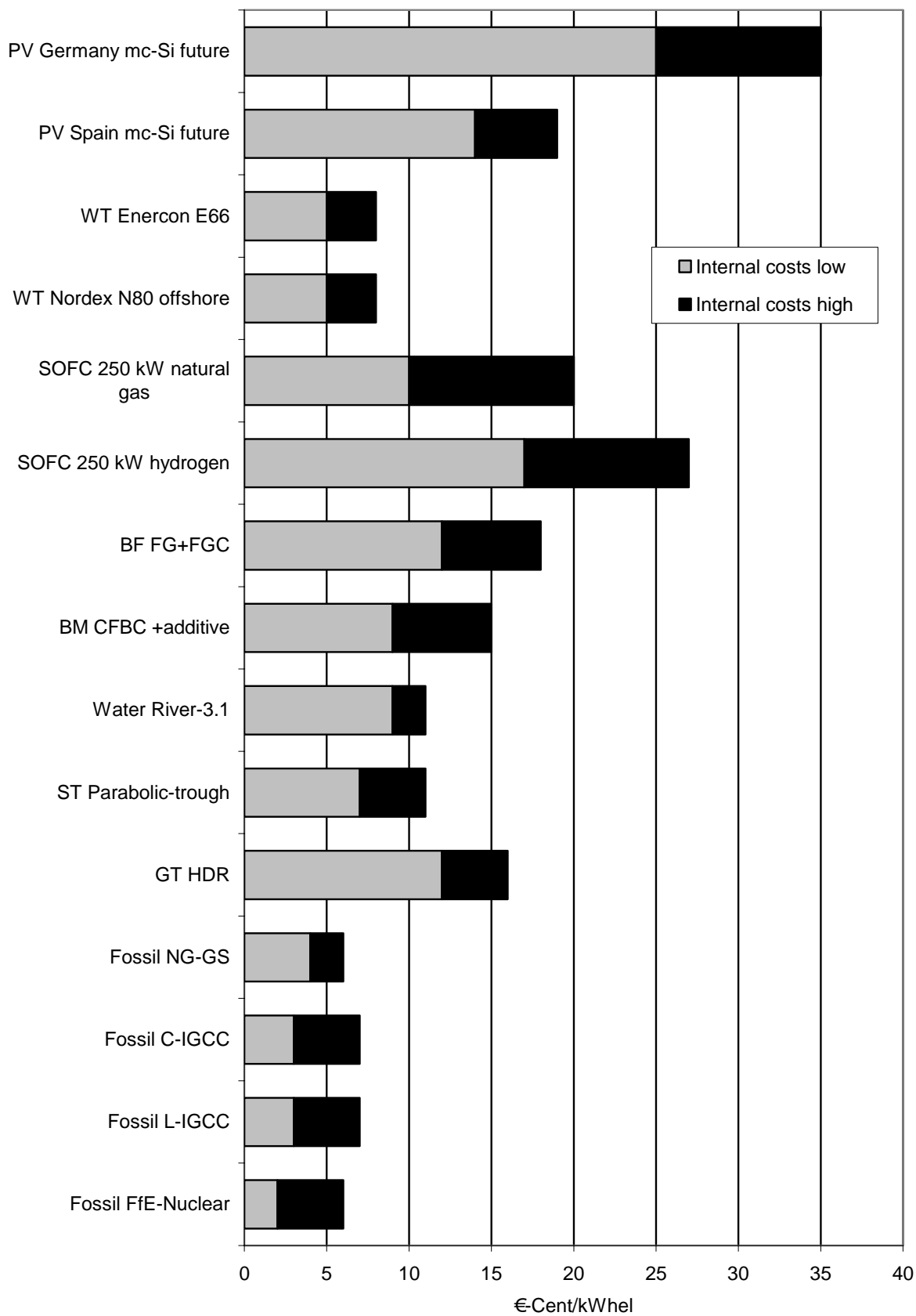
Figure 7-2:   Internal costs of selected examples estimated for 2010 (in $€_{2003}$-Cent/kWh$_{el}$)
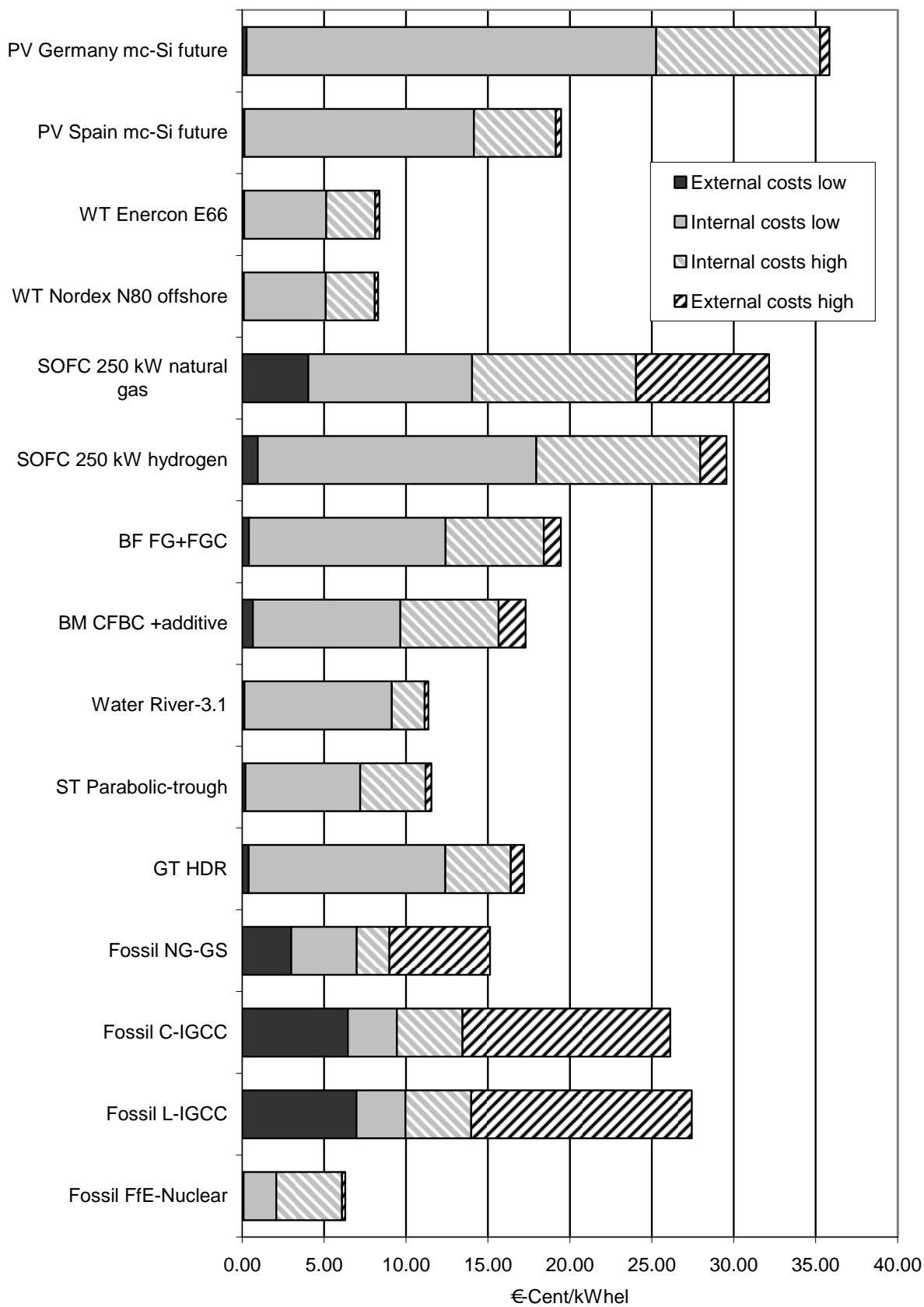
Figure 7-3   Internal and external costs of selected examples estimated for the year 2010 (in €$_{2003}$-Cent/kWh$_{el}$)

Table 7-2:   Ranking of the selected examples under consideration of external and internal costs (extreme values)

Rank	Lower estimate for external costs / Lower estimate for internal costs	Upper estimate for external costs / Upper estimate for internal costs
1	Fossil FfE-Nuclear	Fossil FfE-Nuclear
2	WT Nordex N80 offshore	WT Nordex N80 offshore
3	WT Enercon E66	WT Enercon E66
4	Fossil NG-GS	Water River-3.1
5	ST Parabolic-trough	ST Parabolic-trough
6	Water River-3.1	Fossil NG-GS
7	Fossil C-IGCC	GT HDR
8	BM CFBC +additive	BM CFBC +additive
9	Fossil L-IGCC	BF FG+FGC
10	GT HDR	PV Spain mc-Si future
11	BF FG+FGC	Fossil C-IGCC
12	SOFC 250 kW natural gas	Fossil L-IGCC
13	PV Spain mc-Si future	SOFC 250 kW hydrogen
14	SOFC 250 kW hydrogen	SOFC 250 kW natural gas
15	PV Germany mc-Si future	PV Germany mc-Si future

The lowest internal and external costs of power generation for all four cost considerations are caused by nuclear power plants (rank 1), followed by wind turbine systems (rank 2-3), whereas the highest costs are caused by PV systems in Germany (rank 15). Technologies with relatively low internal and external costs are solar thermal parabolic-trough power plants (rank 4-6), river power plants (rank 4-6) and natural gas-fired power plants (rank 4-7). In contrast, technologies with high internal and external costs are FC systems (rank 10-14) and PV systems in Spain (rank 10-13). In between are biomass systems (rank 6-9), bio-fuelled CHP systems (rank 9-11) and geothermal power plants (rank 7-10). Coal and lignite-fired IGCC power plants show a high sensitivity to different cost considerations. With the low estimate for external costs and the upper estimate for internal costs, both technologies are at rank 7-8 with specific internal and external cost which are lower than those of biomass and bio-fuelled systems as well as PV systems in Spain and fuel cell systems. In contrast, in case of a cost consideration with upper estimate for external costs and the lower estimate for internal costs, both technologies are at rank 12-14 with specific internal and external cost which

are higher than those of the biomass and bio-fuelled systems as well as geothermal power plants, hydrogen fuelled fuel cells and PV systems in Spain.

Table 7-3:   Ranking of the selected examples under consideration of external and internal costs (mixed values)

Rank	Upper estimate for external costs / Lower estimate for internal costs	Lower estimate for external costs / Upper estimate for internal costs
1	Fossil FfE-Nuclear	Fossil FfE-Nuclear
2	WT Nordex N80 offshore	WT Nordex N80 offshore
3	WT Enercon E66	WT Enercon E66
4	ST Parabolic-trough	Fossil NG-GS
5	Water River-3.1	Water River-3.1
6	BM CFBC +additive	ST Parabolic-trough
7	Fossil NG-GS	Fossil C-IGCC
8	GT HDR	Fossil L-IGCC
9	BF FG+FGC	BM CFBC +additive
10	PV Spain mc-Si future	GT HDR
11	SOFC 250 kW hydrogen	BF FG+FGC
12	Fossil C-IGCC	PV Spain mc-Si future
13	SOFC 250 kW natural gas	SOFC 250 kW natural gas
14	Fossil L-IGCC	SOFC 250 kW hydrogen
15	PV Germany mc-Si future	PV Germany mc-Si future

Summarizing the results, it should be noted that with consideration of external and internal costs nuclear power plants and wind turbines are the technologies with the lowest costs whereas PV systems in Germany have the highest ones. While the quantifiable social costs of natural gas-fired fossil power plants are in the order of solar thermal power plants and river power plants with comparably low social costs, the other fossil power plants, which are fired by coal or lignite, have comparably high costs.

Regarding the internal costs, the future development tends to reduce the internal costs of PV systems, fuel cell systems, geothermal power plants, solar thermal power plants and wind turbines because of the above mentioned reasons. In contrast, the internal costs of fossil-fuelled power plants tend to increase due to restricted fuel resources. This development may change the rank significantly. For example, a sensitivity analysis is performed for the development of internal costs of PV systems for the year 2020 as described above. Ceteris paribus,

German PV systems in the year 2020 have the rank of 11-14. At these ranks, they have lower internal and external costs compared to coal or lignite-fired fossil power plants for the cost considerations with the upper external cost estimate. The Spanish PV systems in the year 2020 are estimated to have an improved ranking at rank 4-8 (ceteris paribus). Thus, they have lower internal and external costs than coal or lignite-fired fossil power plants, biomass and bio-fuelled systems as well as geothermal power plants and fuel cells. This sensitivity analysis aims to show that future cost reductions of PV systems may improve their rank significantly. The cost reductions may result in lower social costs than those of coal or lignite-fired power plants.

The comparison so far considers internal and external costs of the analysed power plants. However, technologies using fluctuating energy sources, e.g. solar radiation and wind, do not generate electricity in the same quality as others with constant fuel supply and constant electricity generation. However, the power market demand needs a supply without interruptions. Therefore, PV and wind turbine systems need to be backuped with power plants which deliver power as required. This is causing additional costs which should be attributed to the fluctuating power suppliers. In the following chapter, the backup costs are estimated.

8 Backup costs

Power generation technologies can be differentiated into technologies with constant energy supply, e.g. coal and natural gas, and technologies with fluctuating energy supply, e.g. solar insolation and wind (see **Figure 8-1**). For the latter ones, the power generation may not always match with the electricity demand so that there may be a high demand while the solar insolation is reduced by clouds or the wind is very calm. Therefore, storage technologies or backup plants should be available to balance supply and demand. Backup plants are controllable power plants which can be used to substitute the missing power. In order to compare different technologies a power supply task has to be defined. This power supply task is defined by an assured supply of energy so that power from wind and PV has to be supported with storage technologies or backup power plants.
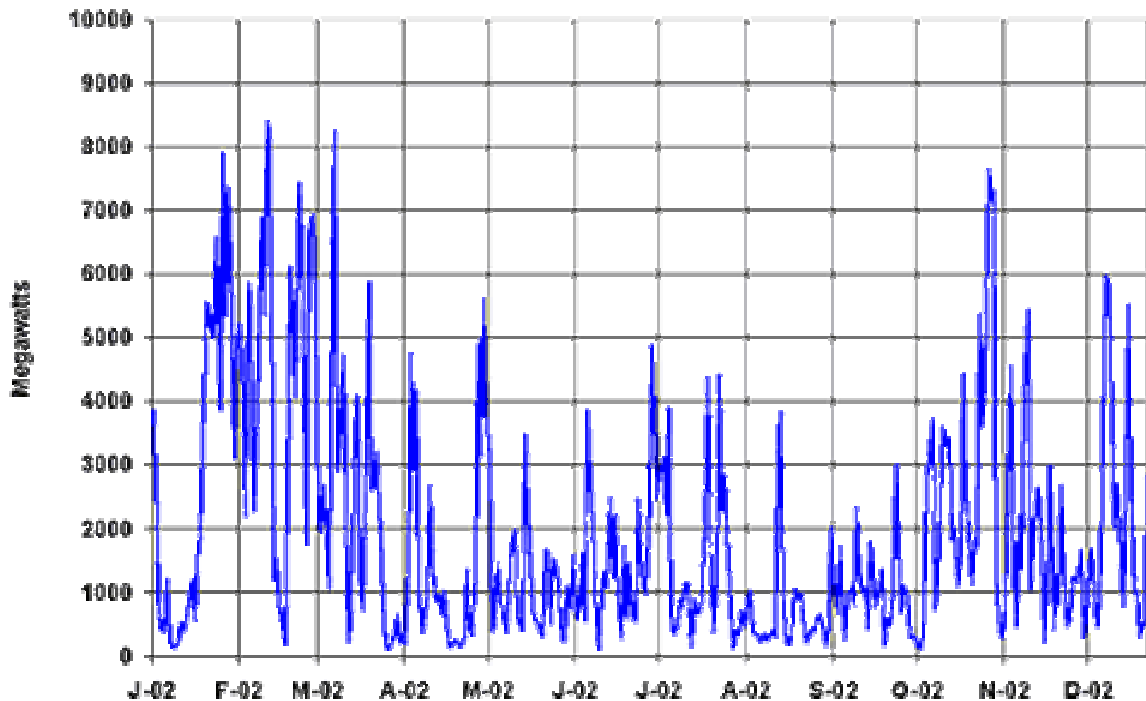
Figure 8-1:   Computed wind power time series of all wind turbines in Germany 2002 /ISET 2004/

In this chapter, the focus lies on PV and wind power generation which have to be integrated into the power network. Technologies investigated as backup plants are coal-fired power plants, gas-fired CHP plants, biomass power plants, fuel cells and wind turbine systems. With these technologies, an energy supply matching the market demand becomes possible. However, there will also arise some disadvantages because these backup plants should keep reserve capacity ready. Additionally, they may have to operate with more start-ups and rundowns as well as longer runtime in part load. These inconveniences may increase the environmental and economic impacts of the backup plants which should be attributed to the backed up PV and wind turbine systems.

The capacity credit is used to define the proportion of the installed power of renewable energy technologies which determines the amount of capacity of the conventional power supply system which can be turned off in a mixed system. This mixed system includes conventional and renewable energy technologies without a reduction in reliability.

Initially, it is assumed that the demand side as well as the supply of fluctuating renewable energies and base load power plants can not be influenced in a significant way so that this input and output should be considered as given and the balance of the supply and demand side is only achieved with controllable power plants. The additional costs in the sense of internal as well as external costs are called *backup costs*. These backup costs are added to the costs of the fluctuating renewable energies which are causing them. In the following two chapters, firstly, the external backup costs are estimated and, secondly, the internal backup costs are estimated. Both calculations are performed with assumptions simplifying the calculations. For detailed analyses, a calculation with more exactness has to be performed in future studies.

8.1   Calculation of external backup costs

For the calculation of external backup costs, the approach of /Hartmann 2001/ is applied. Actually, the calculation has to be performed for every substance which is considered in the life cycle analysis. In the study at hand, this is not performed in such a degree of detail because of the uncertainties discussed in chapter 3.1 and the uncertainties in the required components of this calculation. Therefore, the calculation is not performed for every type of emission but estimated for the external costs as a whole. Thus the following description of the calculation uses the term *costs* instead of *emissions*.

The costs can be differentiated into fixed costs and variable costs. Fixed costs accrue without operating the power plant (e.g. for construction and demolition). They are assumed to be proportional to the installed capacity. Fixed costs arise from additional reserve capacity needed to backup the fluctuations of the renewable energy supply. Variable costs accrue during the operation of the power plant. They are assumed to be reciprocally proportional to the utilization degree of the power plant. Variable costs arise from lower utilization degree due to more part load runtime and additional start-ups and rundowns.

In order to calculate the backup costs, two power systems are compared (see **Figure 8-2**). Firstly, the single conventional system which produces the energy E_c as efficient as possible with costs $S_{c,s}$. Secondly, the renewable system which produces the energy E_r with costs S_r. Thirdly, the mixed system (renewable together with the conventional system) which produces the summed energy $E_m = E_c + E_r$ with the costs S_m. The costs of the mixed systems include the costs of the renewable system so that the costs of the conventional part of the mixed system $S_{c,m}$ are the difference of S_m and S_r. With these assumptions the backup costs S_b can be calculated with the following equation:

$$S_b = S_m - \left(S_{c,s} + S_r\right) = (S_{c,m} + S_r) - \left(S_{c,s} + S_r\right) = S_{c,m} - S_{c,s} \qquad (8\text{-}1)$$
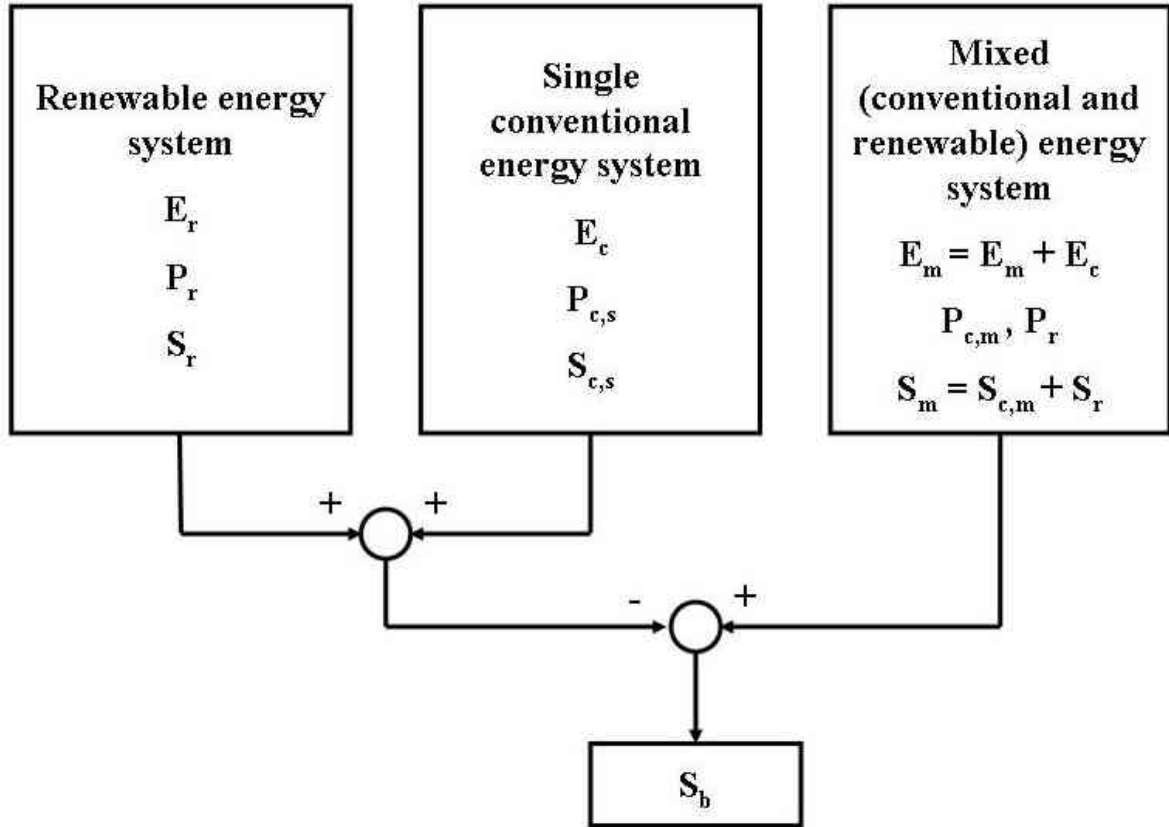
Figure 8-2: Approach for the determination of backup costs

The costs S_i with index i which account for the other indices is calculated with:

$$S_i = S_{fix,i} + S_{var,i} = S_{fix,i} + s_{var,i} \cdot E_j \qquad (8\text{-}2)$$

In this term, the costs S_i are split up into fixed costs $S_{fix,i}$ and variable costs $S_{var,i}$. The variable costs $S_{var,i}$ are dependent on the amount of energy produced E_j so that the specific variable costs per energy unit (e.g. kWh$_{el}$) $s_{var,i}$ can be used. In a similar way, the total backup costs S_b can be expressed in backup costs per kWh$_{el}$ of renewable energy s_b by dividing S_b by the amount of renewable energy E_r which is responsible for these costs:

$$s_b = \frac{S_b}{E_r} \qquad (8\text{-}3)$$

The specific costs of the conventional single system can be defined in the same way:

$$s_{c,s} = \frac{S_{c,s}}{E_c} \tag{8-4}$$

It is assumed that fixed costs are proportional to the installed capacity. Thus, the ratio of the fixed costs is proportional to the ratio of the capacities. The ratio of the conventional system as a single system (indexed c,s) and the conventional system within the mixed system (indexed c,m) is:

$$\frac{S_{fic,c,s}}{S_{fic,c,m}} = \frac{P_{c,s}}{P_{c,m}} \tag{8-5}$$

Another relation for the variable costs is possible due to the mentioned reciprocal proportionality with the utilization degree ζ of the respective system:

$$\frac{s_{\text{var},c,s}}{s_{\text{var},c,m}} = \frac{\zeta_{c,m}}{\zeta_{c,s}} \tag{8-6}$$

With these relations the backup costs per kWh$_\text{el}$ renewable energy can be calculated with:

$$s_b = \frac{S_b}{E_r} = \frac{S_{c,m} - S_{c,s}}{E_r} = \frac{\left(S_{fix,c,m} + s_{\text{var},c,m} \cdot E_c\right) - \left(S_{fix,c,s} + s_{\text{var},c,s} \cdot E_c\right)}{E_r}$$

$$= \frac{\left(S_{fix,c,m} - S_{fix,c,s}\right) + \left(s_{\text{var},c,m} - s_{\text{var},c,s}\right) \cdot E_c}{E_r}$$

$$= \frac{S_{fix,c,s} \cdot \left(\dfrac{P_{c,m}}{P_{c,s}} - 1\right) + s_{\text{var},c,s} \cdot \left(\dfrac{\zeta_{c,s}}{\zeta_{c,m}} - 1\right) \cdot E_c}{E_r} \tag{8-7}$$

The capacity credit CC determines the proportion of the installed renewable energy power which supplies energy as reliable as the conventional power system. It is used to calculate the installed power of the conventional system in the mixed system $P_{c,m}$ by:

$$P_{c,m} = P_{c,tot} - CC \cdot P_r \tag{8-8}$$

In this term, the power $P_{c,tot}$ is the power of a conventional power system which would be needed to generate the total amount of electricity E_m generated by the mixed system. Due to the capacity credit of the renewable energy system the power $P_{c,tot}$ can be reduced in a mixed system. Thus, the backup costs per kWh$_\text{el}$ renewable energy can be calculated by the term:

$$s_b == \frac{S_{fix,c,s} \cdot \left(\frac{P_{c,tot} - CC \cdot P_r}{P_{c,s}} - 1 \right) + s_{var,c,s} \cdot \left(\frac{\zeta_{c,s}}{\zeta_{c,m}} - 1 \right) \cdot E_c}{E_r} \qquad (8\text{-}9)$$

Since the costs in the chapters above are given per kWh$_{el}$ the backup costs per renewable kWh$_{el}$ s_b are determined with the specific backup costs $s_{fix,c,s}$ and $s_{var,c,s}$.

$$s_b = \frac{S_{fix,c,s} \cdot \left(\frac{P_{c,tot} - CC \cdot P_r}{P_{c,s}} - 1 \right) + s_{var,c,s} \cdot \left(\frac{\zeta_{c,s}}{\zeta_{c,m}} - 1 \right)}{E_r} \cdot E_c \qquad (8\text{-}10)$$

A further simplification is achieved by calculating with the total backup costs per kWh$_{el}$ $s_{c,s}$, which is listed in the result tables in the chapters above. The determination of the fixed and variable backup costs can be performed with the proportion $r_{fix,c,s}$ of fixed costs over the total costs of the backup power plant:

$$r_{fix,c,s} = \frac{s_{fix,c,s}}{s_{c,s}} \qquad (8\text{-}11)$$

This proportion can be derived from the figures in chapter 5 which show the contribution of the different life cycle phases. Every life cycle phase, except for the operation, is assumed to be attributable to $s_{fix,c,s}$. Thus, the specific backup costs can be calculated with:

$$s_b = \frac{s_{c,s} \cdot r_{fix,c,s} \cdot \left(\frac{P_{c,tot} - CC \cdot P_r}{P_{c,s}} - 1 \right) + s_{c,s} \cdot \left(1 - r_{fix,c,s} \right) \cdot \left(\frac{\zeta_{c,s}}{\zeta_{c,m}} - 1 \right)}{E_r} \cdot E_c \qquad (8\text{-}12)$$

The penetration R is the proportion of the renewable energy system to the total electricity generation of the considered system. With this parameter the electricity generation of the conventional system E_c and the electricity generation of the renewable energy system can be calculated by the equations:

$$E_r = R \cdot E_m \qquad (8\text{-}13)$$

$$E_c = (1 - R) \cdot E_m \qquad (8\text{-}14)$$

With these terms the specific backup costs are:

$$s_b = \frac{1-R}{R} \cdot \left[s_{c,s} \cdot r_{fix,c,s} \cdot \left(\frac{P_{c,tot} - CC \cdot P_r}{P_{c,s}} - 1 \right) + s_{c,s} \cdot \left(1 - r_{fix,c,s} \right) \cdot \left(\frac{\zeta_{c,s}}{\zeta_{c,m}} - 1 \right) \right] \quad (8\text{-}15)$$

The full load hours of a power plant describe how many hours per year a power plant should be operated at nominal power to generate the annual electricity produced with fluctuating load. Assuming constant full load hours for all the power plants of a considered technology leads to the following relations with the full load hours of the renewable energy power plants f_r and the full load hours of the conventional backup power plants in a single system f_c:

$$P_r = \frac{E_r}{f_r} = \frac{R \cdot E_m}{f_r} \quad (8\text{-}16)$$

$$P_{c,tot} = \frac{E_m}{f_c} \quad (8\text{-}17)$$

$$P_{c,s} = \frac{E_c}{f_c} = \frac{(1-R) \cdot E_m}{f_c} \quad (8\text{-}18)$$

These relations can be implemented in the equation for the specific backup costs:

$$s_b = \frac{1-R}{R} \cdot \left[s_{c,s} \cdot r_{fix,c,s} \cdot \left(\frac{\frac{E_m}{f_c} - CC \cdot \frac{R \cdot E_m}{f_r}}{\frac{(1-R) \cdot E_m}{f_c}} - 1 \right) + s_{c,s} \cdot \left(1 - r_{fix,c,s} \right) \cdot \left(\frac{\zeta_{c,s}}{\zeta_{c,m}} - 1 \right) \right]$$

$$= \frac{1-R}{R} \cdot \left[s_{c,s} \cdot r_{fix,c,s} \cdot \left(\frac{1 - R \cdot CC \cdot \frac{f_c}{f_r}}{1-R} - 1 \right) + s_{c,s} \cdot \left(1 - r_{fix,c,s} \right) \cdot \left(\frac{\zeta_{c,s}}{\zeta_{c,m}} - 1 \right) \right]$$

$$= \frac{1-R}{R} \cdot \left[s_{c,s} \cdot r_{fix,c,s} \cdot \left(\frac{R \cdot \left(1 - CC \cdot \frac{f_c}{f_r} \right)}{1-R} \right) + s_{c,s} \cdot \left(1 - r_{fix,c,s} \right) \cdot \left(\frac{\zeta_{c,s}}{\zeta_{c,m}} - 1 \right) \right]$$

$$= s_{c,s} \cdot r_{fix,c,s} \cdot \left(1 - CC \cdot \frac{f_c}{f_r} \right) + s_{c,s} \cdot \left(1 - r_{fix,c,s} \right) \cdot \left(\frac{\zeta_{c,s}}{\zeta_{c,m}} - 1 \right) \cdot \left(\frac{1}{R} - 1 \right) \quad (8\text{-}19)$$

The capacity credit CC and the utilization degree ratio have to be indexed with R as they depend on the penetration and are determined for specific situations. This and the simplifications above leads to the following equation for the specific backup costs:

$$s_b = s_{c,s} \cdot \left\{ r_{fix,c,s} \cdot \left(1 - CC_R \cdot \frac{f_c}{f_r}\right) + \left(1 - r_{fix,c,s}\right) \cdot \left[\left(\frac{\zeta_{c,s}}{\zeta_{c,m}}\right)_R - 1 \right] \cdot \left(\frac{1}{R} - 1\right) \right\} \quad (8\text{-}20)$$

In the following paragraphs the elements of this equation are determined step by step.

The capacity credit is calculated on the basis of the reliability of the power network. It is not possible to achieve 100 % reliability because there are uncertainties about disturbances. With reserve capacity it is possible to improve the reliability by balancing supply and demand in the case that disturbances have brought the transmission grid out of balance. The reserve capacity can be classified into primary control, secondary control and tertiary control. With the primary control reserve (second reserve), the power-frequency is controlled within 30 seconds for the case that the grid frequency is not at nominal value in order to avoid deviations which are too large. In the UCTE transmission grid, the primary control reserve is 3 GW. With the secondary control reserve, the capacity balance is evened to reduce the second reserve. Therefore, the nominal value is adjusted by the secondary reserve within 15 minutes. The tertiary control reserve (minute reserve) is provided mainly by storage stations, pumped-storage stations, gas turbines and by thermal power stations that operate at less than full output. It is required to even the capacity balance of the transmission grid operators within 15 minutes. In contrast to the primary and secondary control reserve which is self-controlled, the tertiary control reserve has to be activated manually.

The capacity credit CC_R and the utility degree ratio $\zeta_{c,s}/\zeta_{c,m}$ are determined in the following paragraphs for a wind power or PV power penetration R of 5 % and 10 %. The capacity credit must not be larger than the ratio of full load hours f_r/f_c. In chapter 6, the specific external costs of the conventional single system $s_{c,s}$ are given. The proportion $r_{fix,c,s}$ of fixed external costs over the total external costs of the backup power plant can be derived from chapter 5. In this chapter, the contribution of the life cycle phases to the emissions is illustrated. The emissions correspond to the external costs because damage factors are used. Also full load hours f_c and f_r are partly given in chapter 5. Nevertheless, many of the values have to be estimated because detailed analyses are not available. Thus, the calculated external backup costs are only rough estimates and should be analysed in further research in more detail.

8.1.1   Fluctuation characteristics from wind turbines

Figure 8-3 shows a statistical analysis of the gradients of 15 minutes mean values for a time frame of four hours. The analysis is performed for the German power grid (the most inner

curve) and other plant groups. In the diagram, the frequency distribution of the relative power changes in relation to the total installed power is illustrated. For the German power grid, there is no fluctuation of the wind power from one interval of four hours to the next with a probability of 40 % and a maximum fluctuation of plus or minus 5 % with a probability of approximately 90 %.
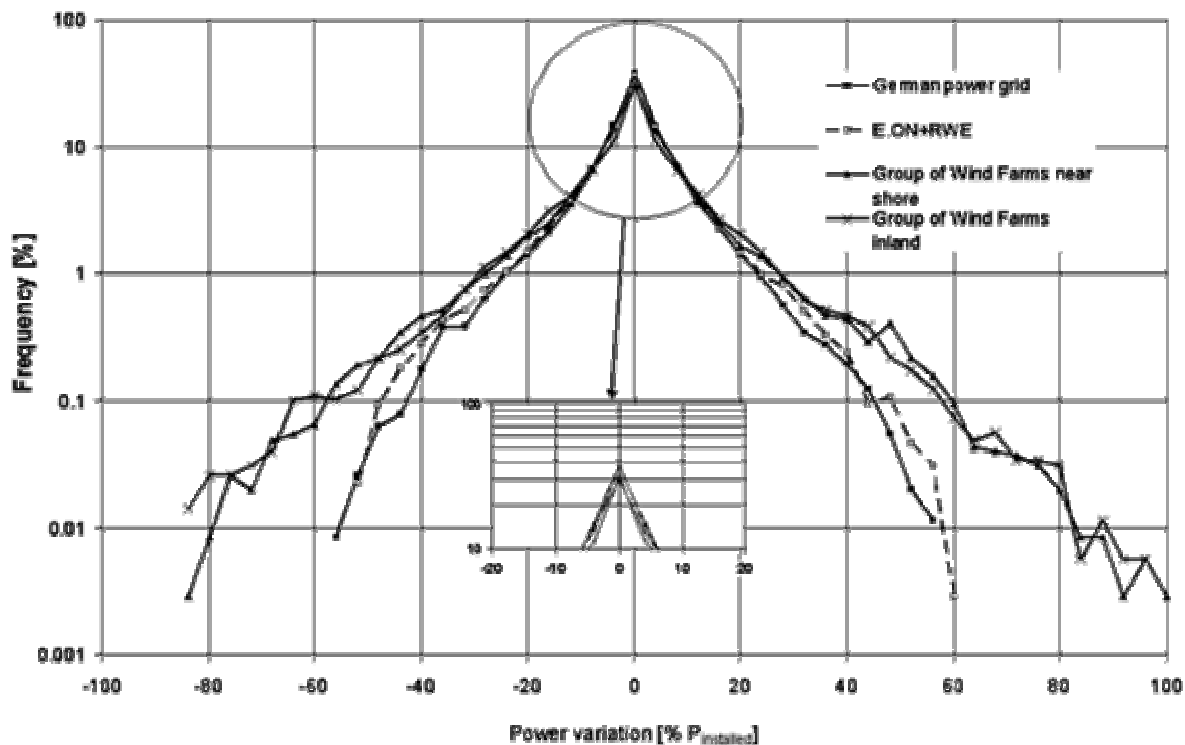
Figure 8-3:   Frequency (in %) of wind power variations (in % of installed power) in four hour periods in the year 2002 /ISET 2004/

/Wiese 1994/ determines the capacity effect with a methodology based on convolution and states that a combination of wind and PV increases the overall capacity credit. He calculates that a ratio of 10 % PV and 90 % wind power achieves approximately a maximum of capacity credits. /Wiese 1994/ determines the capacity credit of wind power systems for Germany with data from 1990 and on the basis of 97 % reliability of the power network. /Hartmann 2001/ calculates with the capacity credit for 1.5 MW wind turbines and 2,450 full load hours. /Lux et al. 1999/ study a power network which is similar to the region in the North of Germany with high wind power penetration. The reliability of uninterrupted service is assumed to be 93 % and the wind power energy substitutes about 80-90 % energy from coal-fired power plants. The capacity credit is 19-24 % in the case of a penetration of 5 %. With increasing penetration, the capacity decreases. The capacity credit of the respective penetration is given in **Table 8-1**.

With the values in **Table 8-1**, the capacity credit in the study at hand is assumed to be 19-28 % for a penetration of 5 % and 16-24 % for a penetration of 10 % of wind turbine systems.

Table 8-1:   Capacity credit of wind turbine systems

Study	/Wiese 1994/			/Hartmann 2001/		/Lux et al. 1999/		
R	1 %	5 %	10 %	5 %	10 %	5 %	10 %	20 %
CC$_R$	33.6 %	28 %	23.4 %	23.12 %	18.07 %	19-24 %	16-24 %	11-18 %

/Dany; Haubrich 2000/ state that the fluctuations of wind power concerning the primary control reserve are evened due to uncorrelated wind situations together with the high number of wind turbines. Thus, fluctuations concerning the primary control reserve are negligible compared to breakdowns of conventional power plants and even the fluctuations of the total grid load. Even with offshore wind farms, which have a high installed power, the primary control reserve can be neglected by the use of appropriate control concepts. However, fluctuations of wind power concerning the secondary control reserve may increase the requirements of the amount and the dynamics of the secondary control. The secondary control is available in form of rotating reserve in steam power plants, fast starting gas turbines and hydro-storage power plants. At present, it seems that there will be no significant increase in the secondary control reserve due to a higher wind power penetration. The need of tertiary control reserve (manual minute reserve) for wind turbines is determined by forecast errors. For the general load, the standard deviation of the forecast is about 3-7 %. At present, the forecast correctness for wind power is worse. /Rohrig et al. 2003/ describe a prediction model which is implemented in the German load dispatcher of E.ON Netz since July 2001. The prediction model delivers a forecast for the wind power up to 72 hours in advance. Therefore, 16 representative wind farms are equipped with measurement technologies and the *Deutscher Wetterdienst* (DWD) provides meteorological parameters in one-hour intervals with a spatial dispersion of seven kilometres. The forecast error of the model using an artificial neural network is about 8.8 % of the installed capacity for the day-ahead forecast and about 6 % for the short-term prediction of 1-8 hours. Further improvements with more wind farms equipped with measurement technology and higher time and spatial resolution may increase the accuracy of the forecast so that the range of the general load forecast is achieved. In **Figure 8-4**, /Rohrig et al. 2003/ show the frequency distribution of the forecast error for a period of 680 days. It can be seen that the forecast error in the range of -10 % to +10 % of the installed capacity is not exceeded in 86 % of the days. /Dany; Haubrich 2000/ simulate the manual minute reserve capacity for wind power penetration and determine a quite linear relation for higher penetrations of more than 10 % in a 20 GW transmissions grid of approximately 300 MW per GW installed wind power for a forecast error of 10 %. For lower penetrations, there is a smaller increase of manual minute reserve.

The need for manual minute reserve is approximately proportional to the forecast error. Thus, a forecast error of 6 %, which is determined in /Rohrig et al. 2003/, leads to additional 180 MW manual minute reserve per GW installed wind power for a penetration of more than

10 %. Improvements in forecast models will decrease the forecast error and thus the additional manual minute reserve.
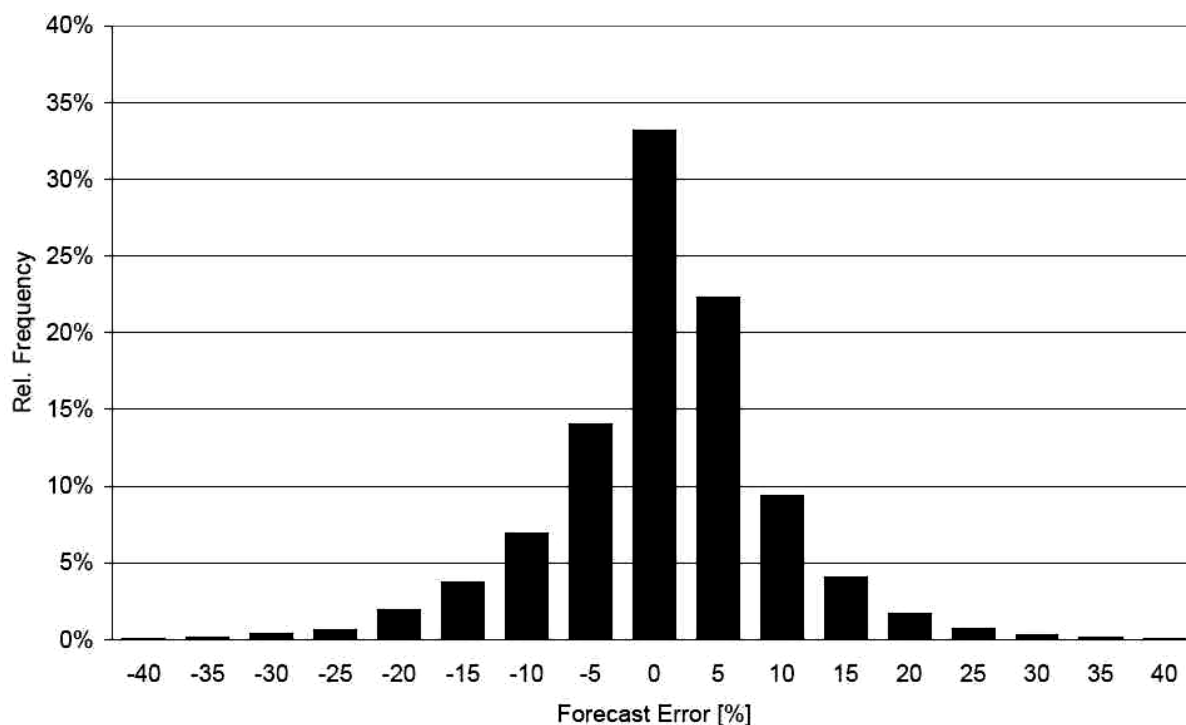
Figure 8-4:   Frequency distribution of the forecast error /Rohrig et al. 2003/

8.1.2   Fluctuation characteristics from PV

/Wiese 1994/ determines the capacity credit of PV systems for Germany with data from 1990 and on the basis of a 97 % reliability of the power network. /Hartmann 2001/ calculates with the capacity credit for 5 kW PV generators and 880 full load hours. The capacity credit of the respective penetration is given in **Table 8-2**. With these values, the capacity credit in the study at hand is assumed to be 5-15 % for a penetration of 5 % and 2-15 % for a penetration of 10 % of PV systems. The upper estimate of 15 % is used because the capacity credit should not be larger than the ratio of full load hours f_r/f_c. With $f_r = 905$ h/a and $f_c = 6000$ h/a in the following calculation, this means that the capacity credit should be lower than 15.1 %.

Table 8-2:   Capacity credit of PV systems

Study	/Wiese 1994/			/Hartmann 2001/	
R	1 %	5 %	10 %	5 %	10 %
CC$_R$	18.1 %	16.6 %	14.6 %	5.41 %	2.61 %

8.1.3 Backup with coal power plants

/Hartmann 2001/ calculates with the utilization degree ratios in **Table 8-5** depending on the penetration referring to /Lux 1999/. /Lux 1999/ describes the impacts of different wind power penetration levels and the impact on a considered power network with the technical parameters in **Table 8-3**. Different scenarios for power generation from wind turbines are considered (see **Table 8-4**). The calculations show that most (ca. 80-90 %) of the substituted electricity generation is economized in coal-fired power plants.

Table 8-3: Elements of the power network considered in /Lux 1999/

Element	Net nominal capacity (MW)	Nominal efficiency (%)	Electricity generation (TWh/a)	Share of the electricity generation (%)	Full load hours (h/a)
Nuclear power plants	4,564	34	33.7	49.3	7,384
Coal power plants	4,541	39	26.3	38.5	5,792
Gas-fired power plants	1,577	41	0.3	0.4	190
Lignite power plants	610	32	3.7	5.4	6,066
Gas turbines[38]	520	34	-	-	-
Pumped-hydro storage	800	75	-0.3	-0.4	375
Run-of-the-river power plant	69	100	0.3	0.5	4,348
Contract benefits	1,385	-[39]	3.2	4.7	2,310
Possible Spot market benefits	1,500	33[40]	1.1	1.7	733

/Lux 1999/ describes that the efficiency of coal power plants decreases by ca. 5 % (1 %) in the operation case of 50 % (75 %) of the net nominal load. There are 23 start-ups per TWh of coal-fired power plants without wind power. With a wind power penetration of 5 % the number of start-ups increases by ca. 30 % and with a penetration of 10 % by ca. 70 %. Another aspect of changes in operation characteristics are the number of power changes. A coal-fired power plant has power changes of 66 MW per GWh without wind power. This value increases by 23 % for a penetration of 5 % and by ca. 50 % for a penetration of 10 %. In contrast to these significant changes by wind power penetration, the part load behaviour changes

---

[38] Gs turbines are not further analysed in /Lux 1999/.

[39] No average values are available.

[40] The German electricity mix is used.

only marginally with increasing wind power penetration. On the one hand, the share of 82 % in the load range of 75-100 % of the nominal power decreases to ca. 80 % with 5 % penetration and to ca. 79 % with 10 % penetration. On the other hand, the share of 10 % in the load range smaller than 50 % of the nominal power increases to ca. 12 % with 5 % penetration and to ca. 14 % with 10 % penetration. The described aspects of wind power penetration result in a change of the average net utilization degrees. For coal-fired power plants the utilization degree decreases from the reference of 39 % by ca. 0.3 % in the case of 5 % penetration and by ca. 0.6 % in the case of 10 % penetration.

Table 8-4:   Scenarios of wind power penetration considered in /Lux 1999/

Scenario (R)	Nominal capacity (MW)	Electricity genera-tion (TWh/a)	Full load hours (h/a)
Coast (5 %)	1,435	3.3	2,278
Inland (5 %)	1,686	3.4	2,035
Coast (10 %)	2,415	6.6	2,725
Inland (10 %)	3,537	6.8	1,920

In the study at hand, the ratio of utilization degrees is assumed to be 1.001-1.003 for a penetration of 5 % and 1.002-1.006 for a penetration of 10 %.

Table 8-5:   Utilization degree ratio for coal power plants

Study	/Hartmann 2001/		/Lux 1999/	
R	5 %	10 %	5 %	10 %
$(\zeta_{c,s}/\zeta_{c,m})_R$	1.00083	1.00186	1.003	1.006

8.1.4   Backup with gas-fired CHP

/Lux 1999/ describes that the efficiency of gas turbines decreases by ca. 20 % (4 %) in the operation case of 50 % (75 %) of the net nominal load and the efficiency of gas-fired power plants decreases by ca. 5 % (1 %) in the operation case of 50 % (75 %) of the net nominal load. In the analysed power network, there are 558 start-ups per TWh of gas-fired power plants without wind power. With a wind power penetration of 5 % the number of start-ups increases by ca. 13 % and with a penetration of 10 % by ca. 16 %. A gas-fired power plant has power changes of 353 MW per GWh without wind power. This value increases by ca. 6 % for a penetration of 5 % and by ca. 2 % for a penetration of 10 %.

Another aspect of penetration of wind power is the change in the part load behaviour of the conventional power plants. On the one hand, the share of 8 % in the load range of 75-100 % of the nominal power decreases to ca. 4 % with 5 % penetration and to ca. 2 % with 10 % penetration. On the other hand, the share of 47 % in the load range smaller than 50 % of the nominal power increases to ca. 51 % with 5 % penetration and to ca. 60 % with 10 % penetration.

The described aspects of wind power penetration result in a change of the average net utilization degrees. For gas-fired power plants the utilization degree decreases from the reference of 35 % by 1.4-1.9 % ($\zeta_{c,s}/\zeta_{c,m} = 1.014$-$1.019$) in the case of 5 % penetration and by ca. 0.5-1.9 % ($\zeta_{c,s}/\zeta_{c,m} = 1.005$-$1.019$) in the case of 10 % penetration. These are rough values. Therefore, in the study at hand, the utilization degree ratio is estimated in the range of 1.005-1.020 for 5 % as well as 10 % penetration.

8.1.5 Backup with biomass power plants

Biomass power plants can be assumed to be similar to coal-fired power plants. Therefore, the utilization degree ratio is assumed to be in the same range as the one for a coal-fired power plant.

8.1.6 Backup with fuel cells

Fuel cells have excellent part load behaviour. This is shown in **Figure 8-5** for a PAFC. Even a better part load behaviour is illustrated in /Bokämper; Erdmann 2001/ for a PEFC and a SOFC. All three fuel cells have an approximately constant electrical efficiency in the range of 50 -100 % of the rated power. Thus, the utilization degree ratio is assumed to be one and the specific backup costs are reduced to a simplified equation:

$$s_b = s_{c,s} \cdot r_{fix,c,s} \cdot \left(1 - CC_R \cdot \frac{f_c}{f_r} \right) \tag{8-21}$$

Using CHP plants as backup plants requires the consideration of the heat supply besides the power generation. The heat supply has to be ensured. This requirement can be assured by storage technologies.
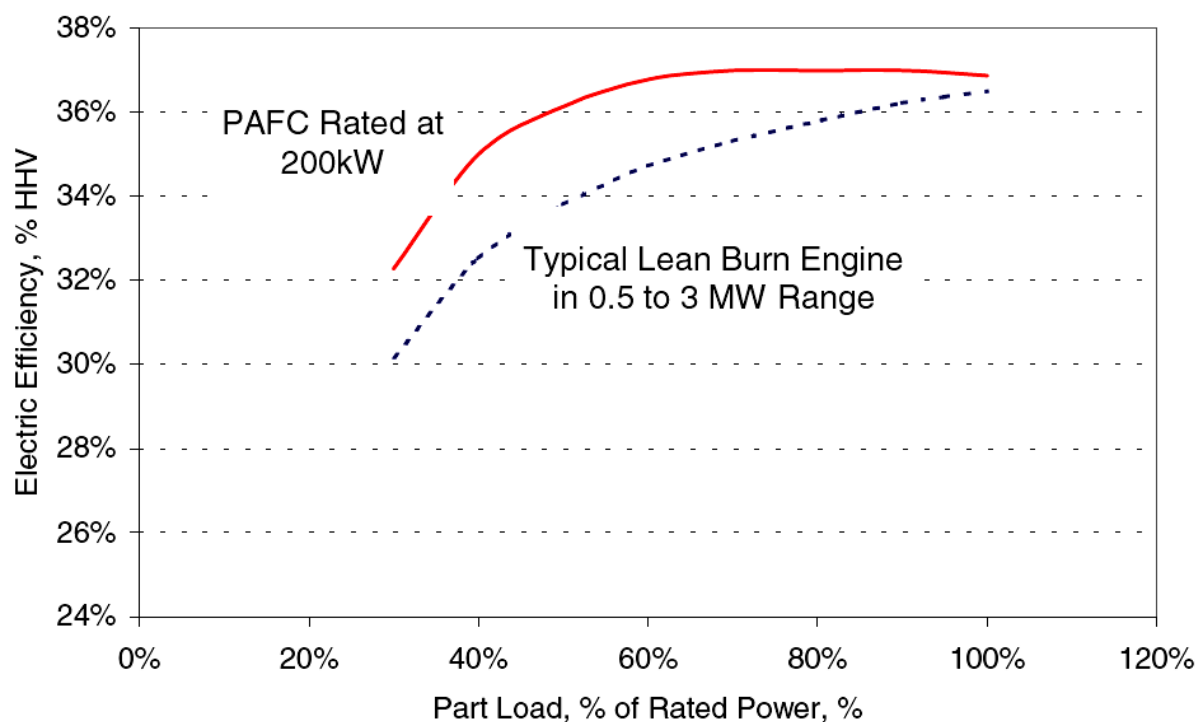
Figure 8-5:   Part load behaviour of 200 kW PAFC /Energy Nexus Group 2002/

HHV: higher heating value

8.1.7   Backup with wind turbines

Technically it is possible to operate wind turbines below the optimal efficiency by suboptimal adjustment of the blades. This enables the operators of wind turbines to supply reserve capacity. It is assumed that the efficiency of the wind turbine is reduced as far as the utilization degree ratio is 1.1.

8.1.8   External backup costs

The external backup costs are calculated with equation (8-20) and the derived or estimated values for the variables which are given in **Table 8-6** and **Table 8-7**. **Table 8-8** summarizes the ranges of the external backup costs. It can be seen that the external backup costs, which should be attributed to the wind turbines and PV systems, are estimated to be in the range of 0.0-3.6 €-Cent/kWh$_{el}$. The lower estimate is found for the wind turbine and the biomass system whereas the upper estimate is found for the fossil power plants. Before the technologies can be compared, the internal backup costs should be calculated. This is performed in the following chapter.

Table 8-6: Components for the calculation of external backup costs

Penetration R	WT Enercon E66		PV Germany mc-Si future	
	5 %	10 %	5 %	10 %
CC_R	19-28 %	16-24 %	5-15 %	2-15 %
f_r	2,500 h/a		905 h/a	

Table 8-7: Components of the backup plant for the calculation of external backup costs

Backup plant	$\zeta_{c,s}/\zeta_{c,m}$		f_c	$r_{fix,c,s}$	$s_{c,s}$ ($€$-Cent/kWh$_{el}$)
	5 %	10 %			
Fossil C-IGCC	1.001-1.003	1.002-1.006	5,000 h/a	5 %	6.45-19.13
Fossil NG-GS	1.005-1.020		5,000 h/a	5 %	2.99-9.13
BM CFBC-additive	1.001-1.003	1.002-1.006	5,000 h/a	5 %	0.66-2.30
SOFC 250 kW hydrogen	1.0		5,000 h/a	95 %	0.95-2.56
Nordex N80 offshore	1.1		4,000 h/a	90 %	0.10-0.30

Table 8-8: External backup costs ($€$-Cent/kWhel)

Power plant	WT Enercon E66		PV Germany mc-Si future	
Penetration R	5 %	10 %	5 %	10 %
Fossil C-IGCC	0.3-1.6	0.3-1.6	0.2-1.7	0.1-1.8
Fossil NG-GS	0.3-3.6	0.2-1.9	0.3-3.6	0.2-2.0
BM CFBC-additive	0.0-0.2	0.0-0.2	0.0-0.2	0.0-0.2
SOFC 250 kW hydrogen	0.4-1.5	0.5-1.7	0.2-1.8	0.2-2.2
Nordex N80 offshore	0.1-0.2	0.1-0.2	0.0-0.3	0.0-0.3

8.2   Calculation of internal backup costs

For the calculation of internal backup costs, the same approach as for the external backup costs is performed. The only difference is that the internal costs are used for the component $s_{c,s}$ and that the ratio $r_{fix,c,s}$ describes not the contribution of the fixed emissions (or external costs) to the total specific emissions but the contribution of the fixed internal costs to the total internal costs. Thus, the estimations of these parameters are listed in **Table 8-9**. The results of the calculation are displayed in **Table 8-10** showing the range of the internal backup costs of the different backup plants for the considered wind turbines and PV systems. Internal backup costs are in the range of 0.2-14.4 €-Cent/kWh$_{el}$. The lower values are found for the fossil power plants while the upper values are found for the fuel cell and the wind turbine.

It should be noted that these calculations are only rough estimations as most of the calculations above. This is mainly caused by the poor data quality which is available for the ratio of utilization degrees, the external costs, the internal costs and the capacity credit.With the calculation of the internal and external backup costs the total backup costs of the power generation technologies can be compared. This is performed in the next chapter.

Table 8-9:   Components of the backup plant for the calculation of the internal backup costs

Backup plant	$r_{fix,c,s}$	$s_{c,s}$ (€-Cent/kWh$_{el}$)
Fossil C-IGCC	30 %	3-7
Fossil NG-GS	10 %	4-6
BM CFBC-additive	20 %	9-15
SOFC 250 kW hydrogen	60 %	17-27
Nordex N80 offshore	90 %	5-8

Table 8-10:   Internal backup costs (€-Cent/kWh$_{el}$)

Power plant	WT Enercon E66		PV Germany mc-Si future	
Penetration R	5 %	10 %	5 %	10 %
Fossil C-IGCC	0.4-1.6	0.5-1.7	0.2-1.8	0.2-2.1
Fossil NG-GS	0.5-2.4	0.4-1.4	0.4-2.5	0.2-1.5
BM CFBC-additive	0.9-2.5	1.1-2.7	0.4-2.9	0.4-3.3
SOFC 250 kW hydrogen	4.5-10.0	5.3-11.0	1.7-11.7	1.7-14.4
Nordex N80 offshore	3.4-6.5	3.2-6.1	2.5-7.1	2.0-7.3

8.3   Calculation of total backup costs

The external and internal backup costs should be summed up to the total backup costs which are listed in **Table 8-11**. It can be seen that the estimated backup costs of the fuel cell as well as the wind turbine are in a range of 1.9-16.6 €-Cent/kWh$_{el}$. The estimated backup costs of the coal-fired IGCC power plant, the natural gas-fired power plant and the biomass system are in the range of 0.4-6.1 €-Cent/kWh$_{el}$. This results in a preference for the latter technologies for the use as backup power plants. The reasons for the high backup costs of the former technologies are the high internal costs for the fuel cell and the high share of fixed costs together with the high utilization degree ratio for the wind turbine. Due to these results the final comparison assumes backup costs in the range of 0.4-6.1 €-Cent/kWh$_{el}$ for wind turbines as well as PV systems. Since solar thermal power plants are also depending on the fluctuating radiation of the sun the considered power plant of this type is also burdened with this backup cost range. These rough estimates should be improved in further research.

Table 8-11:   Total backup costs (€-Cent/kWh$_{el}$)

Power plant	WT Enercon E66		PV Germany mc-Si future	
Penetration R	5 %	10 %	5 %	10 %
Fossil C-IGCC	0.7-3.2	0.8-3.3	0.4-3.5	0.4-4.0
Fossil NG-GS	0.9-6.0	0.6-3.3	0.7-6.1	0.4-3.5
BM CFBC-additive	1.0-2.7	1.1-2.9	0.5-3.1	0.5-3.5
SOFC 250 kW hydrogen	4.9-11.5	5.8-12.7	1.9-13.5	1.9-16.6
Nordex N80 offshore	3.5-6.8	3.3-6.3	2.5-7.4	2.0-7.6

9 Comparison of the social costs of power generation

The estimation of the external, internal and backup costs in the previous chapters is merged in this chapter which compares the technologies on the basis of these types of costs. All estimations concerning greenhouse gases are based on the assumption of the avoidance cost approach described in chapter 4. It is assumed that this approach will be commonly accepted until 2010. The results are illustrated in **Figure 9-1**. The filled parts of the bars display the lower estimate of the external, internal and backup costs while the striped parts of the bars display the range between the lower and upper estimate.

If all three types of costs are calculated with their lower estimates the ranking in **Table 7-2** does not change by the inclusion of the backup costs (see **Table 9-1**). However, the ranking does changes if all three types of costs are calculated with their upper estimates (see **Table 9-1** compared to **Table 7-3**). Thus, the river power plant has lower social costs than the wind turbines which have additional 6.1 €-Cent/kWh$_{el}$ backup costs. The solar thermal power plant changes from rank 5 to rank 8 due to the additional backup costs. In other respects, the ranking is unchanged.

Table 9-1: Ranking of the selected examples under consideration of quantifiable external, internal and backup costs (abbreviations are linked in **Table 6-2**)

Rank	Lower estimate for all types of costs	Upper estimate for all types of costs
1	Fossil FfE-Nuclear	Fossil FfE-Nuclear
2	WT Nordex N80 offshore	Water River-3.1
3	WT Enercon E66	WT Nordex N80 offshore
4	Fossil NG-GS	WT Enercon E66
5	ST Parabolic-trough	Fossil NG-GS
6	Water River-3.1	GT HDR
7	Fossil C-IGCC	BM CFBC +additive
8	BM CFBC +additive	ST Parabolic-trough
9	Fossil L-IGCC	BF FG+FGC
10	GT HDR	PV Spain mc-Si future
11	BF FG+FGC	Fossil C-IGCC
12	SOFC 250 kW natural gas	Fossil L-IGCC
13	PV Spain mc-Si future	SOFC 250 kW hydrogen
14	SOFC 250 kW hydrogen	SOFC 250 kW natural gas
15	PV Germany mc-Si future	PV Germany mc-Si future
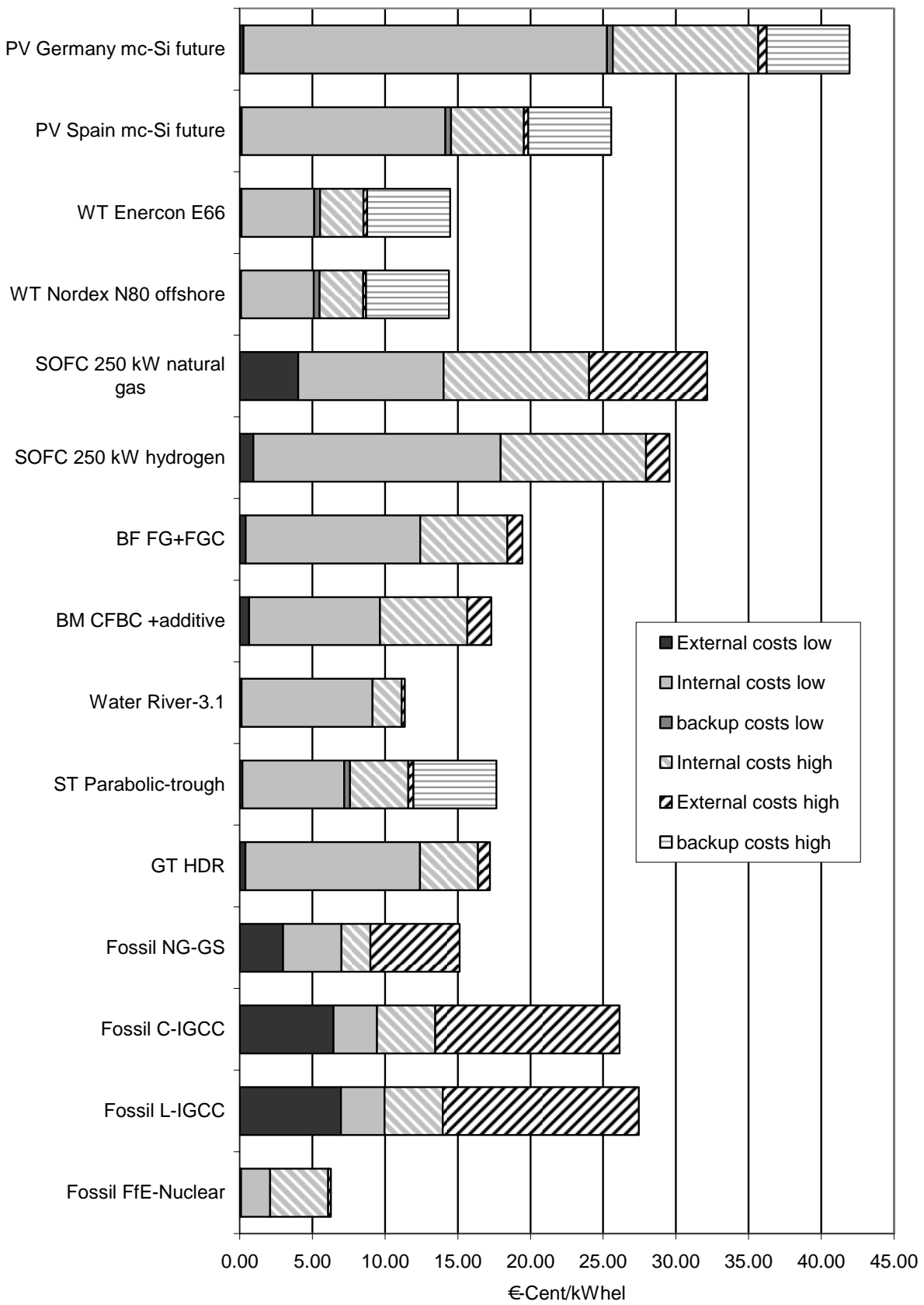
Figure 9-1:   Comparison of the technologies with quantifiable internal, external and backup costs (in €$_{2003}$-Cent/kWh$_{el}$)

Altogether, five technology clusters can be distinguished by their social costs with the upper estimates. The first cluster (< 10 €-Cent/kWh$_{el}$) includes the nuclear power plant alone which has by far the lowest social costs. In the range of 10-15 €-Cent/kWh$_{el}$, the second cluster can be situated with the river power plant and the wind turbines. Cluster three includes the bio-fuelled CHP system, the biomass power plant, the solar thermal power plant, the geothermal power plant and the natural gas-fired power plant. They have social costs in the range of 15-20 €-Cent/kWh$_{el}$. The fourth cluster includes technologies with social costs in the range of 20-35 €-Cent/kWh$_{el}$. Technologies with such high costs are the PV systems in Spain, the fuel cells and the coal or lignite-fired power plants. Within in this cluster, PV systems as well as fuel cells have a future trend of cost reduction which may enable them to change to another cluster with a lower cost range. The fifth cluster includes PV systems in Germany with social costs of more than 35 €-Cent/kWh$_{el}$.

In the following, a sensitivity analysis is performed with another approach for global warming which is used in many publications. It is an avoidance costs approach with the goal to give the real willingness to pay for CO_2 reductions of the present generation. Therefore, the German goal of CO_2 reduction in the Kyoto protocol is taken because it was determined in a political discourse and the politicians were elected as the representatives of the people. The goal of Germany is to reduce national CO_2 emissions from 1990 to 2010 by 25 %. This is analysed with the model E^{3}Net described in /Fahl et al. 1999/. The result of this analysis is that the marginal avoidance costs of 1 t CO_2 in 2010 are 38 DM$_{1995}$ (ca. 19 €/tCO$_2$). This estimation is similar to several other studies with similar goals (cf. /Friedrich; Bickel 2001/). The approach shows the real willingness to pay for the avoidance of CO_2-Emissions in 2010. However, the willingness to pay in the years after 2010 is not available. Nevertheless, it can be assumed that the willingness to pay after 2010 is at minimum the willingness to pay in 2010 because it can be used as a reference value for further discussions on reductions. Despite showing the real willingness to pay, the sustainability goals are difficult to achieve with this approach. This results from deviant positions of people. On the one hand, most people agree to sustainability goals, e.g. equity between generations, on the other hand, most people do not want to pay the amount of money which would be necessary to reach the goals certainly. Thus, the present willingness to pay is not sufficient to accomplish the avoidance cost approach developed in this study. Therefore, the sensitivity analysis with the real willingness to pay is performed.

A calculation of the social costs including the value of 19 €/tCO$_2$ for the avoidance of greenhouse gases results in a different ranking of the technologies compared to the base case. This is shown in **Figure 9-2**. The figure illustrates that fossil-fuelled power plants have lower social costs than renewable energy systems. Additionally, **Table 9-2** shows the different ranking compared to **Table 9-1**.

Table 9-2:   Ranking of the selected examples under consideration of quantifiable external, internal and backup costs with carbon dioxide avoidance costs of 19 €/tCO_2 (abbreviations are linked in **Table 6-2**)

| Rank	Lower estimate for all types of costs	Upper estimate for all types of costs
1	Fossil FfE-Nuclear	Fossil FfE-Nuclear
2	Fossil NG-GS	Fossil NG-GS
3	Fossil C-IGCC	Fossil C-IGCC
4	WT Nordex N80 offshore	Fossil L-IGCC
5	Fossil L-IGCC	Water River-3.1
6	WT Enercon E66	WT Nordex N80 offshore
7	ST Parabolic-trough	WT Enercon E66
8	Water River-3.1	GT HDR
9	BM CFBC +additive	BM CFBC +additive
10	SOFC 250 kW natural gas	ST Parabolic-trough
11	GT HDR	BF FG+FGC
12	BF FG+FGC	SOFC 250 kW natural gas
13	PV Spain mc-Si future	PV Spain mc-Si future
14	SOFC 250 kW hydrogen	SOFC 250 kW hydrogen
15	PV Germany mc-Si future	PV Germany mc-Si future
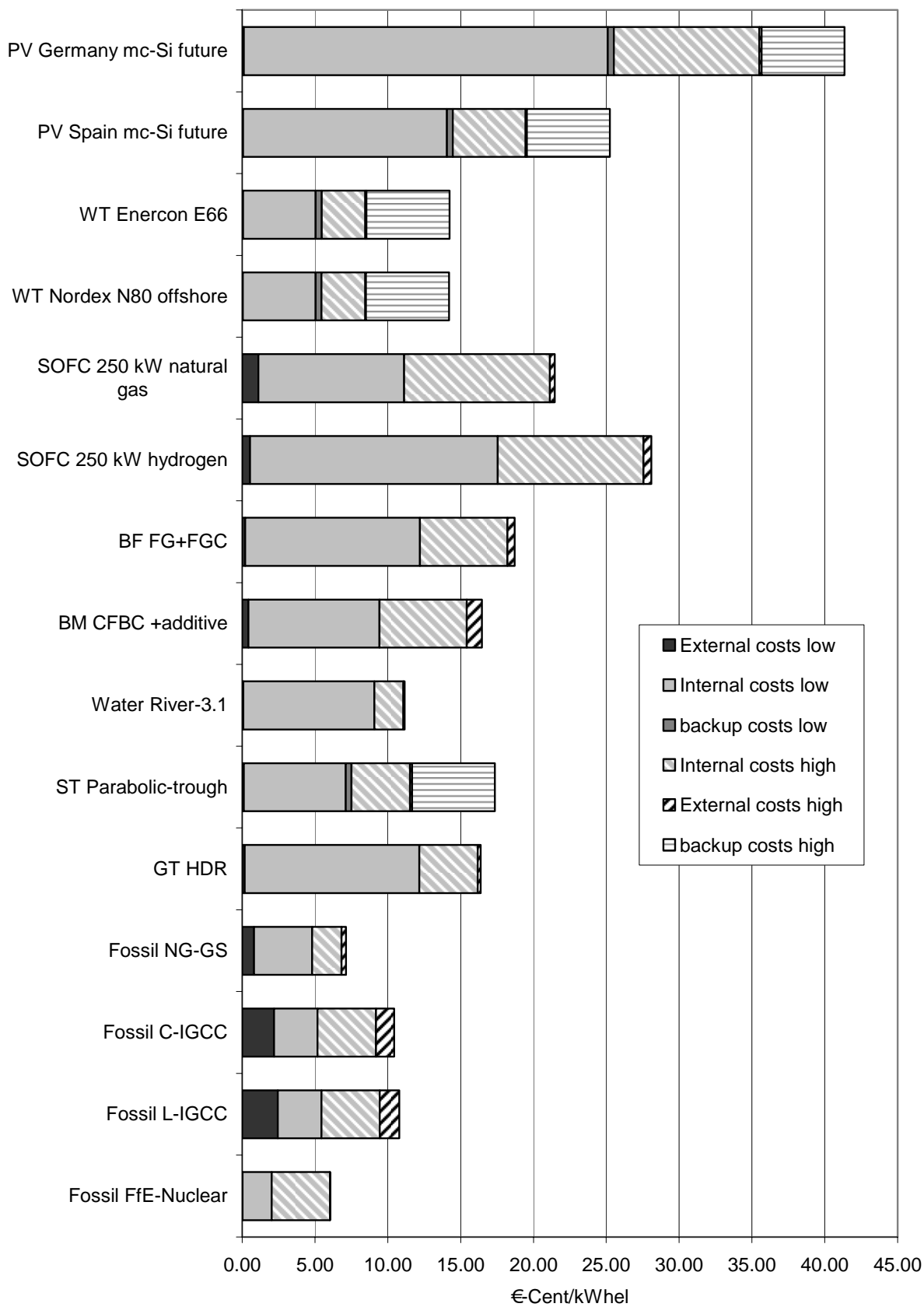
Figure 9-2: Comparison of the technologies with quantifiable internal, external and backup costs with avoidance costs of 19 €/tCO$_2$ (in €$_{2003}$-Cent/kWh$_{el}$)

10   Conclusions

This study makes the attempt to give a comparison of the external and internal costs of different power generation technologies in the year 2010 in order to support the decision-making process of future power plant investments in the framework of a sustainable development. In chapter 3 and 4, the uncertainties inherent in the estimation of external costs are described. Only a part of the environmental aspects corresponding to emissions and no social aspects are taken into account. Therefore, there are many issues which should be analysed in more detail in order to get a more confident comparison of possible future power plants. Nevertheless, the life cycle analysis in chapter 5 gives considerable life cycle data for the analysed technologies. This database is used for the estimation of the external costs in chapter 6 which is based on updated factors of damage and avoidance costs of the emissions considered. The results show that greenhouse gases have the main influence on the external cost estimates. These results for global warming due to greenhouse gases are discussed in chapter 4. Global warming and the issue of discounting future impacts are considered to be the hot spots in the external costs discussion. In chapter 4, it is described why an emission reduction goal has to be constituted in a social, political and scientific discourse in order to estimate the avoidance costs for greenhouse gas emissions. This is required because the damages are difficult to quantify. However, it is not sufficient to have a reduction goal only for the coming few years such as the Kyoto Protocol with reduction goals for 2008-2012. A reduction goal for the coming decades is required because power plant investments have a planning horizon of several decades. Since there is no globally ratified reduction goal, an attempt is made to estimate a possible reduction goal based on political ratifications and scientific recommendations fulfilling sustainability criteria. At present, the willingness to pay is not high enough, however, it is assumed to increase. With this assumption, the external costs are estimated for different technologies. Nevertheless, a sensitivity analysis is performed in chapter 9 showing the results with the assumption that the present willingness to pay does not change in the future. The comparison in chapter 6 shows that external costs of power generation technologies using renewable energies and nuclear power plants are in the range of 0.03-3.79 €-Cent/kWh$_{el}$ whereas the external costs of power generation technologies using organic fossil fuels are in the range of 3.37-27.98 €-Cent/kWh$_{el}$. However, this comparison only takes into account the quantifiable environmental and human health aspects. Internal costs are estimated in chapter 7. The comparison of the internal costs shows that, in contrast to the external costs, fossil-fuelled power plants have the lowest internal costs compared to the other technologies analysed. This trade-off between external and internal costs requires a comparison of the social costs which are the sum of internal and external costs. Beforehand, photovoltaic systems and wind turbines are burdened with additional backup costs. Backup costs arise due to the fluctuating power supply from the photovoltaic systems and wind turbines. This variability requires controllable power plants, e.g. fuel fired power plants, which assure that power is sup-

plied without interruptions. The costs for this backup service are added to the respective photovoltaic systems and wind turbines. These backup costs are estimated in chapter 8 and added to the external and internal costs of the power plants concerned. The final comparison in chapter 9 shows five social cost clusters of the analysed technologies for the year 2010 with the assumption that society is willing to achieve the sustainability goal of limiting the temperature increase due to global warming to a maximum of ca. 2 °C:

- Cluster 1 (< 10 €-Cent/kWh$_{el}$):

  Nuclear power plants

- Cluster 2 (10-15 €-Cent/kWh$_{el}$):

  Wind turbines and river power plants

- Cluster 3 (15-20 €-Cent/kWh$_{el}$):

  Biomass power plants, bio-fuelled CHP systems, solar thermal power plants, geothermal power plants and natural gas-fired power plants

- Cluster 4 (20-35 €-Cent/kWh$_{el}$):

  PV systems in Spain, fuel cells, coal-fired power plants and lignite-fired power plants

- Cluster 5 (>35 €-Cent/kWh$_{el}$):

  PV systems in Germany

Beyond 2010, shifts between these clusters are possible for many technologies:

Nuclear power plants have the lowest social costs. However, the probability of occurrence, e.g. of core melt, misuse of plutonium and terror acts, which is inherent in the use of nuclear power, is extremely small but the extent of potential damage is enormous. /Beck; May 2003/ state that the consequential damage costs for the Tschernobyl catastrophe will be 600,000 million € until 2015. A risk of such type is called Damocles risk /WBGU 1998/. It lies partly in the transition area and partly in the prohibited area (cf. chapter 4.4). Therefore, the standard risk policy using the expectance value for assessment is debated. Special risk policy is demanded which is not developed yet. If these impacts or necessary avoidance technologies for inherently save nuclear power plants are included in the external or internal cost estimation it may be possible that nuclear power plants are responsible for higher social costs and may thus shift to another cluster.

Wind turbines have potentials to shift to cluster 1. These potentials arise from the reduction potentials of their internal costs. This is possible due to large wind potentials and a low learning factor.

In contrast, river power plants only have small cost reduction potentials. Electricity costs from river power plants will increase because possible plant sites are noticeably rare, environmental restrictions are imposed and external costs are already very low.

Solar thermal power plants and geothermal power plants both have high internal cost reduction potentials because they are at the beginning of their market development. Future developments may lead to a shift to lower social cost clusters.

The cost reduction potentials of biomass power plants, bio-fuelled CHP systems and natural gas-fired power plants, which are located in cluster 3 are small because the plant components are already well developed. Internal and external costs will probably decrease but a shift to a lower cost cluster is not expected.

PV systems and fuel cells have large internal cost reduction potentials because the technological development is not finished yet. This enables both technologies to change to another cluster with a lower cost range. Experiences with the development of photovoltaic systems support this assumption whereas sufficient experiences with fuel cells are not available. However, many interesting portable, mobile and stationary applications for fuel cells are possible so that a fast market development seems probable.

Coal and lignite-fired power plants are located in cluster 4. Internal cost reduction is not expected due to the well developed technologies. Nevertheless, external cost reduction is possible with sequestration technologies for carbon dioxide and other flue gas cleaning technologies. This may reduce external costs. However, additional components for the power plant will increase internal costs. This trade-off has to be analysed in order to recognize the optimal configuration. The analysis is not performed in this study. Therefore, a cost reduction tendency can not be stated.

If society can not be convinced to follow the sustainability goals described in this study and only the current willingness to pay is used (cf. chapter 9) the ranking of the technologies is different as compared in **Table 10-1**. For this comparison, the upper estimates are used. The comparison shows that the ranking with the current willingness to pay (with avoidance costs of 19 €/tCO$_2$) ranks fossil-fired power plants at the top ranks. In contrast, the ranking with a willingness to pay which is necessary to achieve assumed sustainability goals (with avoidance costs of 225 €/tCO$_2$) ranks fossil-fired power plants in the middle ranks. The other power generation technologies have a similar order. From this sensitivity analysis it can be derived that the ranking of fossil-fired power generation technologies depends significantly on the willingness to pay.

In further research it is recommended to reduce the uncertainties inherent in the whole calculation of external costs. Additionally, it is necessary to study the impact pathways of more than just a few emissions, e.g. impacts of other emissions, impacts to water, impacts to ecosystems, noise, land occupation, visual effects, vibrations and effects from accidents. Especially, in the case of biomass, ammonia seems to have a significant contribution to the external costs but it is not analysed in this study. For detailed calculation of external costs, it is necessary to include also emissions which have minor contributions, e.g. nitrous oxide. Using the assumptions of this study, global warming shows the largest contribution to external costs. Therefore, it is recommended to constitute an emission reduction path for the coming decades which enables the estimation of the required avoidance costs. Besides uncertainties

in the impact pathways, there are also uncertainties in the life cycle inventories of the analysed technologies. The life cycle analysis in this study uses out-dated life cycle data for upstream processes. Therefore, it is recommended to implement life cycle data from /Dones et al. 2003/ or other updated studies. Additionally, it is necessary to update the life cycle inventory regularly because process chains change, particularly in the case of new technologies. For instance, the life cycle inventory of photovoltaic systems will probably be influenced by the development of recycling processes and the use of solar grade silicon which is produced directly for photovoltaic applications. An example for an out-dated life cycle inventory is the hydrogen-fuelled fuel cell in chapter 5.3. It uses out-dated data for power generation by wind turbines for the production of the hydrogen. An update seems necessary in order to improve the comparability with other updated technologies.

Table 10-1:   Ranking of the selected examples under consideration of quantifiable external, internal and backup costs with carbon dioxide avoidance costs of 19 €/tCO$_2$ and with avoidance costs of 225 €/tCO$_2$ (abbreviations are linked in **Table 6-2**)

Rank	Avoidance costs of 19 €/tCO$_2$	Avoidance costs of 225 €/tCO$_2$
1	Fossil FfE-Nuclear	Fossil FfE-Nuclear
2	Fossil NG-GS	Water River-3.1
3	Fossil C-IGCC	WT Nordex N80 offshore
4	Fossil L-IGCC	WT Enercon E66
5	Water River-3.1	Fossil NG-GS
6	WT Nordex N80 offshore	GT HDR
7	WT Enercon E66	BM CFBC +additive
8	GT HDR	ST Parabolic-trough
9	BM CFBC +additive	BF FG+FGC
10	ST Parabolic-trough	PV Spain mc-Si future
11	BF FG+FGC	Fossil C-IGCC
12	SOFC 250 kW natural gas	Fossil L-IGCC
13	PV Spain mc-Si future	SOFC 250 kW hydrogen
14	SOFC 250 kW hydrogen	SOFC 250 kW natural gas
15	PV Germany mc-Si future	PV Germany mc-Si future

In order to enable a comparison of different technologies many aspects should be considered. For instance, the life cycle inventory of power generation in the case of combined heat and power plants is sensitive to the applied allocation method and the assumed parameters.

Therefore, a comparison requires comparable allocation methods. Also the comparison of unknown particulates mixes is not appropriate for detailed analyses. A classification in PM10 and PM2.5 is necessary in order to apply the respective exposure-response functions because the impact of a mixture of particulates with unknown diameters is difficult to estimate.

Generally, a life cycle analysis does not consider the place and time of the substance emissions. However, for detailed calculations it is essential to know the emission site in order to apply the impact pathway approach. This disaggregation of emissions is recommended in more detailed future research. Since most of the emissions from renewable energy technologies are caused in the production process, it is not consistent to distribute them over the amount of electricity generation because it may be possible that the plant considered is not able to produce as much as estimated. Moreover, the power generation itself does not produce emissions and thus no external costs. In contrast, the emissions of fossil-fired power plants mainly arise in the operation phase. However, the damages of emissions which arise in future operation can only be estimated including many inherent uncertainties. Thus, the comparison of a technology contributing the main part of the emissions in the building phase, e.g. wind turbine systems, with a technology contributing the main part of the emissions in the operation phase, e.g. coal-fired power plants, is not consistent. It is suggested that this inconsistency is considered in future research.

The comparison of three different studies in chapter 5 shows that the results vary significantly. This difference is assumed to be based on different assumptions, e.g. with regard to upstream processes and the electricity mix. It is recommended to determine the hot spots of the technologies and their sensitivity to different assumptions in order to enable a comparison and an understanding of significantly varying results of different studies.

Chapter 8 estimates the backup costs of power generation technologies with fluctuating supply. Therefore, an equation is applied which simplifies the complex behaviour of power grids in order to enable the estimation of backup costs. However, the capacity credit and the ratio of utilization degrees used in this equation should be analysed in more detail. The available values are determined with real or assumed regional power grids which are not transferable to the European power grid.

Altogether, it can be stated that the variety of uncertainties and the lack of good quality data requires extensive further research in order to enable improved and more detailed comparison of power generation technologies with regard to external costs. Additionally, considerable discourses on sustainable development are necessary. These discourses should include economic, environmental and social aspects. With the outcomes of these discourses it should be possible to compare power generation technologies not only with their internal costs but also with their external costs and under consideration of social aspects.

11   Annotations

11.1   Exchange rates

For US$ figures, the inflation is calculated with U.S. consumer price index for all urban con-
sumers given in **Table 11-1**. The U.S. consumer price index is used because it has no inter-
ruptions in the 1990s in contrast to the European one. In the case of € figures, in the years
1997-2003, the inflation is calculated with the harmonised annual average consumer price
index of EU-15 given in **Table 11-2**.

Table 11-1:   Annual average of U.S. consumer price index for all urban consumers /U.S. Depart-
ment of Labor 2004/

Year	Inflation index
1990	130.7
1991	136.2
1992	140.3
1993	144.5
1994	148.2
1995	152.4
1996	156.9
1997	160.5
1998	163.0
1999	166.6
2000	172.2
2001	177.1
2002	179.9
2003	184.0

Table 11-2: Harmonised annual average consumer price index of EU-15 /Eurostat 2004/

Year	Inflation index
1997	101.7
1998	103.0
1999	104.3
2000	106.2
2001	108.6
2002	110.8
2003	113.0

The exchange rates between US$ and € are listed in **Table 11-3**.

Table 11-3: Exchange rates for the first trade day of the respective year between € and US$ /Triacom 2004/

Year	€ / US$
1999	0.8462
2000	0.9944
2001	1.0566
2002	1.1069
2003	0.9534

With **Table 11-1**, **Table 11-2** and **Table 11-3**, the exchange ratios in this study are those given in **Table 11-4**.

Table 11-4: Exchange ratios

€$_{2003}$ / US\$$_{1990}$	1.342
€$_{2003}$ / €$_{2000}$	1.064

11.2 Conversion factors

In some studies emissions are given in tC and in others in tCO_2. For harmonisation, this study calculates with tCO_2. The conversion factor is based on the atomic mass of C and CO_2. It is 12.01 u for C and 44.01 u for CO_2. In the form of gaseous emissions 1 tC corresponds to 44.01/12.01 tCO_2 or 3.664 tCO_2. Thus, costs per emissions can be converted from 1 currency unit/tC to 0.2729 currency units/tCO_2.

Bibliography

/Azar; Rodhe 1997/

> Azar, C., Rodhe, H.: Targets for stabilization of atmospheric CO_2. In: Science Vol. 276, Issue 5320, p. 1818-1819, 1997
> http://www.sciencemag.org/cgi/content/full/276/5320/1818

/Bartmann 1996/

> Bartmann, H.: Umweltökonomie - ökologische Ökonomie. Kohlhammer. Stuttgart 1996

/Beck; May 2003/

> Beck, J., Hanne, M.: Offene Rechnungen. In: Neue Energie, Issue 12 2003

/BMU 2004/

> Bundesministerium für Umwelt, Naturschutz und Reaktorsicherheit (BMU) (Ed.): Ökologisch optimierter Ausbau der Nutzung erneuerbarer Energien in Deutschland. Stuttgart, Heidelberg, Wuppertal 2004
> http://www.bmu.de/files/nutzung_ee_lang.pdf

/BMWA 2003/

> Bundesministerium für Wirtschaft und Arbeit (BMWA): Research and Development Concept for Zero-Emission Fossil-Fuelled Power Plants - Summary of COORETEC. Berlin 2003
> http://www.bmwi.de/Redaktion/Inhalte/Downloads/doku-527-en,property=pdf.pdf

/BMWA 2004/

> Bundesministerium für Wirtschaft und Arbeit (BMWA): Lebenszyklusanalysen ausgewählter zukünftiger Stromerzeugungstechniken. Berlin 2004
> http://www.ier.uni-stuttgart.de/lci_bmwi (in press)

/Bokämper; Erdmann 2001/

> Bokämper, S., Erdmnn, G.: Wirtschaftlichkeit von Brennstoffzellen-Heizgeräten unter den Rahmenbedingungen eines liberalisierten Elektrizitäts- und Erdgasmarktes. In: VDI-Bereichte 1594: Fortschrittliche Energiewandlung und – anwendung. Düsseldorf 2001

/Borken et al. 1999/

> Borken, J., Patyk, A., Reinhardt, G.A.: Basisdaten für ökologische Bilanzierungen: Einsatz von Nutzfahrzeugen in Transport, Landwirtschaft und Bergbau. Braunschweig und Wiesbaden 1999

/Briem 2003/

> Briem, S.: ECLIPSE Gas-fired Combined Heat and Power systems – Internal Combustion Engines. Internet publication 2003
> http://www.ECLIPSE-eu.org/zip/gas_fired.zip

/Bundesverband Windenergie 2004/
        Bundesverband Windenergie e.V.. Internet publication 2004
        http://www.wind-energie.de

/BUWAL 1998/
        Bundesamt für Umwelt, Wald und Landschaft (BUWAL): Bewertung in Ökobi-
        lanzen mit der Methode der ökologischen Knappheit - Ökofaktoren 1997 - SRU
        297. Bern 1998

/Carter 2001/
        Carter, R.L.: EE 4345 – Semiconductor Electronics Design Project. Spring 2002.
        Lecture 09a. University of Texas at Arlington 2001
        http://www.uta.edu/ronc/4345sp02/lectures/L09a_4345_Sp02.pdf

/Chataignere; Le Boulch 2003/
        Chataignere, A., Le Boulch, D.: ECLIPSE Wind turbine (WT) systems. Internet
        publication 2003
        http://www.ECLIPSE-eu.org/zip/wind.zip

/Cherubini 2001/
        Cherubini, A.: Processo produttivo di moduli fotovoltaici in silicio policristallino.
        Thesis. Universita di Roma 1 La Sapienza. Roma, Italy 2001

/Clarkson; Deyes 2002/
        Clarkson, R., Deyes, K.: Estimating the Social Cost of Carbon Emissions. Gov-
        ernment Economic Service Working Paper 140. London 2002
        http://www.hm-treasury.gov.uk/media//2E817/SCC.pdf

/Cuperus 2003/
        Cuperus, M.A.T.: ECLIPSE Biomass systems. Internet publication 2003
        http://www.ECLIPSE-eu.org/zip/biomass.zip

/Danish Wind Industry Association 2003/
        Danish Wind Industry Association: Guided Tour on Wind Energy. Internet publi-
        cation 2003
        http://www.windpower.org/en/tour/index.htm

/Dany; Haubrich 2000/
        Dany, G., Haubrich, H.-J.: Anforderungen an die Kraftwerksreserve bei hoher
        Windenergieeinspeisung. In: Energiewirtschaftliche Tagesfragen, Issue 12, 2000

/De Moor et al. 2003/
        De Moor, H.C.C., Schaeffer, G.J., Seebregts, A.J., Beurskens, L.W.M., Durste-
        witz, M., Alsema, E., van Sark, W., Laukamp, H., Boulanger, P., Zuccaro, C.:
        Experience Curve Approach for more Effective Policy Instruments. Paper pre-
        sented at the 3rd World Conference on Photovoltaic Energy Conversion, Osaka,
        Japan, 2003
        http://www.ecn.nl/docs/library/report/2003/rx03046.pdf

/Dones et al. 2003/
> Dones, R., Bauer C., Burger B., Faist M., Frischknecht R., Heck T., Jungbluth N., Röder A.: Sachbilanzen von Energiesystemen: Grundlagen für den ökologischen Vergleich von Energiesystemen und den Einbezug von Energiesystemen in Ökobilanzen für die Schweiz. Paul Scherrer Institut Villigen, Swiss Centre for Life Cycle Inventories, Duebendorf, CH 2003

/EAA 2002/
> European Aluminium Association (EAA): LCA and its application to aluminium products. Internet publication 2002
> http://www.eaa.net/environment/lca.asp

/Eckhardt et al. 2002/
> Eckhardt, V., Kafermann, R., Lehmann, K.-P., Övermöhle, K., Rennert, I., Wollert, W.: Offshore Windenergie – Chancen und Herausforderungen im Überblick. In: Elektrie Vol. 56, Issue 7-9, 2002
> www.lco.lineas.de/pdf/artikel_elektrie_56.pdf

/E.E.I.G. 2004/
> European Economic Interest Grouping (E.E.I.G.): European Deep Geothermal Energy Programme. Internet publication 2004
> http://www.soultz.net

/Endres 2000/
> Endres, A.: Umweltökonomie. 2nd Edition. Kohlhammer. Stuttgart 2000

/Endres; Holm-Müller 1998/
> Endres, A., Holm-Müller, K.: Die Bewertung von Umweltschäden. Kohlhammer. Stuttgart 1998

/Energy Nexus Group 2002/
> Energy Nexus Group: Technology Characterization: Fuel Cells. Internet Publication. Arlington 2002
> http://www.epa.gov/chp/pdf/EPA%20Fuel%20Cell%20final%206-18-02.pdf

/European Commission 1999a/
> European Commission: ExternE – Externalities of Energy Vol. 7 Methodology 1998 Update. Luxemburg 1999

/European Commission 1999b/
> European Commission: ExternE – Externalities of Energy Vol. 8 Global Warming. Luxemburg 1999

/European Commission 1999c/
> European Commission: ExternE – Externalities of Energy Vol. 10 National Implementation. Luxemburg 1999

/European Parliament 2003/
> European Parliament and Council: Directive 2003/30/EC. Brussels 2003
> http://www.dft.gov.uk/stellent/groups/dft_roads/documents/page/dft_roads_0284 06.pdf

/European Commission 2004/
European Commission: Work Package 6: Revision of external cost estimates. In: New Elements for the Assessment of External Costs from Energy Technologies (NewExt). Final Report. Contract No. ENGI-CT2000-00129. 2004 (in press)

/Eurostat 2004/
Eurostat: FREE DATA, Longterm indicators, Economy and ecology, Prices, wages and finance, Consumer prices, Harmonised annual average consumer price indices. Internet publication 2004
http://europa.eu.int/comm/eurostat/newcronos/queen/display.do?screen=welcome&open=/&product=LT&depth=2&language=en

/EWEA 2004a/
European Wind Energy Association (EWEA): Wind Energy The Facts: An analysis of wind energy in the EU25. Internet publication 2004
http://www.ewea.org/06projects_events/proj_WEfacts.htm

/EWEA 2004b/
European Wind Energy Association (EWEA): Europe's Installed Wind Capacity – end 2003. Internet publication 2004
http://www.ewea.org/documents/europe_windata_jan20041.pdf

/Fahl et al. 1999/
Fahl, U., Schaumman, P., Remme, U.: E^3Net. In: Forum für Energiemodelle und Energiewirtschaftliche Systemanalysen in Deutschland (Hrsg.): Energiemodelle zum Klimaschutz in Deutschland. Physica-Verlag. Heidelberg 1999

/FfE 1996/
Forschungsstelle für Energiewirtschaft (FfE): Ganzheitliche energetische Bilanzierung der Energiebereitstellung: Energetische Untersuchung eines Steinkohlekraftwerkes. FfE 1996
http://www.ffe.de/download/gabie/sk_kw.pdf

/FfE 1999/
Forschungsstelle für Energiewirtschaft (FfE): Ganzheitliche energetische Bilanzierung der Energiebereitstellung (GaBiE) Teil VII Emissionen der Strombereitstellung aus thermischen und nuklearen Kraftwerken. FfE 1999
http://www.ffe.de/download/gabie/kw_emi.pdf

/Forschungszentrum Jülich 2003/
Forschungszentrum Jülich: Brennstoffzellenseiten. Internet publication 2003
http://www.fuelcells.de

/Frankl 1996/
Frankl, P.: Analisi del ciclo di vita di sistemi fotovoltaici. Ph.D. dissertation thesis. Universita di Roma 1 La Sapienza. Roma, Italy 1996

/Frankl et al. 2004/
Frankl, P., Corrado, A., Lombardelli, S.: ECLIPSE Photovoltaic (PV) Systems. Internet publication 2004
http://www.ECLIPSE-eu.org/zip/photovoltaic.zip

/Frankl; Gamberale 1998/

Frankl, P., Gamberale, M.: Analysis of Energy and CO_2 aspects of building integration of photovoltaic systems. BNL/NREL Workshop "PV and the environment 1998". Keystone, CO 1998

/Friedrich 2003a/

Friedrich, R.: Technology Assessment and Environmental Economics (Lecture summer term 2003). Stuttgart 2003
http://www.ier.uni-stuttgart.de/public/de/lehre/skripte/waste/index.html

/Friedrich 2003b/

Friedrich, R.: Energie und Umwelt (Vorlesung Sommersemester 2003). Stuttgart 2003
http://www.ier.uni-stuttgart.de/public/de/lehre/skripte/energumw/index.html

/Friedrich; Bickel 2001/

Friedrich, R., Bickel, P.: Environmental External Costs of Transport. Springer-Verlag. Berlin, Heidelberg 2001

/Frischknecht et al. 1996/

Frischknecht, R., Bollens, U., Bosshart, S., Ciot, M., Ciseri, L., Doka, G., Dones, R., Gantner, U., Hischier, R., Martin, A.: Ökoinventare von Energiesystemen. Zürich 1996

/Frischknecht 2003/

Frischknecht, R.: Ecoinvent Database Methodology. Presentation for Special LCA forum. ETH Lausanne December 5, 2003
http://www.ecoinvent.ch/download/Frischknecht_DF_eng.zip

/Gürzenich et al. 1998/

Gürzenich, D., Mathur, J., Bansal, N.K., Wagner, H.-J.: Cumulative Energy Demand for Selected Renewable Energy Technologies. In: The International Journal of Life Cycle Assessment, Vol. 3, Issue 2, 1998

/Harmon 2000/

Harmon, C.: Experience Curves of Photovoltaic Technology. IIASA Interim Report 2000
http://www.iiasa.ac.at/Publications/Documents/IR-00-014.pdf

/Hart; Hörmandinger 1998/

Hart, D., Hörmandinger, G.: Environmental benefits of transport and stationary fuel cells. In: Journal of Power Sources. Vol. 71, Issue 1-2, p. 348-353, 1998

/Hartmann 2001/

Hartmann, D.: Ganzheitliche Bilanzierung der Stromerzeugung aus regenerativen Energien. IER, Universität Stuttgart. Forschungsbericht Band 83. Stuttgart 2001

/Horlacher 2003/

Horlacher, H.-B.: Globale Potenziale der Wasserkraft. Externe Expertise für das WBGU-Hauptgutachten 2003 „Welt im Wandel: Energiewende zur Nachhaltigkeit". Berlin, Heidelberg 2003
http://www.wbgu.de/wbgu_jg2003_ex03.pdf

/IEA 2003/

International Energy Agency (IEA): Renewables Information. Online Database 2003
http://library.iea.org/renew/eng/ReportFolders/Rfview/Explorerp.asp

/IEA-PVPS 2001/

IEA-PVPS: Potential for Building Integrated Photovoltaics. Report IEA-PVPS T7-4 (Summary) 2001
http://www.oja-services.nl/iea-pvps/products/download/rep7_04.pdf

/IEA-PVPS 2002/

IEA-PVPS: Basics of PV. Internet Publication 2002
http://www.oja-services.nl/iea-pvps/pv/pv.htm

/IEA-PVPS 2003/

IEA-PVPS: TRENDS IN PHOTOVOLTAIC APPLICATIONS Survey report of selected IEA countries between 1992 and 2002. Internet publication 2003
http://www.oja-services.nl/iea-pvps/products/download/rep1_12.pdf

/IISI 2000/

International Iron and Steel Institute (IISI): Life cycle Inventory. Internet publication 2000
http://www.worldsteel.org/lci

/IPCC 2001a/

Intergovernmental Panel on Climate Change: Climate Change 2001: The Scientific Basis. Cambridge 2001
http://www.grida.no/climate/ipcc_tar/wg1/index.htm

/IPCC 2001b/

Intergovernmental Panel on Climate Change: Climate Change 2001: Impacts, Adaptation and Vulnerability. Cambridge 2001
http://www.grida.no/climate/ipcc_tar/wg2/index.htm

/IPCC 2001c/

Intergovernmental Panel on Climate Change: Climate Change 2001: Mitigation. Cambridge 2001
http://www.grida.no/climate/ipcc_tar/wg3/index.htm

/IPCC 2001d/

Intergovernmental Panel on Climate Change: Climate Change 2001: Synthesis Report. Cambridge 2001
http://www.grida.no/climate/ipcc_tar/vol4/english/index.htm

/ISET 2004/

Institut für Solare Energieversorgungstechnik (ISET): Renewable Energy Information System on Internet. Internet publication 2004
http://reisi.iset.uni-kassel.de

/Ito et al. 2004/

Ito, M., Kato, K., Komoto, K., Kichima, T., Sugihara, H., Kurokawa, K.: An Analysis of Variation of Very Large-Scale PV (VLS-PV) Systems in the World Deserts. Internet publication 2004
http://pv.ei.tuat.ac.jp/paper/wcpec3/wcpec3_ito.pdf

/Kaltschmitt et al. 2003/

Kaltschmitt, M., Merten, D., Fröhlich, N., Nill, M.: Energiegewinnung aus Biomasse. Externe Expertise für das WBGU-Hauptgutachten 2003 „Welt im Wandel: Energiewende zur Nachhaltigkeit". Berlin, Heidelberg 2003
http://www.wbgu.de/wbgu_jg2003_ex04.pdf

/Karkakoussis et al. 2000/

Karakoussis, V., Leach, M., van der Vorst, R., Hart, D., Lane, J., Pearson, P., Kilner, J.: Environmental Emissions of SOFC and SPFC System Manufacture and Disposal. Internet publication 2000
http://www.dti.gov.uk/energy/renewables/publications/pdfs/f100164.pdf

/KEMA 1999/

KEMA: LCA of different thermal conversion technologies. Phase 2: data collection. KEMA Report Nr. 530144-KPS/MEC 99-3039, 1999

/Krewitt et al. 2004/

Krewitt, W., Pehnt, M., Fischedick, M.,Temming, H. (Ed.): Brennstoffzellen in der Kraft-Wärme-Kopplung – Ökobilanzen, Szenarien, Marktpotenziale. Berlin 2004

/Ledjeff-Hey et al. 2001/

Ledjeff-Hey, K., Mahlendorf, F.,Roes, J.: Brennstoffzellen – Entwicklung, Technologie, Anwendung. C.F. Müller. Heidelberg 2001

/Luterbacher et al. 2004/

Luterbacher, J., Dietrich, D., Xoplaki, E., Grosjean, M., Wanner, H.: European Seasonal and Annual Temperature Variability, Trends and Extremes Since 1500. In: Science, Vol 303, Issue 5663, p. 1499-1503, 2003
http://www.sciencemag.org/cgi/reprint/303/5663/1499.pdf

/Lux 1999/

Lux, R.: Auswirkungen fluktuierender Einspeisung auf die Stromerzeugung konventioneller Kraftwerkssysteme. IER, Universität Stuttgart. Forschungsbericht Band 60 1999

/Lux et al. 1999/

Lux, R. Sontow, J., Voß, A., Kaltschmitt, M.: Windstrom im Kraftwerksverbund. In: Energiewirtschaftliche Tagesfragen, Issue 8, 1999

/Majer 2003a/

Majer, H.: Umwelt- und Ressourcenökonomik (Grundlagen der Umweltöko-
nomik). Vorlesung Wintersemester 2003/2004. Stuttgart 2003
http://www.ivr.uni-stuttgart.de/umwelt/downloads/Umwelt_Skript.pdf

/Majer 2003b/

Majer, H.: Nachhaltige Entwicklung – Leitbild für Zukunftsfähigkeit. In: WISU,
Issue 7, p. 935-942, 2003

/Marheineke 2002/

Marheineke, T.: Lebenszyklusanalyse fossiler, nuklearer und regenerativer Stro-
merzeugungstechniken. IER, Universität Stuttgart. Forschungsbericht Band 87
2002

/McCulloch et al. 2000/

McCulloch, M., Raynolds, M., Laurei, M.: Life-Cycle Value Assessment of a
Wind Turbine. Pembina Institute for Appropriate Development. Alberta, Canada
2000
http://www.pembina.org/pdf/publications/windlcva.pdf

/Mulligan et al. 2004/

Mulligan, W.P., Rose, D.H., Cudzinovic, M.J., De Ceuster, D.M., McIntosh,
K.R., Smith, D.D., Swanson, R.M.: Manufacture of Solar Cells with 21 % Effi-
ciency. White Paper SunPower Cooperation. Internet publication 2004
http://www.sunpowercorp.com/html/Technical%20Papers/pdf/bmpaper.pdf

/Nakicenovic; Riahi 2003/

Nakicenovic, N., Riahi, K.: Model Runs With MESSAGE in the Context of the
Further Development of the Kyoto Protocol. Externe Expertise für das WBGU-
Sondergutachten "Welt im Wandel: Über Kioto hinausdenken. Kli-
maschutzstrategien für das 21. Jahrhundert". Laxenburg 2003
http://www.wbgu.de/wbgu_sn2003_ex03.pdf

/Neij et al. 2003/

Neij, L., Andersen, P.D., Durstewitz, M., Helby, P., Hoppe-Kilpper, M.,
Morthorst, P.E.: Experience Curves: A Tool for Energy Policy Assessment. Inter-
net publication. Lund, Sweden 2003
http://www.iset.uni-kassel.de/extool/Extool_final_report.pdf

/NTM 2000/

Network for Freight Transport and the Environment (NTM): Environmental data.
Internet publication 2000
http://www.ntm.a.se/eng-miljodata/frameset_inner.htm

/Pearce; Turner 1994/

Pearce, D.W., Turner, R.K.: Economics of natural resources and the environment.
9th Edition. Harvester Wheatsheaf. New York 1994

/Pehnt 2002/

Pehnt, M.: Ganzheitliche Bilanzierung von Brennstoffzellen in der Energie- und
Verkehrstechnik. Fortschritt-Berichte VDI, Reihe 6, Nr. 476. Heidelberg 2002

/PHOTON 2004/
PHOTON Spezial: Netzgekoppelte Solarstromanlagen 2004.

/Pick et al. 1998/
Pick, E., Wagner, H.-J., Bunk, O.: Kumulierter Energieaufwand von Windkraftanlagen. In: BWK, Vol. 50, Issue 11/12, 1998

/Rohrig et al. 2003/
Ensslin, C., Ernst, B., Rohrig, K., Schlögl, F.: Online-monitoring and prediction of wind power in German transmission system operation centres. ISET Kassel. Internet publication 2003
http://www.iset.uni-kassel.de/abt/FB-I/publication/03-06-17_EWEC.pdf

/Schmela 2004/
Schmela, M.: Sharp und der Rest der Welt. In: Photon – Das Solarstrom-Magazin, Issue 4, 2004

/Statistisches Bundesamt Deutschland 2004/
Statistisches Bundesamt Deutschland: Ausgewählte lange Reihen zu den Volkswirtschaftlichen Gesamtrechnungen ab 1970. Statistisches Bundesamt. Fachserie 18, Reihe S.21. Online publication 2004
http://www.destatis.de/download/veroe/lreihe04.pdf

/Swanson 2004/
Swanson R.M.: A Vision for Crystalline Silicon Solar Cells. Sunpower white paper. Internet publication 2004
http://www.sunpowercorp.com/html/Technical%20Papers/pdf/swanson.pdf

/Setterwall et al. 2003/
Setterwall, C., Münter, M., Sarközi, P., Bodlund, B.: ECLIPSE Bio-fuelled Combined Heat and Power Systems. Internet publication 2003
http://www.ECLIPSE-eu.org/zip/bio_fuelled.zip

/Setterwall et al. 2004/
Setterwall, C., Münter, M., Sarközi, P., Bodlund, B.: ECLIPSE Methodological guidelines. Internet publication 2004
http://www.ECLIPSE-eu.org/pdf/methodological_guidelines.pdf

/Slootweg; de Vries 2003/
Slootweg, H., de Vries, E.: Inside Wind turbines – Fixed vs. variable speed. Renewable Energy World. Vol. 6, Issue 1, 2003
http://www.jxj.com/magsandj/rew/2003_01/inside_wind.html

/Tol 2003/
Tol, R.S.J.: The Marginal Costs of Carbon Dioxide Emissions: An Assessment of the Uncertainties. Working Paper FNU-19. Internet Publication 2003
http://www.uni-hamburg.de/Wiss/FB/15/Sustainability/margcostunc.pdf

/Tol; Heinzow 2003/

    Tol, R.S.J., Heinzow, T.: Estimates of the external and sustainability costs of climate change. Working Paper FNU-32. Internet Publication 2003
    http://www.cru.uea.ac.uk/tourism/greensense.pdf

/Triacom 2004/

    Triacom: Historical exchange rates- USD. Internet publication 2004
    http://www.triacom.com/archive/exchange.en.html

/United Nations 1992/

    United Nations (UN): United Nations Framework Convention on Climate Change. United Nations 1992
    http://unfccc.int/resource/docs/convkp/conveng.pdf

/UNDP 2000/

    United Nations Development Programme (UNDP): World Energy Assessment – energy and the challenge of sustainability. New York 2000
    http://www.undp.org/seed/eap/activities/wea/drafts-frame.html

/U.S. Department of Energy 2004/

    U.S. Department of Energy: How Wind Turbines Work. Internet publication 2004
    http://www.eere.energy.gov/windandhydro/wind_how.html

/U.S. Department of Labor 2004/

    U.S. Department of Labor: Consumer Price Index
    ftp://ftp.bls.gov/pub/special.requests/cpi/cpiai.txt

/Viebahn; Krewitt 2003/

    Viebahn, P., Krewitt, W.: ECLIPSE Fuel Cell (FC) Systems. Internet publication 2003
    http://www.ECLIPSE-eu.org/zip/fuell_cell.zip

/VIK 1999/

    Verband der Industriellen Energie- und Kraftwirtschaft (VIK): Brennstoffzellen. VIK-Berichte Nr. 214. Essen 1999

/Voß 2003/

    Voß, A.: Energiesysteme I. Vorlesungsmanuskript. Stuttgart 2003
    http://www.ier.uni-stuttgart.de/public/de/lehre/skripte/esys1/index.html

/WBGU 1998/

    Wissenschaftlicher Beirat der Bundesregierung globale Umweltveränderungen (WBGU): Welt im Wandel – Strategien zur Bewältigung globaler Umweltrisiken (Jahresgutachten). Berlin 1998
    http://www.wbgu.de/wbgu_jg1998.pdf

/WBGU 2003/

Wissenschaftlicher Beirat der Bundesregierung globale Umweltveränderungen (WBGU): Über Kioto hinaus denken – Klimaschutzstrategien für das 21. Jahrhundert (Sondergutachten). Berlin 2003
http://www.wbgu.de/wbgu_sn2003.pdf

/Werner 2004/

Werner, J. H.: Second and Third Generation Photovoltaics – Dreams and Reality. In: Advances in Solid State Physics, Vol. xx, Issue xxx, 2004 (in press)

/Wiese 1994/

Wiese, A.: Simulation und Analyse einer Stromerzeugung aus erneuerbaren Energien in Deutschland. IER, Universität Stuttgart. Forschungsbericht Band 16 1994

/Willeke 2004/

Willeke, G. P.: The Crystalline Silicon Solar Cell – History, Achievements and Perspectives. Presented at the 19th European Photovoltaic Solar energy conference. Paris 7-11 June 2004
http://www.ise.fhg.de/german/current_topics/events/events2004/pdf/Willeke_2C P.1.1.pdf